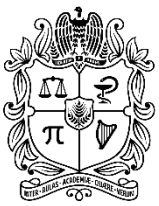

UNIVERSIDAD
NACIONAL
DE COLOMBIA

Optimization of the structural design of asphalt pavements for streets and highways

OPTIMIZACIÓN DEL DISEÑO ESTRUCTURAL DE PAVIMENTOS ASFÁLTICOS PARA CALLES Y CARRETERAS

Luis Ricardo Vásquez Varela

Universidad Nacional de Colombia

Facultad de Ingeniería y Arquitectura, Departamento de Ingeniería Eléctrica y Electrónica

Manizales, Colombia

2022

Optimization of the structural design of asphalt pavements for streets and highways

OPTIMIZACIÓN DEL DISEÑO ESTRUCTURAL DE PAVIMENTOS ASFÁLTICOS PARA CALLES Y CARRETERAS

Luis Ricardo Vásquez Varela

A thesis presented as a partial requirement to qualify for the title of

Ph.D. in Engineering – Automatic

Advisor:

Ph.D. Francisco Javier García Orozco

Universidad Nacional de Colombia

Facultad de Ingeniería y Arquitectura, Departamento de Ingeniería Eléctrica y Electrónica

Manizales, Colombia

2022

For my beloved family.

Acknowledgments

The author profoundly thanks the enthusiastic support and guidance of Professor F. J. García–Orozco, Ph.D., as Director of this research project. This work would not have been possible without his indefatigable compromise, as it has been in every conjoint endeavor in almost two decades of academic cooperation and friendship.

Proper recognition goes to Professor M. Granada–Echeverri, Ph.D., at Universidad Tecnológica de Pereira (UTP) for his valuable contribution to the genesis of this project. Professor Granada's invitation to his Metaheuristics course was fundamental for formulating this research project.

The author wishes to thank the valuable contributions and comments of Professors D. A. Álvarez–Marín, Ph.D.; J. A. Paredes-López, Ph.D.; and A. Salas-Montoya, Ph.D., to the research project presented in mid-2016. Contributions by Ph.D. Álvarez-Marín increased the potential value of this research.

Likewise, the author thanks the jurors of the thesis Professors F. A. Reyes-Lizcano, Ph.D.; W. D. Fernandez-Gomez, Ph.D.; and J. E. Hurtado-Gómez, Ph.D., for their observations, criticisms, and contributions.

The author is also grateful to the Universidad Nacional de Colombia for its support through these doctoral years with tuition exemptions and a two-year study commission.

Abstract

The construction of asphalt pavements in streets and highways is an activity that requires optimizing the consumption of significant economic and natural resources. Pavement design optimization meets contradictory objectives according to the availability of resources and users' needs. This dissertation explores the application of metaheuristics to optimize the design of asphalt pavements using an incremental design based on the prediction of damage and vehicle operating costs (VOC). The costs are proportional to energy and resource consumption and polluting emissions. The evolution of asphalt pavement design and metaheuristic optimization techniques on this topic were reviewed. Four computer programs were developed: (1) UNLEA, a program for the structural analysis of multilayer systems. (2) PSO-UNLEA, a program that uses particle swarm optimization metaheuristic (PSO) for the backcalculation of pavement moduli. (3) UNPAVE, an incremental pavement design program based on the equations of the North American MEPDG and includes the computation of vehicle operating costs based on IRI. (4) PSO-PAVE, a PSO program to search for thicknesses that optimize the design considering construction and vehicle operating costs. The case studies show that the backcalculation and structural design of pavements can be optimized by PSO considering restrictions in the thickness and the selection of materials. Future developments should reduce the computational cost and calibrate the pavement performance and VOC models.

Keywords: Asphalt pavement, design, backcalculation, metaheuristics.

Resumen

La construcción de pavimentos asfálticos en calles y carreteras es una actividad que requiere la optimización del consumo de cuantiosos recursos económicos y naturales. La optimización del diseño de pavimentos atiende objetivos contradictorios de acuerdo con la disponibilidad de recursos y las necesidades de los usuarios. Este trabajo explora el

empleo de metaheurísticas para optimizar el diseño de pavimentos asfálticos empleando el diseño incremental basado en la predicción del deterioro y los costos de operación vehicular (COV). Los costos son proporcionales al consumo energético y de recursos y las emisiones contaminantes. Se revisó la evolución del diseño de pavimentos asfálticos y el desarrollo de técnicas metaheurísticas de optimización en este tema. Se desarrollaron cuatro programas de computador: (1) UNLEA, programa para el análisis estructural de sistemas multicapa. (2) PSO-UNLEA, programa que emplea la metaheurística de optimización con enjambre de partículas (PSO) para el cálculo inverso de módulos de pavimentos. (3) UNPAVE, programa de diseño incremental de pavimentos basado en las ecuaciones de la MEPDG norteamericana, y el cálculo de costos de construcción y operación vehicular basados en el IRI. (4) PSO-PAVE, programa que emplea la PSO en la búsqueda de espesores que permitan optimizar el diseño considerando los costos de construcción y de operación vehicular. Los estudios de caso muestran que el cálculo inverso y el diseño estructural de pavimentos pueden optimizarse mediante PSO considerando restricciones en los espesores y la selección de materiales. Los desarrollos futuros deben enfocarse en reducir el costo computacional y calibrar los modelos de deterioro y COV.

Palabras clave: Pavimento asfáltico, diseño, cálculo inverso, metaheurística.

Contents

List of figures

Page

List of tables

Page

List of symbols and abbreviations

Symbols with Latin letters

Symbol	Concept	SI unit	Definition
a	*The radius of the loaded area*	*mm*	*The radius of a uniformly loaded area on the surface of the pavement used in the layered elastic theory*
A	*The aggressiveness of an axle*	*--*	*Relationship between the damage caused by an axle and the reference axle of 130 kN in the French method*
A	*Temperature susceptibility of the bitumen*	$\frac{\log(pen)}{°C}$	*The slope of the line plot between the logarithm of penetration and temperature used to estimate stiffness and fatigue properties in the Shell Oil method*
A	*The number of activities for an optimizing problem*	*--*	*Space search of a combinatorial double-exponential allocation problem*
A	*Integration constant*	*--*	*Integration constant obtained from the continuity conditions in the interfaces of a layered system*
A	*Viscosity-temperature susceptibility*	*--*	*Regression intercept of the ASTM viscosity-temperature relationship*
age	*The age of pavement*	*years*	*Prediction model of the pavement smoothness in the MEPDG*
A_r	*Regression coefficient in the rutting model in the French Design Method*	*--*	*A traffic-based coefficient to adjust the strain-based rutting law in the French Design Method*
$AREA$	*The normalized area of a vertical section of a deflection basin*	*mm*	*A descriptor of the deflection bowl that relates to pavement type and behavior*
b	*The slope of the bi-logarithmic fatigue law*	*--*	*Regression coefficient in strain-based or stress-based fatigue laws in the French Design Method*
$(BC)_T$	*The area of block cracking (user input, not modeled by MEPDG)*	*% Of the total lane area*	*Part of the IRI prediction model in the MEPDG*
B	*Integration constant*	*--*	*Integration constant obtained from the continuity conditions in the interfaces of a layered system*
c	*User-defined cracking progression parameters*	*--*	*Reflection cracking model in hot-mix asphalt overlays of cracks and joints in existing flexible, semi-rigid, composite, and rigid pavements in MEPDG*
c	*Coefficient linking the variation in strain (or stress) to the random variation in thickness*	*cm^{-1}*	*Related to fatigue in bituminous materials in the French Design Method*
c_1	*The cognition weight*	*--*	*Learning or condition factor of the PSO*
c_2	*The social weight*	*--*	*Learning or condition factor of the PSO*
C	*Cracked area*	*ft^2 / ft^2 (m^2/ m^2)*	*The cracked area in the PSI prediction equation for asphalt pavements obtained at the AASHO Road Test*

Symbol	Concept	SI unit	Definition
C	*The transverse depth of the crack*	*in*	*Part of the non-load transverse cracking model in the MEPDG*
C	*The CSM layer cracking in feet of cracking per 500 feet long sections*	*ft / 500 ft*	*The empirical relationship that relates CSM damage to cracking*
C	*Integration constant*	*--*	*Integration constant obtained from the continuity conditions in the interfaces of a layered system*
CC	*Construction cost in US dollars per kilometer*	*U$ / km*	*Pavement initial construction cost for a road 7.2 meters wide. It is used to optimize the design*
C_0	*A coefficient to estimate the ρ function of the soil rutting model*	*--*	*Part of the rutting model of unbound layers in the MEPDG*
C_0	*The current transverse crack length*	*feet*	*Part of the non-load transverse cracking model in the MEPDG*
C_1, C_2	*The depth confinement factor coefficients*	*--*	*Part of the rutting model of HMA in the MEPDG*
$C_1, C'_1, C_2, C_{,2}$	*Coefficients to calculate alligator fatigue cracking from the fatigue damage*	*--*	*Part of the load-related alligator cracking or bottom-up cracking models in the MEPDG*
C_f	*Shift factor*	*--*	*Field calibration coefficient for fatigue laws obtained in the laboratory*
C_f	*The observed amount of thermal cracking*	*--*	*Part of the non-load transverse cracking model in the MEPDG*
C_H	*The thickness correction term for fatigue cracking prediction*	*--*	*Part of the load-related alligator cracking or bottom-up cracking models in the MEPDG*
CBR	*California Bearing Ratio*	*%*	*A relative measure of soil shear strength developed in California by Porter*
COV_{RD}	*The coefficient of variation of the rut depths (assumed to be 20%)*	*%*	*Part of the IRI prediction model for pavements with unbound aggregate base and subbase in the MEPDG*
d	*User-defined cracking progression parameters*	*--*	*Reflection cracking model in hot-mix asphalt overlays of cracks and joints in existing flexible, semi-rigid, composite, and rigid pavements in MEPDG*
d_i	*The measured deflection at point i*	*μm*	*The pavement displacement due to a known load applied on the surface*
d_i^k	*The input deflection information obtained from the field at sensor k*	*μm*	*Field time-history deflection for dynamic moduli backcalculation*
d_o^k	*The output deflection information obtained from forward-calculation at sensor k*	*μm*	*Computed time-history deflection for dynamic moduli backcalculation*
$\{d^k\}_{max}$	*The maximum value of the input deflection information obtained from the field at sensor k*	*μm*	*Field maximum deflection for dynamic moduli backcalculation*
D	*The depth below the surface*	*in*	*Part of the rutting model of HMA in the MEPDG*
D	*The fatigue damage*	*--*	*Part of the load-related alligator cracking or bottom-up cracking models of HMA and CSM in the MEPDG*
D	*Integration constant*	*--*	*Integration constant obtained from the continuity conditions in the interfaces of a layered system*
D	*The dimensions of the search space*	*--*	*Used in the particle swarm optimization to define the position of each particle*
D_a	*Asphalt Institute's allowable superficial deflection*	*mm*	*The maximum allowable superficial deflection for an asphalt pavement that will support N repetitions of the standard single axle load of 80 kN*

Symbol	Concept	SI unit	Definition
D_i	*The measured deflection at point i*	*μm*	*The pavement displacement due to a known load applied on the surface*
D_j	*A measured deflection at the point j*	*μm*	*Part of the quadratic error function of pavement moduli backcalculation*
E	*Young modulus*	*MPa*	*Elastic parameter of isotropic materials*
E_1	*Modulus of the pavement*	*kPa*	*Modulus of the pavement layer in the simplified two-layer model*
E_2	*Modulus of the subgrade*	*kPa*	*Modulus of the semi-infinite subgrade layer in the simplified two-layer model*
$E(10°C)$	*Elastic modulus of the asphalt mixture at 10°C*	*MPa*	*Modulus of the bituminous layers in the French Design Method*
$\|E*\|$	*Dynamic modulus of the asphalt mix*	*MPa*	*The absolute value of the viscous and elastic components of the dynamic response due to cyclic loading in the Asphalt Institute method*
$\{E\}$	*The unknown moduli vector*	*--*	*Part of the matrix equation to solve moduli in the gradient relaxation method*
$E_{CSM}(max)$	*The maximum CSM layer modulus for the intact layer*	*psi*	*Part of the incremental modulus reduction of CSM in the MEPDG*
$E_{CSM}(min)$	*The minimum CSM layer modulus after total layer destruction*	*psi*	*Part of the incremental modulus reduction of CSM in the MEPDG*
$E_{CSM}(t)$	*The CSM layer modulus at a damage level D*	*psi*	*Part of the incremental modulus reduction of CSM in the MEPDG*
E_{HMA}	*The HMA indirect tensile modulus*	*psi*	*Part of the non-load transverse cracking model in the MEPDG*
E_{HMA}	*The dynamic modulus of the HMA measured in compression*	*psi*	*Part of the load-related alligator cracking or bottom-up cracking models in the MEPDG*
$E(\theta_{eq})$	*Elastic modulus of the asphalt mixture at the equivalent temperature*	*MPa*	*Modulus of the bituminous layers in the French Design Method*
f	*A fitness function in an optimization process*	*--*	*A function of the relative root-mean-square error of measured versus computed deflections in a backcalculation process*
FC_{bottom}	*Transfer function to calculate alligator fatigue cracking from the fatigue damage*	*% Of lane area*	*Part of the load-related alligator cracking or bottom-up cracking models in the MEPDG*
FI	*The average annual freezing index*	*°C-days °F-days*	*Part of the site factor equation in the roughness prediction model in MEPDG*
$\overline{FC_i}$	*The predicted cracking based on mean inputs*	*% ft/mile*	*The load-related alligator cracking or bottom-up cracking reliability in the MEPDG*
FC_P	*The predicted cracking at a reliability level of P*	*% ft/mile*	*The load-related alligator cracking or bottom-up cracking reliability in the MEPDG*
FC_{top}	*Transfer function to calculate longitudinal fatigue cracking from the fatigue damage*	*ft/mile*	*Part of the load-related alligator cracking or bottom-up cracking models in the MEPDG*
$(FC)_T$	*The fatigue cracking in the wheel path*	*% Of the total lane area*	*Part of the IRI prediction model in the MEPDG*
GWT	*The groundwater table depth*	*feet*	*Part of the rutting model of unbound layers in the MEPDG*
h_1	*The total thickness of the pavement*	*mm*	*The thickness of the pavement layer in the simplified two-layer model*
h_{AC}	*The thickness of the asphalt layer*	*in*	*Part of the non-load transverse cracking model in the MEPDG*
H	*The total depth of a pavement structure*	*m*	*Used in the layered system solution to normalize the coordinates of any point. Also used to normalize the radius of the loaded areas*
H_{eff}	*The effective overlay thickness*	*in*	*Reflection cracking model in hot-mix asphalt overlays of cracks and joints in existing*

Symbol	Concept	SI unit	Definition
			flexible, semi-rigid, composite, and rigid pavements in MEPDG
$h_{(HMA)}$ H_{HMA}	*The total thickness of the HMA layer*	*in*	*Part of the rutting model of HMA in the MEPDG*
h_{soil}	*The thickness of the unbound layer*	*in*	*Part of the rutting model of unbound layers in the MEPDG*
J_0	*The Bessel function of the first kind and order zero*	--	*A function used to solve the stresses and displacements due to a loaded area in an axisymmetrical system*
J_1	*The Bessel function of the first kind and first order*	--	*A function used to solve the stresses and displacements due to a loaded area in an axisymmetrical system*
IRI	*International Roughness Index*	*mm/m*	*Cumulative displacement of the quarter-of-car model over the road profile*
IRI	*The predicted IRI based on mean inputs (reliability 50%)*	*mm/m*	*Part of the prediction model of the pavement smoothness in the MEPDG*
IRI_P	*The predicted IRI at the reliability level P*	*mm/m*	*Part of the prediction model of the pavement smoothness in the MEPDG*
IRI_0	*The initial IRI of the pavement*	*mm/m*	*Part of the prediction model of the pavement smoothness in the MEPDG*
K	*Coefficient according to the type of axle*	--	*A coefficient that considers the type of axle (single, tandem, tridem) in the aggressiveness computation in the French method*
K_{0TC_i}	*A coefficient determined through global calibration for each hierarchical input level in the MEPDG*	--	*Part of the non-load transverse cracking model in the MEPDG*
k_1, k_2, k_3	*Regression coefficients*	--	*Regression coefficients in strain-based fatigue law*
k_{1r}, k_{2r}, k_{3r}	*Global field calibration parameters for rutting*	--	*Part of the rutting model of HMA in the MEPDG*
k_4, k_5	*Regression coefficients*	--	*Regression coefficients in strain-based rutting model*
k_c	*Regression coefficient in fatigue model in the French Design Method*	--	*A coefficient that adjusts the working strain or stress to the performance observed on pavements of the same type*
k_d	*Regression coefficient in fatigue model in the French Design Method*	--	*A coefficient that considers the effect of joints or shrinkage cracks in cement-treated materials or concrete slabs*
k_{f1}, k_{f2}, k_{f3}	*Global field calibration parameters for fatigue cracking*	--	*Part of the load-related alligator cracking or bottom-up cracking models in the MEPDG*
k_r	*Regression coefficient in fatigue model in the French Design Method*	--	*A coefficient that adjusts the working strain or stress values to the design reliability*
k_s	*Regression coefficient in fatigue model in the French Design Method*	--	*A reducing factor that considers the heterogeneity of the bearing capacity of the roadbed*
k_{s1}	*Global calibration factor:* $k_{s1} = 1.673\ [granular\ soil]$ $k_{s1} = 1.350[fine\ soil]$	--	*Part of the rutting model of unbound layers in the MEPDG*
k_t	*A coefficient determined through global calibration for each hierarchical input level in the MEPDG*	--	*Part of the non-load transverse cracking model in the MEPDG*
K_{TC_i}	*A coefficient determined through global calibration for each hierarchical input level in the MEPDG*	--	*Part of the non-load transverse cracking model in the MEPDG*
k_z	*The depth confinement factor in the HMA rutting model*	--	*Part of the rutting model of HMA in the MEPDG*

Symbol	Concept	SI unit	Definition
$(LC_{SNWP})_{MH}$	*The length of moderate and high severity sealed longitudinal cracks outside the wheel path (user input, not modeled by MEPDG)*	*m/km*	*Part of the IRI prediction model in the MEPDG*
m	*A parameter derived from the indirect tensile creep compliance curve measured in the laboratory*	*--*	*Part of the non-load transverse cracking model in the MEPDG*
m	*The number of deflection points or measuring sensors*	*--*	*Part of the quadratic error function of pavement moduli backcalculation*
m	*A parameter in Burmister's or Huang's stress function*	*--*	*A parameter used in the Hankel transformation to solve the stresses and displacements due to a loaded area in an axisymmetrical system*
$MAAT$	*Mean annual air temperature*	*°C*	*Temperature to estimate the long-term aging of binder*
M_r	*Resilient modulus*	*psi*	*Resilient modulus of the pavement materials or subgrade in the AASHTO 1993 method*
M_r	*Resilient modulus*	*psi*	*Part of the rutting model of unbound layers in the MEPDG*
MR	*The 28-day modulus of rupture of the CSM*	*psi*	*Part of the load-related fatigue cracking model of CSM in the MEPDG*
n	*The number of axle-load repetitions*	*--*	*Part of the rutting models in the MEPDG*
N	*Expected traffic on the pavement*	*ESAL*	*Repetitions of the standard single axle load of 80 kN in the Asphalt Institute's deflection criterion*
N_d	*The allowable number of load repetitions in the rutting model*	*--*	*The allowable number of load repetitions until the development of ruts of a certain depth in an asphalt pavement*
NE	*Number of load repetitions to failure with a 50% probability*	*--*	*Repetitions of the standard single axle load of 130 kN in the French Design Method*
N_f	*The allowable number of load repetitions in the cracking model*	*--*	*The allowable number of load repetitions to fatigue failure of an asphalt material*
$N_{f(HMA)}$	*The allowable number of axle-load applications*	*--*	*Part of the load-related alligator cracking or bottom-up cracking models in the MEPDG*
$N_{f(CTB)}$	*The number of repetitions to fatigue cracking of the chemically stabilized (CSM) layer*	*--*	*Part of the load-related fatigue cracking model of CSM in the MEPDG*
n_i	*The actual traffic for period i*	*--*	*Part of the load-related alligator cracking or bottom-up cracking models in the MEPDG*
N_i	*The allowed traffic under conditions prevailing in period i*	*--*	*Part of the load-related alligator cracking or bottom-up cracking models in the MEPDG*
$N_{(z)}$	*The standard normal distribution evaluated at z*	*--*	*Part of the non-load transverse cracking model in the MEPDG*
$p_{i,d}^k$	*The d^{th} dimension best personal position of particle i in cycle k*	*--*	*Best position of a particle in a PSO*
$p_{g,d}^k$	*The d^{th} dimension best global position of particle i in cycle k*	*--*	*The best global position of a particle in a PSO*
pen_0	*Penetration of a recovered bitumen*	*0.1 mm*	*Penetration of a recovered bitumen to estimate the asphalt concrete modulus with Shell equations*
pen_t	*Penetration of an aged bitumen*	*0.1 mm*	*Penetration of an aged bitumen to estimate the change of asphalt concrete modulus with time*
P	*Applied wheel load*	*lb. (kN)*	*Applied load by a single wheel in the USACE CBR equation or by an axle in the French method*
P	*Patched area*	*ft² / ft² (m²/ m²)*	*The patched area in the PSI prediction equation for asphalt pavements*

Symbol	Concept	SI unit	Definition
P	*The desired reliability level in the MEPDG design process*	--	*Part of the rutting model in the MEPDG*
P_{34}	*Cumulative percentage retained on the ¾ sieve*	%	*Part of the MEPDG dynamic modulus model*
P_{38}	*Cumulative percentage retained on the ⅜ sieve*	%	*Part of the MEPDG dynamic modulus model*
P_4	*Cumulative percentage retained on the No.4 sieve*	%	*Part of the MEPDG dynamic modulus model*
P_{200}	*Percent passing the No. 200 sieve*	%	*Part of the MEPDG dynamic modulus model*
P_{02}	*The percent passing the 0.02 mm sieve*	%	*Part of the site factor equation in the roughness prediction model in MEPDG*
P_{075}	*The percent passing the 0.075 mm sieve*	%	*Part of the site factor equation in the roughness prediction model in MEPDG*
PI	*The plasticity index of the soil*	%	*Part of the site factor equation in the roughness prediction model in MEPDG*
PI	*Bitumen penetration index*	--	*A measure of the temperature susceptibility of bitumen used to estimate stiffness and fatigue properties in the Shell Oil method*
P_S	*The number of pavement sections for an optimizing problem*	--	*Space search of a combinatorial double-exponential allocation problem*
PSI	*Present Serviceability Index*	--	*A subjective evaluation of the condition of pavement based on roughness and distress*
$(P)_H$	*The area of high-severity patches as a percent of the total lane area*	%	*Part of the IRI prediction model for pavements with asphalt-treated bases in the MEPDG*
q	*The inflation wheel pressure*	*kPa*	*Applied pressure by a single wheel in the USACE CBR equation, and the layered elastic theory*
r_i	*Radial distance*	*mm*	*The distance from the load to any sensor in a deflectometer*
$r_1 or\ r_2$	*Random values uniformly distributed in the range [0, 1]*	--	*Used to include randomness in the updated velocity of the particles in PSO*
RC	*Percentage of cracks reflected*	%	*Reflection cracking model in hot-mix asphalt overlays of cracks and joints in existing flexible, semi-rigid, composite, and rigid pavements in MEPDG*
RD	*Rut depth*	*in (mm)*	*Average rut depth on both wheel tracks in a flexible pavement*
RD_{Total}	*The total permanent deformation*	*in*	*The sum of all rutting components in MEPDG*
RD_{AC}	*Predicted average permanent deformation or rutting of the asphalt concrete*	*in*	*Rutting component of HMA*
RD_{GB}	*Predicted mean permanent deformation or rutting of the aggregate bases*	*in*	*Rutting component of granular bases*
RD_{SG}	*Predicted average permanent deformation or rutting of the subgrade*	*in*	*Rutting component of subgrade*
RD_p	*The predicted rutting at a reliability level of P*	*in*	*Part of the rutting model in the MEPDG*
$\overline{RD_i}$	*The predicted rutting based on mean inputs (reliability of 50%)*	*in*	*Part of the rutting model in the MEPDG*
R_m	*The average annual rainfall*	*mm*	*Part of the site factor equation in the roughness prediction model in MEPDG*
$RMAE$	*The relative mean absolute error of measured versus computed deflections*		*A statistical comparison between measured and computed pavement deflection for moduli backcalculation*

Symbol	Concept	SI unit	Definition
$RMSE$	*The root-mean-square error of measured versus computed deflections*	*%*	*A statistical comparison between measured and computed pavement deflection for moduli backcalculation*
R_{SD}	*The standard deviation of the monthly rainfall*	*mm*	*Part of the site factor equation in the roughness prediction model in MEPDG*
RSS	*The squared differences summation of measured versus computed deflections*	*μm²*	*A statistical comparison between measured and computed pavement deflection for moduli backcalculation*
SD_{RD}	*The standard deviation of rut depths*	*mm*	*Part of the IRI prediction model for pavements with chemically stabilized bases in the MEPDG*
S_e^2	*The variance of the overall model error for IRI prediction*	*0.15 (mm/m) ²*	*Part of the IRI dispersion model in the MEPDG*
Se_{FCi}	*The standard error of cracking at the predicted level of mean cracking*	*% ft/mile*	*The load-related alligator cracking or bottom-up cracking reliability in the MEPDG*
Se_{FC_bottom}	*The standard error of bottom-up cracking at the predicted level of mean cracking*	*% ft/mile*	*The load-related alligator cracking or bottom-up cracking reliability in the MEPDG*
Se_{FC_top}	*The standard error of top-down cracking at the predicted level of mean cracking*	*% ft/mile*	*The load-related alligator cracking or bottom-up cracking reliability in the MEPDG*
Se_{IRI}	*The standard deviation of IRI at the predicted level of mean IRI*	*mm/m*	*Part of the prediction model of the pavement smoothness in the MEPDG*
Se_{TC_i}	*The standard error of estimate for thermal cracking per 500 ft*	*feet*	*Part of the non-load transverse cracking model in the MEPDG*
Se_{RDi}	*The standard error of rutting at the predicted level of mean rutting*	*in*	*Part of the rutting model in the MEPDG*
Se_{RDAC}	*The standard error of rutting at the predicted level of mean rutting of the asphalt concrete*	*in*	*Part of the rutting model in the MEPDG*
Se_{RDBG}	*The standard error of rutting at the predicted level of mean rutting of the aggregate bases*	*In*	*Part of the rutting model in the MEPDG*
Se_{RDSG}	*The standard error of rutting at the predicted level of mean rutting of the subgrade*	*in*	*Part of the rutting model in the MEPDG*
SF	*The site factor of the IRI prediction model*	*--*	*Part of the prediction model of the pavement smoothness in the MEPDG*
Sh	*The standard deviation of the dispersion of the layer thickness*	*cm*	*Dispersion due to construction in the strain-based fatigue model in the French Design Method*
S_{ji}	*A simplified model for the moduli-deflection relation in backcalculation*	*μm / log(kPa)*	*Part of the gradient relaxation method for moduli backcalculation*
S_m	*Stiffness of the asphalt mix*	*Pa*	*Stiffness modulus of an asphalt mix in the Shell Oil method*
SN	*The standard deviation of the logarithm of the number of cycles at failure*	*--*	*Dispersion due to traffic in the strain-based fatigue model in the French Design Method*
SN	*Structural number*	*--*	*The summation of the products of the layer thickness times a non-dimensional layer coefficient*
S_n	*The standard deviation of the pavement condition assessment*	$\log W_{18}$	*The dispersion of the pavement condition in the AASHTO 1993 method*
S_o	*The overall standard deviation of the pavement design*	$\log W_{18}$	*The total dispersion of the pavement design in the AASHTO 1993 method*
S_s	*The size of a search space for an optimizing problem*	*--*	*Space search of a combinatorial double-exponential allocation problem*

Symbol	Concept	SI unit	Definition
S_w	*The standard deviation of the traffic estimation*	$\log W_{18}$	*The dispersion of the traffic estimation in the AASHTO 1993 method*
SV	*Slope variance*	*10-6*	*Slope variance of a road profile measured with the CHLOE profilograph*
t	*Time for the reflection cracking process*	*years*	*Reflection cracking model in hot-mix asphalt overlays of cracks and joints in existing flexible, semi-rigid, composite, and rigid pavements in MEPDG*
t	*Accumulated time of an in-service bitumen*	*months*	*Accumulated time to estimate bitumen aging and asphalt concrete modulus*
t	*The current generation in PSO*	*--*	*Elapsed generations in a PSO*
T	*The total thickness of the pavement*	*mm*	*Pavement thickness in the USACE CBR equation*
T	*The pavement temperature*	*°F*	*Part of the rutting model of HMA in the MEPDG*
T	*The analysis period for an optimizing problem*	*years*	*Space search of a combinatorial double-exponential allocation problem*
T	*The total number of years in the pavement's analysis period*	*years*	*Part of the load-related alligator cracking or bottom-up cracking models in the MEPDG*
T_{max}	*The maximum evolution generation*	*--*	*End of the generations in a PSO*
$(TC_L)_T$	*The total length of transverse cracks*	*m/km*	*Part of the IRI prediction model in the MEPDG*
$(TC_S)_H$	*The average spacing of high-severity transverse cracks estimated from the thermal cracking model*	*m*	*Part of the IRI prediction model for pavements with asphalt-treated bases in the MEPDG*
$Thermal$	*The predicted thermal cracking per 500 ft*	*feet*	*Part of the non-load transverse cracking model in the MEPDG*
T_{rb}	*The softening point of a bitumen*	*°C*	*The softening point of bitumen obtained with the ring-and-ball test (ASTM D36)*
t_w	*Time of loading*	*s*	*Time of loading as a function of traffic speed to estimate asphalt concrete modulus*
u	*The horizontal displacement*	*m*	*The translation of a point in the radial direction in a multilayered system*
$v_{i,d}^{k+1}$	*The d^{th} dimension updated velocity of particle i in cycle $k+1$*	*--*	*The updated velocity of a particle in a PSO*
V_a	*The air voids by volume*	*%*	*Part of the load-related alligator cracking or bottom-up cracking models in the MEPDG*
V_b	*Percentage of bitumen*	*%*	*The relative volume of bitumen in an asphalt mix used to estimate stiffness and fatigue properties in the Shell Oil and the Asphalt Institute methods*
V_{be}	*The effective asphalt content by volume*	*%*	*Part of the load-related alligator cracking or bottom-up cracking models in the MEPDG*
$V[(BC)_T]$	*The variance of the area of the block cracking*	*(% of the total lane area) ²*	*Part of the IRI dispersion model in the MEPDG*
$V[COV_{RD}]$	*The variance of the coefficient of variation of the rut depth*	*%²*	*Part of the IRI dispersion model for pavements with unbound aggregate base and subbase in the MEPDG*
$V[(FC)_T]$	*The variance of fatigue cracking in the wheel path*	*(% of the total lane area) ²*	*Part of the IRI dispersion model in the MEPDG*
$V(IRI_0)$	*The variance of the initial International Roughness Index*	*(mm/m) ²*	*Part of the IRI dispersion model in the MEPDG*
$V[(LC_{SNWP})_{MH}]$	*The variance of the length of moderate and high severity sealed longitudinal cracks outside wheel paths*	*(m/km) ²*	*Part of the IRI dispersion model in the MEPDG*

Symbol	Concept	SI unit	Definition
VOC	*Vehicle operating cost in US dollars per kilometer*	*U$ / km*	*Vehicle operating cost for a road 7.2 meters wide. It is used to optimize the design*
$V(P_H)$	*The variance of the area of high-severity patches estimated from typical values*	*%²*	*Part of the IRI dispersion model for pavements with asphalt-treated bases in the MEPDG*
$V[SD_{RD}]$	*The variance of rut depths*	*mm²*	*Part of the IRI dispersion model for pavements with chemically stabilized bases in the MEPDG*
$V(SF)$	*The variance of the site factor*	*--*	*Part of the IRI dispersion model for pavements with unbound aggregate base and subbase in the MEPDG*
$V[(TC_L)_T]$	*The variance of the total length of transverse cracks at all severity levels*	*(m/km) ²*	*Part of the IRI dispersion model in the MEPDG*
$V[(TC_S)_H]$	*The variance of average spacing of high-severity transverse cracks estimated from the thermal cracking model*	*m²*	*Part of the IRI dispersion model for pavements with asphalt-treated bases in the MEPDG*
VTS	*Viscosity-temperature susceptibility*	*--*	*Regression slope of the ASTM viscosity-temperature relationship*
V_v	*Percentage of air-voids*	*%*	*The relative volume of air voids in an asphalt mix used to estimate stiffness and fatigue properties in the Asphalt Institute method*
w	*The vertical displacement or "deflection."*	*M*	*The translation of a point in the vertical direction in a multilayered system*
W_{18}	*Traffic in the AASHTO 1993 design method*	*ESAL*	*Expected number of repetitions of the standard single axle load of 18-kips on the design lane for the design period of analysis*
W_C	*Water content*	*%*	*Part of the rutting model of unbound layers in the MEPDG*
x_i	*A vector of D dimensions*	*--*	*Defines the position of a single particle in the particle swarm optimization (PSO)*
$x_{i,d}^{k}$	*The d^{th} dimension current position of particle i in cycle k*	*--*	*The current position of a particle in a PSO*
$x_{i,d}^{k+1}$	*The d^{th} dimension next position of particle i in cycle $k+1$*	*--*	*Updated position of a particle in a PSO*
Z_r	*Standardized normal distribution*	*--*	*The accumulated value of the standardized normal distribution for a given reliability level*

Symbols with Greek letters

Symbol	Concept	SI unit	Definition
α	*A material behavior-related power for aggressiveness computation*	*--*	*A power depending on the type of material and structure in the aggressiveness computation in the French method*
α	*An adjustment factor*	*--*	*A factor used to provide significant figures in a fitness function based on RMSE*
α	*The normalized radius of the loaded area applied on a layered system*	*--*	*The ratio of the radius of the applied load and the full depth of the pavement*
β	*The slope of Wohler's curve*	*--*	*Related to fatigue in cement-treated materials in the French Design Method*
β	*A parameter of the rutting model for unbound materials*	*--*	*Part of the rutting model of unbound layers in the MEPDG*
β	*An adjustment factor*	*--*	*A factor used to avoid "division by zero" errors in RMSE computing when computed deflections have low values*

Symbol	Concept	SI unit	Definition
β_1	*A regression coefficient determined through field calibration*	--	*Part of the non-load transverse cracking model in the MEPDG*
$\beta_{1r}, \beta_{2r}, \beta_{3r}$	*Local field calibration constants for rutting*	--	*Part of the rutting model of HMA in the MEPDG*
$\beta_{f1}, \beta_{f2}, \beta_{f3}$	*Local field calibration constants for fatigue cracking*	--	*Part of the load-related alligator cracking or bottom-up cracking models in the MEPDG*
β_{c1}, β_{c2}	*Field calibration factors for CSM fatigue prediction*	--	*Part of the load-related fatigue cracking model of CSM in the MEPDG*
β_{s1}	*Local calibration constant*	--	*Part of the rutting model of unbound layers in the MEPDG*
β_t	*Local calibration factor*	--	*Part of the non-load transverse cracking model in the MEPDG*
χ	*A convergence factor for the updated velocity in PSO*	--	*A function of the cognition and social weights in the PSO*
δ	*Standard deviation associated with the load repetitions given the dispersion of the fatigue law and the layer thickness*	--	*Related to fatigue in bituminous materials in the French Design Method*
ΔC	*The change in the crack depth due to a cooling cycle*	*in*	*Part of the non-load transverse cracking model in the MEPDG*
$\Delta h_{i,j}$	*Thicknesses of all rutting-susceptible layers and sublayers*	*in*	*Part of the rutting model in the MEPDG*
Δ_j	*The predicted deflection at the point j as a function of the moduli of the pavement*	*μm*	*Part of the quadratic error function of pavement moduli backcalculation*
$\Delta_{p(HMA)}$	*The accumulated plastic vertical deformation in the HMA layer*	*in*	*Part of the rutting model of HMA in the MEPDG*
$\Delta_{p(soil)}$	*The plastic deformation of unbound materials*	*in*	*Part of the rutting model of unbound layers in the MEPDG*
ΔPSI	*Delta of PSI*	--	*The estimated loss of serviceability in the service period in the AASHTO 1993 method*
Δt	*The time increment between cycles k and $k+1$*	--	*Elapsed time for the updated position of a particle in a PSO. It is equal to 1.0*
ε_0	*The intercept determined from laboratory repeated load permanent deformation tests*	*in/in*	*Part of the rutting model of unbound layers in the MEPDG*
$\varepsilon_6(10°C, 25Hz)$	*The tensile strain of the fatigue law at 10°C, 25 Hz, and one million load repetitions*	*mm/mm*	*Constant of the bi-logarithmic fatigue law in the French Design Method*
ε_c	*Vertical compressive strain*	*mm/mm*	*The structural response related to the rutting of the subgrade in the Shell Oil procedure*
$\varepsilon_{p\ i,j}$	*Plastic strain due to the i^{th} traffic load in the j^{th} period*	*in/in*	*Part of the rutting model in the MEPDG*
$\varepsilon_{r(HMA)}$	*The resilient strain calculated at the mid-depth of the HMA layer*	*in/in*	*Part of the rutting model of HMA in the MEPDG*
ε_r	*The resilient strain imposed in the laboratory to obtain material properties ε_0, ε, and ρ*	*in/in*	*Part of the rutting model of unbound layers in the MEPDG*
ε_t	*Horizontal tensile strain*	*mm/mm*	*The structural response in a layered media related to fatigue in bituminous materials*
ε_t	*The calculated tensile strain at critical locations*	*in/in*	*Part of the load-related alligator cracking or bottom-up cracking models in the MEPDG*
$\varepsilon_{t,ad}$	*Allowable tensile strain in the asphalt layer*	*mm/mm*	*The structural response in a layered media related to fatigue in bituminous materials in the French Design Method*
ε_v	*The calculated average vertical resilient strain in the layer*	*in/in*	*Part of the rutting model of unbound layers in the MEPDG*

Symbol	Concept	SI unit	Definition
ε_z	*Vertical compressive strain*	*mm/mm*	*The structural response in a layered media related to the rutting of all materials*
$\varepsilon_{z,ad}$	*The allowable compressive strain on the top of untreated or subgrade layers*	*mm/mm*	*The structural response in a layered media related to rutting in the subgrade and untreated materials in the French Design Method*
ϕ	*The Burmister's or Huang's stress function*	*--*	*A stress function that satisfies the governing differential equation at any point in a layered system*
φ	*A function of the cognition and social weights in the PSO*	*--*	*A modifier of the updated velocity in PSO*
λ_i	*The normalized vertical coordinate of an i^{th} point in a layered system*	*--*	*The ratio between the z-coordinate of any point in a layered system and the full depth of the pavement*
ν	*Poisson ratio*	*--*	*Elastic parameter of isotropic materials*
π	*Circumference/radius ratio*	*--*	*3.1141592*
θ_{eq}	*Equivalent temperature*	*°C*	*A single equivalent site temperature in the French Design Method*
η	*Viscosity*	*Pa. s*	*Binder viscosity in the A-VTS model*
$\eta_{original}$	*Original viscosity*	*Pa. s*	*Unaged viscosity*
$\eta_{t=0}$	*Mix/lay-down viscosity*	*Pa. s*	*Short-term aged viscosity*
η_{aged}	*In-service viscosity*	*Pa. s*	*Long-term aged viscosity*
η_{aged_va}	*In-service viscosity adjusted for air voids*	*Pa. s*	*Long-term aged viscosity adjusted for the air void ratio*
$\eta_{t,z}$	*Aged viscosity for a time t and a depth z*	*Pa. s*	*Long-term aged viscosity adjusted for the air void ratio and depth*
ρ	*A coefficient to estimate the rutting rate of unbound materials*	*--*	*Part of the rutting model of unbound layers in the MEPDG*
ρ_i	*The normalized radial coordinate of an i^{th} point in a layered system*	*--*	*The ratio between the r-coordinate of any point in a layered system and the full depth of the pavement*
σ	*The standard deviation of the logarithm of the depth of cracks in the pavement*	*--*	*Part of the non-load transverse cracking model in the MEPDG*
σ_c	*Vertical compressive stress*	*kPa*	*Structural response in a layered media related to rutting in unbounded materials*
σ_i	*Normal stress in the i^{th} direction*	*kPa*	*Any of the normal stresses in an infinitesimal volume. According to the coordinate system, the suffix "i^{th}" may be:* • *X, Y, Z in cartesian coordinates.* • *R, θ, Z in cylindrical coordinates.* • *R, θ, ψ in spherical coordinates.*
σ_m	*The HMA tensile strength*	*psi*	*Part of the non-load transverse cracking model in the MEPDG*
σ_t	*Horizontal tensile stress*	*kPa*	*Structural response in a layered media related to fatigue in cement-treated materials*
σ_t	*The maximum traffic-induced tensile stress at the bottom of the CSM layer*	*psi*	*Part of the load-related fatigue cracking model of CSM in the MEPDG*
$\sigma_{t,ad}$	*Allowable tensile stress at the bottom of tensile-stressed layers*	*kPa*	*The structural response in a layered media related to fatigue in cement-treated materials in the French Design Method*
σ_{tip}	*The computed far-field stress at a depth of the crack tip*	*psi*	*Part of the non-load transverse cracking model in the MEPDG*
σ_0	*The indirect tensile strength of the material*	*kPa*	*Related to fatigue in cement-treated materials in the French Design Method*

Symbol	Concept	SI unit	Definition
τ_{ij}	*Shear stress in the i^{th} direction on a j^{th} plane*	*kPa*	*Any of the shear stresses in an infinitesimal volume. According to the coordinate system, the suffixes "i^{th}" and "j^{th}" may be:* • *X, Y, Z in cartesian coordinates.* • *R, θ, Z in cylindrical coordinates.* • *R, θ, ψ in spherical coordinates.*
ω	*The inertia weight parameter of PSO*	--	*Controls the relationship between exploration and exploitation in the PSO*
ω_{max}	*The maximum inertia weight parameter of PSO*	--	*Avoid local minima in PSO*
ω_{min}	*The minimum inertia weight parameter of PSO*	--	*Improves the convergence speed in PSO*

Subscripts

Subscript	Concept
0	*Reference initial or maximum value*
18	*18 kips*
1r, 2r, 3r	*HMA rutting calibration coefficient*
a, or ad	*Allowable or admissible*
AC	*Asphalt concrete*
b	*Bitumen*
c	*Compressive stress or strain; water content*
eq	*Equivalent*
f	*Failure; factor*
GB	*Granular base*
h	*Horizontal stress or strain; thickness dispersion*
i^{th}	*Number of a particle in a swarm*
HMA	*Hot-Mix Asphalt*
m	*Mix*
n	*Serviceability dispersion*
p	*Incremental plastic deformation*
r	*Radial stress or strain; resilient; reliability*
s	*Search space*
s1	*The unbound material rutting calibration coefficient*
SG	*Subgrade*
soil	*Subgrade*
t	*Tensile stress or stress*
v	*Voids*
w	*Traffic loading*
x or y	*Horizontal stress or strain*
z	*Vertical stress or strain*

Superscripts

Superscripts	Concept
k	*The cycle of optimization in PSO*
n	*Exponent, power*

Abbreviations

Abbreviation	Concept
AASHO	American Association of State Highways Officials (until 1970)
AASHTO	American Association of State Highways and Transportation Officials
ACO	Ant Colony Optimization
AI	The Asphalt Institute
AMADEUS	Advanced Models for Analytical Design of European Pavement Structures
ANN	Artificial Neural Network
CBR	California Bearing Ratio
COV	Coefficient Of Variation
FAA	Federal Aviation Administration
FEM	Finite Element Method
FORM	First-Order Reliability Method
FOSM	First-Order Second Moment Method
FWD	Falling Weight Deflectometer
GA	Genetic Algorithm
GB	Granular Base
HMA	Hot-Mix Asphalt
LCCA	Life Cycle Cost Analysis
LCPC	Laboratoire Central des Ponts et Chausses
LEA	Layered Elastic Analysis
LET	Layered Elastic Theory
LRFD	Load and Resistance Factor Design
MCMV	Markov Chain Monte Carlos Simulation
MCS	Monte Carlo Simulation
M-E	Mechanistic-Empirical
MEPDG	Mechanistic-Empirical Pavement Design Guide
MET	Method of Equivalent Thickness
NAASRA	National Association of Australian State Road Authorities, today AUSTROADS
NCHRP	National Cooperative Highway Research Program
PEM	Point Estimate Method
PSO	Particle Swarm Optimization
PSO-UNLEA	Particle Swarm Optimization based on Universidad Nacional Layered Elastic Analysis
PSO-PAVE	Particle Swarm Optimization Pavement Design
PMS	Pavement Management System
RBD	Reliability-Based Design
RBDO	Reliability-Based Design Optimization
RC	Resultant Cost
RRL	Road Research Laboratory
RSM	Response Surface Model
SA	Simulated Annealing Algorithm
SORM	Second-Order Reliability Method
SPDM	Shell Pavement Design Manual
TC	Total Cost
TRL	Transportation Research Laboratory
UNLEA	Universidad Nacional Layered Elastic Analysis
UNPAVE	Universidad Nacional Pavement Design Software
USACE	United States Army Corps of Engineers
VOC	Vehicle Operating Cost
WASHO	Western Association of State Highway Officials
WESLEA	Waterways Experiment Station Layered Elastic Analysis

1 Introduction

"These trucks helped ruin the highways, and then his roadbuilding firm, with lucrative state contracts, repaired the damage wrought."

About Anthony Stracci. The Godfather, Mario Puzo.

Pavements are ubiquitous elements of highway assets worldwide, and their condition indicates the welfare associated with public infrastructure. Table 1-1 shows the extent of this infrastructure component in several countries.

Table 1-1: Length of road networks in different countries

Country (year)	Length of the road network (km)	Paved length (km)	Unpaved length (km)
USA (2012)	6,586,610	4,304,715 76,334 km of highways	2,281,895
China (2011)	4,106,387	3,453,890 84,946 km of highways	652,497
Brazil (2010)	1,580,964 (rural only)	212,798	1,368,166
Canada (2011)	1,042,300	415,600 17,000 km of highways	626,700
France (2010)	1,028,446 (metropolitan)	1,028,446 11,416 km of highways	5,100 (overseas)
Australia (2011)	823,217	356,343	466,874
Germany (2010)	645,000 (including local roads)	645,000. 12,800 km of highways	
UK (2009)	394,428	394,428 3,519 km of highways	
Argentina (2004)	231,374	69,412 734 km of highways	161,962
Colombia (2014)	204,855 (public roads) Primary network: 11,194 INVIAS & 6,240 ANI Secondary network: 45,137 Departments Tertiary network: 13,959 Departments, 100,748 Municipalities & 27,577 INVIAS	Primary network: 8,457 INVIAS, 6,240 ANI	Primary network: 2,459 INVIAS
Bolivia (2010)	80,448	6,850	73,638
Chile (2010)	77,764	18,119 2,387 km of highways	59,645
Ecuador (2007)	43,670	6,472	37,198
Costa Rica (2010)	39,018	10,133	28,885
Haiti (2009)	4,266	768	3,498

Source: Adapted from Central Intelligence Agency (2013) and Ministerio de Transporte (2014).

There has been substantial progress in pavement engineering through the twentieth century, considering the resources spent on designing, constructing, and maintaining streets, roads, parking lots, airports, ports, and industrial platforms.

The structural design of asphalt pavements for streets and roads evolved from applying empirical rules proposed in the 18th century by McAdam, Telford, and Trésaguet (Babkov & Zamakhayev, 1967). Nowadays, the mechanistic-empirical (ME) methodology applies a scientific approach to the interaction between the subgrade, the construction materials, the weather conditions, and the traffic loadings in pavement design. The *"Mechanistic-Empirical Pavement Design Guide"* –MEPDG– from the United States (NCHRP, 2004) and the *"Conception et dimensionnement des structures de chaussée – Guide technique"* from France (LCPC - SETRA, 1994) represent these analytical procedures. The ME design philosophy and pavement management systems (PMS) are the primary tools in a subject that evolved from an art to a science in the 20th century.

1.1 Problem statement

The development of analytical design procedures increased the complexity of optimizing pavement thickness and technical specifications. The materials properties, the climate effects, and the scattering of traffic estimations add to the uncertainty of pavement behavior and affect the ability to predict pavement condition evolution. Pavement conditions directly impact the agency and user costs, including construction, fuel and tire consumption, and vehicle maintenance expenses.

A significant effort in pavement management seeks to maximize the economic benefits or reduce the present total costs by incorporating the *"Life-Cycle Cost Analysis"* (LCCA) in the design process, both in new structures and in-service pavements. A purely economic approach is attractive to decision-makers. However, it assumes deterministic modeling for a problem that requires more sophisticated methodologies and extensive input information (Mallick & El-Korchi, 2009). Therefore, the application of present total cost minimization models (Walls & Smith, 1998) or the forecast of potential benefits to the users (Watanatada, et al., 1987) have to apply more intricate models that may overcome the available resources in pavement analysis and design.

According to Thom (2008), pavement design and construction must consider environmental aspects such as the consumption of non-renewable resources, space occupation at the expense of other social objectives, atmospheric emissions, and energy consumption for construction activities. Yang et al. (2014) indicate that the requirements to consider in the optimization process are the economy, behavior, sustainability, recyclability, and energetic efficiency. There is an intersection of interests in the previous definitions that explicitly call for research in pavement design optimization.

> *According to the above, this dissertation explores the problem of the structural design of asphalt pavements in streets and roads based on optimizing evolutionary algorithms or bio-inspired techniques aimed to minimize the total project costs, including construction and user costs. The optimizing process focuses on defining feasible solutions and considering design criteria that involve pavement behavior, such as roughness and damage evolution, for a given set of traffic, materials, environmental conditions, and user costs.*

This research contributes to pavement engineering advancement by encouraging the current transition from empirical design practices to the mechanistic-empirical method taking advantage of the analytical design approach.

1.2 Objectives

1.2.1 Main objective

To formulate a methodology for optimizing the structural design of asphalt pavements for streets and roads based on evolutionary algorithms and bio-inspired techniques. The methodology must consider the design's behavior requirements, cost, environmental sustainability, recyclability, and energy efficiency. The objective function considers the net present value of the initial and maintenance costs throughout the analysis period.

1.2.2 Specific objectives

1. Develop and codify an algorithm to analyze elastic layer systems that serve as a calculation engine in applying evolutionary algorithms and bio-inspired techniques to optimize the structural design of asphalt pavements for streets and roads.

2. To adapt different evolutionary algorithms and bio-inspired techniques (hybrid solutions) to optimize the structural design of asphalt pavements for streets and roads.

1.3 Methodology

This dissertation deals with applied technological research on the specific problem of optimizing asphalt pavement design in streets and roads by applying metaheuristics.

The author developed two detailed reviews on asphalt pavement design for streets and roads and applied metaheuristics in pavement engineering to understand the scope of the problem. Those reviews cover an extensive bibliography, from early developments to the latest research in each area, with subsequent conclusions for both topics.

From the review of the structural design of pavements, the author selected the incremental design method to estimate the deterioration and progression of pavement roughness with traffic and environmental conditions by applying the national-calibrated equations of the American MEPDG published between 2004 and 2008 (Chapter 2).

From the review of the metaheuristics applied to pavement engineering, the author selected the particle-swarm optimization (PSO) metaheuristic for two complementary applications: moduli backcalculation and incremental pavement design (Chapter 3). The PSO is a straightforward metaheuristic based on a set of limited parameters, and it does not require decoding and repair procedures as genetic algorithms. With recent developments, PSO evolved as a swarm-intelligence metaheuristic to balance its ability to explore the search space and avoid local minima implementing chaos and runtime adaptations.

The incremental design requires the intensive use of the layered-elastic analysis method (LEA). The author developed the UNLEA algorithm to analyze N-layer systems without restrictions on the number of layers, analysis points, and loads applied to the surface. The software development included a procedure to improve the response obtained at points close to the surface, a recognized drawback in LEA computations (Chapter 4).

The International Roughness Index (IRI) progression represents the pavement condition through the performance period. Each vehicle in the traffic mix has a vector of fuel

consumption, tire consumption, and maintenance costs per kilometer as functions of the IRI. The total cost of pavement is the sum of the construction costs plus the vehicle operating costs, which is the base of the objective functions for design optimization. Methodologically, the combination of the incremental pavement design procedure, the computation of construction and user costs, and the PSO metaheuristic constitute a novel approach for optimizing asphalt pavement design for streets and roads. A series of study cases demonstrate the potential of the methodological approach (Chapter 5).

1.4 Scope

The scope of the research is to propose a methodology. It proposes a procedure and develops its implementation tools. Future research may evaluate the results under controlled conditions in test tracks or in-service roads. The development of this research will be limited to the following specific points:

1. The research does not include experimental activities, only computer programs and case analysis development.
2. The type of pavements under study corresponds to asphalt pavements, with surface layers like chip seals or asphalt concrete between 50 and 350 millimeters, untreated granular bases between 150 mm and 800 mm, and subgrades with CBR values between 3% and 15%.
3. The method of structural analysis is the layered elastic theory.
4. The material properties are the Young modulus and Poisson ratio. The selection of elastic properties for non-linear and viscoelastic materials depends on the load levels and environmental conditions selected for the analysis.
5. The optimization criterion will minimize the initial construction and vehicle operating costs.

The document has six chapters; this Introduction is the first of them. The second chapter reviews asphalt pavement design in streets and roads. The third chapter presents a summary of applied optimization in pavements. The fourth chapter presents the development of the N-layer code UNLEA. The fifth chapter presents the development of the PSO-UNLEA, UNPAVE, and PSO-PAVE programs for asphalt pavement design

optimization based on the particle swarm optimization (PSO) algorithm. The sixth chapter presents conclusions and recommendations for future research.

2 An overview of asphalt pavement design in streets and roads

Parks are but pavement disguised with a growth of grass.
George Gissing.

An abridged version of this chapter was published as a review in "Revista de la Facultad de Ingeniería de la Universidad de Antioquia" No. 98 (Vásquez-Varela & García-Orozco, 2020).

Schwartz & Carvalho (2007) stated that pavement structural design is a daunting task even though the design outcome is as simple as drawing a cross-section with thicknesses and some notes regarding construction specifications. Traffic characterization and forecasting, pavement materials and subgrade assessments, environmental effects, and life-cycle economic analysis cause difficulties in all pavement projects regardless of their longitude, intended purpose (road, port, or airport), and strategic value (local, collector, or highway).

Monismith (2004) considers that the structural design of durable asphalt pavements has two fundamental premises:

1. One can design long-term asphalt pavements by taking advantage of the developments achieved for more than 50 years in the mechanistic-empirical design methodology, and
2. Although it is possible to design long-term asphalt pavements, good behavior will always require adequate construction.

This chapter presents an overview of asphalt pavement design for streets and roads, divided into four sections. The first section introduces the geotechnical framework for asphalt pavement design. The second section presents the design principles of asphalt

pavements in streets and roads. The third section summarizes the evolution of the structural design of asphalt pavements from the empirical approaches to the current mechanistic-empirical methodologies. The fourth section encompasses the author's views about the subject.

2.1 The geotechnical framework of asphalt pavements

Pavements are geotechnical problems. Engineers built pavements on cuts, embankments, tunnels, or at the bottom of human-made ponds.

Pavement materials include natural and artificial constituents such as soil, rock, lime, Portland cement and bitumen, polymers and geo-synthetics, and various chemical products to enhance their natural characteristics. Pavement failure usually does not compromise life or property, but pavements require a systemic approach to include the analysis, design, construction, and monitoring activities. Pavement or modern asset management systems also include economic aspects (Wu, Flintsch, Ferreira, & de Picado-Santos, 2012).

Regarding pavements as a geotechnical problem, Figure 2-1 shows five constitutive elements required for the engineering solution of pavements based on a general framework devised by Alarcón-Guzmán for any geotechnical problem (2004). This dissertation focuses on the *"Design"* of asphalt pavements for streets and roads, the evolution of the design methods, and the current trends.

2.2 Design principles of asphalt pavements in streets and roads

Pavement design is complicated because there is no unique solution to each problem. There are many materials and construction methods. Likewise, the performance of several alternatives may differ, even if both solutions are acceptable for a specific situation. All pavements require maintenance; thus, their short-term and long-term characteristics are significant for proper analysis.

Yang (1972) proposed that pavement design must consider users' expectations since the dynamic interaction between the vehicle and the pavement substantially affects their evaluation. Functional pavement design must focus on the users' satisfaction considering

five primordial aspects: speed, smoothness, safety, maintenance, and cost. Therefore, Yang presents a systematic approach to pavement design considering the *"optimization of the pavement"* when all the components (subgrade, structure, wearing course) have the same structural reliability, including their general response to environmental conditions.

Figure 2-1: The geotechnical framework of pavements

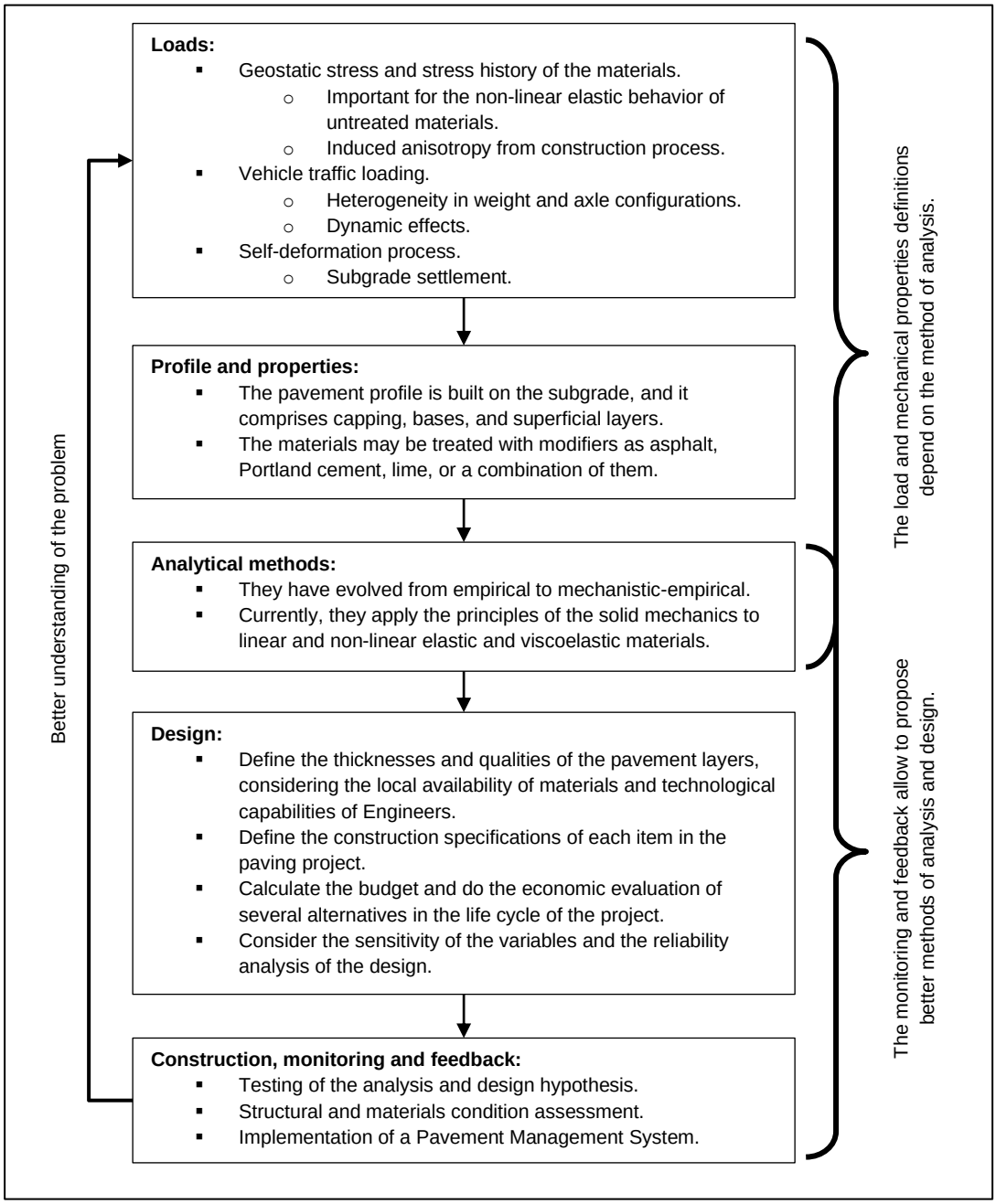

The design problem has a cost associated with reliability, which is extensible to the project life cycle of construction, maintenance, operation, and contingency costs. If all the elements have the same reliability, obtaining a balanced pavement design is possible. Furthermore, achieving a functional pavement design is impossible without analyzing the cost-benefit ratio.

Yoder and Witczak (1975) stated that pavement design consists of two broad categories: (a) design of the pavement mixtures and (b) structural design of the pavement components, which is different from the structural design of bridges and buildings since environmental factors greatly influence the pavement structure. Improper structural design is one of many factors that may cause pavement distress, including insufficient quality control in construction or lack of maintenance. Serviceability and the intended use of the pavement are the main topics in designing a pavement structure. Design is a tradeoff process based on the cost analysis according to the performance models and the available materials.

Ullidtz (1987) postulated that a pavement design system has two main tasks: (a) define the structure to avoid an unacceptable level of distress, and (b) estimate the structural (bearing capacity) and functional (ride quality) distresses in time. The structural behavior prediction must consider the combined effects of traffic, environmental conditions, material degradation, and construction practices.

Croney & Croney (1998) stated that pavement design requires understanding the processes influencing pavement behavior under traffic and time. The necessary information for pavement design includes the climatic environment, the soil conditions, and the traffic to be served.

Thom (2008) proposed that the engineering principles in pavement design should consider the following:

1. Protect the subgrade from the action of the traffic loads. Subgrade protection is the first principle of modern pavement engineering.
2. Minimize the permanent deformation in all the pavement layers by keeping stress levels compatible with the materials.
3. Minimize the failure probability of the materials.

4. Minimize the adverse effects of environmental conditions, for example, with the proper drainage of the structure.
5. Provide an acceptable surface regarding smoothness, skid resistance, and noise generation.
6. Preserve the pavement without unnecessary expenses or extended closures of the roads.

Any engineering alternative must provide a satisfactory solution under various design requirements. Pavement design substantially differs from other design problems in civil engineering because the wear and tear are progressive throughout the service life, depending on the materials, traffic, and climate conditions.

2.3 Evolution of the asphalt pavement design methods for streets and roads

Throughout the twentieth century, the structural design of pavements evolved from *"art to science."* However, empiricism will always be necessary for the design process because it is indispensable to calibrate actual pavement behavior with the analytical model responses.

The first modern asphalt pavements appeared at the end of the nineteenth century, built by combining techniques developed a century before by McAdam, Telford, and Trésaguet (Babkov & Zamakhayev, 1967) with innovative materials in the upper layers to water-proof the structure and control the dust production (Huang, 2004).

One can classify the asphalt pavement design methods into two main groups: empirical and mechanistic-empirical (ME), also called analytical or rational methods.

2.3.1 Empirical methods

The empirical methods include those based on the subgrade engineering classification (Bureau of Public Roads), the relative shear resistance of the soil (CBR), and road experiments such as the WASHO Road Test (1952 – 1955) and the AASHO Road Test (1958 – 1962). The design method considers the observed behavior of in-service pavements under traffic, environmental, and construction conditions like those in observed sections (Mallick & El-Korchi, 2009). For a short period, and in parallel with the

developments of Soil Mechanics and Foundation Engineering, pavement design used the bearing capacity theory to design pavements (Huang, 2004). This approach wrongly assumes that *"pavements are a type of foundation,"* but there are differences between the behavior and the deterioration of both structures. However, it is interesting to note that the Mohr-Coulomb failure model, applied in the analysis of the bearing capacity of foundations, has also been used to characterize asphalt mixtures to evaluate their resistance (Monismith, 2004).

2.3.1.1 The method based on the CBR test

The method based on the California Bearing Ratio test (ASTM D1833) emerges from the work in soil mechanics by Omer James Porter in the California State Highway Division in the 1920s (Porter, 1942). The CBR is the relative undrained shear strength compared with high-quality material. Figure 2-2 shows the original curves for pavement design in California for two traffic levels. The United States Army Corps of Engineers (USACE) developed a correlation between CBR, pavement thickness, and the magnitude of the wheel load based on calibration studies on roads and aerodromes during World War II (Gonzales, Barker, & Bianchini, 2012):

$$T = \sqrt{P\left(\frac{1}{8.1 \cdot CBR} - \frac{1}{q \cdot \pi}\right)}$$

Eq. 2-1

Where T is the total thickness of the pavement in inches (1 inch = 25.4 mm), P is the applied wheel load in pounds (1 lb = 4.4482 Newton), CBR is the California Bearing Ratio in percent, and q is the tire pressure in psi (1 psi = 6.8948 kPa). Figure 2-3 shows the evaluation of Eq. 2-1 for three levels of wheel load and tire pressure of 224 psi (1,682 kPa), representing the landing gear of a World War II bombardier.

Figure 2-2: Curves for pavement design in California Highways Department (1942)

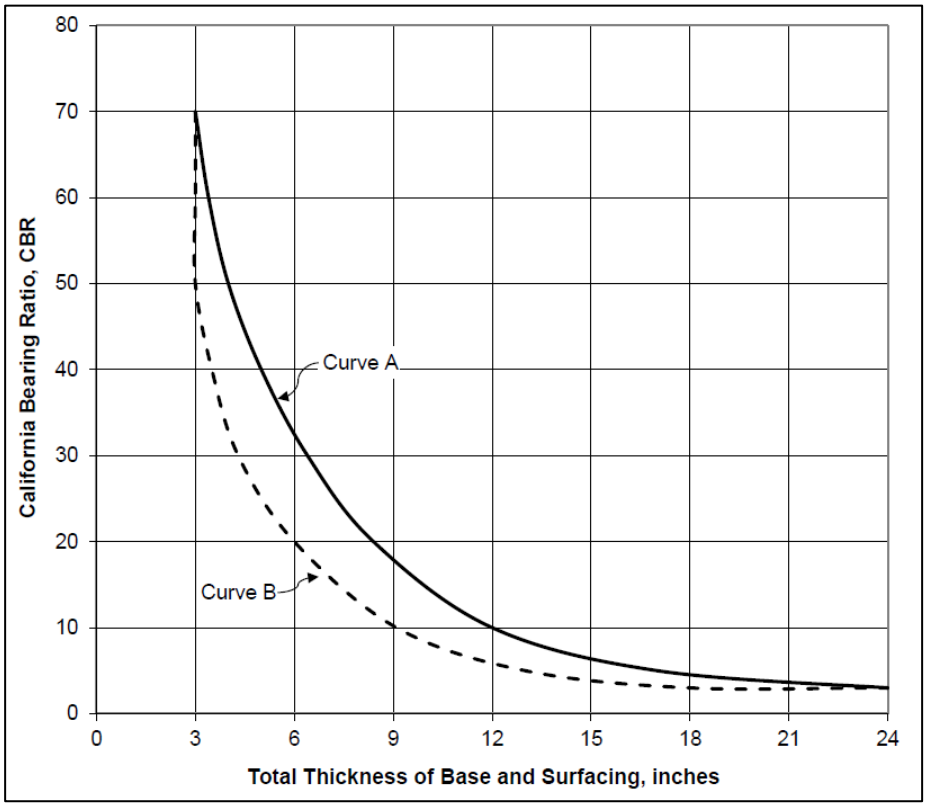

Source: Porter (1949) in Gonzalez (2015).

According to the CBR method, pavement failure is the permanent deformation due to excessive shear stress in the soil. Therefore, the design principle protects the subgrade with a minimum thickness of better material but disregards other distresses (Brown S. F., 1967).

After the AASHO Road Test results were published, Road Agencies modified the CBR method to characterize the vehicular traffic as repetitions of an 18-kip standard single axle. Jameson (1996) summarized the Australian experience of adopting the equivalent axle load of 18 kips by the British Road Research Laboratory. The procedure involves several assumptions to transform the single wheel load to the AASHO standard axle load repetitions. The former Ministerio de Obras Públicas in Colombia adopted the same procedure in the pavement design methods of 1970 and 1975.

Figure 2-3: Extrapolation of CBR curves for three levels of wheel loads (1949)

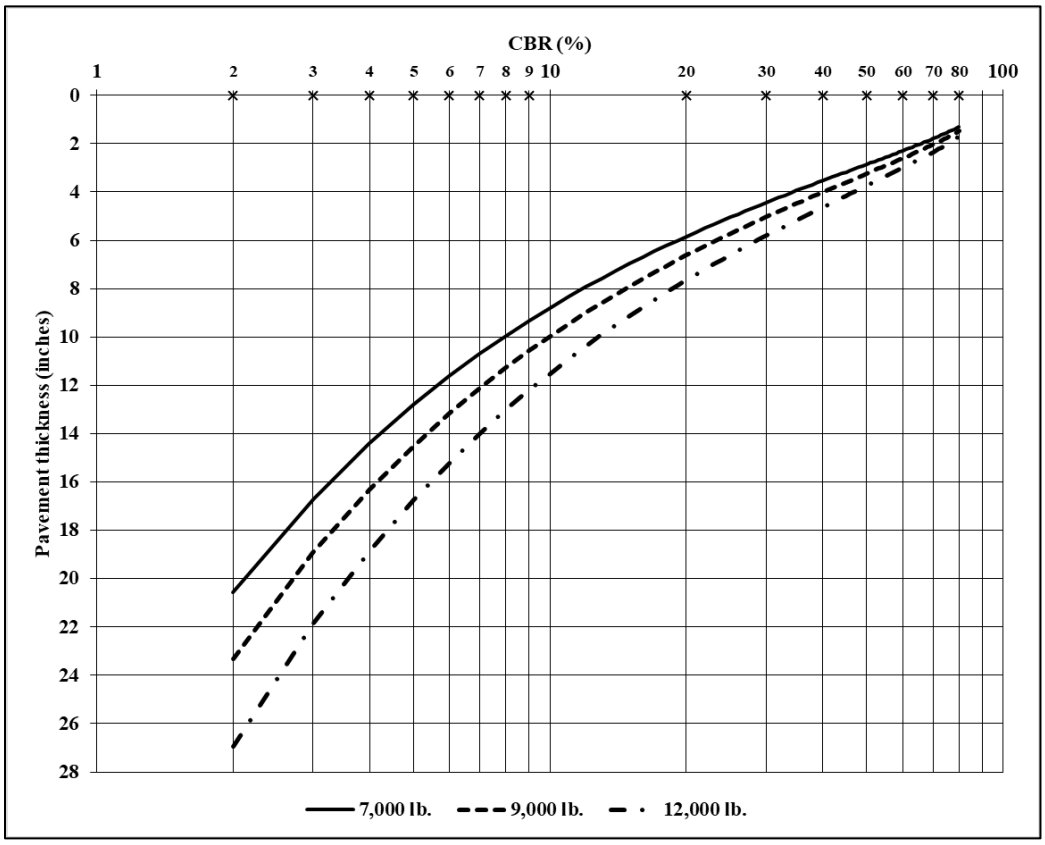

Source: Drawn from Jameson (1996).

Figure 2-4 shows the 1979 NAASRA pavement design method for traffic intensities up to 50 million repetitions of the AASHTO standard axle of 80 kilonewtons and CBR values between 2 and 30 percent. Austroads (1992) updated this chart to design pavements with thin asphalt surfacing.

For over 50 years, the CBR-based method was the preferred procedure for designing asphalt pavements in airports and roads (Gonzales, Barker, & Bianchini, 2012). The original CBR method persisted for asphalt pavement design in airports until the twentieth century (Federal Aviation Administration, 1995). One must note that the CBR method is still under analysis, for example, with the *"beta-CBR"* procedure to design pavements controlling the shear deformations in the subgrade soil (Gonzalez, 2015). Recently, Mendoza & Caicedo presented an elastoplastic framework for CBR and Young modulus (2018).

Figure 2-4: NAASRA design curves for pavements whit thin asphalt surfacing

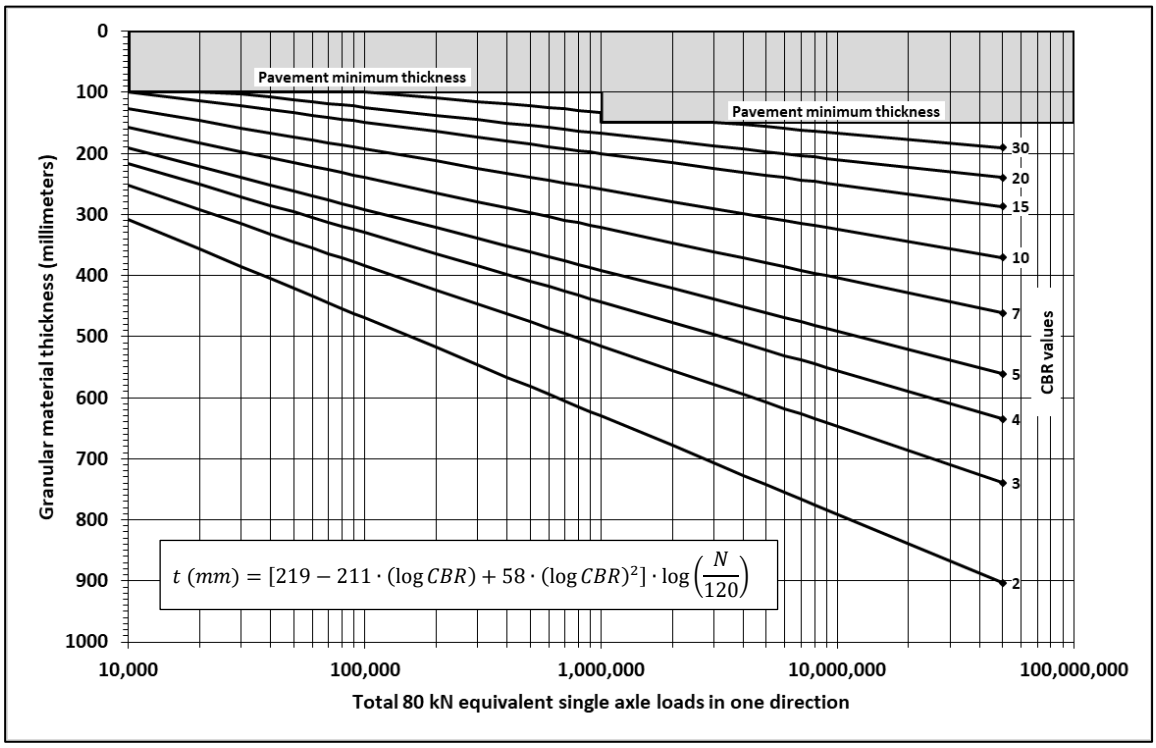

Source: Drawn with the 1979 NAASRA CBR equation (Jameson, 1996).

2.3.1.2 American Association of State Highways and Transportation Officials (AASHTO) method

The AASHTO method is based on the statistical analysis of pavement behavior data obtained between 1958 and 1960 in the AASHO Road Test, a full-scale facility built in Ottawa, IL. (U.S.A.). Although the method has a robust empirical component, its successive versions incorporated mechanistic analysis to interpret and extrapolate the Road Test results on asphalt pavements. In the latest version, the design method incorporated mechanistic concepts into a *"semi-empirical"* approach that considers two primary design criteria: serviceability and reliability (AASHTO, 1993).

Serviceability, represented by the Present Serviceability Index (PSI), was developed in the 1950s. It is based on the subjective evaluation of pavement sections with the Present Serviceability Rating and its statistical correlation with measurable characteristics like roughness and distress (cracking, deformation, patching). Theoretically, PSI varies between zero (a failed pavement) and five (a good pavement); however, the Road Test data indicates that asphalt pavements may range from 4.2 to 1.5 or less. The relationship

between the PSI and several measurable characteristics of asphalt pavements was (Croney & Croney, 1998):

$$PSI = 5.03 - 1.91 \times \log_{10}(SV + 1) - 1.38 \times \overline{RD}^2 - 0.01 \times \sqrt[2]{C + P}$$

Eq. 2-2

Where RD is the average rut depth in inches (1 inch = 25.4 mm) on both wheel tracks, and SV is the slope variance of the average slope of both wheel tracks (x10^6) measured with the CHLOE profilograph (see Figure 2-5). C is the cracked area with alligator pattern in square feet over 1000 ft², and P is the patched area in square feet over 1000 ft² (1 ft² = 0.0929 m²).

Figure 2-5: CHLOE profilograph for roughness measurement in the longitudinal profile

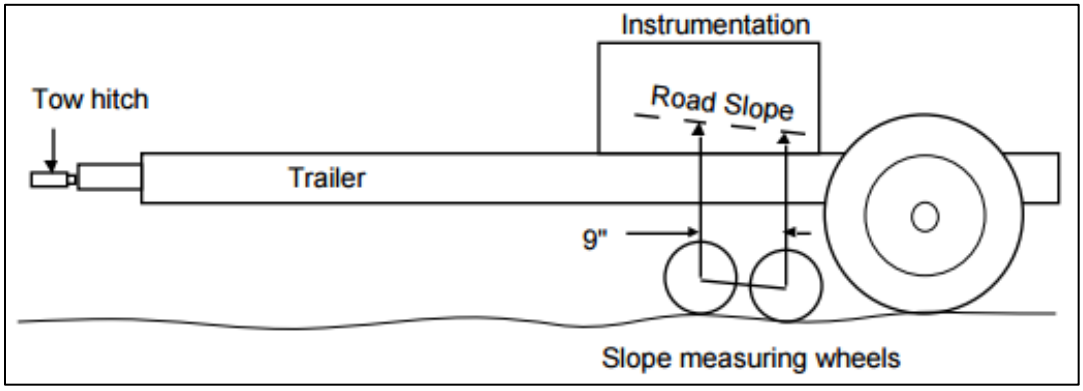

Source: Gillespie (1992).

Several authors correlate PSI with roughness. The roughness is the computed effect of the road profile over a standard vehicle, i.e., the International Roughness Index (IRI) (Papagiannakis & Masad, 2008).

Figure 2-6 shows three equations between PSI and IRI that substitute Eq. 2-2. Experience in Vietnam (Nguyen, 2017) indicates possible functional correlations on a project or national scale.

Figure 2-6: PSI versus IRI empirical relationships

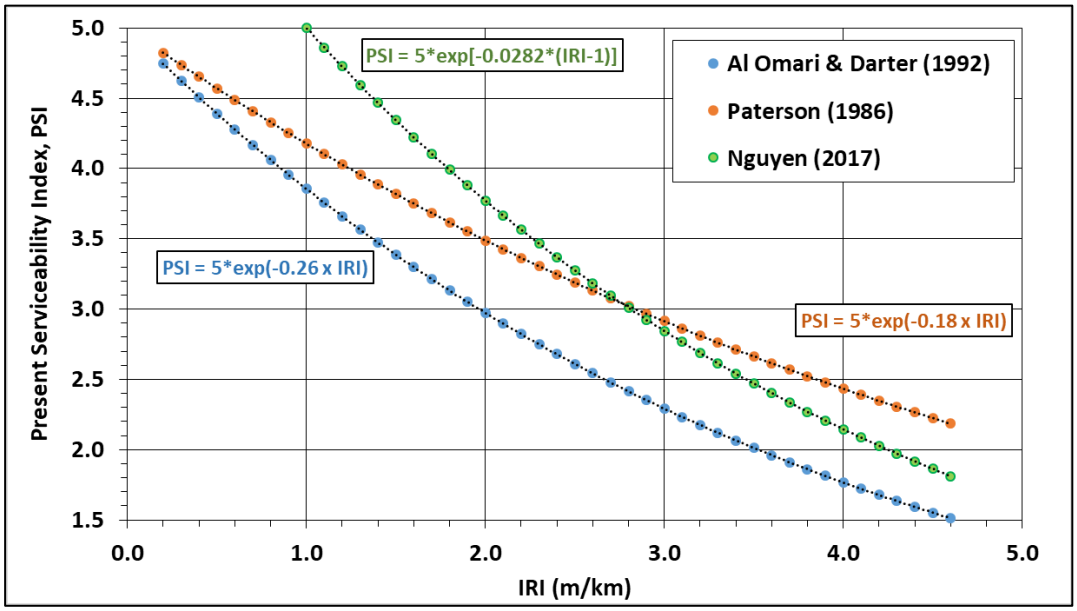

Source: Drawn from Al-Omary & Darter (1994) and Nguyen (2017).

The reliability in the AASHTO method considers two sources of uncertainty in pavement design: (a) future traffic on the structure and (b) the pavement serviceability in any future moment after supporting the traffic loading. Both uncertainties are standard deviations of the logarithm of the accumulated standard 18-kip (80 kilonewtons) single-axle loads. Thus, the overall standard deviation for the pavement design (S_o) is:

$$S_o = \sqrt[2]{S_w^2 + S_n^2}$$

Eq. 2-3

Where S_w is the standard deviation of the traffic estimation and S_n is the standard deviation of the pavement condition assessment.

The structural design of asphalt pavements with the AASHTO 1993 procedure uses the following algorithm of pavement behavior (AASHTO, 1993):

$$\log_{10}(W_{18}) = Z_r \cdot S_o + 9.36 \times \log_{10}(SN+1) - 0.20 + \frac{\log_{10}\left(\frac{\Delta PSI}{4.2-1.5}\right)}{0.40 + \frac{1094}{(SN+1)^{5.19}}} + 2.32 \cdot \log_{10}(M_r) - 8.07$$

Eq. 2-4

Where W_{18} is the expected number of repetitions of the standard single axle load of 18-kips on the design lane for the design period of analysis (ESAL); Z_r is the accumulated value of the standardized normal distribution for a given reliability level; S_o is as previously defined in Eq. 2-3; SN is the *"structural number"*, an abstract representation of the pavement equal to the summation of the products of the layer thickness (D_i, in inches) times a non-dimensional coefficient that represents the layer quality (a_i), [$SN = \sum D_i \times a_i$]; ΔPSI is the estimated loss of serviceability in the service period; and M_r is the resilient modulus in psi of the pavement materials or subgrade (1 psi = 6.8948 kPa). Eq. 2-4 must be satisfied with the design of each layer and the whole structure. Figure 2-7 shows a design chart for flexible asphalt pavements with 50% reliability.

Figure 2-7: Flexible pavement design chart based on the 1993 AASHTO method

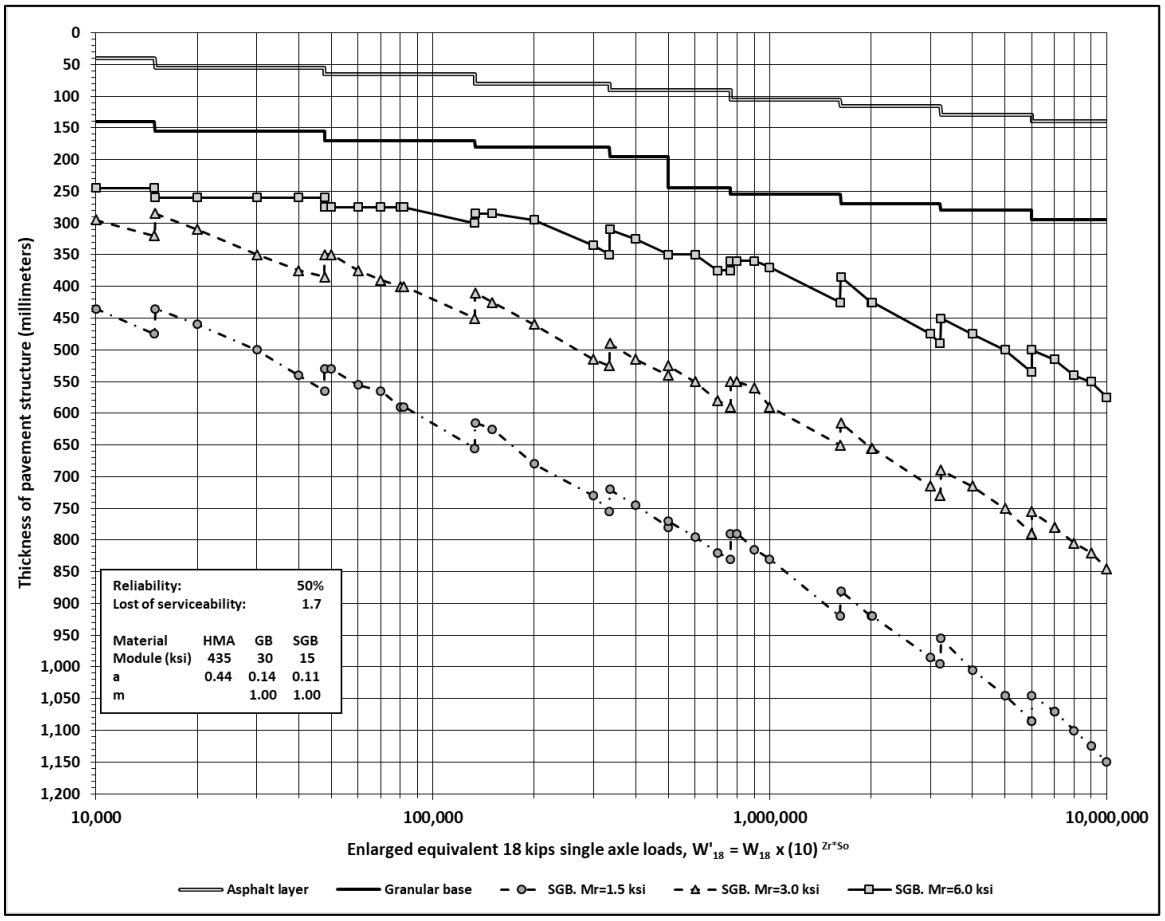

To use the previous chart, one must multiply the estimated traffic for the safety factor [$FS = 10^{(Z_r \times S_o)}$]. The chart includes three values of resilient moduli of the subgrade: 1500

psi, 3000 psi, and 6000 psi. The properties of the pavement materials are summarized in the same chart. The thicknesses are in millimeters allowing comparison with Figure 2-4.

The increase in layer thickness is similar to the Australian method based on the CBR test. Some discontinuities in the granular subbase thickness curves are associated with the minimum requirements for the asphalt and granular base layers.

Engineers still use the AASHTO method to design new or rehabilitated pavements in many countries. However, the design practice is based only on the CBR test. Practitioners apply the AASHTO method with several uncertain presumptions and correlations for local or regional conditions. Therefore, it is not appropriate to disqualify the AASHTO method based on an improper application since the same situation will affect the more advanced analytical methods.

2.3.2 Mechanistic-empirical methods

2.3.2.1 Analysis method

The mechanistic-empirical method became convenient with the introduction of the layered elastic theory by Burmister (1943). The theory became an accurate analysis method for pavements at the 1962 *"First International Conference on the Structural Design of Asphalt Pavements"* (Monismith, 2004). The initial application of layered elastic theory considered systems with two or three layers simplified in tables and charts [Yoder & Witczak (1975), Poulos & Davis (1974)]. These solutions are still valuable for teaching purposes as they graphically illustrate multiple pavement responses under traffic loads. The two and three-layer graphical solutions focused on measurable structural responses calibrated with in-service behavior as the vertical deflection or stress.

For example, Figure 2-8 shows a chart to obtain the vertical displacement at the surface of a two-layer system (w_0) due to a uniformly loaded circular area of radius (a) with an applied pressure (q). The solution depends on the modular relationship of the layers (E_1/E_2) and the normalized pavement thickness (h_1/a).

Figure 2-8: Vertical displacement of the surface of a two-layer pavement

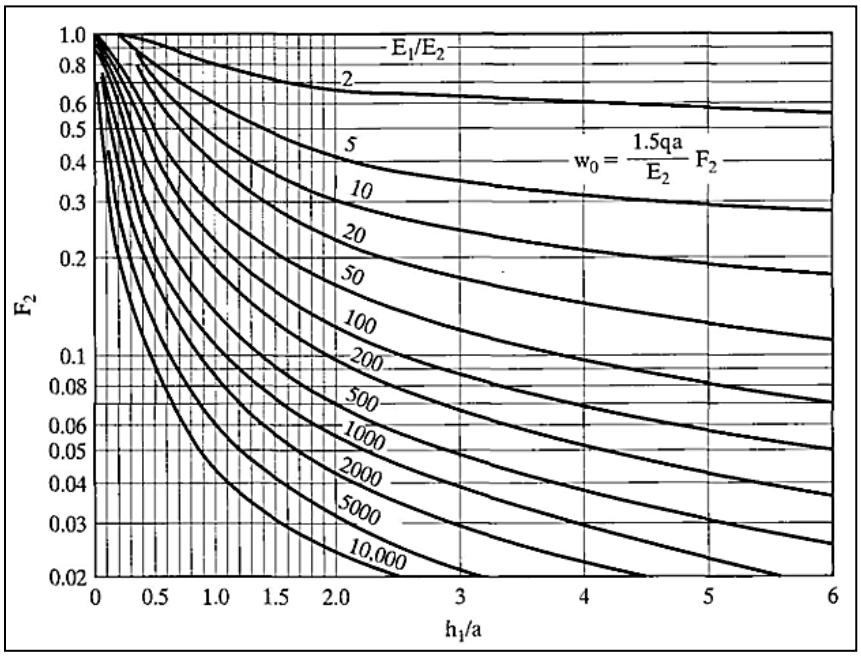

Source: Yoder & Witczak (1975).

The vertical deflection is compared with field values measured with the Benkelman beam or the Falling Weight Deflectometer (FWD) (Monismith, 2004). Figure 2-9 shows both deflections measuring devices.

Figure 2-9: Vertical deflections measuring systems: (a) Benkelman beam, (b) FWD

(a) Benkelman Beam

(b) Falling Weight Deflectometer – FWD

The deflection analysis is part of the pavement evaluation procedures. The empirical information about deflection and behavior defines deflection thresholds as a function of traffic like the Asphalt Institute equation (Asphalt Institute, 2000):

$$D_a = \frac{25.64}{N^{0.2383}}$$

Eq. 2-5

Where D_a is the maximum allowable superficial deflection in millimeters for an asphalt pavement that will support N repetitions of the single axle load of 80 kN. One must note that more significant traffic requires a less deformable structure, i.e., with a larger capacity to absorb the deformation energy induced by the traffic loadings.

Figure 2-10 shows a chart to obtain the vertical stress (σ_c) in the interface of a two-layer pavement under the axis of a uniformly loaded circular area of radius (a) with an applied pressure (q). The solution depends on the modular relationship of the layers (E_1/E_2) and the ratio of the loaded area radius and pavement thickness (a/h_1).

Figure 2-10: Vertical stress in the interface of a two-layer pavement

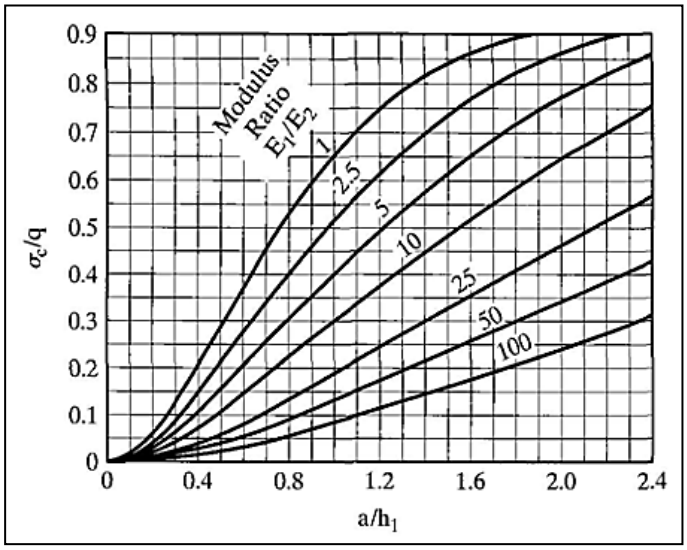

Source: Huang (2004).

The vertical stress correlates with pressures measured by load cells in test tracks. The reduction of the stress intensity on the subgrade depends on the rigidity of the pavement system (E_1), and the thickness of the structure (h_1). This model may explain the mechanical background of the empirical method based on the CBR test.

Figure 2-11 shows a chart to obtain the horizontal tensile strain (ε_t or e) in the bottom of the upper layer under the axis of a uniformly loaded circular area of radius (a) with an applied pressure (q). The solution depends on the modular relationship of the layers (E_1/E_2) and the normalized pavement thickness (h_1/a).

Figure 2-11: Chart of the horizontal strain in the interface of a two-layer pavement

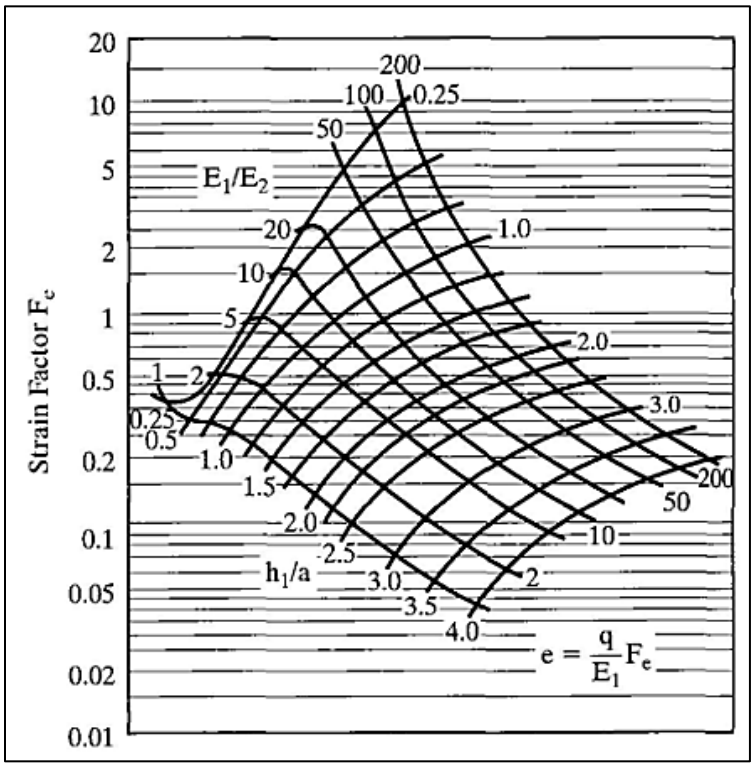

Source: Huang (2004).

There is no specific definition of the constitutive material in these solutions for the two-layer system. For example, in pavements with a thin asphalt wearing course, the modulus of the first layer, E_1, represents the untreated granular materials on the subgrade with a modulus equal to E_2. Otherwise, in full-depth asphalt pavements, modulus E_1 represents the asphalt concrete, and modulus E_2 represents the weighted rigidity of the untreated bases and the subgrade.

The analysis method (LEA or FEM) is not the pavement design procedure. The challenge with the layered elastic theory is to characterize and calibrate the materials' actual behavior. Such behavior includes the non-linearity of soils and untreated granular bases, the

viscoelasticity and thermal susceptibility of asphalt materials, and the permanent deformation under repeated loading.

2.3.2.2 Pavement performance in M-E design

Layered theory application in pavement design was accomplished in the 1962 *"First International Conference on Design of Asphalt Pavements,"* with substantial contributions to analyzing the deterioration of asphalt pavements (Monismith, 2004). The proceedings of the conference included the principles of the structural design of asphalt pavements considering two distresses (Croney & Croney, 1998):

Permanent deformation

The permanent or irrecoverable deformation appears in the pavement surface as ruts or depressions in the wheel path, as shown in Figure 2-12. This damage is known as *"rutting"* (Shahin, 2006), and it is due to the following:

1. The plastic deformation of the unbounded materials due to the change in volumetric phases by secondary compaction under traffic or general shear failure in very thin pavements.
2. The plastic deformation of asphalt mixes with excessive amounts of bituminous binder or mixes subjected to high temperatures.

Rutting is a compound failure mode; however, the usual empirical model relates the unrecoverable surface deformation with the elastic response of the subgrade as follows:

$$N_d = \frac{k_4}{\varepsilon_z^{k_5}}$$

Eq. 2-6

Where N_d is the allowable number of load repetitions until the development of ruts of a certain depth, and ε_z is the vertical compressive strain at the top of the subgrade due to the traffic loading. The values k_4 and k_5 are obtained with a regression analysis from the observation of in-service pavements. There is substantial dispersion in the published models due to the differences in the rut depth threshold and the lack of knowledge about each layer's contribution to the total plastic deformation.

Figure 2-12: Rutting in asphalt pavements

(a) Due to traffic and climate in the Buga – Tuluá highway (Valle del Cauca, Colombia)

(b) Due to a high content of bitumen in the asphalt mix in the Supía – Riosucio road (Caldas, Colombia)

Source: Courtesy of Luis Carlos Vásquez Torres.

Figure 2-13 evidences the complexity of plastic deformation in asphalt pavements as observed by the British Transport Research Laboratory in the Alconbury Hill road test.

Figure 2-13: Development of permanent deformation in the Alconbury Hill road test

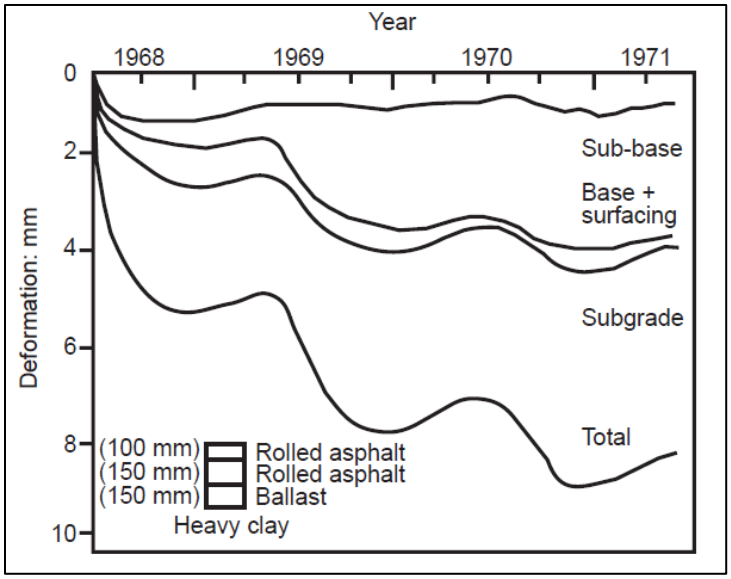

Source: Brown (1993).

Half of the plastic deformation accumulated between 1968 and 1971 is due to the pavement structure layers and not exclusively to the subgrade (Brown S. F., 1993). It is accepted that the rutting estimation in all the pavement layers must be part of any rigorous mechanistic-

empirical design methodology. For example, since 1978, the Shell design method has assessed the asphalt mix's permanent deformation (Shell Oil, 1978). The incremental plastic deformation analysis is part of the new MEPDG (NCHRP, 2004).

Fatigue cracking

Fatigue cracking (Figure 2-14) is a series of interconnecting cracks caused by fatigue failure of asphalt concrete under repeated traffic loading (Shahin, 2006).

Figure 2-14: Cracking due to fatigue in asphalt pavements

The properties of asphalt materials change throughout the pavement service life with the aging of the bitumen caused by environmental conditions. Materials treated with hydraulic binders (Portland cement, lime, fly ash, and slag) present changes in their mechanical properties throughout the service life.

The traditional fatigue model considers that cracking starts at the bottom of the bituminous layers due to tensile stresses under traffic loading, i.e., *"bottom-up cracking."* Rolt et al. (Transport Research Laboratory, 2002) indicate that fatigue cracking tends to develop from top to bottom, or *"top-down,"* and the opposite is less frequent on in-service pavements. The MEPDG considers both cases of fatigue cracking (NCHRP, 2004).

The horizontal tensile strain correlates with the fatigue behavior of the asphalt layers. This structural response depends primarily on the layer thickness and the rigidities of the asphalt

and base layers. The following relationship characterizes the fatigue behavior of asphalt materials:

$$N_f = C_f \cdot \frac{k_1}{\varepsilon_t^{k_2} \cdot E^{k_3}}$$

Eq. 2-7

Where N_f is the number of load repetitions to fatigue failure of the asphalt material subjected to a repetitive horizontal strain (ε_t) at a temperature and load conditions that mobilize a specific modulus (E). The values k_1, k_2 & k_3, are obtained by regression from laboratory fatigue tests and the C_f coefficient, known as the shift factor, calibrates the laboratory-controlled conditions with the actual behavior of in-service pavements.

The allowable number of load repetitions to failure reduces with the increase in the tensile strain, i.e., with the load intensity and the stiffness. Eq. 2-7 is a general fatigue law for asphalt materials whose behavior is controlled by the tensile strain (ε_t). Similar relationships exist for materials treated with hydraulic binders as a function of tensile stress (σ_t).

2.3.2.3 Mechanistic-empirical design general procedure

Figure 2-15 shows a flowchart for a mechanistic-empirical pavement design procedure with multiple seasons (climatic sub-periods) and load groups. The conventional M-E design may consider one season with weighted or critical climatic values and standard axle load repetitions. The incremental design method requires considering multiple climatic seasons and load groups by type (single, tandem, triple, and quad) and magnitude (load spectra). The following paragraphs present some general aspects of three mechanistic-empirical methodologies (Shell, Asphalt Institute, and the French Design Method) and the new MEPDG.

Figure 2-15: Flowchart of a mechanistic-empirical pavement design procedure

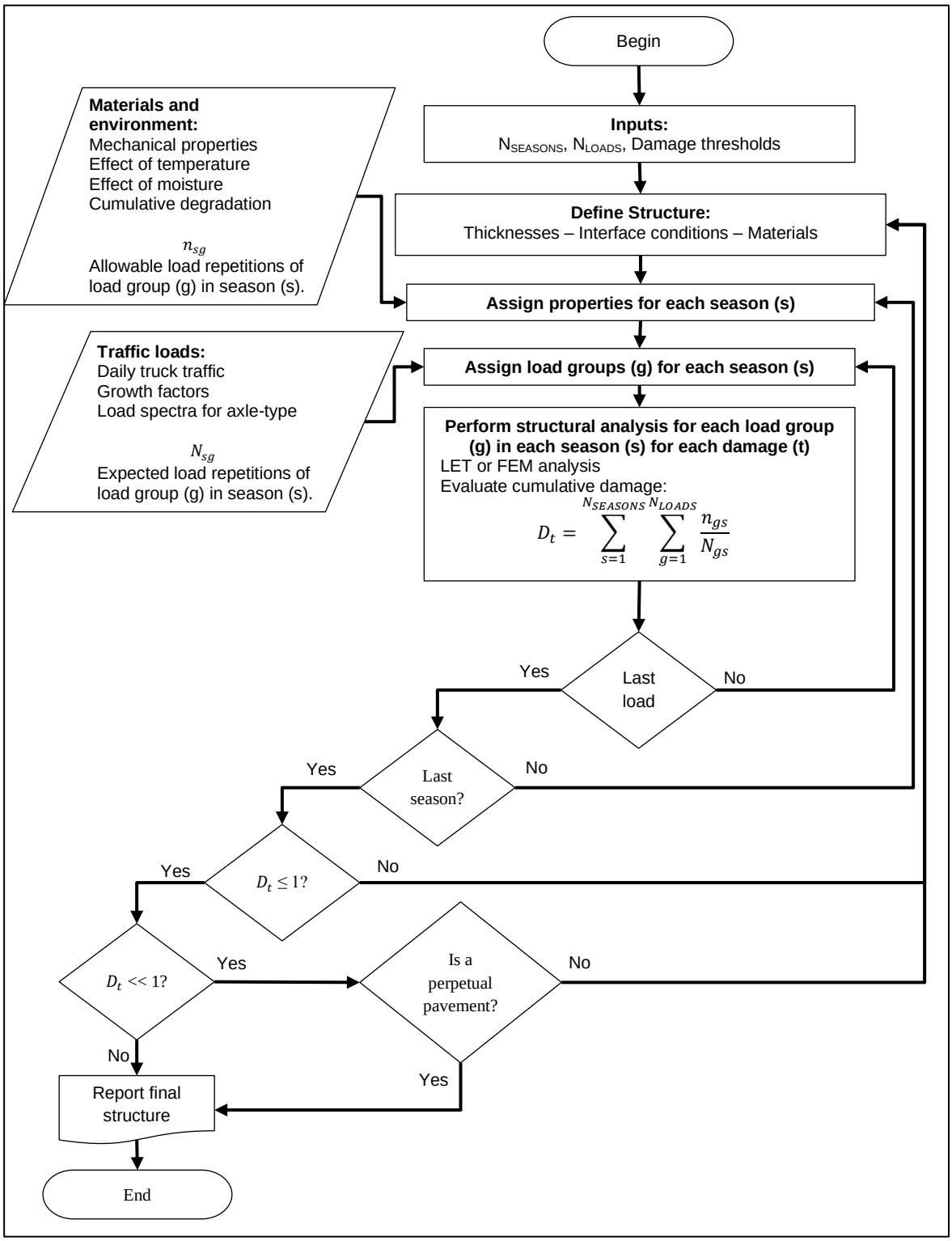

Other countries as Australia and New Zealand (Austroads, 1992), South Africa (The South African National Roads Agency, 2014), Mexico (Garnica Anguas & Hernández Domínguez, 2013), and Costa Rica (Trejos Castillo, Leiva Padilla, & Loría Salazar, 2014) have M-E procedures.

Shell Oil method

The first edition of the Shell method dates from 1963. The *"Shell Pavement Design Manual (SPDM)"* of 1978 and the 1985 addendum replaced it. The method is based on the layered elastic theory and presents the design alternatives in charts and tables. The last version of the Shell method, SPDM 3.0, is a software suite published in 1993 without any known updates to date (Strickland, 2000).

The SPDM versions between 1978 and 1985 consider a three-layer structure composed of asphalt materials, untreated granular bases, and subgrade soil. The mechanical properties of each material are the modulus (E) and Poisson ratio (ν). Repetitions of a 40 kN semi-axle load with dual wheels of 105 mm radius, center-to-center separation of 315 mm, and contact pressure of 577 kPa represent the traffic.

Failure criteria in the Shell method are fatigue cracking and permanent deformation of the asphalt layers and the subgrade.

The expected life is the allowable repetitions of the standard axle load, and the design aims to have the materials working with strains smaller than the acceptable values (Whiteoak, 1991). The following equations summarize the design criteria of the Shell Oil method (Huang Y. H., 2004):

- Fatigue of bituminous mixtures based on constant stress tests:

$$\varepsilon_t = \frac{[36.43 \cdot PI - 1.82 \cdot PI \cdot V_b + 9.71 \cdot V_b - 24.04]}{10^6} \cdot \left(\frac{S_m}{5 \times 10^9}\right)^{-0.28} \cdot \left(\frac{N_f}{10^6}\right)^{-0.20}$$

Eq. 2-8

- Fatigue of bituminous mixtures based on constant strain tests:

$$\varepsilon_t = \frac{[36.43 \cdot PI - 1.82 \cdot PI \cdot V_b + 9.71 \cdot V_b - 24.04]}{10^6} \cdot \left(\frac{S_m}{5 \times 10^{10}}\right)^{-0.36} \cdot \left(\frac{N_f}{10^6}\right)^{-0.20}$$

Eq. 2-9

In both equations, ε_t is the tensile strain, PI is the bitumen penetration index, V_b is the percentage of bitumen volume in the mix, S_m is the stiffness modulus of the mix in N/m², and N_f is the number of repetitions to failure. The penetration index of the bitumen (PI) is:

$$PI = \frac{20 - 500 \cdot A}{1 + 50 \cdot A}$$

Eq. 2-10

Where A is the temperature susceptibility of the bitumen or the slope of the line plot between the logarithm of penetration (pen = 0.1 mm) and temperature (°C):

$$A = \frac{\log(pen\ at\ T_1) - \log(pen\ at\ T_2)}{T_1 - T_2}$$

Eq. 2-11

- Rutting associated with the subgrade response (Ali & Shiraz, 1998):

$$N_d = 6.15 \times 10^{-7} \cdot (\varepsilon_c)^{-4.00}$$

Eq. 2-12

Where N_d is the number of load repetitions to failure (rutting equal to 13 mm), corresponding to 50% reliability, and ε_c is the vertical compressive strain at the top of the subgrade.

Figure 2-16 shows the HN 45 design chart of the 1978 Shell manual to obtain multiple flexible pavement designs over a subgrade with a modulus of 50 MPa (a relatively soft soil) and a weighted mean annual air temperature of 12°C. The asphalt mix code is S1–F1–100, i.e., it has stiffness and fatigue corresponding to a dense-graded mix, while the number *"100"* means that the bitumen is an 80-120 pen grade bitumen according to ASTM D946.

Figure 2-16: Design chart HN 45 from the Shell pavement design method of 1978

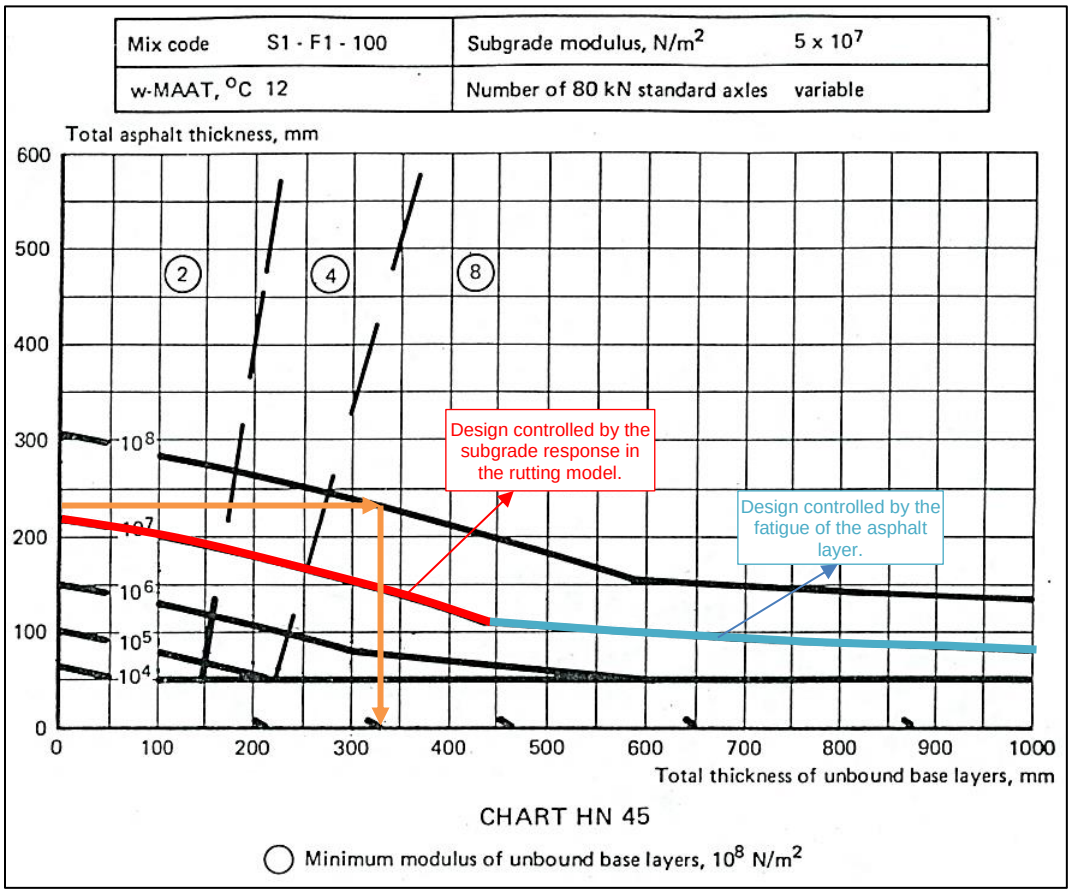

Source: Modified from Shell Oil (1978).

The horizontal axis represents the total thickness of unbound base layers, and the vertical axis represents the total thickness of the asphalt layers. The chart includes five curves with traffic levels of 10^4, 10^5, 10^6, 10^7, and 10^8 repetitions of the single axle load of 80 kN. When the user defines the design traffic, all proposed or interpolated points in the curves represent a possible solution. The plastic deformation associated with the subgrade controls the thin structures (small thickness of unbound base and asphalt), and the fatigue of the asphalt mix controls the thicker ones.

Figure 2-16 contains two broken diagonal lines that define three sections for moduli of the unbound base according to its thickness. The first section has a modulus of 200 MPa with a thickness between 150 mm for 10^4 load repetitions and 170 mm for 10^7 load repetitions. The second section has a modulus of 400 MPa with a thickness between 75 mm, for 10^4

load repetitions and 100 mm for 10^7 load repetitions. The third section has a modulus of 800 MPa with a thickness of up to 770 mm for 10^4 load repetitions.

This feature calls for some discussion because it implies that the modulus of the unbound layers doubles with thicknesses increments that are not feasible in the construction process, e.g., 75 millimeters. Likewise, moduli of 800 MPa are unrealistic for the unbound layer considering other references like the French design guide (LCPC - SETRA, 1994) and the elastic method of the USACE (Joint Departments of the Army and Air Force, 1994) that restrict the maximum modulus of untreated base materials to 700 MPa.

Figure 2-17 shows the USACE proposal with a maximum modulus of 280 MPa for the granular subbase and 700 MPa for the granular base. Therefore, some solutions from the Shell charts may be theoretically plausible but impracticable.

Figure 2-17: Young moduli relations between two successive untreated layers

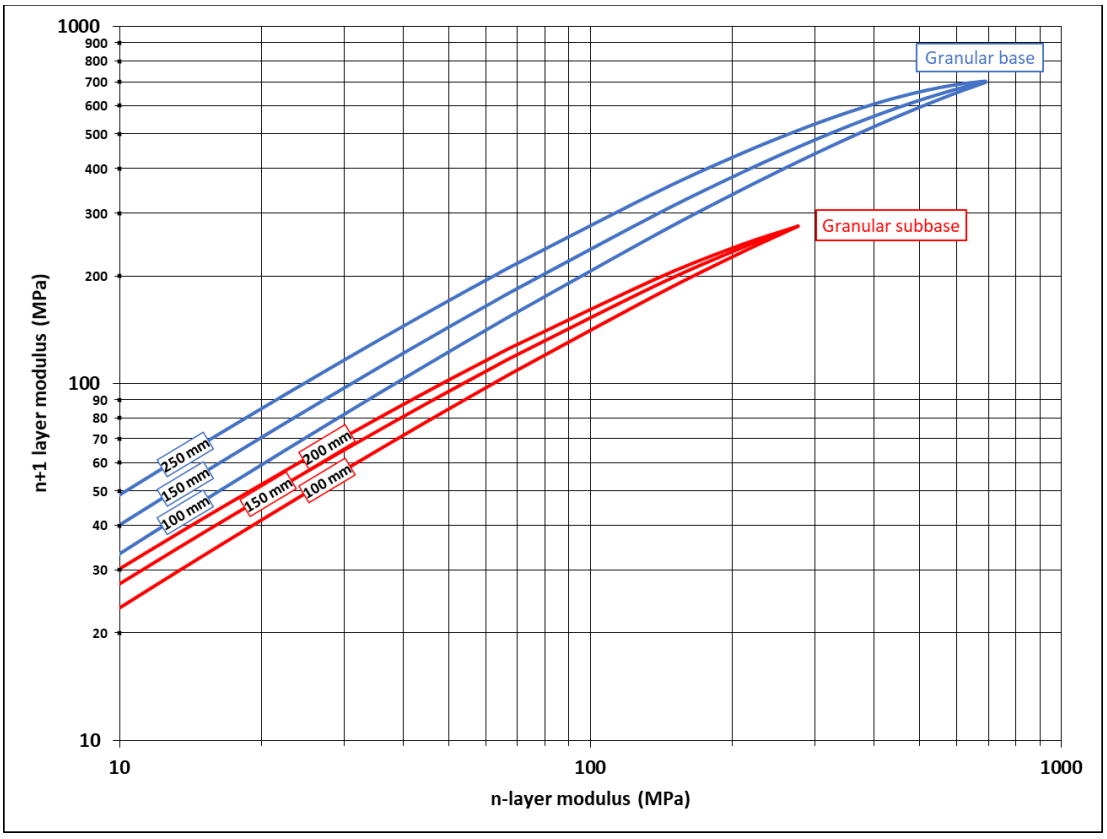

Source: Adapted to SI units from Joint Departments of the Army and Air Force (1994).

Engineers used the Shell procedure for decades as the archetype of the mechanistic-empirical design method before the emergence of the MEPDG. The method resources increased by converting the charts into the SPDM 3.0 software; however, today, the program is unavailable for modern computers with 64 bits operative systems.

Asphalt Institute method

The Asphalt Institute (AI) published its first design manual in 1955, with six subsequent editions until 1962. In 1963 AI published the seventh edition based on the WASHO and AASHO road tests, the test tracks in the United Kingdom, and contemporary design methods like USACE.

In 1969, AI published the eighth edition considering equivalent axle loads and new design charts. These empirical procedures were based on the relationships between traffic and thickness obtained in the AASHO Road Test. In 1977, AI launched the research for the ninth edition of the manual with mechanistic-empirical methodology, thus suppressing the limitations of the AASHO Road Test data and other practices like thickness equivalence factors between layers.

The ninth edition of the AI method incorporates the joint evaluation of structural and functional characteristics used in the calibration with in-service pavements (end-of-service PSI of 2.5). The structural characteristics are the asphalt layers fatigue, adjusted for a cracked area of 20% to 25% of the total pavement area according to the AASHO Road Test results, and a calibrated depth of rutting up to 13 millimeters according to data from California (U.S.A.). Asphalt rutting is a construction defect by secondary compaction, and it does not have an independent distress model (Asphalt Institute, 1982).

The pavement model is a layered elastic system characterized by moduli (E) and Poisson ratios (v). The method considers several materials as asphalt concrete, asphalt-treated bases, and untreated granular bases, in three and four layers over a linear elastic subgrade. The method presents a regression model to estimate the asphalt concrete dynamic modulus with the volumetric proportions and the rheological characteristics of the bitumen. Also, it presents a non-linear elastic model to estimate the modulus of untreated materials (Mallick & El-Korchi, 2009).

Repetitions of the AASHTO standard axle load of 80 kilonewtons, applied by two wheels with a radius of 115 mm, a center-to-center spacing of 345 mm, and a contact pressure of 483 kPa, represent the traffic loading. This geometry is different from the one proposed by Shell. AI used the elastic N-layer program DAMA to analyze the pavement structures and produce design charts based on the critical solicitation between the asphalt layers fatigue and the rutting associated with the subgrade response (Asphalt Institute, 2005).

The following equations summarize the design criteria of the Asphalt Institute method (Asphalt Institute, 1982):

- Fatigue of asphalt materials:

$$N_f = 18.4 \cdot \left(10^{4.84 \cdot \left(\frac{V_b}{V_v + V_v} - 0.69 \right)} \right) \cdot (6.167 \times 10^{-5} \cdot \varepsilon_t^{-3.291} \cdot |E*|^{-0.854})$$

Eq. 2-13

Where N_f are the load repetitions; V_v and V_b are the volume of voids and bitumen of the asphalt mixture, ε_t is the tensile strain in the asphalt layer (mm/mm), and $|E*|$ is the dynamic modulus (MPa).

- Rutting associated with the subgrade response:

$$N_d = 1.365 \times 10^{-9} \cdot (\varepsilon_c)^{-4.477}$$

Eq. 2-14

Where N_d are the load repetitions to failure (13 mm), and ε_c is the vertical compressive strain at the top of the subgrade.

Figure 2-18 shows the design chart for pavements with asphalt concrete over an untreated granular base of 18 inches (457 mm) thick. The horizontal axis presents the accumulated 80 kN axle loads in the design life (usually 20 years). The vertical axis presents the resilient modulus of the subgrade in psi. Numbers in curves represent the thickness of asphalt concrete in inches. The Asphalt Institute method yields thicker asphalt concrete layers than

those obtained by the CBR-based empirical method. Therefore, it has a lower acceptance than the Shell method, especially for the structural alternatives between 50 mm and 100 mm of asphalt concrete.

Figure 2-18: Chart for asphalt concrete pavement with 18 in of untreated materials

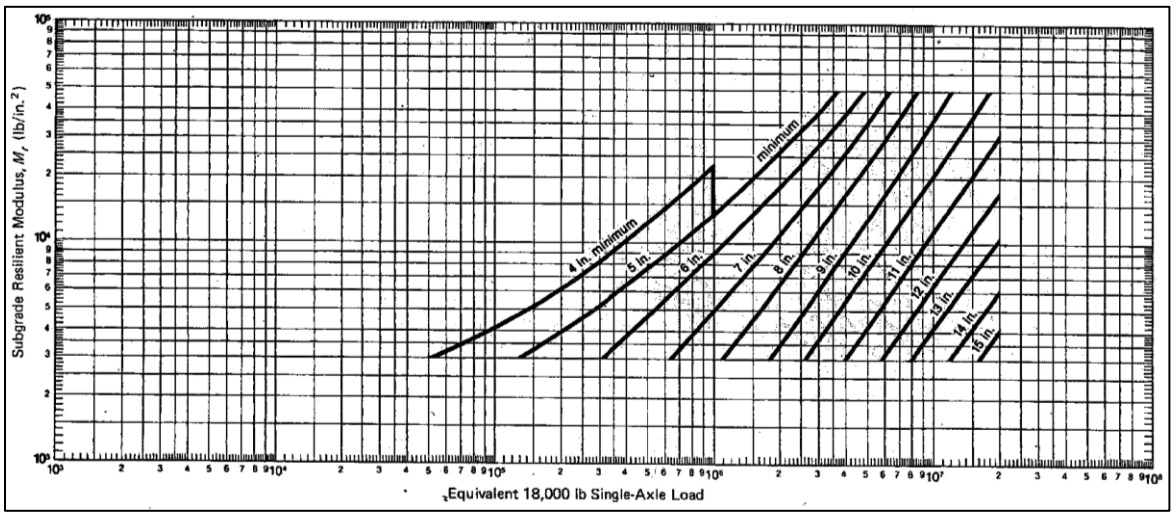

Source: Asphalt Institute (1982). 1 inch = 25.4 mm, 1 psi = 6.89 kPa.

The French Design Guide

After World War II, the French design practice applied experimental procedures based on the CBR test. The increase in heavy traffic and new materials in road construction required new design methods in the 1970s. The first procedure used charts based on mechanical analysis with the layered elastic program Alizé and in situ performance criteria based on the roadbed's compressive strain and the surface's vertical deflection.

The current French design method combines an analytical method to compute stresses and strains and laboratory tests to evaluate fatigue resistance. One significant feature of the method is the detailed consideration of embankments or capping layer design on the subgrade and the calibration of permanent deformation performance with test sections and tracks (Corté & Goux, 1996). The method also includes a risk assessment of pavement design, considering the random mechanical response of materials.

The different axle loads are converted to repetitions of a single reference axle of 130 kN, applied by two wheels with a 125 mm radius, a center-to-center spacing of 375 mm, and a 662 kPa contact pressure (LCPC - SETRA, 1994). The following equation gives the relation between the damage caused by any axle and the reference axle:

$$A = K \cdot \left(\frac{P}{130\ kN}\right)^{\alpha}$$

Eq. 2-15

Where A is the *"aggressiveness"* of any axle, K is used to consider the kind of axle (single, tandem, tridem), P is the axle weight in kilonewtons, and α is a function of the type of material and structure. Table 2-1 summarizes the average values of α and K for French conditions on average and highly trafficked new pavements. In Colombia, the *"α"* parameter may be near four (4.0) for flexible and bituminous pavement design (Figueroa, Reyes, Hernández, Jiménez, & Bohórquez, 2007).

Table 2-1: Values for parameters K and α used in calculating the aggressiveness

Type of structure	Parameter α	Parameter K		
		Single axle	Tandem axle	Tridem axle
Flexible and bituminous pavements	5	1	0.75	1.1
Semi-rigid pavements	12	1	12	113
Concrete pavements				
Slabs	12	1	12	113
Continuously reinforced concrete	12	1	12	?

Source: LCPC – SETRA (1994)

The following equations summarize the design criteria of the procedure (LCPC - SETRA, 1994; Corté & Goux, 1996):

- Fatigue of bonded or cemented materials:

The following equation defines the working strain for asphalt pavements:

$$\varepsilon_{t,ad} = \varepsilon_6(10°C, 25Hz) \cdot \sqrt[2]{\frac{E(10°C)}{E(\theta_{eq})}} \cdot \left(\frac{NE}{10^6}\right)^{b} \cdot k_r \cdot k_c \cdot k_s$$

Eq. 2-16

Where $\varepsilon_{t,ad}$ is the allowable tensile strain in the asphalt layer; $\varepsilon_6(10°C, 25Hz)$ is the tensile strain of the fatigue law at 10°C, 25 Hz, and 10^6 load repetitions; $E(\theta_{eq})$ is the elastic modulus of the asphalt mixture at the equivalent temperature (θ_{eq}); NE is the number of load repetitions to failure with a 50% probability, and b is the slope of the bi-logarithmic fatigue law.

The following equation defines the working stress for pavements with hydraulic-binder-treated bases or concrete pavements:

$$\sigma_{t,ad} = \sigma_0 \cdot (1 + 6\beta) \cdot \left(\frac{NE}{10^6}\right)^b \cdot k_r \cdot k_d \cdot k_c \cdot k_s$$

Eq. 2-17

Where $\sigma_{t,ad}$ is the allowable tensile stress at the bottom of tensile-stressed layers; σ_0 is the indirect tensile strength of the material; β is the slope of the Wohler's curve $(\sigma/\sigma_0 = 1 + \beta \cdot \log N)$; NE is the number of load repetitions to failure with a 50% probability; and $b = -0.5 \cdot \log\left(\frac{1+5\beta}{1+7\beta}\right)$ for load repetitions between 10^5 and 10^7.

The coefficient k_r adjusts the working strain or stress values to the design reliability:

$$k_r = 10^{-Zr \cdot b \cdot \delta}$$

Eq. 2-18

Where Z_r is the accumulated value of the standardized normal distribution for a given reliability (or risk) level, b is the slope of the bi-logarithmic fatigue law, and δ is the standard deviation associated with the load repetitions given the dispersion of the fatigue law and the layer thickness:

$$\delta = \sqrt[2]{SN^2 + \left(\frac{c \cdot Sh}{b}\right)^2}$$

Eq. 2-19

Where SN is the standard deviation of the logarithm of the number of cycles at failure, Sh is the standard deviation of the layer thickness, c is the coefficient linking the variation in

strain (or stress) to the random variation in thickness ($\log \varepsilon = \log \varepsilon_0 - c \cdot \Delta h$), and b is the slope of the bi-logarithmic fatigue law.

The calibration coefficient k_c adjusts the working strain or stress to the performance observed on pavements of the same type. The coefficient k_s is a reducing factor that considers the heterogeneity of the bearing capacity of the roadbed. The coefficient k_d considers the effect of joints or shrinkage cracks in cement-treated materials or concrete slabs. Table 2-2 summarizes the suggested values of the coefficients for French conditions:

Table 2-2: Coefficients for calculation of working strains and stress

Coefficient	**Pavement material**				
k_c	Semi-coarse graded aggregate base asphalt concrete	Asphalt concrete	High-modulus asphalt concrete	Cement-treated graded aggregates	Cement concrete and slag-treated graded aggregates
	1.3	1.1	1.0	1.4	1.5
k_s	**Subgrade modulus**				
	E < 50 MPa	50 MPa ≤ E ≤ 120 MPa			E > 120 MPa
	1 / 1.20	1 / 1.10			1.0
k_d	**Pavement material**				
	Treated gravels class G2 & G3	Treated gravels classes G4 & G5 and rolled concrete	Un-dowelled cement concrete slabs	Dowelled cement concrete slabs	Continuously reinforced concrete
	1.0	1 / 1.25	1 / 1.27	1 / 1.10	1 / 1.10

Source: Corté & Goux (1996).

- Rutting associated with the subgrade and untreated layers responses:

$$\varepsilon_{z,ad} = A_r \cdot (NE)^{-0.222}$$

Eq. 2-20

Where $\varepsilon_{z,ad}$ is the allowable compressive strain on the top of untreated or subgrade layers, A_r is 0.012 on pavements with medium or high traffic and 0.016 on pavements with low traffic, and NE is the number of load repetitions.

The French method is a comprehensive and straightforward design methodology. Its suitability to the local practice depends on the field calibration activities and construction specifications that evaluate index properties and mechanical performance. The pavement

design manuals made for Bogotá (Colombia) by Reyes Lizcano et al. (1997) and the Universidad Nacional de Colombia (2013) represent valuable efforts for this purpose.

In a detailed review of European pavement and asphalt mix design practices, Pereira & Pais (2017) state that the French pavement design method "*is the most comprehensive design method in use in Europe.*" Also, the authors highlight the main desirable features for a pavement design procedure proposed by the project "*Advanced Models for Analytical Design of European Pavement Structures - AMADEUS*" (2000) in the European context. Simplicity is a requisite for implementing a pavement design method because many random variables will determine a high level of uncertainty in the result.

Figure 2-19 shows the ideal design procedure proposed by the AMADEUS project. One must note that the incremental European approach anticipated the American MEPDG by several years.

Mechanistic-Empirical Pavement Design Guide (MEPDG)

The MEPDG is the main product of the NCHRP 1-37A project to implement mechanistic-empirical pavement analysis and design procedures in the USA. A mechanic model computes structural responses considering material properties, environmental conditions, and traffic loading characteristics. The structural responses are analyzed with empirical models to evaluate the performance and predict pavement distress (NCHRP, 2004).

The accuracy of the empirical models to predict damage depends on the quality of the field calibration. The method considers two models: one directly predicts the damage (rutting), and another predicts the damage from calibrated observations (fatigue). The design process differs from conventional methods because the result is the estimated distress, not the pavement thickness.

Figure 2-19: Flowchart of an incremental pavement design procedure

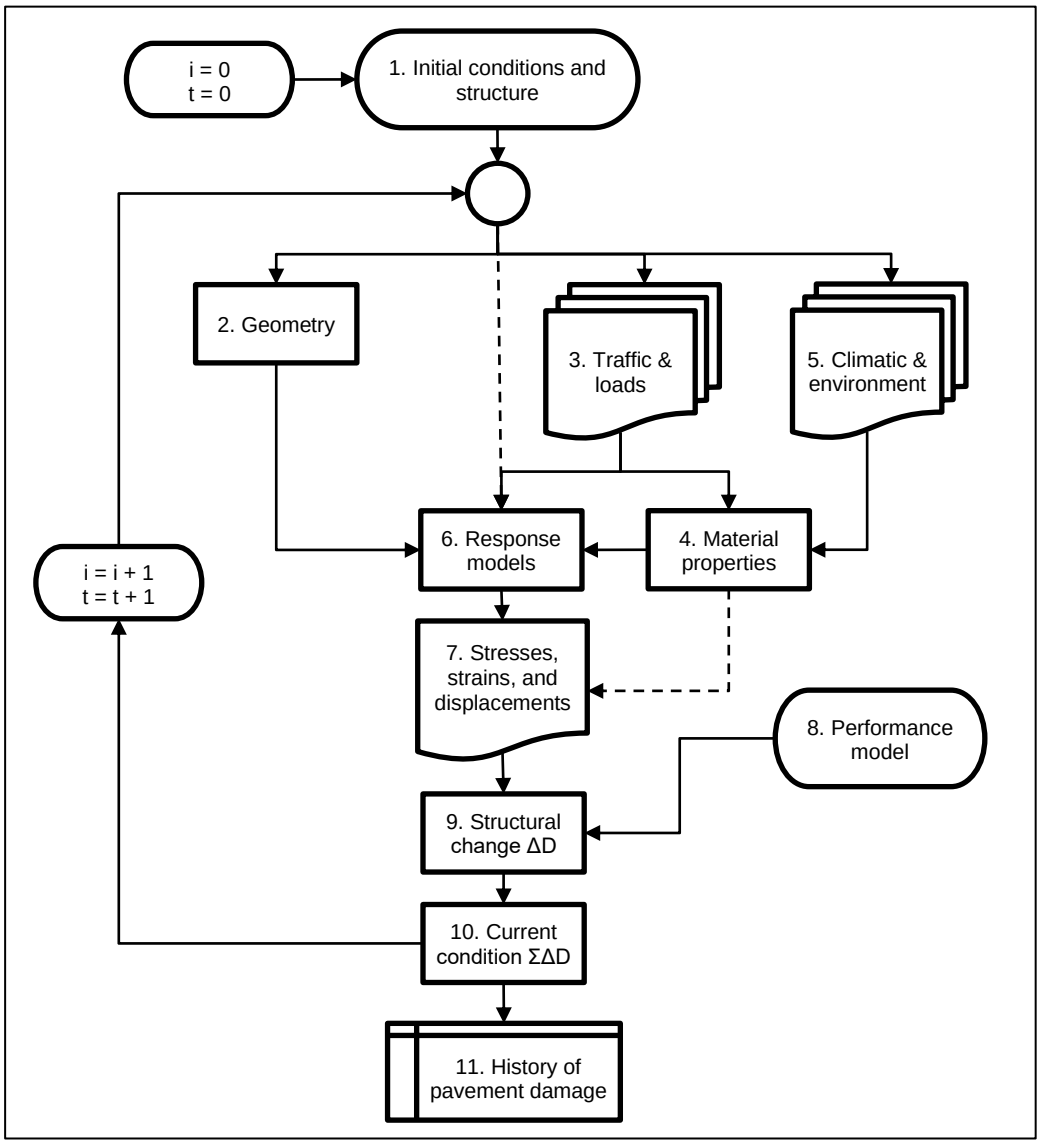

Source: AMADEUS (2000).

The MEPDG procedure may be summarized in the following steps:

1. Define a trial design for specific site subgrade support, material properties, traffic loading, and environmental conditions.
2. Define the design criteria for pavement performance: acceptable levels of rutting, fatigue cracking, thermal cracking, and roughness at the end of the design period.
3. Select the reliability level for each distress considered in the design.
4. Calculate monthly traffic loading and seasonal climate conditions.

5. Modify material properties in response to environmental conditions.
6. Compute structural responses (stresses, strains, and deflections) for each axle type and load and for each time step throughout the design period.
7. Calculate predicted distresses at the end of each time step throughout the design period using the calibrated empirical performance models.
8. Evaluate the predicted performance of the trial design against the specified reliability level. If the trial design does not meet the performance criteria, the design must be modified, and the calculations repeated until the design is acceptable.

Figure 2-20 shows the conceptual schematic of the design process of MEPDG divided into three stages: evaluation, analysis, and strategy selection.

The MEPDG considers three hierarchical levels for the input data: Level 1 demands high-quality laboratory characterization of the materials. Level 2 uses correlations between simple parameters and advanced material characterization. Level 3 uses local or national values by default. The hierarchical level must coincide with the relevance of the project. The initial calibration corresponds to Level 3; thus, road agencies must develop local studies to properly use the MEPDG (Schwartz & Carvalho, 2007).

The analysis method is the layered elastic theory, based on the JULEA program, except for non-linear analysis in the hierarchical Level 1 that uses the DSC2D finite element method program. FEM is not fully calibrated and is only for research. The traffic loading characterization uses load spectra of single, tandem, triple, and quad axles with multiple analysis points in the pavement structure to obtain the critical responses.

Figure 2-21 shows the locations for regular traffic proposed for the MEPDG (NCHRP, 2004). Zhao et al. (2012) questioned the adequacy of this approach for tandem, triple, and quad axles.

The incremental damage analysis divides the design period into sub-periods of one month or even two weeks. For example, a ten-year design period comprises 120 one-month sub-periods. The structural layers support the predicted traffic under the predominant weather and material conditions at each subperiod. The damage is accumulated to predict the progressive deterioration of the structural and functional conditions.

Figure 2-20: Conceptual schematic of the three-stage design process of MEPDG.

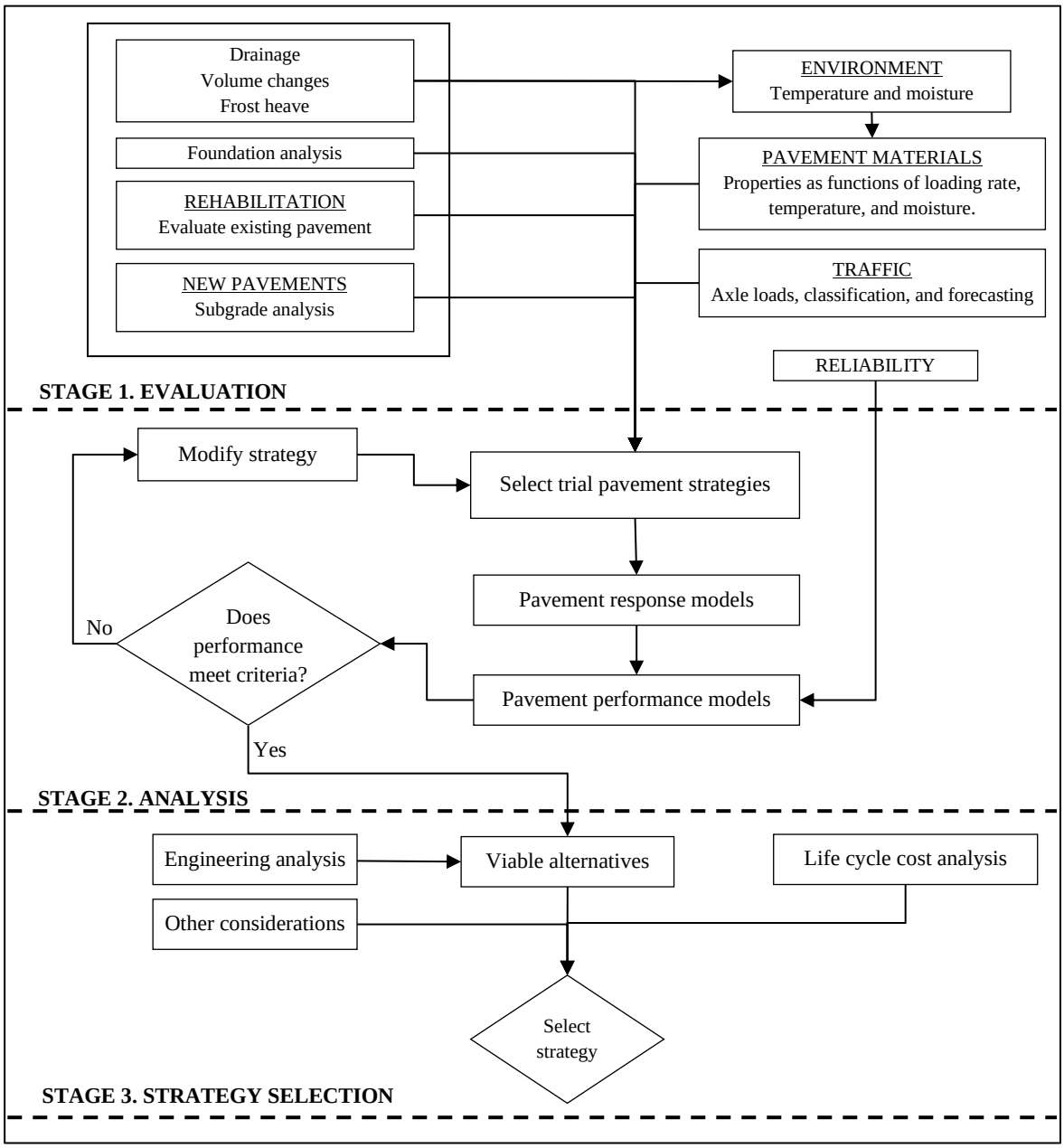

Source: NCHRP (2004).

Figure 2-21: Schematics for horizontal analysis locations for regular traffic

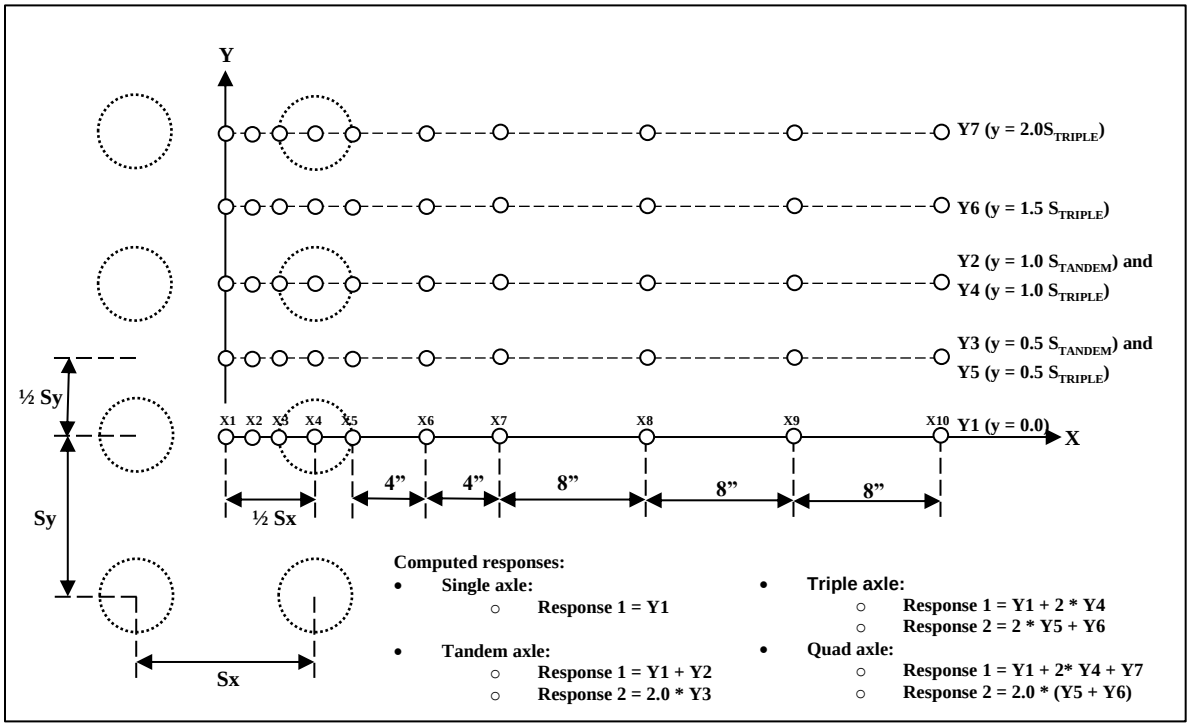

Source: Redrawn from NCHRP (2004) – not to scale.

The MEPDG can consider a wide range of materials: Hot mix dense-graded asphalt concrete, asphalt-treated open-graded permeable base materials, cold mix asphalt, Portland cement concrete, cement-treated or lean concrete base, cement-treated open-graded permeable base materials, untreated base materials (granular base or granular subbase), lime modified or stabilized soils, subgrade soil, and bedrock.

For hot-mix asphalt-surfaced pavements, the specific performance models are [AASHTO, (2008) & NCHRP (2004)]:

1. Total rut depth and rutting of hot-mix asphalt, unbound aggregate base, and subgrade.

a. Plastic deformation for hot-mix asphalt (HMA):

$$\Delta_{p(HMA)} = \left[\beta_{1r} \cdot k_z \cdot \varepsilon_{r(HMA)} \cdot 10^{(k_{1r})}\right] \cdot (h_{HMA}) \cdot \left[n^{(k_{2r} \cdot \beta_{2r})}\right] \cdot \left[T^{(k_{3r} \cdot \beta_{3r})}\right]$$

Eq. 2-21

Where $\Delta_{p(HMA)}$ is the accumulated plastic vertical deformation in the HMA layer (in.); $\varepsilon_{r(HMA)}$ is the resilient strain calculated at the mid-depth of the HMA layer (in./in.); $h_{(HMA)}$ is

the thickness of the HMA layer (in.); n is the number of axle-load repetitions; T is the pavement temperature (°F); k_z is the depth confinement factor; k_{1r}, k_{2r}, k_{3r} are the global field calibration parameters ($k_{1r} = -3.35412, k_{2r} = 0.4791, k_{3r} = 1.506$); and β_{1r} , β_{2r}, β_{3r} are local field calibration constants (1.0 by default). The depth confinement factor is:

$$k_z = (C_1 + C_2 \cdot D) \cdot (0.328196)^D$$

Eq. 2-22

Where:

$$C_1 = -0.1039 \cdot (H_{HMA})^2 + 2.4868 \cdot (H_{HMA}) - 17.342$$

Eq. 2-23

$$C_2 = 0.0172 \cdot (H_{HMA})^2 - 1.7331 \cdot (H_{HMA}) + 27.428$$

Eq. 2-24

Where D is the depth below the surface (in.), and H_{HMA} is the total thickness of the hot-mix asphalt (in.).

b. Plastic deformation for unbound pavement layers and the foundation or embankment soil:

$$\Delta_{p(soil)} = [\beta_{s1} \cdot k_{s1} \cdot \varepsilon_v] \cdot \left[\left(\frac{\varepsilon_0}{\varepsilon_r}\right) \cdot e^{-\left(\frac{\rho}{n}\right)^{\beta}}\right] \cdot h_{soil}$$

Eq. 2-25

Where $\Delta_{p(soil)}$ is the plastic deformation of the layer (in.); n is the number of axle-load repetitions; ε_0 is the intercept determined from laboratory repeated load permanent deformation tests (in./in.); ε_r is the resilient strain imposed in the laboratory to obtain material properties ε_0, ε, and ρ (in./in.); ε_v is the calculated average vertical resilient strain in the layer (in./in.); h_{soil} is the thickness of the unbound layer (in.); k_{s1} is a global calibration factor ($k_{s1} = 1.673\ [granular\ material], k_{s1} = 1.350[fine\ soil]$); and β_{s1} is a local calibration constant (1.0 by default). The models to estimate the parameters β, $(\varepsilon_0/\varepsilon_r)$, and ρ are:

$$W_c = 51.712 \cdot \left[\left(\frac{M_r}{2555}\right)^{\frac{1}{0.64}}\right]^{-0.3586 \cdot (GWT)^{0.1192}}$$

Eq. 2-26

$$\beta = 10^{[-0.61119-0.017683\cdot(W_c)]}$$

Eq. 2-27

$$C_0 = \ln\left[\frac{a_1 \cdot (M_r)^{b_1}}{a_9 \cdot (M_r)^{b_9}}\right]$$

Eq. 2-28

$$\rho = 10^9 \cdot \left[\frac{C_0}{1-(10^9)^{\beta}}\right]^{\frac{1}{\beta}}$$

Eq. 2-29

$$\left(\frac{\varepsilon_0}{\varepsilon_r}\right) = 10^{\frac{\left\{\left[e^{(\rho)^{\beta}}\cdot a_1(M_r)^{b_1}\right]+\left[e^{\left(\rho/10^9\right)^{\beta}}\cdot a_9(M_r)^{b_9}\right]\right\}}{2}}$$

Eq. 2-30

Where W_c is the water content (%); M_r is the resilient modulus of the layer (psi); GWT is the groundwater table depth (feet); and $a_1 = 0.15, b_1 = 0.0, a_9 = 20.0, b_9 = 0.0$.

The total permanent deformation of the pavement is the addition of the contribution of all rutting-susceptible layers:

$$RD_{Total} = RD_{AC} + RD_{GB} + RD_{SG} = \sum_{j=1}^{N_{layers}} \left(\sum_{i=1}^{N_{periods}} \varepsilon_{p\,i,j} \cdot \Delta h_{i,j} \right)$$

Eq. 2-31

Where RD_{Total} is the total permanent deformation made by the contributions of asphalt (AC), granular bases (GB), and subgrade (SG) layers.

The reliability design is obtained by determining the predicted rutting at the desired level of reliability:

$$RD_P = \sum_i (\overline{RD_i}) + \sqrt[2]{{Se_{RDAC}}^2 + {Se_{RDBG}}^2 + {Se_{RDSG}}^2} \cdot Z_r$$

Eq. 2-32

Where RD_P is the predicted rutting at a reliability P (in.); $\overline{RD_i}$ is the predicted rutting based on mean inputs (reliability of 50%) (in.); Se_{RDi} is the standard error of rutting at the predicted

level of mean rutting (in.); and Z_r is the normal standard deviation for a one-tailed distribution.

The following equations estimate the standard errors of predicted rutting (in.) for asphalt concrete, granular bases, and subgrade as functions of the predicted mean rutting values:

$$Se_{RDAC} = 0.1587 \cdot RD_{AC}^{0.4579}$$

Eq. 2-33

$$Se_{RDBG} = 0.1169 \cdot RD_{BG}^{0.5303}$$

Eq. 2-34

$$Se_{RDSG} = 0.1724 \cdot RD_{SG}^{0.5516}$$

Eq. 2-35

The critical responses to compute rutting are the mid-depth of each layer (or sub-layer), the top of the subgrade, and six inches below the subgrade.

2. Non-load transverse cracking:

The amount of transverse cracking expected in the pavement system is predicted by relating the crack depth to an amount of crack frequency as follows:

$$C_f = \beta_1 \cdot N_{(z)} \cdot \left[\frac{\log\left(\frac{C}{h_{AC}}\right)}{\sigma}\right]$$

Eq. 2-36

Where C_f is the observed amount of thermal cracking; β_1 is a regression coefficient determined through field calibration; $N_{(z)}$ is the standard normal distribution evaluated at (z); σ is the standard deviation of the logarithm of the depth of cracks in the pavement; C is the crack depth; and h_{AC} is the thickness of the asphalt layer.

The amount of crack propagation induced by a given thermal cooling cycle is predicted using the Paris law of crack propagation:

$$\Delta C = \left\{10^{[k_t \cdot \beta_t] \cdot \left[4.389 - 2.52 \cdot \log\left(E_{HMA} \cdot \sigma_m \cdot 0.80 \cdot \left(1+\frac{1}{m}\right)\right)\right]}\right\} \cdot \left\{\Delta\left[\sigma_{tip} \cdot \left(0.45 + 1.99 \cdot C_0^{0.56}\right)\right]\right\}^{0.80 \cdot \left(1+\frac{1}{m}\right)}$$

Eq. 2-37

Where ΔC is the change in the crack depth due to a cooling cycle; k_t is a coefficient determined through global calibration for each input level; β_t is a local calibration factor; E_{HMA} is the HMA indirect tensile modulus (psi); σ_m is the mixture tensile strength (psi); m is derived from the indirect tensile creep compliance curve measured in the laboratory; σ_{tip} is the computed far-field stress at a depth of crack tip (psi); and C_0 is the current crack length (feet). Table 2-3 summarizes the USA calibration parameters for the thermal cracking model.

Table 2-3: North American calibration parameters for the thermal cracking model

Hierarchical level	Parameter			
	β_1	σ	E_{HMA}	β_t
1	400	0.769	10,000	5.0
2	400	0.769	10,000	1.5
3	400	0.769	10,000	3.0

Source: NCHRP (2004).

The degree of cracking is expressed as the thermal-transverse cracking occurring in a pavement length of 500 feet. The maximum thermal cracking assumed is 400 feet per 500 feet of pavement length, translating into a crack spacing of one crack (full 12 feet lane width) per 15 feet of pavement length.

The standard error of the thermal cracking reliability is a function of the hierarchical level of data:

$$Se_{TC\_i} = K_{TC\_i} \cdot Thermal + K_{0TC\_i}$$

Eq. 2-38

Where Se_{TC_i} is the standard error of estimate for thermal cracking (feet / 500 feet) for level i of analysis; $Thermal$ is the predicted thermal cracking (feet / 500 feet); K_{TC_i} (Level 1: 0.2474, Level 2: 0.3371, Level 3: 0.6803) and K_{0TC_i} (Level 1: 10.619, Level 2: 14.468, Level 3: 29.197) are regression constants.

3. Load-related alligator cracking or bottom-up cracking:

The estimation of fatigue damage is based upon Miner's law, given by the following relationship:

$$D = \sum_{i=1}^{T} \frac{n_i}{N_i}$$

Eq. 2-39

Where D is the damage; T is the total number of years in the analysis period; n_i is the actual traffic for period i; and N_i is the allowed traffic under conditions prevailing in period i.

The allowable number of axle-load applications needed for the incremental damage index approach to predict alligator and longitudinal fatigue cracks is:

$$N_{f(HMA)} = k_{f1} \cdot \left[10^{4.84 \cdot \left(\frac{V_{be}}{V_a + V_{be}} - 0.69\right)}\right] \cdot C_H \cdot \beta_{f1} \cdot (\varepsilon_t)^{k_{f2} \cdot \beta_{f2}} \cdot (E_{HMA})^{k_{f3} \cdot \beta_{f3}}$$

Eq. 2-40

Where $N_{f(HMA)}$ is the allowable number of axle-load applications; ε_t is the calculated tensile strain at critical locations (in./in.); V_{be} is the effective asphalt content by volume (%); V_a is the air voids by volume (%); E_{HMA} is the dynamic modulus of the HMA measured in compression (psi); k_{f1}, k_{f2}, k_{f3} are the global field calibration parameters ($k_{f1} = 0.007566, k_{f2} = -3.9492, k_{f3} = -1.281$); β_{f1}, β_{f2}, β_{f3} are local field calibration constants (1.0 by default).

The thickness correction term (C_H) is dependent on the cracking. For bottom-up or alligator cracking:

$$C_H = \frac{1}{0.000398 + \frac{0.003602}{1 + e^{(11.02 - 3.49 \cdot H_{HMA})}}}$$

Eq. 2-41

Where H_{HMA} is the total thickness of the hot-mix asphalt (in.)

The final transfer function to calculate alligator fatigue cracking from the fatigue damage is:

$$FC_{bottom} = \left\{\frac{6000}{1 + e^{[C_1 \cdot C'_1 + C_2 \cdot C'_2 \cdot \log_{10}(D \cdot 100)]}}\right\} \cdot \left(\frac{1}{60}\right)$$

Eq. 2-42

Where FC_{bottom} is the bottom-up fatigue cracking (% of lane area); D bottom-up fatigue damage; $C_1 = 1.0$; $C'_1 = (-2.0 \cdot C'_2)$; $C_2 = 1.0$; $C'_2 = -2.40874 - 39.748 \cdot (1 + H_{HMA})^{-2.856}$; and H_{HMA} is the total thickness of the hot-mix asphalt (in.)

4. Load-related longitudinal cracking, or top-down cracking:

The fatigue equation is the same as Eq. 2-40, but the thickness correction term (C_H) is:

$$C_H = \frac{1}{0.01 + \frac{12.0}{1 + e^{(15.676 - 2.8186 \cdot H_{HMA})}}}$$

Eq. 2-43

Where H_{HMA} is the total thickness of the hot-mix asphalt (in.)

The transfer function to calculate longitudinal fatigue cracking from the fatigue damage is:

$$FC_{top} = \left\{\frac{1000}{1 + e^{[7.00 - 3.50 \cdot \log_{10}(D \cdot 100)]}}\right\} \cdot (10.56)$$

Eq. 2-44

Where FC_{bottom} is the top-down fatigue cracking (feet/mile), and D top-down fatigue damage.

The reliability design is obtained by determining the predicted associated fatigue-cracking at the desired level of reliability:

$$FC_P = \overline{FC_i} + Se_{FCi} \cdot Z_r$$

Eq. 2-45

Where FC_P is the predicted cracking at a reliability P (% or feet/mile); $\overline{FC_i}$ is the predicted cracking based on mean inputs (reliability of 50%) (% or feet/mile); Se_{FCi} is the standard error of cracking at the predicted level of mean cracking; and Z_r is the normal standard deviation for a one-tailed distribution.

The following equations estimate the standard errors of predicted alligator (bottom-up) and longitudinal (top-down) cracking as functions of the predicted mean cracking values:

$$Se_{FC\_bottom} = 0.5 + \frac{12}{1 + e^{1.308 - 2.949 \cdot \log(D)}}$$

Eq. 2-46

$$Se_{FC\_top} = 200 + \frac{2300}{1 + e^{1.072 - 2.1654 \cdot \log(D)}}$$

Eq. 2-47

The critical responses to compute fatigue are at the pavement surface, 0.5 inches from the surface, and at the bottom of each bonded or stabilized layer.

5. Fatigue cracking in chemically stabilized bases:

$$\log\left(N_{f(CTB)}\right) = \frac{0.972 \cdot \beta_{c1} - \left(\frac{\sigma_t}{MR}\right)}{0.0825 \cdot \beta_{c2}}$$

Eq. 2-48

Where $N_{f(CTB)}$ is the number of repetitions to fatigue cracking of the CSM layer; σ_t is the maximum traffic-induced tensile stress at the bottom of the CSM layer (psi); MR is the 28-day modulus of rupture (psi); and β_{c1}& β_{c2} are field calibration factors (both are uncalibrated and equal to 1.0).

The computational analysis of CSM fatigue cracking is conducted in the predefined 2 to 4 weeks analysis period. The incremental damage per analysis period considers the reduction of the CSM modulus at the following analysis period:

$$E_{CSM}(t) = E_{CSM}(min) + \frac{E_{CSM}(max) - E_{CSM}(min)}{1 + e^{(-4+14D)}}$$

Eq. 2-49

Where $E_{CSM}(t)$ is the CSM layer modulus at damage level D; $E_{CSM}(max)$ is the maximum CSM layer modulus for the intact layer (psi); $E_{CSM}(min)$ is the minimum CSM layer modulus after total layer destruction (psi), and D is the CSM damage level (decimal form).

The empirical relationship that relates CSM damage to cracking is:

$$C = \frac{1000}{1 + e^{(1-D)}}$$

Eq. 2-50

Where C is the CSM layer cracking in feet of cracking per 500 feet long sections; D is the CSM damage level.

The reliability is the standard deviation associated with normal HMA fatigue cracking because this model is uncalibrated.

6. Reflection cracking in hot-mix asphalt overlays from cracks and joints in existing flexible, semi-rigid, composite, and rigid pavements.

$$RC = \frac{100}{1 + e^{\{[3.5+0.75\cdot(H_{eff})]\cdot(c)+[-0.688684-3.37302\cdot(H_{eff})]\cdot t(d)\}}}$$

Eq. 2-51

Where RC is the percentage of cracks reflected (%); t is the time (years); H_{eff} is the effective overlay thickness; c & d are user-defined cracking progression parameters (1.0 by default).

7. Smoothness (IRI).

The prediction models consider the damage, age, and type of asphalt pavement in three groups: pavements with unbound aggregate bases, pavements with asphalt-treated bases, and pavements with chemically stabilized bases (NCHRP, 2004).

a. Unbound aggregate base and subbase:

$$IRI = IRI_0 + 0.0463 \cdot \left[SF \cdot \left(e^{\frac{age}{20}} - 1\right)\right] + 0.00119 \cdot (TC_L)_T + 0.1834 \cdot (COV_{RD}) + 0.00384 \cdot (FC)_T + 0.00736 \cdot (BC)_T + 0.00115 \cdot (LC_{SNWP})_{MH}$$

Eq. 2-52

Where IRI is the IRI at any given time (mm/m); IRI_0 is the initial IRI (mm/m); SF is the site factor; age is the age of pavement in years; $(TC_L)_T$ is the total length of transverse cracks

(m/km); COV_{RD} is the coefficient of variation of the rut depths (assumed to be 20%); $(FC)_T$ is the fatigue cracking in the wheel path (% of total lane area); $(BC)_T$ is the area of block cracking as a percent of total lane area (user input, not modeled by MEPDG); and $(LC_{SNWP})_{MH}$ is the length of moderate and high severity sealed longitudinal cracks outside the wheel path in meters per kilometer (user input, not modeled by MEPDG). The site factor is:

$$SF = \left\{\frac{(R_{SD}) \cdot (P_{075} + 1) \cdot (PI)}{2 \times 10^4}\right\} \cdot \left\{\frac{\ln(FI + 1) \cdot (P_{02} + 1) \cdot \ln(R_m + 1)}{10}\right\}$$

Eq. 2-53

Where R_{SD} is the standard deviation of the monthly rainfall (mm); P_{075} is the percent passing the 0.075 mm sieve; PI is the plasticity index of the soil (%); FI is the average annual freezing index (°C-days); P_{02} is the percent passing the 0.02 mm sieve; and R_m is the average annual rainfall (mm).

The predicted IRI for hot-mix asphalt over unbound granular bases and subbases at the desired level of reliability is:

$$IRI_P = IRI + Se_{IRI} \cdot Z_r$$

Eq. 2-54

Where IRI_P is the predicted IRI at the reliability level P (mm/m); IRI is the predicted IRI based on mean inputs (reliability 50%) (mm/m); Se_{IRI} is the standard deviation of IRI at the predicted level of mean IRI; and Z_r is the normal standard deviation.

The standard deviation of IRI for hot-mix asphalt over unbound granular bases and subbases is derived from the variance of IRI as follows:

$$Se_{IRI} = \sqrt[2]{\begin{array}{c} V(IRI_0) + \left\{0.0367 \cdot \left[e^{(age/20)} - 1\right]\right\}^2 \cdot V(SF) + 1.05625 \times 10^{-5} \cdot V[(FC)_T] + \\ 1.67445 \times 10^{-5} \cdot V[COV_{RD}] + 1.1236 \times 10^{-6} \cdot V[(TC_L)_T] + \\ 4.9562 \times 10^{-5} \cdot V[(BC)_T] + 2.4336 \times 10^{-6} \cdot V[(LC_{SNWP})_{MH}] + S_e^2 \end{array}}$$

Eq. 2-55

Where Se_{IRI} is the standard deviation of IRI at the predicted level of mean IRI; $V(IRI_0)$ is the variance of the initial IRI; $V(SF)$ is the variance of the site factor (estimated from typical values); $V[(FC)_T]$ is the variance of fatigue cracking in wheel path (estimated from models);

$V[COV_{RD}]$ is the variance of the coefficient of variation of the rut depth (estimated with typical values); $V[(TC_L)_T]$ is the variance of the total length of transverse cracks at all severity levels; $V[(BC)_T]$ is the variance of the area of block cracking (estimated); $V[(LC_{SNWP})_{MH}]$ is the variance of the length of moderate and high severity sealed longitudinal cracks outside wheel paths (estimated using typical values); and S_e^2 is the variance of the overall model error = 0.15 (m/km)².

b. Asphalt-treated bases:

$$IRI = IRI_0 + 0.0099947 \cdot (age) + 0.0005138 \cdot (FI) + 0.00235 \cdot (FC)_T + 18.36 \cdot \left[\frac{1}{(TC_S)_H}\right] + 0.9694 \cdot (P)_H$$

Eq. 2-56

Where $(TC_S)_H$ is the average spacing of high-severity transverse cracks (m) estimated from the thermal cracking model; $(P)_H$ is the area of high severity patches as a percent (%) of the total lane area (user input). All other variables are as previously defined.

The predicted IRI for hot-mix asphalt pavements over asphalt-treated bases at the desired level of reliability is obtained with Eq. 2-54. The corresponding standard deviation is:

$$Se_{IRI} = \sqrt[2]{V(IRI_0) + 3.047 \times 10^{-5} \cdot V[(FC)_T] + \left\{\frac{-33.59}{[(TC_S)_H + 1]^2}\right\}^2 \cdot V[(TC_S)_H] + 0.90802 \cdot V(P_H) + S_e^2}$$

Eq. 2-57

Where $V[(TC_S)_H]$ is the variance of average spacing of high severity transverse cracks estimated from the thermal cracking model; $V(P_H)$ is the variance of the high-severity patches area estimated from typical values. All other variables are as previously defined.

c. Chemically stabilized bases:

$$IRI = IRI_0 + 0.00732 \cdot (FC)_T + 0.07647 \cdot (SD_{RD}) + 0.0001449 \cdot (TC_L)_T + 0.00842 \cdot (BC)_T + 0.0002115 \cdot (LC_{SNWP})_{MH}$$

Eq. 2-58

Where all the variables are as previously defined.

The predicted IRI for hot-mix asphalt pavements over asphalt-treated bases at the desired level of reliability is obtained with Eq. 2-54. The corresponding standard deviation is:

$$Se_{IRI} = \sqrt[2]{\begin{matrix} V(IRI_0) + 5.358 \times 10^{-5} \cdot V[(FC)_T] + 5.848 \times 10^{-3} \cdot V[SD_{RD}] + \\ +2.0996 \times 10^{-8} \cdot V[(TC_L)_T] + 7.0896 \times 10^{-5} \cdot V[(BC)_T] \\ +4.473 \times 10^{-8} \cdot V[(LC_{SNWP})_{MH}] + S_e^2 \end{matrix}}$$

Eq. 2-59

Where all the variables are as previously defined. The model to estimate SD_{RD} of predicted rutting is:

$$SD_{RD} = 0.665 + 0.2126 \cdot (RD)$$

Eq. 2-60

Where SD_{RD} is the standard deviation of rut depths (mm), and RD is the mean rut depth (mm).

d. Updated roughness equations:

AASHTO (2008) presented an updated form for the roughness equations for new asphalt pavements or asphalt overlays disregarding the base material type, as follows:

$$IRI = IRI_0 + 0.015 \cdot SF + 0.400 \cdot FC_{total} + 0.008 \cdot TC + 40.0 \cdot RD$$

Eq. 2-61

Where IRI is the IRI at any given time (in./mile); IRI_0 is the IRI after construction (in./mile); SF is the site factor; FC_{total} is the area of fatigue cracking (% of total lane area) due to alligator cracking, longitudinal cracking, and reflective cracking in the wheel path; TC is the length of transversal cracking, including reflective transverse cracking, in ft./mile; and RD is the average rut depth in inches. Note the use of imperial system units. The updated site factor equation is as follows:

$$SF = Age \cdot [0.02003 \cdot (PI + 1) + 0.007947 \cdot (Precip + 1) + 0.000636 \cdot (FI + 1)]$$

Eq. 2-62

Where SF is the site factor; Age is the pavement age in years; PI is the plasticity index of the subgrade soil; $Precip$ is the mean annual rainfall in inches; FI is the mean annual freezing index in °F-days.

In the MEPDG, there is an improvement in pavement design thanks to other distress and functional models. However, the published comparisons between the measured and estimated distress (AASHTO, 2008) show that the proposed models are quite dispersed, with coefficients of correlation (R^2) of 0.577 for rutting, 0.275 for alligator cracking, 0.544 for longitudinal cracking, and 0.56 for IRI. Also, the observed values were proportionally distributed between the layers from a single measurement of total superficial rutting.

The proper use of the MEPDG requires the models' calibration and the assessment of variability of the design factors to evaluate the reliability. Although the MEPDG develops the idea of incremental design, it lacks simplicity, and maybe some models should be reviewed for applicability for road agencies and practitioners.

Schwartz & Carvalho (2007) compared flexible pavement designs between the 1993 AASHTO pavement design guide and the MEPDG; they found that the 1993 AASHTO method overestimates the performance in warm climates and heavier traffic levels than those of the original AASHO Road Test.

Li et al. (2011) identified future research areas for MEPDG development and improvement in robust sensitivity analysis, enhancements of the climate model and the potential impact of climate change, traffic data quality control, local calibration, and new materials. The extent of the calibration efforts for the MEPDG covers multiple reports with different results, from the proper bias and error reduction in some cases to the unavailability of sufficient local data in others.

Schwartz et al. (2011) evaluated the pavement performance sensitivity to the design inputs in MEPDG; they found that flexible pavement distress is significantly sensitive to the asphalt mix properties and thickness.

Von Quintus et al. (2012) produced the NCHRP Report 719 about calibrating new rutting models for MEPDG. They concluded that repeated-load plastic deformation tests (triaxial and shear) are cost-effective and may be included in the MEPDG software with new transfer functions for rutting (Kaloush, modified Leahy, and WesTrack).

Romanoschi et al. (2014) verified the MEPDG models for flexible pavements with accelerated pavement testing and found that MEPDG underpredicts HMA longitudinal strains and overpredicts permanent deformation.

Pierce & McGovern (2014) prepared the NCHRP Synthesis 457 about MEPDG adoption in the United States and found that 48 agencies used empirical design methods. Three agencies implemented MEPDG (Indiana, Missouri, and Oregon), and 46 had plans to implement the new method.

Tran et al. (2017) presented a case study that compared designs conducted with global and local calibration coefficients to illustrate the importance of local calibration in implementing the MEPDG.

The MEPDG implementation progresses in North America according to numerous publications:

- Velasquez et al. (2009) implemented MEPDG for Minnesota pavement design; they found several software issues and weak correlations for longitudinal cracking in flexible pavements.
- Mallela et al. (2009) implemented M-E design procedures in Ohio.
- Baus & Stires (2010) implemented MEPDG for South Carolina pavement desi, particularly concerned about the longitudinal cracking model.
- Kim et al. (2011) implemented MEPDG for North Carolina pavement design but was limited to rutting and fatigue cracking calibration based on extensive materials characterization and implementing a genetic algorithm.
- Li et al. (2011) revised the pavement thickness design catalog for Washington DOT using both the 1993 AASHTO procedure and the MEPDG with WSDOT historical performance data; they found that the 1993 AASHTO procedure provided accurate results for flexible pavements with a modified layer coefficient for HMA and that MEPDG was not able to model or predict all the desired distresses according to the observed data in the Washington pavement system.
- Williams & Shaidur (2013) calibrated the MEPDG for pavement rehabilitation in Oregon and reported issues with the longitudinal and transverse cracking models.

- Ceylan et al. (2013) and Kim et al. (2014) calibrated the performance models of the MEPDG for Iowa pavement systems, both flexible and rigid; they found that the national and the local-calibrated models for rutting, cracking, and roughness provide good predictions, while the national longitudinal cracking model underestimates the distress.
- Tarefder & Rodriguez-Ruiz (2013) calibrated the MEPDG for flexible pavements in New Mexico; they only calibrated the total rutting model and partially improved the alligator and longitudinal cracking models.
- Nabhan (2015) calibrated the MEPDG for flexible pavements in Nevada, limited to alligator cracking and permanent deformation, and emphasized polymer-modified asphalt binder technologies.
- Kasperick & Ksaibati (2015) calibrated the MEPDG for local paved roads in Wyoming and produced custom axle load spectra and calibration coefficients for the Darwin-ME program.
- Cunha (2016) calibrated the MEPDG performance models for flexible pavement distresses to local conditions in Ontario (Canada), limited to alligator cracking and total permanent deformation, and improved the bias and standard error of the models.
- Sufian (2016) calibrated the MEPDG for Kansas for both rigid and flexible pavements; the rutting and roughness models for flexible pavement yielded a proper calibration, while the fatigue cracking models, both top-down and bottom-up, were not calibrated due to variability and lack of data.

The published research about MEPDG is extensive (Pierce & McGovern, 2014). The author of this dissertation does not pretend to offer a comprehensive review of every document but gives an overview of the mainstream work lines.

Perpetual Pavement Design

The perpetual pavement design is a subset of mechanistic-empirical design with two main features: (a) It pursues to achieve a long life with no deep structural distress as bottom-up fatigue and rutting below the concrete layers, and (b) the method recognizes that all materials have endurance limits below which no damage will occur. In consequence, the method seeks to avoid a terminal structural condition, and the damage ratio as$\left(D = N_{expected}/N_{allowable}\right)$ must be lesser than 1.0 (Timm, Robbins, Tran, & Rodezno,

2014). Accordingly, these pavements are expected to perform for 50 years without major structural rehabilitation or reconstruction (Tarefder & Bateman, 2012).

The typical section of perpetual pavement consists of three hot-mix asphalt layers over a pavement foundation: the bottom layer is a fatigue-resistant material (rich in asphalt, low air-voids, 75 – 100 mm thick), the intermediate layer is a rut-resistant material (high modulus, 100 – 175 mm thick), and the wearing surface is also rut resistant, but durable and impermeable (40 – 75 mm thick) (Newcomb, Buncher, & Huddleston, 2001).

According to different authors, the tensile strain fatigue endurance limit (FEL) of asphalt mixes varies between 60 to 200 με. The structural rutting is controlled by a vertical compressive strain in the subgrade of 200 με or a vertical stress / unconfined compressive strength ratio lower than 0.42. Illinois, Texas, Wisconsin, and West Virginia have provisions for perpetual pavement design. Some use the PerROAD software developed by D. H. Timm for the Asphalt Pavement Alliance (Op. Cit., 2014).

In Israel, Sidess & Uzan (2009) developed a design method for perpetual flexible pavement with an FEL of 70 με (under a single axle load of 130 kN) and Finn's fatigue equation for crack initiation at the end of a 30-year design period. The high cost of asphalt binder requires a subbase layer with a modulus limited to 200 MPa to consider the decreasing confinement stress under the thick asphalt layers. The design does not consider the compressive strain in the subgrade; instead, the authors use the CBR extended method proposed by Uzan as a better approach to protect the pavement foundation.

Tarefder & Bateman (2012) presented an optimal perpetual pavement design implementation for New Mexico with the MEPDG. The authors evaluated structures with and without rich-binder layers and found that the latter is the most economical (and feasible) for HMA thicknesses up to 254 mm. The authors also evaluated the HMA debonding effect and found a marked increment in top-down cracking and some rutting increment.

Perpetual pavements, as a subset of asphalt pavements, also benefit from analysis methods and materials characterization improvements. Cao et al. (2016) applied viscoelastic continuum damage to predict perpetual pavement fatigue performance in

China, with promising results in understanding the performance of asphalt pavements regarding gradation size and distribution and the use of modified binders.

2.4 Summary

Asphalt pavement design for roads and streets evolved from purely empirical to mechanistic-empirical procedures in the twentieth century. Empirical methods are simple, but the original experimental data limit their applicability. CBR-based procedures only address one design issue: protecting the subgrade from excessive load-induced stresses. Later refinements led to the AASHTO guides from 1972 to 1993. Timm et al. (2014) point out that the empirical character of the AASHTO method is particularly troublesome for contemporary design given the limitations of factors such as the structural and drainage coefficients, the ESAL equations, and the limited experience with thick asphalt layers and mix design. Also, the increase in loads and tire pressures in present-day heavier vehicles has surpassed the limits of those applied in the Road Test. Thanks to the layered elastic theory, the analytical approach gained popularity with progressive implementation in personal computers. The main advantage of mechanistic-empirical methods is adapting to changing conditions (Op. Cit., 2014).

Compared with layered elastic theory, the finite element method better represents the stresses, strains, and displacements in non-linear, viscoelastic, real-world materials. However, the increased complexity of models requires a similar advance in laboratory and field characterization. The necessary research, calibration, and training investments can be compensated by the large-scale benefits obtained from a more reliable road network.

The main breakthrough in pavement design is the shift from thickness design procedures to incremental damage analysis procedures. The implementation of MEPDG faces significant challenges in calibrating the national (USA) performance equations and models to local conditions. Hasan et al. (2018) reported that the lack of calibration yields questionable results.

Table 2-4 presents some well-known M-E methods and their characteristics.

Table 2-4: Examples of M-E design procedures for asphalt pavements

Organization	Pavement model	Failure modes	Environmental effects	Pavement materials	Design format
Shell International Petroleum Company (Shell Oil, 1978) (Strickland, 2000).	Layered elastic solid	Fatigue in treated layers Rutting: Subgrade strain Estimate in asphalt-bound layer	Temperature	Asphalt concrete Untreated aggregates Cement stabilized aggregates	Design charts BISAR analysis program SPDM 3.0 design program
NCHRP Project 1–10B AASHTO procedure (Finn et al., 1977)	Layered elastic solid	Fatigue in treated layers Rutting	Temperature	Asphalt concrete Asphalt stabilized bases Untreated aggregates	Design charts MTC093 computer program
The Asphalt Institute, Lexington, KY, USA (MS-1, MS-11, MS-23) (Asphalt Institute, 1981)	Layered elastic solid	Fatigue in asphalt-treated layers Rutting: Subgrade strain	Temperature Soil freezing and thawing cycle	Asphalt concrete Asphalt emulsion-treated bases Untreated aggregates	Design charts DAMA computer program
Laboratoire Central de Ponts et Chaussés (LCPC - SETRA, 1994)	Layered elastic solid	Fatigue in treated layers Rutting	Temperature	Asphalt concrete Asphalt-treated bases Cement stabilized aggregates Untreated aggregates	Design catalog ALIZE computer program
Centre de Recherches Routières, Belgique (Verstraeten, Veverka, & Francken, 1982)	Layered elastic solid	Fatigue in treated layers Rutting	Temperature	Asphalt concrete Asphalt-stabilized bases Untreated aggregates	Design charts MTC093 computer program
National Institute for Transportation and Road Research (NITRR), South Africa (Walker, Patterson, Freeme, & Marias, 1977)	Layered elastic solid	Fatigue in asphalt layers Rutting: Subgrade strain Shear in granular layers	Temperature	Gap-graded asphalt mix Asphalt concrete Cement-stabilized aggregate Untreated aggregates	Design catalog PADS computer program
National Cooperative Highway Research Program (NCHRP) Project 1-26 Procedure (AASHTO) (Thompson & Barenberg, Calibrated Mechanistic Structural Analysis Procedures for Pavements: Phase I—Final Report, NCHRP Project 1-26, 1989)	Idealization with FEM Layered elastic solid	Fatigue in treated layers Rutting: Subgrade strain	Temperature	Asphalt concrete Untreated aggregates	ILLI-PAVE Linear elastic program ELSYM5
Federal Highway Administration U.S. DOT, Washington (Kenis, Sherwood, & McMahon, 1982)	Layered elastic or viscoelastic solid	Fatigue in treated layers Rutting: Estimate at surface Serviceability measured by PSI	Temperature	Asphalt concrete Cement-stabilized aggregate Untreated aggregates Sulfur-treated aggregates	VESYS computer program.
University of Nottingham, Great Britain (Brown, Bunton, & Pell, 1982)	Layered elastic solid	Fatigue in treated layers Rutting: Subgrade strain	Temperature	Continuous or gap-graded asphalt mixes of known volumetric on standard UK materials	Design charts ANPAD computer program
Austroads (Austroads, 1994)	Layered elastic solid	Fatigue in treated layers Rutting: Subgrade strain	Temperature Moisture	Asphalt concrete Untreated aggregates Cement-stabilized aggregates	Design charts CIRCLY computer program .

Organization	Pavement model	Failure modes	Environmental effects	Pavement materials	Design format
Pavement Design for Roads, Streets, and Open Storage Areas, Layered Elastic Method. TM 5-822-13/AF JMAN 32-1018 (Joint Departments of the Army and Air Force, 1994)	Layered elastic solid	Fatigue in treated layers Rutting: Subgrade strain	Temperature	Asphalt concrete Cement-stabilized aggregate Untreated aggregates	LEDROADS computer program (based on JULEA)
Ministry of Transportation of Ontario (He, Cai, & Haas, 1996)	Simplified two-layer elastic equivalent	Progression of IRI as a function of age and traffic	Climatic regions	Asphalt concrete Treated or untreated base and subbase layers	Computer package Ontario Pavement Analysis of Costs – OPAC 2000
National Cooperative Highway Research Program (NCHRP) Project 1-37A (AASHTO MEPDG) (NCHRP, 2004)	Layered elastic solid	Fatigue in treated layers Rutting: Subgrade strain Asphalt concrete time hardening Low-temperature cracking	Temperature Moisture	Asphalt concrete Untreated aggregates Chemical-stabilized materials	JULEA computer program
Flexible Pavement Design System FPS 21 (Liu & Scullion, 2011)	Layered elastic solid	Fatigue in the bottom HMA layer Rutting: Subgrade strain	Temperature Moisture	Asphalt concrete Treated or untreated base and subbase layers	FPS 21 computer program
IMT-PAVE 1.1 (Garnica Anguas & Hernández Domínguez, 2013)	Simplified layered elastic solid by MET	Fatigue in the bottom HMA layer Rutting: Subgrade strain	Temperature Moisture	Asphalt concrete Treated or untreated base and subbase layers	IMT-PAVE 1.1 computer program
CR-ME Ver. 1 (Trejos Castillo, Leiva Padilla, & Loría Salazar, 2014)	Layered elastic solid (3-4 layers) LET analysis not included	Fatigue in the HMA layer, as in MEPDG Rutting in the structure, as in MEPDG	Temperature Moisture	Asphalt concrete Treated or untreated base and subbase layers	CR-ME 1.0 computer program

Source: Adapted from Monismith (2004) and Haas et al. (2007).

A subset of the M-E method is the perpetual pavement design approach that considers low damage ratios to avoid deep structural distress as bottom-up fatigue cracking and rutting of the pavement foundation.

All M-E methods apply the design principles formulated five decades ago. These principles will remain under the premise of understanding the material behavior and the mechanistic approach adaptability. Haas et al. (2007) summarize the *"options and factors"* to consider choosing an M-E design procedure:

- *Options:*
    1. Retain the existing empirical procedure.

2. Update existing empirical procedures.
3. Adopt a new empirical procedure.
4. Retain existing simplified M-E procedures.
5. Implement new simplified M-E- procedures.
6. Phase into the new MEPDG procedure.

- *Factors:*
  1. Calibration requirements, update needs, and frequency.
  2. Implementation plan schedule.
  3. Inputs characterization/properties requirements (traffic data collection, materials, climate)
  4. Balancing complexity/comprehensiveness with understandability and practicality.
  5. Resource needs (people, equipment, training) and costs.
  6. Criteria for validation or assessing the success of the implementation.
  7. The comprehensiveness of the LCCA component of the design procedure package.
  8. Stability of the software.

Adopting an M-E design procedure is not trivial for any Public Highway Agency. Interestingly, Haas et al. (Op. Cit., 2007) suggest the need for some simplification in catalogs of representative designs to check designs from M-E analysis; also, they suggest avoiding the use of M-E *"black box"* packages and implementing checks on the fairness of results. Even more, there is not a consensus in the USA about the pavement design method as the Department of Transportation of the State of California (Caltrans) keeps developing the CalME software and postulates that *"its models and ideas will become part of a multistate or national long-term research and development programs"* (Ullidtz, et al., 2010).

A mechanistic-only approach will be insufficient for the adequate structural design of asphalt pavements. The empirical component is still necessary for pavement design. There is still a gap between the theoretical approach and the expectations of those in charge of the construction and maintenance of the pavements.

3 Applied optimization in pavement engineering

People are the nature of the city, and you can feel it in the pavement.

Andy Goldsworthy.

An abridged version of section 3.2.2 was published as "Applied Metaheuristic Optimization in Asphalt Pavement Management" in Ciencia e Ingeniería Neogranadina (Vásquez-Varela & García-Orozco, 2021).

An abridged version of sections 3.2.3 and 5.1 is under review for publication under the title "Pavement moduli backcalculation based on particle swarm optimization."

Optimization is the art of selecting the best alternative in a set of valid options (Gallego, Toro, & Escobar, 2015) or finding the best solution from a feasible solutions pool (Dede, Kripka, Togan, Yepes, & Rao, 2019). These definitions relate to sound engineering practice because optimization implies reducing cost or energetic consumption and the maximization of the profitability of a system.

Optimization is a three-step decision-making process: (a) know or model the system or process, (b) define the objective function, and (c) apply the theory of optimization (Diwekar, 2008). Pavement design optimization may be *"making an assemblage of materials sustain loads in the best way"* (Christensen & Klarbring, 2009), for example, with long-duration or high bearing capacity subjected to budget or environmental constraints.

This chapter presents the fundamentals of optimization theory and reviews its application in pavement-related problems.

3.1 Optimization algorithms

According to Yang (2013), there are three integrated components of the optimization process applied to complex simulations of any problem:

1. An optimization algorithm: It is the tool to find the desired optimum. It must consider the uncertainty of the actual world to be robust and adaptable to exceptional situations. Two of the three primordial problems of optimization relate to the algorithm selection: (a) The efficiency of the algorithm considering different perspectives, e.g., whether it depends on a gradient or if it is determinist or stochastic, and (b) the adequacy of the algorithm to analyze the problem.
2. An efficient numerical simulator: This is the third primordial problem and determines if one can obtain relevant results in an acceptable time for the analysis and design process. A simulator can be a simple function subroutine, a multiphysics solver, or an external black-box evaluator with running times from milliseconds to days or weeks.
3. A realistic representation of a physical process requires adequate comprehension of the problem.

Figure 3-1 shows a classification of optimization algorithms based on several criteria. One must recall that no single algorithm is appropriate for all problems, and sometimes, it is necessary to combine algorithms to achieve better results (Op. Cit., 2013).

3.1.1 Heuristics and metaheuristics

A heuristic is a search method for an optimum through trial and error, which does not follow a rigorous course. The *"aleatory search"* and *"local search"* algorithms are examples of the first algorithms with heuristic rules in size selection, stopping criteria, starting points determination, and identification of new possible solutions (Toklu, 2014).

Etymologically, a metaheuristic implies a higher level. Metaheuristic algorithms are *"stochastic optimization methods inspired by the observation of several sources"* such as nature, physics, mathematics, music, animal sociology, and politics. These techniques appeared in the last quarter of the twentieth century, and today, more than fifty algorithms are available to solve different engineering and design problems (Op. Cit., 2014).

Figure 3-1: Optimization algorithms classification

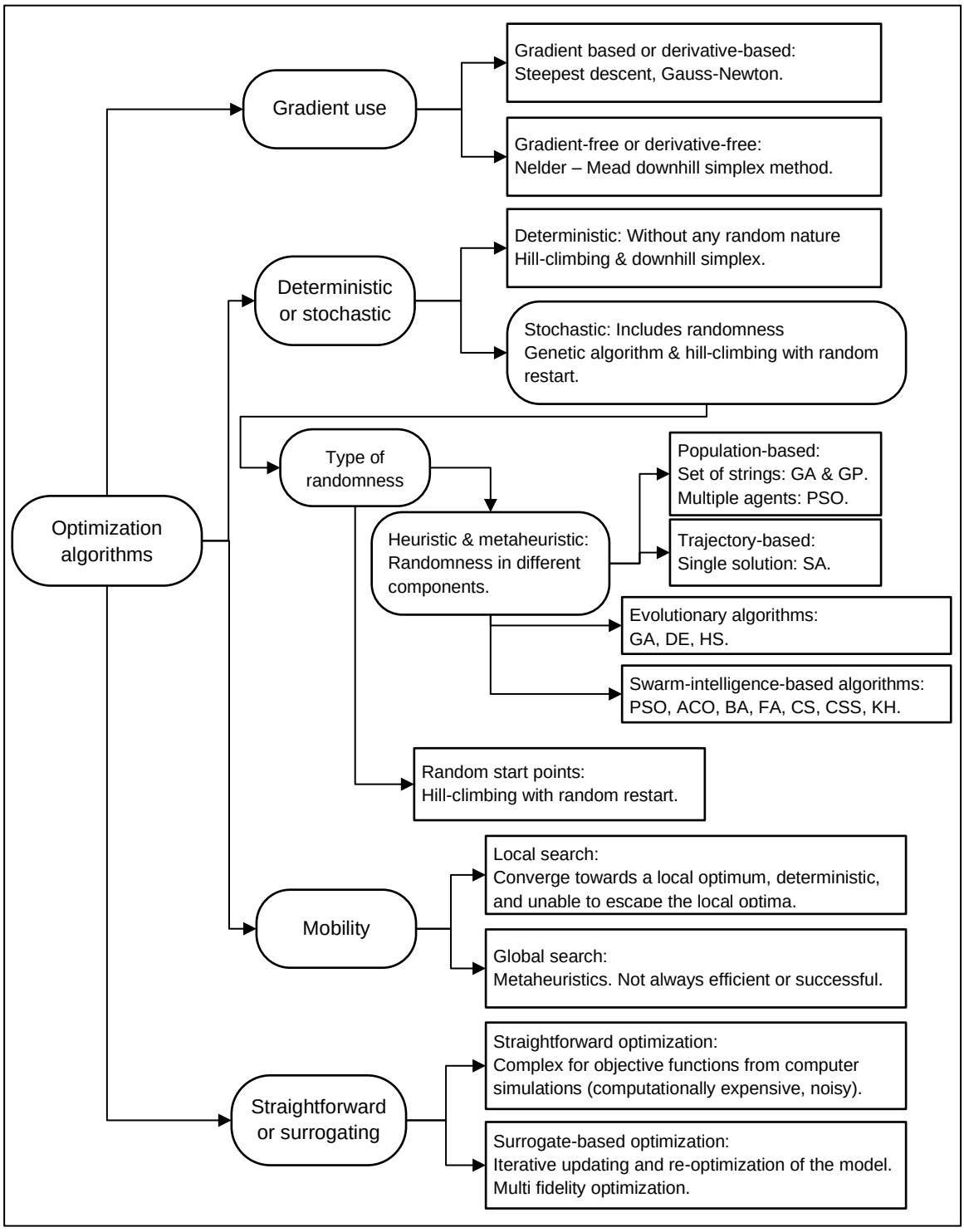

Source: Adapted from Yang (2013) and Gandomi et al. (2013).

Metaheuristics have a delicate balance between intensification (intensive local search) and diversification (global exploration of the search space) by introducing randomness inside the algorithm components. Also, proper mechanisms select and keep the best solutions, for example, the survival of the fittest in one generation and elitism in the following (Yang X. S., 2013). Figure 3-2 shows a general flowchart for metaheuristic methods.

Figure 3-2: A general flow chart for metaheuristic methods

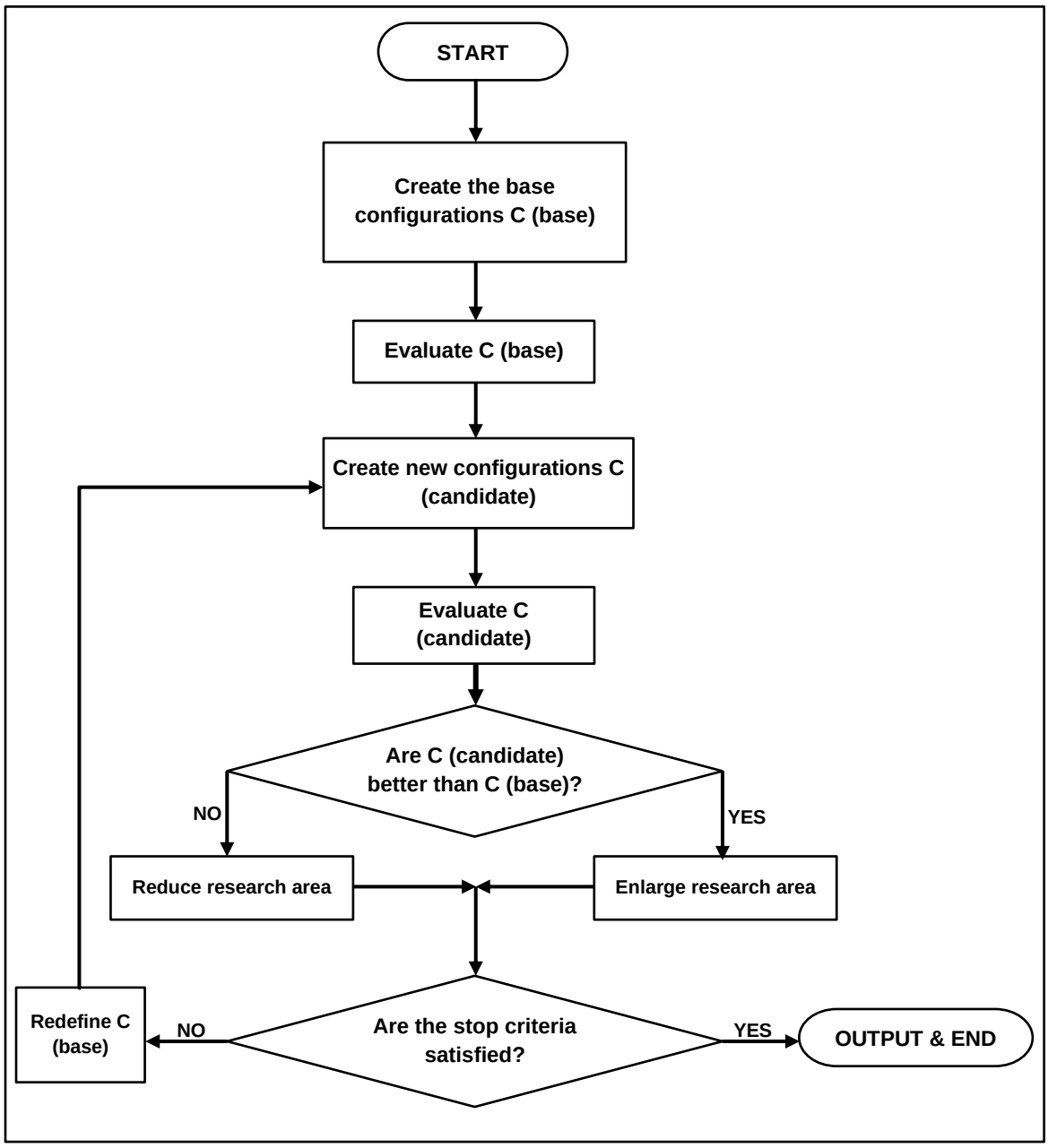

Source: Toklu (2014).

Metaheuristic optimization algorithms are often inspired by nature. Bio-inspired algorithms use biological evolution or the collective behavior of animals as their models. Science-inspired algorithms imitate the physics or chemistry process. Art-inspired algorithms implement the creative behavior of musicians or architects. Social-inspired algorithms simulate social behavior to optimize (Gandomi, Yang, Talatahari, & Alavi, 2013). Table 3-1 summarizes some metaheuristic algorithms and their general features; however, it is an ongoing research topic, and researchers propose new algorithms yearly.

Table 3-1: Some metaheuristic optimization algorithms

Algorithm & authors	Type of algorithm	Year of introduction	Inspiration or analogy
Genetic algorithm (GA) Holland	Population-based Evolutionary	1975	It is based on Darwin's theory of the evolution of the species. It applies concepts like crossover, mutation, and selection of the fittest. The possible solutions are codified in "*chromosomes*," for example, as binary chains, subjected to generational evolution with the crossing of parents, mutation of small proportions of the offspring, and emphasis on preserving the best adapted according to the objective function (elitism). The algorithm operates in multiple, randomly created base vectors, crossed and mutated to create candidate vectors. The genetic algorithms have hundreds of applications, including hybrid techniques or combinations with other algorithms.
Simulated annealing (SA) Kirkpatrick, Gelatt & Vecchi	Single solution-based	1983	It mimics the metallurgical process of controlled metal cooling to change their properties. The algorithm operates on a single base vector preserved or improved in each iteration to create a candidate vector. The algorithm uses an aleatory search for a Markov chain that accepts changes that improve the objective function and preserves, with a probability P, some minor changes from the pursued objective.
Taboo search (TS) Glover	Single solution-based	1989	It explores the search space by a sequence of moves and escapes from local optima with moves listed in a forbidden (taboo) list. The algorithm includes the taboo list, neighborhood, aspiration criterion, termination criterion, and cost function. The aspiration criterion determines the best search move from the current neighborhood by finding a new one at a lower cost.
Ant Colony Optimization (ACO) Dorigo	Population-based Swarm-intelligence	1992	It mimics the behavior of ants to find the shortest paths between their colony and food sources. The quality of the path depends on the pheromone concentration left by the ants. The path marked with the pheromone's high intensity represents the system's global memory.
Cultural Algorithm (CA) Reynolds	Population-based	1994	The principle of cultural evolution inspires it. The agents or individuals consider outlining, dominant belief, acceptance, and selection to update the next generation's agents. The experiences of individuals generate the problem-solving knowledge stored in the belief space.
Particle swarm optimization (PSO) Kennedy & Eberhart	Population-based Swarm-intelligence	1995	It mimics the behavior observed in nature in bird flocks or fish shoals. It is based on studying individual particles' trajectories in the search space, attracted to the optimum solution. The process is stochastic and uses the memory of each particle.
Differential evolution (DE) Storn & Price	Population-based Evolutionary	1996	It is an evolutionary algorithm based on vectors that allow cross, mutation, and selection operations on each codified solution chain component. Unlike genetic algorithms, DE carries out operations over each dimension of the solution.
Harmony search (HS) Geem, Kim & Loganathan	Population-based Evolutionary	2001	It is an algorithm based on the inspiration process of a musician under three scenarios: (a) he or she will play by heart a famous piece (series of tones in harmony), (b) he or she will play something like a famous piece but changing some tones, and (c) he or she will compose something with new or random notes. These scenarios are equivalent

Algorithm & authors	Type of algorithm	Year of introduction	Inspiration or analogy
			to the three components of optimization: harmonic memory (a form of elitism), tone adjustment (a form of mutation for local search), and randomness (to generate diversity in search of a global optimum). The algorithm operates in multiple base vectors processed with HS's three parameters to create a candidate vector for evaluation.
Ant algorithms (AA)	Population-based Swarm-intelligence	2004	They are based on ant colonies' behavior. A pheromone concentration indicates the quality of a solution to a problem represented by a path between nodes. It is suitable for discrete optimization problems.
Bee algorithm (VBA or ABC) Karaboga & Basturk	Population-based Swarm-intelligence	2004 – 2007	They are based on bees' collecting behavior, although some versions also employ pheromones. The maximization of the nectar recollection is the indicator of the quality of the solution to a problem. Some algorithms allocate forager bees to different food sources, and others define specialized classes of bees (forager, observer, and scouts). They are suitable for discrete optimization problems like routing.
Big Bang – Big Crunch algorithm (BBBC) Osman & Eksin	Population-based	2006	It uses a randomly created initial population called the Big Bang phase. The individuals from the Big Band phase are uniformly dispersed through the search space. A convergence operator then obtains one output from the Big Crunch phase's feasible inputs to create a new population to search for optimal solutions.
Firefly algorithm (FA) Yang	Population-based Swarm-intelligence	2008	It is based on the flight patterns of fireflies considering three rules: (a) fireflies are asexual and attracted to each other without gender preference, (b) their appeal is proportional to their glow, and both are reduced with distance, (c) the landscape of the objective function determines the firefly glow.
League championship algorithm (LCA) Kashan	Population-based	2009	It is based on the championship process in a sports league. The league represents the population; each team represents the individuals; team formation represents a solution. An iteration represents a week. The playing strength represents the value of the objective function.
Glowworm swarm optimization (GSO) Krishnanand & Ghose	Population-based Swarm intelligence	2009	It mimics the behavior of glowworms that represent a feasible solution set. Glowworms contain a luminescent quantity called luciferin, whose intensity determines the value of the objective function. The best solution has the highest density of luciferin. The glowworms move toward brighter individuals using a probabilistic mechanism to create new individuals.
Cuckoo search (CA) Yang & Deb	Population-based Swarm-intelligence	2009	It is based on the Cuckoo bird's progress, a parasite bird that lays its eggs on other birds and other species' nests to favor its offspring. The Cuckoo search considers three idealized rules: (a) Each Cuckoo lays an egg at a time in a random-selected nest, (b) the best nest with high-quality eggs passes to the next generation, and (c) the number of available nests is fixed, and there is a probability that the cuckoo egg will be discovered by the bird that owns the nest, which will discard it or leave the nest to build a new one. The eggs in the nests represent the solutions.
Bats algorithm (BA) Yang	Population-based Swarm-intelligence	2010	The echo-localization technique is based on bats' ability to detect food, prey, and obstacles. Its codification has similarities to simulated annealing.
Charged System Search (CSS) Kaveh & Talatahari	Population-based Swarm-intelligence	2010	It is based on the governing laws of charged systems. It uses multiple agents or *"charged particles"* (CP) that interact according to the Coulomb and Gauss laws of electrostatics and Newton's laws of motion. CP moves considering the resultant forces and their previous velocity at each iteration. A charged memory stores the number of positions for the best agents.
Teaching-learning-based optimization (TLBO) Rao, Savsani & Vakharia	Population-based	2011	This algorithm has two phases: The Teacher phase and the Learner phase. In the first phase, the best solution is defined as a teacher. The new solution is created in the teacher's neighborhood using the mean solution and the teaching factor. If the new solution is better than the old one, it replaces the former teacher. In the learner phase, the solutions are students, and new solutions arise in the neighborhood.
Krill Herd (KS)	Population-based	2012	It is based on simulating the herding behavior of krill individuals. The movement objectives are the minimum distances of each krill from

Algorithm & authors	Type of algorithm	Year of introduction	Inspiration or analogy
Gandomi & Alavi	Swarm-intelligence		food and the herd's highest density. The components of the time-dependent motion of the krill individuals are (a) movement induced by other individuals, (b) foraging activity, and (c) random diffusion. The calibration of the KH algorithm used empirical data from real-world krill systems. It only requires tuning the time intervals.
Back-tracking search (BSA) Civicioglu	Population-based	2013	It has five components: initialization, first selection, mutation, crossover, and second selection. The first selection phase determines the historical population using memory. The mutation and crossover process generates the initial and final forms of the trial population. The second selection phase takes the best selection of individuals as a solution.
Jaya (*"Victory"*) Rao	Population-based	2016	Jaya starts with a randomly created population and identifies the best and worst solutions. The new individuals are generated around the best solution avoiding the worst one.
The innovative gunner (AIG) Pijarski & Kacejko	Population-based	2019	Also called the *"ballistic algorithm."* It is inspired by the mathematical idea of the projectile motion theory. The decision vector components are subjected to *"multiplicative"* modifications in each successive step instead of *"additive"* modifications like those in PSO or SA. The theoretical justification of its usefulness is currently under study.

Source: Adapted from Yang (2013), Toklu (2014), Gandomi et al. (2013), Dede et al. (2019), and Pijarski & Kacejko (2019).

The increasing formulation of new algorithms may not imply differences in performance for any given problem. In 1997, Wolpert & Macready postulated the *"no-free-lunch"* (NFL) theorem, which states, *"any algorithm is as good/bad as random search when averaged over all possible problems/functions."* Thus, there is no universally efficient algorithm considering a limited search space closed under permutation.

A review by Yang (2011) reported that Corne & Knowles in 2003 suggested that *"some multi-objective optimizers are better than others."* Also, in the same reference, Auger & Teytaud in 2009 claimed that the NFL theorem is not valid for continuous domains, but Rowe, Vose & Wright refuted them in 2011. At the same time, Marshall and Hinton alleged that, without closed permutation, the NFL theorem does not hold and is unproved for unlimited or continuous domains for multiobjective optimization.

Gandomi et al. (2013) identified several challenges concerning future developments in metaheuristics:

1. There is a lack of a unified framework.
2. There are many open problems:
    a. The effect of algorithm-dependent parameters on efficiency.
    b. The optimal balance between exploration and exploitation.

   c. The effect of algorithm-memory on performance.
3. There is a gap between theory and practice because metaheuristic applications expand faster than mathematical analysis.
4. The multiplicity of new algorithms challenges the general understanding of metaheuristics mechanisms.

Kuyu & Vatansever (2021) reviewed several advanced metaheuristic algorithms and concluded that it is not easy to identify the best algorithm. They considered several performance metrics and found that some algorithms have more robust and stable structures to solve complex problems. Any comparison should guide researchers in choosing the proper algorithm for specific problems.

3.1.2 Multiobjective optimization

Multiobjective or multicriteria optimization considers more than one objective or cost function (Yang X. S., 2013). Most engineering applications in the real world are multiobjective. Multiobjective optimization is computationally expensive. Most studies consider two or three objectives, while real problems may require dozens of design objectives (Yang, Koziel, & Leifsson, 2014).

A multiobjective optimization tries to find a variable vector that satisfies the constraints and optimizes an objective vector function whose elements represent the individual objective functions. The multiple objectives are usually in conflict, and the solutions are a trade-off between good and not-so-good features. Correspondingly, one must expect an increase in the computing cost of the problems. The optimization algorithms apply the concept of dominance to find when a solution is better than others. A solution dominates another solution when it is better in all the objectives or strictly better in one objective. The set of non-dominated solutions in the objective space is a Pareto front (Gallego, Toro, & Escobar, 2015). Figure 3-3 shows the Pareto optimum sets for different combinations of two objective functions based on the maximization or minimization of the objective function. A Pareto front may converge to a single point, i.e., the optimal solution to the problem.

Figure 3-3: Pareto optimum sets for different combinations of two objectives

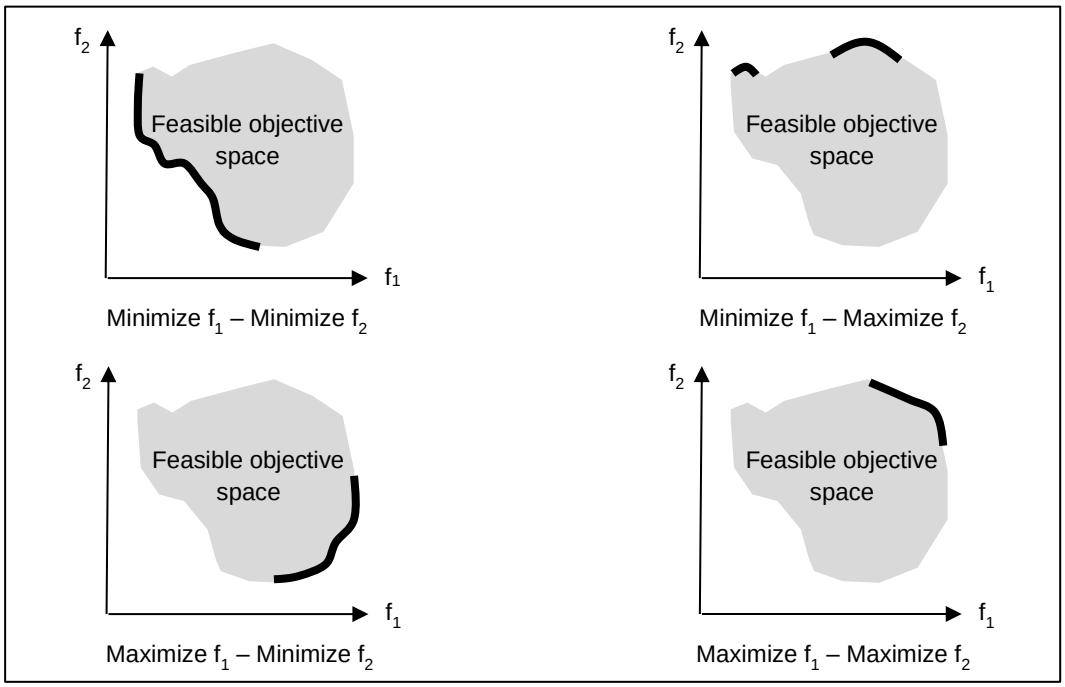

Source: Gallego et al. (2015).

According to Wu et al. (2012), multiobjective optimization in highway asset management will be more used when the concept of optimization permeates the decision process in highway agencies. The highway systems require multiobjective optimization due to their environmental impact on economic development, ecological sustainability, and social desirability. A highway system is a three-dimensional interacting system of objectives, facilities, and operational functions that demands trade-offs in resource allocation. The resource allocation must satisfy the public demands for better infrastructure beyond the least-cost solutions.

3.2 Applied optimization in pavement engineering

Cercevik et al. (2014) identified several metaheuristics applications to civil engineering problems, including structural design and structural analysis, hydraulic works, construction management & scheduling, geotechnical engineering, transportation engineering, and construction materials. Likewise, Dede et al. (2019) did an extensive review of civil engineering optimization techniques for 1999 – 2019. They summarized multiple optimization algorithms in geotechnical, transportation, construction management,

structural, hydraulic, and mechanical engineering problems. Although the authors did not claim a comprehensive review in all areas, one must notice that they only reported two applications in pavement design and management among 147 references.

Pavement engineering is a crossroads between geotechnical and transportation engineering with a sound base in construction materials. It is not surprising that there are multiple applications of optimization algorithms in this area, emphasizing pavement management for its socioeconomic implications and backcalculation of mechanical properties for its complexity.

In the following sections, the author summarizes several examples of applied optimization in pavement engineering considering five broad areas: (a) pavement design, (b) pavement management systems, (c) backcalculation of pavement moduli from deflections, (d) data fitting, and (e) reliability-based design optimization (RBDO). At the end of the chapter, the author summarizes each subject.

Most of the applications use genetic algorithms (GA). Figure 3-4 presents a flowchart and some distinctive features of this metaheuristic.

Darwinism inspired genetic algorithms (Chan, Fwa, & Tan, 1994). Natural evolution takes place in chromosomes that encode the structure of living things. A *"chromosome"* represents a set of feasible solutions or *"genotypes."* Each genotype is encoded in bits values known as *"alleles."* Genetic algorithms create an initial (random) population representing a set of feasible solutions. The initial population evolves through genetic selection to give a proper solution according to a *"fitness function."*

The fitness function may be the objective function or a modified form of the latter. The better solutions may reproduce according to their relative fitness ranking, i.e., the better genotypes reproduce and remain in the next generation (*"elitism"*). The usual genetic operators are *"crossover,"* or the combination (in one or many points) of unchanged alleles of two genotypes, and *"mutation,"* or the random change of one or more alleles. The genetic operators work in binary codification (0, 1); however, integer or real codifications are also possible. The evaluation, offspring creation, and solution-pool selection converge to an optimum solution or ends on a preset number of generations.

Figure 3-4: Flow chart and distinctive features of problem-solving with GA

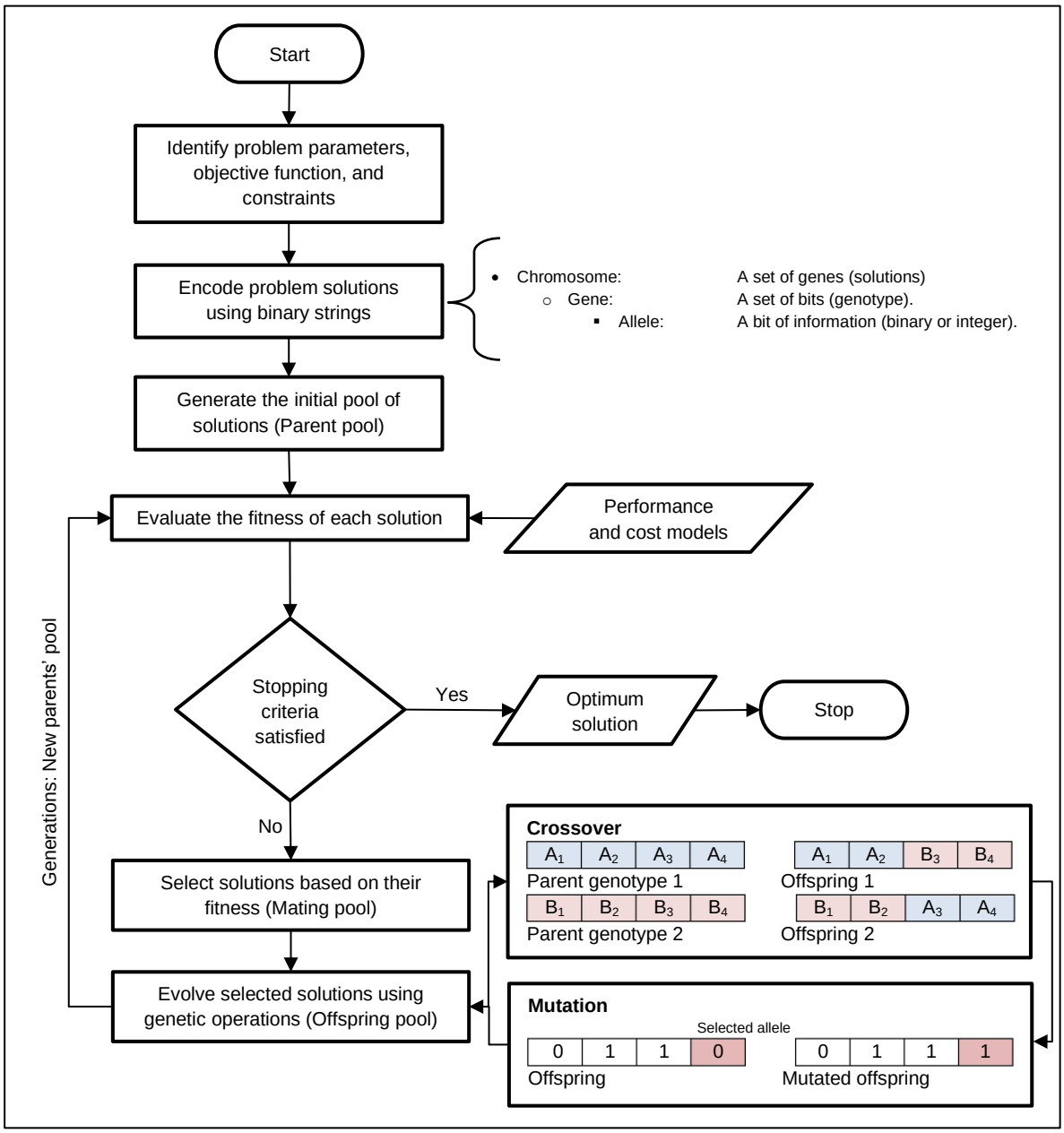

Source: Adapted from Morcous & Lounis (2005) and Chan et al. (1994).

There are three issues in encoding and decoding of solutions in chromosomes: (a) feasibility of the given solution, (b) legality of the decoded chromosome, and (c) uniqueness, i.e., each decoded chromosome only represents one feasible solution (Morcous & Lounis, 2005). The encoding issues require implementing penalty functions or repairing procedures into the fitness function with an increased computing cost of unfeasible solutions.

3.2.1 Applications in pavement design

The pavement design applications are a subset of the general pavement management applications, focusing on project-level analysis for specific design conditions of subgrade, traffic, and construction materials. As expected, the problem's treatment has become more complicated in recent years, including incremental pavement design with economic (LCCA) and environmental considerations.

Oppenlander et al. (1971) proposed a method for flexible pavement design optimization based on linear programming with an objective function of minimal cost and nine constraint equations related to the cost of building materials, design requirements, and environmental conditions. The authors considered three different design cross-sections without a subbase, with a subbase through the shoulders, and with a subbase and subdrains. The design must satisfy the required structural number based on the AASHO Road Test performance algorithm and mitigate the freeze-thaw (environmental) process. Other constraints define the range of thicknesses of bituminous surfaces, stabilized bases, and base aggregate bases. Based on worked examples, the authors conclude that it is possible to optimize the pavement design and recommend sensitivity analysis of the unit cost of material, bearing capacity of the subgrade, and freeze-thaw conditions.

Rouphail (1985) formulated a mixed-integer linear-programming model to determine a minimum initial cost for flexible pavement design based on the 1972 AASHTO Interim Guide Procedure. The analysis did not consider overlay construction and assumed that the AASHTO empirical models were valid from two-layer (full-depth asphalt) to four-layer (asphalt over base and subbase courses) structures. The author considered one cost minimization equation and 27 constraints related to the structural number and a range of thicknesses as binary variables. A case study showed the linear programming ability to propose an optimal structure different from the AASHTO algorithm's design. The author suggested expanding the method to consider maintenance and rehabilitation costs.

Mamlouk et al. (2000) developed a methodology based on dynamic programming to optimize the initial thicknesses of the pavement layers and the future HMA overlay activities considering smoothness, fatigue cracking, and rutting by combining the AASHTO design algorithm, the layered elastic software ELSYM5, and the life cycle cost analysis. The objective function minimized the total pavement cost, composed of agency costs (initial

construction and overlay costs) and user costs. The optimization is feasible for project-level management thanks to the combination of empirical and mechanistic methods.

Liu & Wang (2003) implemented a genetic algorithm for asphalt pavement design whose optimizing criteria were rutting, fatigue cracking, and cost. The objective function minimizes the construction cost subjected to a fixed range of thicknesses. The authors described *"promising results,"* but the paper is unclear about the analysis method. The emphasis on Chinese experience with cement-treated bases limited the search space for optimum solutions.

Pryke et al. (2006) presented a genetic algorithm optimization with an objective function based on the pavement cost and restrictions in transfer damage functions and the range of thicknesses. The authors use a simplified layered elastic theory based on the equivalent thickness method. This approach produces lower costs than the Shell Oil design method. Although there is room for improvement in the analysis method and the life-cycle cost analysis, the authors considered promising the genetic algorithm's capacity to optimize the design.

Ghanizadeh (2016) proposed a linear programming model to determine the optimum configuration and thicknesses of asphalt and untreated granular bases with the Iranian practice based on the AASHTO 1993 design method. The objective function minimizes the initial cost of pavement. The author concluded that asphalt-treated layers were not cost-effective for the controlled conditions of the analysis, and subgrade strengthening allows granular subbase removal.

Chong et al. (2018) developed a method to quantify the effects of pavement design and management decisions on the economic and environmental performance of flexible pavements in Hong Kong conditions. The authors used a commercial version of the *"AASHTOWare Pavement ME Design"* to predict the performance of 206 pavement structures with two IRI (1.76 & 2.16 m/km) and one cracking (20%) thresholds for resurfacing or reconstruction activities under three levels of traffic: high (AADTT = 10,000), medium (AADTT = 5000), and light (AADTT = 2500). The predicted IRI, the total life-cycle costs (agency plus user's costs), and the *"roadbase thickness"* (HMA base course in British terminology) defined a 3D search space for the optimum design. The authors computed the

energy consumption and the greenhouse gas emission for each structure and proposed three predictive polynomial equations based on IRI and roadbase thickness.

Three-dimensional Pareto fronts indicated that cost savings require a thinner roadbase and higher IRI threshold for resurfacing. In comparison, greenhouse emissions reduction demands a thicker roadbase and a lower IRI threshold for resurfacing. Energy consumption lies between costs and greenhouse emissions requirements. Non-Preemptive global programming defined the optimum roadbase thickness as 297 mm for heavy traffic, 190 mm for medium traffic, and 135 mm for light traffic with IRI thresholds of 2.48 m/km, 2.20 m/km, and 2.30 m/km, respectively.

3.2.2 Applications in pavement management systems

Pavement management consists of systematic planning and programming expenditures, design, construction, maintenance, operation, and in-service evaluation of pavement structures in roads, airports, and parking lots. The management activities include data acquisition, planning, programming, new construction, maintenance, rehabilitation, and renovation of pavements [Hudson et al. (1997) in Golroo & Tighe (2012)].

The decision process in pavement management has two basic levels: (a) the network level to develop a priority program and schedule work within a budget, and (b) the project level to focus on a particular location and prioritize the physical implementation of network decisions (Sundin & Braban-Ledoux, 2001).

Pavement management systems (PMS) consider multiple objectives like minimizing the discounted total or annual expenditures, maximizing the pavement network condition according to a performance measure (PSI, PSR, and PCI), or maximizing the use of the workforce and machine resources. In general, there are two types of maintenance and rehabilitation scheduling problems in pavement management: the budget planning problem (minimizing cost over time) and the budget allocation problem (maximizing the effectiveness or minimizing user's costs) subjected to budget constraints (Gao, Xie, Zhang, & Waller, 2012). The programming of PMS activities based on ranking methods or subjective priority rules does not guarantee optimal utilization of available resources (Fwa, Chan, & Hoque, 1998), while effective management produces a safe environment for public users (Herabat & Tangphaisankun, 2005).

Figure 3-5 shows the components and activities of a pavement management system. The PMS evolved into Asset Management Systems, combining engineering principles with business practice and economic theory (Flintsch & Chen, 2004). Asset management is a resource allocation and utilization process across several decision-making levels like asset class, category of works, and projects in each asset class and work category (Wu, Flintsch, Ferreira, & de Picado-Santos, 2012).

Figure 3-5: Pavement management system components and activities

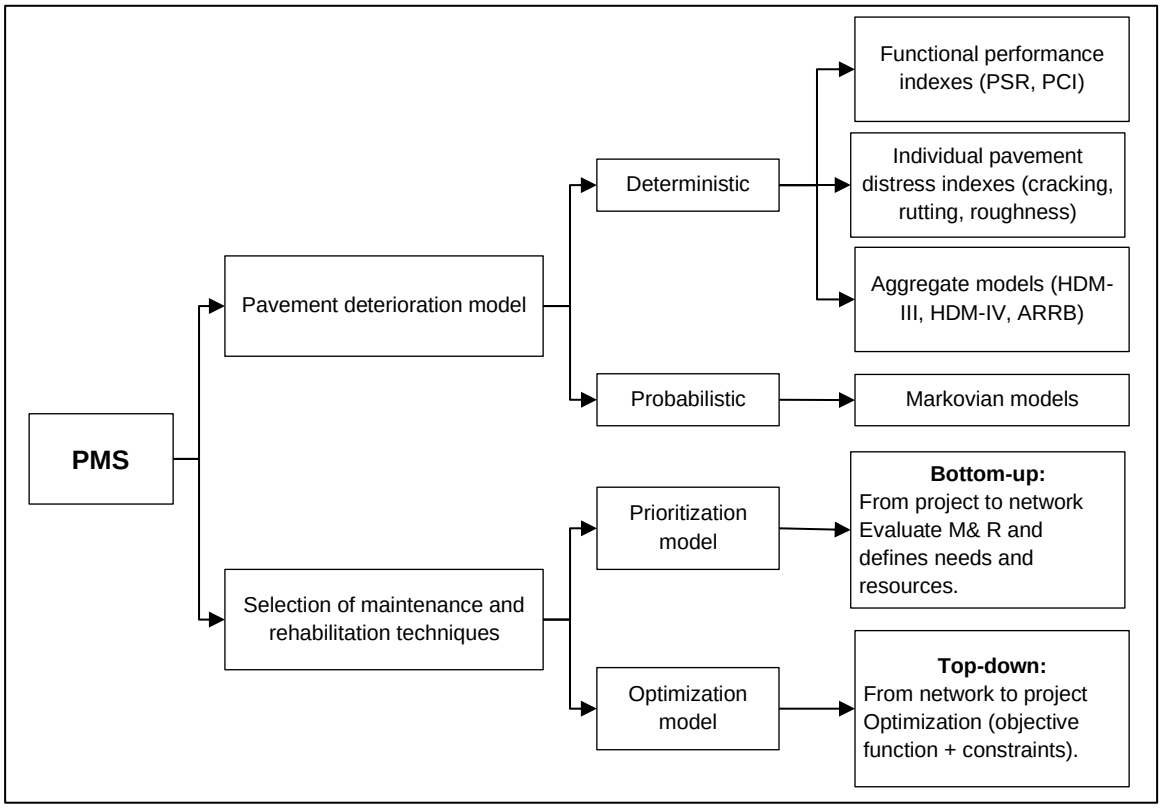

Source: Adapted from Yang et al. (2015).

The need for optimization techniques is evident; for example, in the combinatorial double-exponential budget allocation problem on a pavement network, whose search space of possible solutions is equal to:

$$S_s = (A)^{(P_s)^T}$$

Eq. 3-1

Where S_s is the size of the search space for the optimizing problem, A is the number of activities, P_s is the number of pavement sections, and T is the analysis period (years).

Pavement management systems require a module to solve this combinatorial problem and address the optimization of maintenance alternatives at the network level (Yepes, Torres-Machi, Chamorro, & Pellicer, 2016).

Consequently, if one considers four management activities (0 – do-nothing, 1 – routine maintenance, 3 – rehabilitation, and 4 – reconstruction) and an analysis period of 20 years, the number of pavement sections in the network defines the size of the search space for the problem. A pavement section represents similar climate, traffic, subgrade, materials, and pavement condition. For example, two climatic zones (coastal and in-land; or valley and mountain), three levels of traffic (ESAL ≤ 0.5E06, 0.5E06 < ESAL ≤ 5.0E06, and ESAL > 5.0E06), four types of subgrade (CBR ≤ 3%, 3% < CBR ≤ 6%, 6% < CBR ≤ 10%, and CBR > 10%), two types of pavement (flexible and rigid), and seven categories of pavement condition (PCI by ASTM D6433) yields 336 times N combinations, where N is the actual number of sections in the pavement network. Section longitude may range between hundreds to thousands of meters, so the number of sections in a road network is significant. Thus, for a 20-year analysis period, the combinations of management activities in the network are $(4)^{[336\times \mathrm{N}]^{20}}$. This *"combinatorial explosion"* defines an *"N-hard"* problem which needs significant computer power (Pilson, Hudson, & Anderson, 1999).

A literature review shows multiple optimization techniques applications to the pavement management problem. Before reviewing metaheuristic applications, it is convenient to discuss the more known "What-If" models of pavement management based on *"options evaluation systems"* such as RTIM, HERS, HDM III, HDM-4, or Real Cost.

According to Tsunokawa et al. (2006), What-If models predict the consequences of different maintenance options based on relationships for predicting pavement performance and user benefits over time. However, their optimizing capabilities are limited because they require exogenously specified maintenance options. The authors applied standard optimization algorithms to What-If models to find global optimum maintenance options based on the HDM-IV system. The optimization used two gradient search methods (not metaheuristics) to maximize net user benefits. They found implementing the HDM-IV system feasible with fast convergence into an optimization scheme. However, they also confirmed that the What-If system could not achieve objective optimization. Later, Van Hiep (2009) also applied the gradient search method and defined the efficient pavement design based on the most

significant structural capacity per cost unit; thus, the objective function maximizes a cost-based ratio. The method used existing tools for pavement management, such as HDM III & IV, RTIM, HERS, and Real Cost models, which are *"weak"* because they search the optima in exogenous alternatives. The author stated that road networks do not require prioritization but optimization, which is possible with life-cycle cost analysis.

Wu et al. (2012) reviewed the application of multiobjective optimization techniques at strategic (cross-asset), network, and project levels of highway asset management. They highlighted the advantages of multiobjective optimization techniques over traditional approaches. The authors described several techniques for supporting infrastructure management decisions, considering multiple objectives like the weighting sum method, goal programming, compromising programming, the ε-constraint method, the multi-attribute utility theory, the analytic hierarchy process, and the genetic algorithm. No single multiobjective optimization technique is superior, and the applicability depends on the conditions for the problem and available information. Despite the potential of multiobjective optimization, the authors pointed out that their implementation is difficult because of the resistance to change legacy systems, the difficulty of understanding some sophisticated techniques and their benefits, and the lack of adequate information to develop reliable models.

The following sections summarize several experiences, primarily but not exclusively based on genetic algorithms.

3.2.2.1 Optimization with genetic algorithms

Chan et al. (1994) developed the PAVENET program, adapting the genetic algorithm for analyzing the road maintenance management problem at the network level. The objective function minimizes the present value of maintenance over the planning horizon, maximizes the yearly allocated budgets, or minimizes the fluctuations of the yearly expenditures. The program did not consider any significant rehabilitation within the period of analysis. The authors preferred integer over binary codification for the maintenance activities. The program predicted pavement conditions with deterministic closed-form equations for cracking, rutting, and surface disintegration by dividing the analysis period into active (corrective and preventive activities) and passive planning periods (only corrective repairs).

Fwa et al. (1994) presented a detailed application of PAVENET. The objective function maximizes the management activities subjected to production requirements, budget constraints, workforce availability, equipment availability, material availability, and rehabilitation constraints. The case study considered four highway types, four pavement repair activities, and three need-urgency levels, considering the number of workdays in a month. The authors used an initial population of 80 genotypes, with 80% of invalid penalized individuals considering the problem constraints. The genetic algorithm converged at 28 generations with less computational cost than an integer programming approach used for comparison.

Taha & Hanna (1995) presented a genetic algorithm approach that evolves a neural network model to select the optimum maintenance strategy for flexible pavements from a series of if-then-else rules (expert system). The input factors considered distress type and density, riding condition index, traffic volume, crack type, and distress severity. A backpropagation-trained genetic algorithm provided the artificial neural network with better parameters based on the performance of unseen cases (outside the network training database). The genetic algorithm used ten neural networks trained for 100 epochs.

Fwa et al. (1996) improved the PAVENET-R program to apply genetic algorithms in the programming of pavement maintenance and rehabilitation activities of a road network over a multiple-period planning horizon. The model considered the network division in uniform segments, defined a planning period, and implemented warning levels and prediction models for cracks, ruts, and surface disintegration based on the AASHTO flexible pavement performance algorithm.

The PAVENET-R program considered three maintenance alternatives (crack sealing, patching, and leveling) and one rehabilitation option with a hot-mix asphalt overlay for a PSI lower than 2.5. To describe the proposed intervention, the authors used integer codification for each pavement segment with five-digit codes from 0 to 8. The initial population contained only valid genotypes controlled by a table of feasible alternatives. The objective function minimizes the total present cost, constrained to the relationship between the overlay rehabilitation costs, the combination of the maintenance activities (four cases), and the feasibility of the combined alternatives. The simulation results pointed out that as the

costs of maintenance activities increase concerning rehabilitation, it is more economical to rehabilitate more pavement segments.

Fwa et al. (1998) used genetic algorithms as a programming tool for pavement management, considering different objective functions and developing numerical examples without presenting technical details about the genetic algorithm itself (population, generations, and crossover and mutation rates). The authors concluded that genetic algorithms offered a powerful tool to obtain specific optimal and near-optimal solutions to assess the effect of single or weighted objective functions.

Pilson et al. (1999) considered a multiobjective optimization and applied an interactivity model to predict pavement deterioration. The multi-objective function considered the pavement's cost and performance level and defined an *"efficient"* frontier or Pareto front. This frontier becomes a hypersurface for additional objective functions. The authors estimated the pavement deterioration with a linear-regression interactivity model related to material conditions in four-layer asphalt pavement. A numerical example showed that obtaining efficient (Pareto) network surfaces was possible considering two objectives, including penalties for unfeasible individuals.

Fwa et al. (2000) developed a genetic algorithm-based formulation for multiobjective programming of pavement management activities. The authors reviewed the same problems solved in their previous publications considering two and three objective functions to identify a Pareto front. The original objective function maximizes the labor in total workday units in pavement maintenance. Other objective functions considered minimizing the total maintenance cost and maximizing the overall network pavement condition. A final solution selection may consider the expected budget level or any other form of weighting between criteria.

Shekharan (2000) used genetic algorithms to evaluate five pavement deterioration models from synthetic databases created from multiple regression models. Deterioration models are essential in the pavement management system to estimate pavement condition evolution and trigger the warrants for prescribing treatments or rehabilitation procedures in the analysis period. The deterioration models were the present serviceability rating (PSR), the distress maintenance rating (DMR), the pavement condition rating (PCR), and the

Texan punchouts and patches model. The objective function minimizes the errors between the database and the models based on genetic algorithms. This research was unusual because adjusting data generated from closed-form equations may be trivial. The original equations' regression coefficients nearly match those obtained with the genetic algorithms. The conclusion stated that GA was an appropriate tool to adjust the parameters of complex deterioration models.

Chan et al. (2001) reviewed two constraint-handling methods and proposed a new procedure for applying genetic algorithms in pavement maintenance programming at the network level. The authors analyzed a published example with an objective function to maximize the total weighted work production under production requirements, budget, workforce, equipment, materials, and rehabilitation constraints. The authors summarized the main features of three constraint handling methods: (a) the penalty method (PE), (b) the decoding and repair (DRAM) method, and (c) the genetic algorithms for numerical constrained problems (GENOCOP) with *"prioritized resource allocation method"* (PRAM), which encodes the value decision variables with additional information about the available resources and always satisfies the resource constraints. PE method had the worst results, while DRAM and PRAM showed similar performance. However, the latter achieved the highest objective function value with high resources and concentrated activities on pavements with more distress.

Sundin & Braban-Ledoux (2001) reviewed artificial intelligence-based decision support technologies in pavement management. The primary decision support technologies for unstructured problems are (a) group support systems, (b) executive information analysis, (c) expert or knowledge-based systems, (d) artificial neural networks, and (e) hybrid support systems. Pavement management systems use performance prediction models. These models are deterministic (regression) or probabilistic (Markovian), empirical or mechanistic-empirical. Figure 3-6 shows the applications of AI-based decision-support technologies to the PMS decision-making process with some examples.

Figure 3-6: AI-based decision-support technologies in PMS

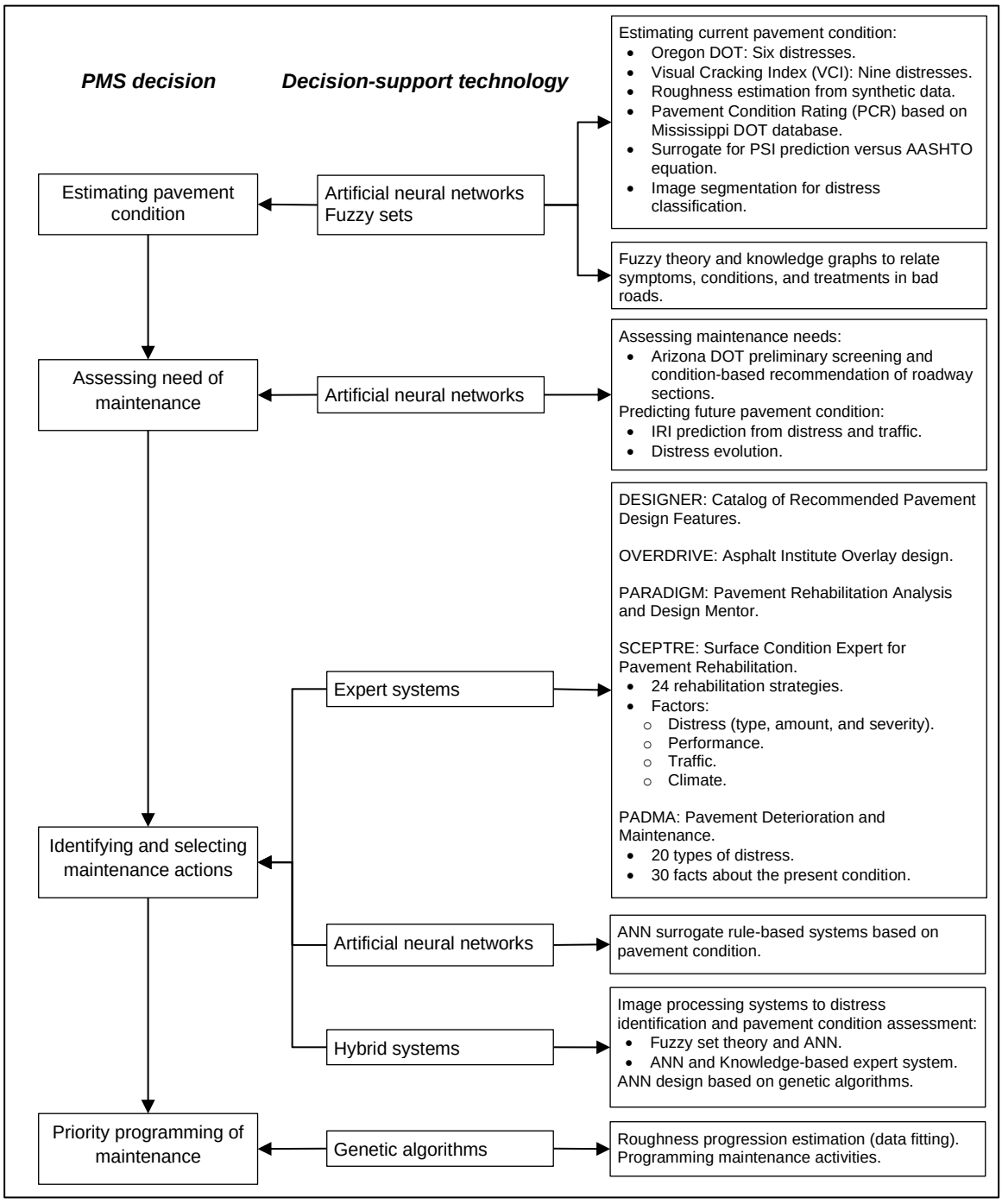

Source: Modified and summarized from Sundin & Braban-Ledoux (2001)

Tack & Chou (2002) compared the results of simple and constrained genetic algorithms with dynamic programming in multiyear pavement repair scheduling. The objective function maximizes the overall average yearly network condition. According to their condition, the

constrained genetic algorithm included an expert system in determining the type of repair to individual pavement sections. The expert system considered two constraints: frequency and application feasibility of a repair. The constrained GA reduced the allowable number of repair combinations. A study showed that the pre-constrained genetic algorithm achieved an optimum solution faster than the simple genetic algorithm; however, dynamic programming was the most accurate optimization technique. The genetic algorithms employed up to 39,000 generations in multiple trial runs. The authors did not present additional detail about the crossover and mutation rates of the GA.

Cheu et al. (2004) presented a hybrid methodology using a genetic algorithm as a search technique coupled with a microscopic traffic simulation model to optimize the daily lane closure scheduling in a network for maintenance activities. The authors did the microsimulation with the commercial software PARAMICS, considering lane but not full road closures and traffic volumes based on 24-hour origin-destination trip distributions. The codification included a one-day program task assignment for multiple teams and jobs with a total workforce, equipment, and materials availability. The objective function tried to minimize the total travel time of vehicles in the network during the day, considering the decoding and repairing of invalid individuals (maintenance schedules) before running the traffic microsimulation. The microsimulations were computationally expensive, but the GA converged after nine generations; consequently, the author recommends future research to reduce the computing time to obtain daily schedules.

Flintsch & Chen (2004) reviewed soft computing applications for infrastructure management. The authors summarized applications of artificial neural networks, fuzzy logic systems, genetic algorithms, and their hybridization for three main tasks in pavement management: (1) asset performance, (2) needs analysis and (3) tradeoff analysis. The tradeoff analysis considers prioritization and optimization. The authors used genetic algorithms and fuzzy mathematical programming with good perspectives; however, they identified several issues for soft computing implementation, like legacy systems, lack of understanding of the techniques and their benefits, and lack of data to develop reliable models.

Morcous & Lounis (2005) combined a genetic algorithm with Markov-chain models for programming pavement maintenance alternatives. Deterioration is a stochastic process

where the probability of a future state depends on the present state. The authors classify the infrastructure facilities by performance-shifting variables like pavement type, material properties, operating loads, and environmental conditions. The maintenance alternatives defined transition probability matrices in a Chapman-Kolmogorov multi-step process for the analysis period with associated discounted costs. The objective function minimizes the present value of the maintenance costs of all facility groups while keeping their condition above a threshold value. The authors developed a case study of bridge decks from Quebec. Although not related to pavement engineering, this problem showed the application of Markov-chain performance prediction for life-cycle cost minimization of the infrastructure network.

Herabat y Tangphaisankun (2005) developed a multi-objective optimization model to support decision-making and provide optimal maintenance programs to the Thailand highway agency. The authors considered two objective functions: minimizing vehicle operating costs and maximizing the road network condition. The operating costs were based on the HDM-III model related to the pavement roughness. The authors considered five maintenance types with closed-form equations to predict their impact on pavement roughness and a roughness degradation model with time. The constraints considered budget limitation (hard constraint) and system preservation based on IRI (soft constraint). The non-dominated sorting genetic algorithm (NSGA) had an initial population of 50 individuals with the combinatorial application of five maintenance activities. The authors evaluated different trigger levels for maintenance application and found an optimum IRI of 2.702 m/km, considering that the base value was 2.0 m/km.

Bosurgi & Trifirò (2005) proposed an optimization procedure for the management of resurfacing interventions on flexible pavements with genetic algorithms based on two indicators: (a) the Sideway Force Coefficient (SFC) and (b) predicted accidents. The SFC and the accident prediction models used artificial neural networks related to SFC variation with time, cumulative traffic, geometric and environmental characteristics, and the number of road accidents. The genetic algorithm minimizes the estimated accidents, and it maximizes the average SFC in the network constrained to a limited budget. A case study considered a population of 924 individuals, or two times the individual chromosome size for three-year programming for 77 kilometers in the A18 Messina – Catania highway (Italy).

The authors propose developing more complex models with operating velocities, safety distances, visibility, and other variables.

Chootinan et al. (2006) developed a pavement maintenance program based on the Markov transition probability matrix (TPM) approach to address the uncertainty in pavement condition prediction. The authors considered the challenge of developing a long-term maintenance plan at the project level consistent with the network-level recommendations with two objective functions: minimizing the maintenance cost and maximizing the pavement performance. The performance prediction used an AASHTO-based serviceability rating (PSR) as a function of the initial condition, pavement structural number, pavement age, cumulative 18-kip axle loads at the specific year, and adjustment factors for climate and function. Although all the variables are sources of uncertainty, only the traffic loads were considered random. The authors combine the genetic algorithm with the condition simulation to solve the stochastic maintenance problem subjected to budget constraints. The stochastic performance simulations used the Latin hypercube sampling (LHS) technique to estimate future traffic load distribution. A case study with 53 pavement segments between 3 to 9 years evaluated the approach against deterministic solutions for a ten-year analysis period. The stochastic simulations showed a faster convergence. The authors noted the need for uncertainty in pavement maintenance programming because deterministic formulations underestimated future deterioration.

Wang et al. (2007) reviewed the Arizona experience with the network optimization system (NOS) based on the application of Markovian transition prediction models. The condition prediction includes linear optimization integrating a genetic algorithm to solve the NOS problem at the network level. NOS considered three pavement factors in establishing the pavement condition and generating decision variables: level of roughness, level of cracking, and index to first crack. Also, the system considers six preserving actions from routine maintenance to overlay construction. The objective function maximized the pavement condition while minimizing agency costs in a combined weighted fitness function. The performance of the genetic algorithm exceeded the original NOS.

Maji & Jha (2007) developed a genetic algorithm optimization model for the highway maintenance scheduling problem under budget and threshold deterioration constraints. The authors considered parabolic deterministic functions for the deterioration and maintenance

costs of guardrails, road signs, and luminaries. The objective function minimizes the total maintenance cost in the design period. A case study showed promising results in integrating road components other than pavement.

Unnikrishnan et al. (2009) proposed a multiobjective bi-level mathematical programming framework to evaluate the impact of maintenance and rehabilitation in Build-Operate-Transfer (BOT) highways, integrating maintenance and capacity improvements decisions with optimal toll pricing. The users select routes with the user equilibrium assignment based on time travel, the toll, and the pavement state. The private operator and the public agency had different objective functions, maximizing the BOT's net present value and minimizing the system's total cost. A case study on a small network with BOT and public roads showed different Pareto fronts for multiple actions from the private and public actors. More frequent maintenance and capacity expansion of the private toll roads reduce the generalized cost. The authors recommended including uncertainty in future research.

Quian (2010) improved performance prediction models for pavements by hybridizing a genetic algorithm and an artificial neural network. The author implemented the genetic algorithm into the back-propagation neural network training to minimize the error between observed and predicted pavement performance; training data corresponded to pavement condition, traffic, and climate of Shenda highway in China. A comparison between ANN and GA-ANN showed better forecasts for the hybrid approach.

Javed (2011) argued that traditional pavement management prioritizes rules like "*worst goes first,*" the effective cost, or is based on a distress index without an exact physical meaning. A genetic algorithm maximizes the pavement behavior under constrained budget conditions and mitigates the sub-optimal alternatives produced by the user's priority preferences employed in pavement management systems. The objective function minimizes the weighted cost of repairing distress subjected to a minimum pavement condition index of PCI = 55 for individual sections and a minimum average of PCI = 70 for the network.

Santos & Ferreira (2012a) developed the OPTIPAV software based on a genetic algorithm. The program optimizes the pavement behavior, the construction and preventive maintenance (and rehabilitation) costs, the user's costs, and the residual value for a given

analysis period. It is based on the AASHTO 1993 algorithm and the present serviceability index (Santos & Ferreira, 2012b). The objective function minimized the total discounted costs over the project analysis period while keeping the pavement above specified quality standards. The constraints corresponded to the yearly pavement condition based on the previous state and maintenance and repair activities. The authors concluded from several case studies that Portuguese pavement design manual structures are not optimal solutions. Pavements with more structural capacity allow savings in terms of life-cycle costs. The authors presented the OPTIPAV application to the life-cycle cost analysis for pavement management at the project level and performance models different than the AASHTO 1993 algorithm (Santos & Ferreira, 2013).

Golroo & Tighe (2012) reviewed the optimum genetic algorithm structure for developing a maintenance system by performing a sensitivity analysis on the problem's outcome concerning the genetic algorithm structure. The authors selected five objective functions: (a) minimization of maintenance costs, (b) maximization of saving in vehicle operating costs, (c) maximization of effectiveness, (d) maximization of saving vehicle operating costs over maintenance costs, and (e) maximization of effectiveness over cost. Effectiveness is the area under the performance curve multiplied by the length of a pavement section and the annual average daily traffic. The constraints were the total budget and the pavement condition index level that triggered the maintenance activities enforced with the penalty method. The authors recommended evaluating the GA operators instead of using typical values from previous publications.

Farhan & Fwa (2012) examined the implications of a priori application of priority weights in the pavement maintenance programming analysis. Traditionally, highway agencies apply priority weights according to pavement distress, pavement condition, road class, or traffic volume to optimize pavement maintenance or rehabilitation activities. However, most agencies ignore the effect of these weights on optimization. The authors applied several combinations of priority weights to a case study based on genetic algorithms. They found that such values define sub-optimal solutions, the worst for multiple priority weights. Consequently, they proposed eliminating priority weights in the optimization process and considering the following phase through a tie-breaking and trade-off analysis to compare non-selected pavement sections with the same objective functions and better conditions.

Meneses (2012) (2013) developed the Multi-Objective Decision-Aid Tool (MODAT), a modified version of the OPTIPAV program, to minimize the cost in a planning period by closing the gap between network and project management by changing the standard design variables (thickness, moduli, weather or traffic) for the damage assessment and future prediction based on the AASHTO 1993 algorithm. The multiple objectives included minimizing the maintenance, rehabilitation, and user costs; and maximizing the residual value. Constraints include pavement structural (thicknesses, moduli, and distresses) and functional characteristics (smoothness). The authors used a vector approach to select the incumbent solution (knee point) from a normalized Pareto front. They concluded that user costs have more influence on the results than agency costs.

Di Mino et al. (2013) developed a two-objective optimization model to minimize road accident risk and rehabilitation costs on network and project levels. The authors presented a case study based on data from the A18 Messina-Catania motorway in Italy. The risk state function (RSF) represented the road's degree of safety related to geometry, surface characteristic, weather and climate conditions, and traffic. The authors modeled pavement deterioration as a Markovian process and used a genetic algorithm to optimize its rehabilitation activities. The authors considered the potential of including a third objective function to minimize user costs.

Abu-Lebdeh et al. (2014) reviewed the performance improvement of genetic algorithms through parallelization and how they could advance transportation systems applications. Several actions increase the algorithm performance, including faster solutions evaluation and the workload division between multiple processors to produce efficient, rapid, and productive algorithms. A parallel genetic algorithm implies a population structure with different migration topologies between islands in free or organized forms. Islands generate discontinuities and require cellular diffusion between neighboring individuals. A case study on traffic control optimization showed a better performance with four and eight subpopulations in terms of convergence and fitness function than a conventional genetic algorithm.

Elhadidy et al. (2015) developed an integrated pavement management system for the Egyptian road network. The authors implemented a genetic algorithm with a Markov-chain deterioration model considering the available budget and road network condition based on

the pavement condition index (PCI). The objective function considered two aspects: (a) minimizing the maintenance and rehabilitation costs and (b) maximizing the pavement condition. Through trial calculations, the authors adopted the genetic algorithm parameters. A numerical example showed a clear Pareto front for Egyptian network and project management conditions.

Yang et al. (2015) proposed a new pavement management system integrating a pavement age gain model to evaluate pavement conditions and NSGA-II to optimize pavement maintenance. The authors evaluated deterministic and probabilistic pavement age models, minimizing maintenance costs and maximizing life. They defined the parameters of the GA through trial and error. Deterministic and probabilistic approaches showed clear Pareto fronts with better results with the stochastic approach because they improved pavement conditions after maintenance.

Rifai et al. (2016) developed a two-objective optimization model considering maximum roughness and minimum maintenance cost for in-service road networks subjected to overloading in West Java. The pavement deterioration model forecasts the IRI using Support Vector Machines for highways with and without overloading. Overloading dramatically affects roughness growth, reducing the pavement life span by 50% for roads with axle weights above the legal limits. The authors considered seven treatment types (including *"do-nothing"*) with representative road construction costs in West Java. According to a Pareto analysis, the case study achieved both objective functions considering three loading/overloading levels.

Santos et al. (2017) presented an adaptive hybrid genetic algorithm (AHGA) for pavement management. The authors combined a genetic algorithm with local search mechanisms for solving the pavement maintenance and rehabilitation strategy selection problem with the OPTIPAV equations. The genetic algorithm used integer coding and the penalty method for handling constraints. The partial local search mechanism aims to either accelerate the discovery of reasonable solutions or find solutions unreachable by evolution or a local method alone. A case study on the Interstate Highway in Virginia (USA) showed that the AHGA gives better results than the GA in convergence speed, minimizing the life-cycle M&R costs of pavement sections.

Matin et al. (2017) compared metaheuristic algorithms for road maintenance planning with a field study in Iran's rural transportation network. The authors compared single-objective and multi-objective optimizations with genetic algorithms and particle swarm optimization. The objective functions maximize pavement performance (PCI) and minimize maintenance costs constrained by budget. The performance model was a quadratic regression equation of PCI versus age. The maintenance and repair actions included three categories: localized preventive (crack sealing), global preventive (surface treatments), and major maintenance (structural overlays). An expert system predicts the effects of maintenance and repair activities on improving PCI. The authors conclude that multi-objective optimization is better than single-objective optimization. Also, in the case study, non-domination sorting genetic algorithm II (NSGA II) performed slightly better than multi-objective particle swarm optimization (MOPSO) since MOPSO gave higher pavement conditions with higher costs but under the defined budget.

3.2.2.2 Optimization with swarm intelligence

Teodorovic (2008) reviewed swarm intelligence systems for transportation engineering, like the ant colony, the particle swarm and the bee colony optimizations, and the stochastic diffusion search. All techniques applied the concept of *"collective intelligence"* of individuals. The author presented vehicle routing and scheduling applications. One must notice that the author highlighted that swarm intelligence is not a specific computational tool but a concept and a thinking pattern.

Shen et al. (2009) applied chaos particle swarm optimization (CPSO) with local solid searching capability and control of population diversity to pavement maintenance decisions. The objective function maximizes the economic benefit and keeps the pavement in an optimal state constrained to the available budget and workforce. A case study against an NSGA-II showed the validity of the CPSO results and faster convergence.

Tayebi (2010) applied particle swarm optimization (PSO) to pavement management activities programming to determine the best maintenance and rehabilitation activities based on four minimizing cost equations. A replication of the case study proposed by Fwa et al. (1996) showed promising results.

Chang (2013) applied the particle swarm optimization method for prioritizing pavement sections for maintenance and rehabilitation activities in the Smooth Roads Project in Taiwan. The pavement condition included the standard deviation for roughness, rutting, deflections, cracking, pothole, bleeding, patching, and shoving. The author used particle swarm optimization to compute the synthetic pavement condition and rank the pavement sections from best to worst to program maintenance activities.

Terzi & Serin (2014) applied ant colony optimization (ACO) to pavement maintenance and rehabilitation programming under budget constraints. The authors proposed a case study previously presented by Fwa et al. (1988) to maximize the routine maintenance workload subjected to budget and resource constraints for four highway classes, four maintenance activities, and three emergency levels. The optimization results were satisfactory compared to the original case study and included a newly implemented budget restriction.

Tayebi et al. (2014) compared a genetic algorithm against a particle swarm optimization to analyze pavement management activities with minimum cost. The authors recognized the complexity of predicting pavement performance and adopted three AASHTO-based distress models (cracking, rutting, and surface disintegration) related to traffic and pavement structural number (SN). The objective function minimizes the M&R activities cost at the network level. The uncertainty of the predicted pavement condition was associated with random traffic loads. The authors found that PSO is an efficient, easy-to-implement optimization model for PMS, even faster and more accurate than the GA proposed for a specific problem based on the case study developed by Fwa et al. (1996).

Ahmed et al. (2018) applied chaos with discrete multiobjective particle swarm optimization (CDMPSO) to pavement maintenance. The authors considered two objective functions minimizing the treatment cost and the sum of all residual pavement condition index (PCI) values. The *“residual pavement condition index”* subtracts the actual PCI from 100 and multiplies it by the annual average daily traffic and the section's area as weighting values. The authors estimate the actual PCI with a regression equation considering cracking areas and lengths, pavement age, and maintenance effect. A small case study with five pavement sections, five alternatives for maintenance and repair, and a ten-year period showed significant computing time reductions compared with published solutions.

Panda & Swamy (2018) developed an improved artificial bee colony algorithm for pavement resurfacing problems. The methodology considers user and agency costs, inflation and interest rates, and reachable roughness levels during pavement resurfacing cycles. The solution yields the frequency and thickness of resurfacing, maximizing the cost-effectiveness without defining the trigger roughness level. The authors used multiple colonies to enhance the exploration and exploitation capabilities of the algorithm. A case study (with closed-form equations to predict deterioration, improvement, and costs) yielded similar results to previous studies; however, the resurfacing activities were simulated for several decades with unrealistic large thicknesses of asphalt concrete.

3.2.2.3 Optimization with genetic programming

Chang & Chao (2010) used genetic programming (GP) to support pavement maintenance and rehabilitation decisions. The authors conducted GP to explore the maintenance and rehabilitation (M&R) decision model between 18 pavement distress types (inputs) and the required M&R treatment among four options (output) based on 2340 records of pavement distress surveys from seven roads in Taiwan. The severity (low, medium, and high) and density (local, medium, extensive) combinations of each distress were codified with a number between one and nine and zero for undamaged. The M&R treatments considered: (a) no-treatment, (b) localized treatment (patching and crack sealing), (c) global treatment (fog seal, slurry seal, and chip seal), and (d) major treatment (milling, hot-recycling, overlay, and reconstruction). The data fitting used equal portions of the data for training, validation, and application. The results were promising, with total accuracies between 0.877 and 0.903. Global and major M&R activities had the worst accuracies due to their low number of cases in the database. Consequently, the model and algorithm are promising but require further refinement with additional data.

Shahnazari et al. (2012) applied artificial neural networks (ANN) and genetic programming (GP) to forecast the pavement condition index (PCI) from a database of 1,250 km of flexible pavements in Iran. Models considered eight out of the twenty distress types, with three severity levels defined in the PCI method: alligator cracking, bleeding, block cracking, edge cracking, longitudinal cracking, patching, pothole, and transverse cracking. The objective function minimizes the error in the predictive models. Both models gave reasonable estimations of the PCI in the database.

3.2.2.4 Optimization with greedy search

Yepes et al. (2016) developed an optimization module based on local search heuristics to optimize the allocation of maintenance funds at the network level subjected to budgetary and technical restrictions. The heuristic consisted of a hybrid algorithm, based on a greedy randomized adaptive search procedure (GRASP), to assemble a viable solutions population considering penalty functions and a Threshold Acceptance (TA) to process the constructed solutions intensifying the search. The problem involved a single-objective optimization of the long-term effectiveness based on the area bound by the treatment time versus the performance curve. The performance measure was a Pavement Condition Index adaptation for urban pavements. A case study in Santiago (Chile) showed improved results than traditional programs based on reactive strategies and an emphasis on preventive activities over maintenance and rehabilitation; for example, although recycling was part of the feasible alternatives, it did not appear in any solution. The long-term effectiveness has a high sensitivity to budget constraints. The authors suggested including sustainability factors in future analyses.

3.2.2.5 Optimization with hybrid methods

Nik et al. (2016) developed various states of hybrid particle swarm optimization and genetic algorithms for the optimal arrangement of surveyed inspection units (SIU) to select the most precise simulation of the distress inspection process with different constraints applied to massive networks. The authors searched for an optimal SIU arrangement to reach a tradeoff between minimum network errors, inspection time, and the number of surveyed units. The inspection procedure corresponded to the pavement condition index (PCI) method. The two objective functions minimize the sampling and network inspection errors. A case study on the road network of a district in Teheran (Iran) indicated that the hybrid implementations yield better results than the systematic sampling procedure suggested in the PCI method. However, one must observe that the authors had the total distress records of the road network, and the comparisons considered different sampling sizes and selection approaches. It is unclear how the PSO-GA hybrid may be helpful in previously uninspected road networks.

Naseri et al. (2021) evaluated several metaheuristic algorithms to solve large-scale pavement network maintenance and rehabilitation scheduling based on the IRI deterioration. A case study with 109 pavement sections indicated that the Water Cycle

Algorithm (WCA) has a better performance than genetic algorithms (GA), particle swarm optimization (PSO), and differential evolutionary (DE) methods. However, the authors do not report multiple runs that may yield a different conclusion in this single aspect, considering the random features of metaheuristics.

3.2.3 Applications in backcalculation of pavement moduli

Backcalculation is a pavement engineering technique to evaluate the *"mobilized"* moduli under pavements with real-life traffic and environmental conditions. Figure 3-7 shows a schematic of the falling weight deflectometer test and the deflection basin. Backcalculation compares measured and computed structural deflections to estimate the moduli given a set of constant thicknesses and a known load. Backcalculation is complicated because several moduli combinations may match the measured deflections without adequately representing the materials.

Figure 3-8 presents a flow diagram of the backcalculation procedure. The layered-elastic theory, the finite element method, the viscoelastic theory, or surrogates of such analysis methods perform the *"Deflection calculation."* The figure represents the conventional backcalculation procedure for road and airport pavements in static conditions based on a defined pavement profile.

Additional time-dependent information is available from the sensor array in modern falling weight deflectometers (FWD). Thus, it is possible to propose a viscoelastic analysis of pavement materials or, in two-layer cases, thickness estimation from surface responses. It is also possible to register Rayleigh surficial waves and, through spectral analysis of surface waves (SASW), evaluate the low-deformation moduli and thicknesses from shear-velocity profiles in the pavement.

Figure 3-7: Surface deflection basin from the FWD test

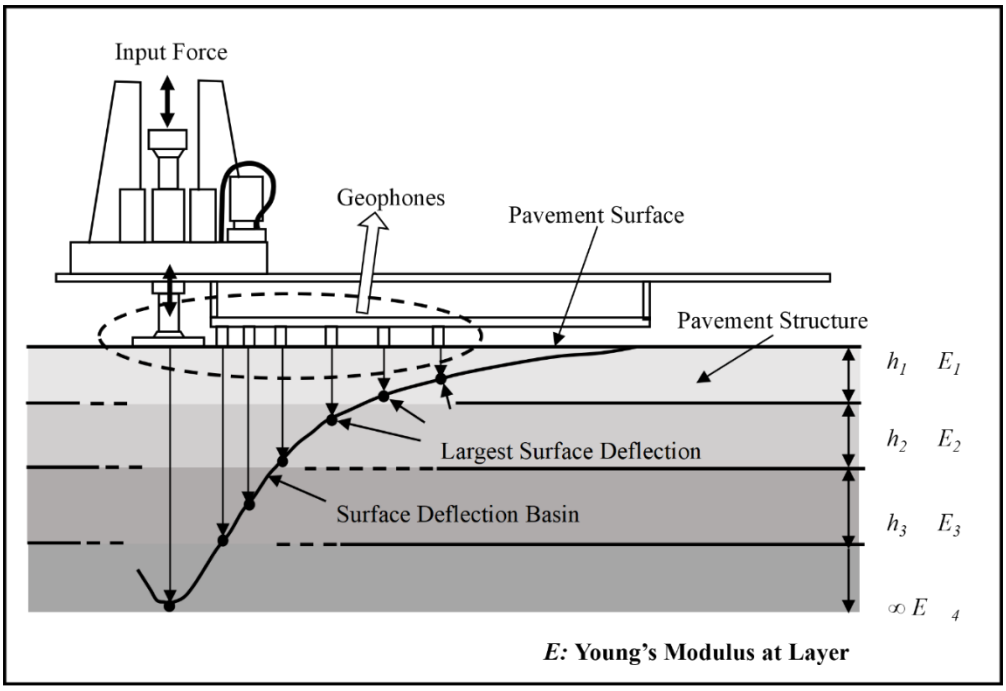

Source: Choi et al. (2010).

Figure 3-8: Conventional backcalculation procedure

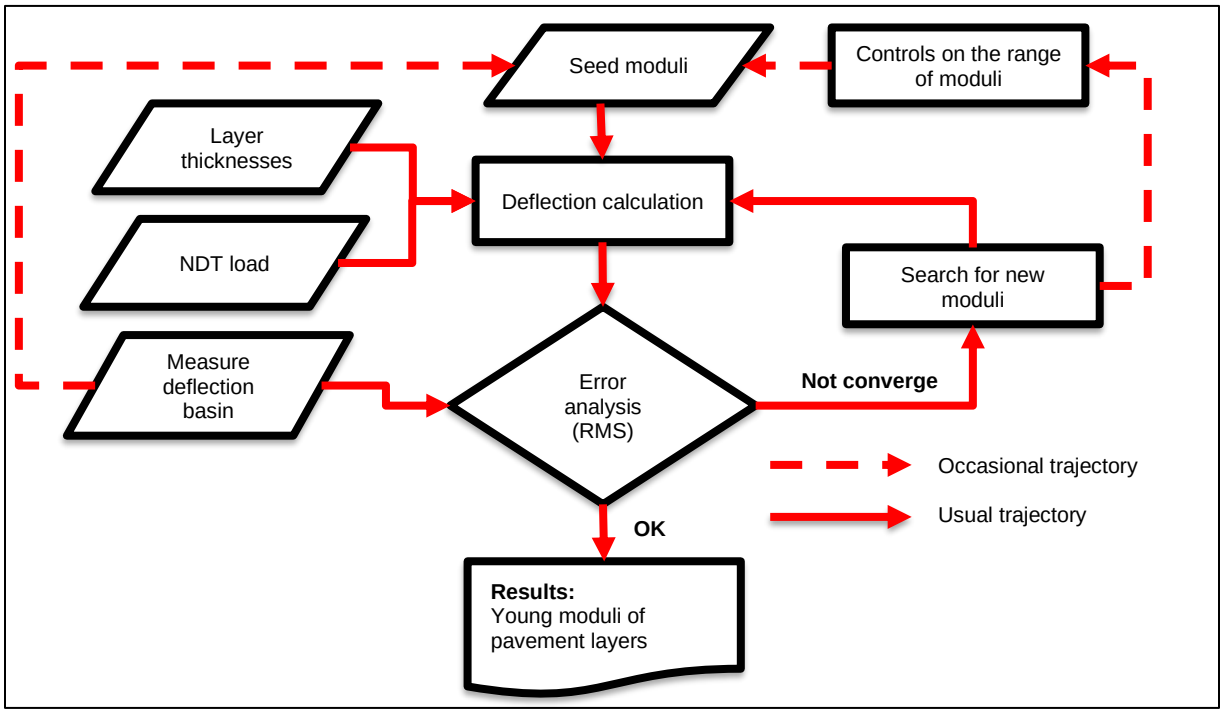

Source: Modified from Lytton (1989).

Anderson (1990) summarized three methods for the backcalculation of pavement moduli from NDT deflection data. Alkasawneh (2007) and Tutumluer & Sarker (2015) reiterated the same classification in two separate publications as follows:

1. Methods based on simplified forward calculation procedures such as the equivalent thickness (MET) method developed by Ullidtz, the surface curvature index method (SCI) developed by Van der Loo, or the Hogg three-layer model.
2. The Gradient Relaxation Method proposed by Michelow is based on gradient matrices to minimize the differences between calculated and measured deflections.
3. The Direct Interpolation Method, as proposed by Uzan and based on a table of pre-calculated responses for a wide range of pavement combinations. Zaabar et al. (2014) developed an artificial neural network as a surrogate *"interpolation"* method from large databases with viscoelastic and non-linear elastic materials.

Gradient relaxation is a standard procedure for backcalculation. It is based on the partial derivation of the quadratic error function (Eq. 3-2) with respect to the unknown moduli of the pavement (Anderson, 1990).

$$\sum_{j=1}^{m}\left(D_j-\Delta_j\right)^2=\sum_{j=1}^{m}\left[D_j-f(E_1,E_2,\dots,E_n)\right]^2$$

Eq. 3-2

Where D_j is the measured deflection at point j, Δ_j is the computed deflection at point j as a function of the moduli of the pavement [$f(E_1,E_2,\dots,E_n)$], and m is the number of deflection points. The partial derivatives are numerically approximated by forming gradient equations by calculating the deflections for an initial set of *"seed"* moduli (E^0) and a sequential change in only one of the unknown moduli (E^1). Thus, the deflection at point j is a function of the gradient equation and the unknown modulus of the layer (E_i):

$$\Delta_j=\Delta_i^0-\left[\frac{\Delta_i^0-\Delta_i^1}{\log_{10}\left(E_i^0\right)-\log_{10}\left(E_i^1\right)}\right]\cdot\log_{10}\left(E_i^1\right)+\left[\frac{\Delta_i^0-\Delta_i^1}{\log_{10}\left(E_i^0\right)-\log_{10}\left(E_i^1\right)}\right]\cdot\log_{10}(E_i)$$

Eq. 3-3

Where Δ_j is the computed deflection at point j, Δ_i^0 is the predicted deflection at point j for E_i^0, and Δ_i^1 is the predicted deflection at point j for E_i^1, which is the modulus for layer i after the variation. Being:

$$S_{ji} = \frac{\Delta_i^0 - \Delta_i^1}{\log_{10}(E_i^0) - \log_{10}(E_i^1)}$$

Eq. 3-4

Where S_{ji} is a simplified model for the moduli-deflection relation. Being:

$$A_{ji} = \Delta_i^0 - S_{ji} \cdot \log_{10}(E_i^1)$$

Eq. 3-5

The general equation for the deflection at sensor location j as a function of all the unknown moduli values is:

$$\Delta_j = \Delta_j^0 + \sum_{i=1}^{n} S_{ji} \cdot \left[\log_{10}(E_i) - \log_{10}(E_i^0)\right]$$

Eq. 3-6

The value of Δ_j^0 is expressed in terms of one of the unknown moduli (e.g., layer 3) as:

$$\Delta_j^0 = A_{j3} + S_{j3} \cdot \log_{10}(E_3^0)$$

Eq. 3-7

Therefore, the expression for Δ_j can be written as:

$$\Delta_j = A_{j3} + S_{j3} \cdot \log_{10}(E_3^0) + \sum_{i=1}^{n} S_{ji} \cdot \left[\log_{10}(E_i) - \log_{10}(E_i^0)\right]$$

Eq. 3-8

The expression for the summation of the squared deviations between measured and computed deflections is:

$$\sum_{j=1}^{m} \left(D_j - \Delta_j\right)^2 = \sum_{j=1}^{m} \left\{ D_j - \left[A_{j3}^0 + S_{j3} \cdot \log_{10}(E_3^0) + \sum_{i=1}^{n} S_{ji} \cdot \left[\log_{10}(E_i) - \log_{10}(E_i^0)\right] \right] \right\}^2$$

Eq. 3-9

To minimize the error function, one takes the partial derivatives of Eq. 3-9 for each of the unknown moduli values and sets them equal to zero to form the following matrix equation:

$$[B] \cdot \{E\} = \{C\}$$

Eq. 3-10

Where $\{E\}$ is the unknown moduli vector and, for i and k equal to the layer number, the matrix terms are:

$$C_k = \sum_{j=1}^{m} \left\{ S_{jk} \cdot \left[D_j - A_{j3} - S_{j3} \cdot \log_{10}(E_3) - \sum_{i=1}^{3} S_{ji} \cdot \log_{10}(E_i) \right] \right\}$$

Eq. 3-11

And

$$B_{ki} = \sum_{j=1}^{m} S_{jk} \cdot S_{ji}$$

Eq. 3-12

The solution of Eq. 3-10 depends on the initial or *"seed"* modulus, which makes the gradient relaxation method prone to converge to local minima without an appropriate representation of the pavement materials. Consequently, the research for different techniques for backcalculation pursues improving the selection of seed moduli or altogether avoiding its utilization.

Laurent et al. (2018) implemented the *"Bound Optimization by Quadratic Approximation"* (BOBYQA) algorithm into the PITRA-BACK software for backcalculation and overlay design for flexible pavements. BOBYQA is based on the NEWUOA program for unconstrained optimization without objective function derivatives (Powell, 2004).

Backcalculation is an attractive field for search techniques based on an objective function (minimum quadratic error of measured versus computed deflections) subjected to a series of constraints (range of moduli, interface conditions, traffic level, and dynamic behavior, among others). The following paragraphs summarize research on the subject.

Fwa et al. (1997) applied a genetic algorithm in pavement-layer moduli backcalculation. The objective function minimizes the root-mean-square difference between the measured and computed deflections subjected to a user-defined restriction in the range of moduli. The forward calculation procedure included the BISAR program and the Odemark equivalent-layer method. It is unclear how the equivalent-layer method was adapted to compute surface deflections. The authors recommended a population of 60 with 150 generations (depending on pavement complexity) and crossover and mutation rates of 0.85

and 0.15. The chromosomes comprised the codified values of the moduli. The authors evaluated three-layer and four-layer structures proposed in the backcalculation literature. They achieved a better performance than solutions based on the method of Newton, like EVERCALC and MICHBACK. The NUS-GABACK program showed good performance with four-layer pavements, including stabilized bases. Also, the GA does not require seed moduli or a minimum number of surface sensors related to pavement layers.

Hunaidi (1998) applied genetic algorithms to the spectral analysis of surface waves. Non-destructive testing of pavements with Rayleigh surface waves considers the dispersion in layered media. Dispersion is wave velocity variation with the propagating wave's frequency or wavelength. High-frequency waves propagate near the surface, while low-frequency waves penetrate the medium and interact with the lower materials. The theoretical models of wave propagation in layered media are non-linear, and the fit with experimental data has multiple solutions. The genetic algorithm minimized the difference between the dispersion curve obtained with the spectral analysis of surface waves (SASW) test and the curve obtained with the theoretical model based on the Thomson-Haskel transfer matrix approach simplified in closed-form equations from the seismological analysis. The fitness function added the absolute differences between phase velocities at different frequencies. The fittest individual represents the shear wave velocity of the pavement. The author presents a case study with a population of 50 individuals, a crossover probability of 0.5, and two kinds of mutation probability: jump mutation (0.02) and creep mutation (0.04). The model's adjustable variables were shear wave velocities and layer thicknesses, but it can also consider *"guessed"* densities and Poisson ratios. In both cases, an optimum solution requires at least 21 generations.

Terzi et al. (2003) hybridized a genetic algorithm and an artificial neural network as a realistic deflection basin modeling approach. They proposed two objective functions: minimization of layer thicknesses and maximization of elastic moduli. It is unclear the purpose of their statement about the backcalculation problem. The constraints limit the ranges for the seven FWD readings and deflection reduction with distance to the applied load.

Reddy et al. (2004) examined the performance of a genetic algorithm for backcalculation according to its population size, number of generations, crossover, and mutation

probabilities. The parameter selection is a trade-off between the accuracy of results and the computational effort. The BACKGA program (based on the forward calculation program ELAYER) implemented an objective function that minimizes the sum of squared differences between calculated and measured deflections. The authors concluded that a population size of 60 with 60 generations, a mutation probability of 0.1, and a crossover probability of 0.74 yielded satisfactory performance for three-layer and four-layer backcalculation theoretical and real-life problems.

Tsai et al. (2004) presented four case studies applying genetic algorithms in backcalculation and experimental data fitting. The authors analyzed the backcalculation of moduli of a three-layer pavement (HMA, granular base, subgrade) from deflections measured in the surface with the falling weight deflectometer (FWD). The objective function minimizes the quadratic error between the measured and calculated superficial basin deflections subjected to restrictions in the range of moduli. The authors consider that the computational cost of the GA is too high compared with traditional (gradient-based) backcalculation techniques.

Terzi (2005) applied gene expression programming (GEP) to model the flexible pavement surface deflection with the Karva language. The program uses 50 chromosomes with eight genes and a mutation rate of 0.044. The one-point and two-point recombination rates were 0.3, and the gene recombination and transposition rates were 0.1. The GEP presented an expression that relates the surface thickness with the deflection in seven sensors. The moduli estimation from such expression and the objective function behind the optimization are not explicit. The result predicted the thickness of the first layer as a function of seven deflections.

Rakesh et al. (2006) implemented an artificial neural network to surrogate the layered-elastic program ELAYER in the BACKGA backcalculation program developed by Reddy et al. (2004). The objective function minimized the quadratic error between the measured and computed deflections. The computed error is used to define the fitness of each solution as its probability of reproduction. The authors kept the 60 generations but changed the crossover and mutation probabilities from 0.74 to 0.90 and 0.10 to 0.02, respectively. The populations varied from 200 to 700 according to pavement layers. Results indicated an accurate backcalculation for the HMA and the subgrade layers. At the same time, more significant errors (up to 40%) appear in the moduli of the intermediate layers (granular base

and subbase) of the four and five-layer systems. The surrogate ANN indistinctly yields better or worse moduli than the LET solution, but the computations are 30 to 40 times faster.

Hu et al. (2007) integrated the genetic algorithms with the dynamic stress wave propagation theory, based on Green's flexibility influence functions, in the DBFWD-GA computer program. Influence functions simulate the propagation behavior of dynamic stress waves in the layered structure. The objective function is the root of the mean square error of measured versus computed deflections. The GA parameters considered populations of 60, 120, and 140; the crossover probability was 0.5; and the mutation rates were 0.1, 0.15, and 0.20. The genome codification used 8 bits. Interestingly, the authors used seed solutions for the backcalculation procedure, which other authors considered unnecessary for the GA. A case study showed coincidence with other backcalculation programs but not with the expected moduli.

Alkasawneh (2007) researched genetic algorithms in the backcalculation of pavement moduli. He concluded that classical backcalculation techniques are prone to misleading results due to premature convergence to local optima and the use of seed moduli. The root-mean-square error (RMSE) of deflections is an unsuitable objective function that should be substituted by the AREA method. A low RMSE (1%) may produce moduli that induce strain errors up to 20%, affecting fatigue and rutting predictions. The backcalculation process improves by increasing the number of sensors. The GA requires large populations and at least 15-bit strings to codify the unknown modulus. The author proposed a new dynamic parameterless genetic algorithm (DPGA) and developed the BackGenetic3D program. The program includes new genetic operators and parameters: jump mutation on coded (genotype) genes, creep mutation of decoded (phenotype) genes, crossover, niching (preserve diversity in small populations), tournament selection, and elitism (retains the chromosome with the best fitness function).

Gopalakrishnan (2009) implemented a hybrid optimization approach to the backcalculation of a three-layer flexible pavement. A trained neural network surrogate for linear-elastic forward calculation based on a 2D finite element solution. The objective function minimizes the squared differences between measured and computed deflections. Particle swarm optimization (PSO) and shuffled complex evolution (SCE) showed excellent prediction capabilities for hot-mix asphalt and subgrade moduli in 150 trial cases. The author does not

provide further details about the PSO or SCE parameters or the quality of the backcalculation of the intermediate base layer modulus.

Park et al. (2010) applied a genetic algorithm and the finite element method to backcalculate layer moduli of flexible pavements. As in previous experiences, a genetic algorithm proved to have a robust global search capacity. The program GAPAVE required measured deflections, load level, layer thicknesses, and a range of genetic algorithm parameters. The objective function minimized the quadratic error between measured and computed deflections. Even though FEM was the analysis method, the examples considered only linear-elastic materials in three-layer structures. The authors made multiple analyses to obtain better parameters for the GA's population, generation, crossover, and mutation rates. Weak pavements appeared to control the appropriate parameters for GA. The authors reported satisfactory results based on a synthetic analysis, but an inspection of the measured versus predicted moduli in their paper indicates a range of error of about ± 100% for hot-mix asphalt and granular bases and up to 25% in subgrade moduli. An additional analysis of sections from the LTPP showed a larger scatter between the measured and predicted modulus.

Gopalakrishnan (2010) proposed a hybrid neural network – particle swarm heuristic optimization (NN–PSO) algorithm for moduli backcalculation. The objective function is the quadratic error between measured and computed pavement surface deflections. The artificial neural network is a surrogate forward calculation response model for a three-layer system (HMA, granular base, and subgrade) based on the ILLI-PAVE program. The NN–PSO accurately predicted the modulus of the HMA (linear-elastic from the ILLI-PAVE training database) and the *"breakpoint"* modulus of the subgrade (bi-linear model from the ILLI-PAVE training database). In contrast, the prediction of aggregate base non-linear characteristics is weak, requiring an independent analysis. The evaluation of two sections of the National Airport Pavement Test Facility (NAPTF) confirms the NN-PSO fitness to estimate the moduli of HMA and subgrade.

Pekcan et al. (2010) developed the SOFTSYS computer program to interpret FWD results over full-depth asphalt pavements. The program can estimate the thicknesses and the layer moduli from surface deflections. It is based on ILLI-PAVE and considers the non-linear behavior of the base course granular materials and fine soil subgrades. SOFTSYS

combines an artificial neural network (ANN), as a surrogate of the finite element method (FEM), with a genetic algorithm (GA). The objective function minimizes the difference between measured and computed deflections. The authors do not explain the population, number of generations, and crossover and mutation rates. Numerical examples show satisfactory HMA and subgrade moduli and full-depth pavement thickness predictions.

Kosasih (2011) implemented a genetic algorithm to backcalculate the moduli of four-layer pavements. Based on closed-form solutions, the GA population contained pseudo-random seed moduli values for the subgrade, granular base, and subbase layers. The objective function minimizes the difference between the measured and computed deflection under the applied load. The surface layer modulus is calculated to match the objective function, subject to the underlying granular base modulus. The fitness function used the difference between the AREA parameters of the measured and computed deflection basins. The GA implementation used real codification and a custom function of the fitness function for crossover operations with a rate of 0.50. The mutation rate was a random ±0.01 change in the genes' current value to exploit the best solution in promising regions. A case study indicated some scattering in the predicted moduli compared to reference values. However, the author carried on an overlay design and proved that the differences were insignificant for practical purposes. One can say that such an analysis is not conclusive because it only considers deflection-reduction, which does not require a detailed characterization of the properties of the in-service pavement before the overlay construction.

Li et al. (2012) applied particle swarm optimization (PSO) to modulus back analysis of pavement structures. The fitness function considered the absolute error between measured and computed deflections. A case study with a three-layer pavement showed remarkable agreement between theoretical and backcalculated moduli.

Senseney et al. (2013) applied a genetic algorithm and a finite element model to back-calculate the top-layer thickness, top-layer modulus, and subgrade modulus of two-layer systems tested with lightweight deflectometer (LWD) based on time history and not the maximum value of deflections. The objective function minimizes the error between measured and computed data, considering the maximum deflection and the time history curves of the LWD sensors. The authors obtained suitable moduli and thickness predictions

in a real-life full-depth reclamation project, avoiding the multiple local minima that affect gradient search algorithms.

Varma et al. (2013) considered the pavement a layered viscoelastic medium. FWD backcalculation yielded viscoelastic properties from time (relaxation modulus) and temperature functions (shift factors). The forward-calculation model was the LAVA layered viscoelastic algorithm based on the quasi-elastic theory of Schapery. The objective function considered the differences between measured and calculated deflections. The backcalculation results for the asphalt concrete layer are not a single value but a four-parameter sigmoidal function for the relaxation modulus [$E(t)$], and a two-parameter polynomial for the shift factors. The constraints included the range of the coefficients of the sigmoidal and polynomial equations, the base and subgrade modulus (considered linear elastic) range, and the depth to a stiff layer under the subgrade. The genetic algorithm used real instead of binary codification, which demanded the GA parameters adjustment by trial and error. The authors do not provide information about the crossover and mutation rates. The best solution requires at least 15 generations, with 300 to 400 individuals. A set of two computer-generated cases created with the LAVA program showed excellent performance in the backcalculation of the sigmoidal relaxation curve. The analysis of two sections of the LTPP encountered some difficulties associated with a stiff layer below the subgrade level. The authors compared the creep compliance data from the LTPP database with the BACKLAVA results. However, they criticized the former based on potential quality problems in testing and viscoplastic effects.

Zaabar et al. (2014) developed DYNABACK-VE, a program that combined viscoelastic dynamic solutions in the time domain with a genetic algorithm for the backcalculation of the HMA modulus master curve and moduli of unbounded bases, subgrade materials, and bedrock (if present) from FWD time histories. The program implements the ViscoWave II model with linear elastic unbound layers as a forward solution. Two case studies showed excellent agreement between the backcalculated relaxation modulus master curve and the measured master curve from laboratory testing on field cores. It is necessary to perform two FWD tests at a specific site with a temperature difference of at least 10°C. The authors do not present further details about genetic algorithm implementation. The authors stressed the advantages of time-domain over frequency-domain analysis for FWD backcalculation to avoid the truncation of deflection time histories.

Scimemi et al. (2016) implemented an Ant Colony Optimization with Lévy perturbation to backcalculate pavement moduli from surface deflection data in airports. The authors implement the minimization of the quadratic error of measured versus computed deflections as the objective function. The objective function has multiple problems for backcalculation: nonlinearity, multimodality, epistasis, and high sensitivity of the solution to noise in measured data. The authors found that the method may accurately estimate pavement properties and avoid local minima. Suggested improvements include implementing a FEM model to consider the nonlinearity of pavement materials.

Li & Wang (2017) developed an ANN-GA program for the backcalculation of pavement moduli under FWD testing. The authors developed FEM models, considering the FWD dynamic loading and the viscoelastic and nonlinear parameters for asphalt and unbound materials, and generated a synthetic database with the ABAQUS software for a wide range of pavement materials and structures, temperatures, and loading levels under axisymmetric conditions to train an artificial neural network. The GA minimized the root mean square error of measured versus computed deflections. The crossover and mutation operators were 0.85 and 0.15, respectively, with 50 generations. Five case studies agreed with field data backed by numerous laboratory tests but restricted to three-layer structures.

3.2.4 Applications in experimental data fitting

Experimental data fitting is necessary for the empirical component of modern Pavement Engineering. Pavement materials behavior challenges data reduction with linear regressions; thus, ad-hoc models require numerical fitting to minimize the quadratic error between measured and estimated values.

Experimental data fitting is an attractive field for implementing search techniques based on an objective function subject to constraints. The following paragraphs summarize some recent applications.

Tsai et al. (2004) and (2009) presented four case studies about applying genetic algorithms in backcalculation and experimental data fitting. The data fitting applications were:

1. The determination of the HMA complex-modulus master curve. It assesses the material response to temperature and frequency load changes based on non-destructive dynamic testing. There is no specific mathematical function for the master curve, so the experimental data is fitted with a spline curve or a gamma function. The objective function minimizes the quadratic error between the measured and estimated moduli restricted to a reference temperature to obtain the loading frequencies.
2. Discrete the relaxation spectrum of the asphalt binder to obtain information about its molecular structure and interpret its behavior as a Maxwell solid. It is an alternative to the master curve. The GA is used to estimate the model's fitting parameters of experimental data.
3. Three-stage Weibull approach to obtain a unique formulation of the asphalt mixes behavior in fatigue and permanent deformation. The GA is used to estimate the model's fitting parameters of experimental data.

Coleri et al. (2010) used a genetic algorithm and curve-shifting to surrogate conventional non-linear constitutive relationships for subgrade resilient modulus. The objective function minimized the error in adjusting the resilient modulus-deviator stress relationship by normalizing the confining pressure effect with a gamma distribution function. The procedure is analogous to the HMA complex-modulus master-curve determination, substituting the normalization by temperature with normalization by the deviator and confining stresses.

Suh et al. (2010) applied a harmony search algorithm to obtain a fatigue cracking model from Accelerated Pavement Testing (APT) data. The objective function minimized the error between the predicted and measured fatigue damage ratios. The authors calibrated the fatigue parameters with elastic-layered theory. They concluded that APT gives a better simulation of pavement performance, predicting longer fatigue lives due to the wandering effect of traffic loads.

Salari and Yu (2011) proposed a pavement segmentation method based on a genetic algorithm and entropy theory for pavement distress detection and classification. The input is a grayscale image of the pavement surface, and the output is the best threshold value for segmentation. The fitness function maximized the threshold levels among the gray levels encoded in 8 bits. The population size is 10, and the crossover and mutation probabilities are 0.7 and 0.04. The distress classification considers cracks and potholes by

dividing the images into tiles. The authors used the measured tiles to train an artificial neural network to quantify cracks and potholes and presented promising results in pavement distress segmentation.

Tao et al. (2013) applied inverse analysis for the inhomogeneous dielectric coefficient of pavement materials based on ground-penetrating radar measurements with a genetic algorithm. The objective function minimized the difference between measured (reflected) and computed waveforms. The crossings and mutation probabilities were 0.60 and 0.15 in a case study with promising results.

Nazzal & Tatari (2013) evaluated the use of neural networks and genetic algorithms to predict subgrade resilient modulus. The approach is a case of data fitting and not of backcalculation because the authors tried to improve the estimation of the three regression parameters (k_1, k_2, k_3) of the non-linear soil modulus model adopted by the MEPDG. Authors consider multiple combinations of indirect soil properties to estimate the non-linear parameters like moisture, density, plasticity, and grain size. The ANN gave better correlation coefficients than the published equations in the MEPDG. The genetic algorithm optimized the artificial neural networks (one for each non-linear parameter) with an objective function to maximize the classification accuracy. A sensitivity analysis showed that an inaccurate prediction of the resilient modulus significantly influences rutting and longitudinal cracking predictions.

Montoya-Rodriguez (2015) proposes a hybrid of artificial neural networks and genetic algorithms to estimate mechanical properties from easy-to-obtain parameters from small databases. The genetic algorithm optimizes the artificial neural network's bias and weights, and its applications may extend to all areas of geotechnical engineering. The objective function minimizes the prediction error of the ANN.

Sharma et al. (2017) developed an artificial neural network to predict the soil moduli for geotechnical and transportation applications based on the index and size-grain properties of three soil deposits in India. The authors employed up to 1000 epochs to train the ANN, obtaining better prediction capabilities than the multiple regression models.

3.2.5 Applications in reliability-based design optimization

Flexible pavement design requires the application of probabilistic concepts to make the design process responsive to the variabilities and uncertainties associated with the design, construction, and performance of pavements. A probabilistic approach may quantify the design risk for a specified reliability level (Darter & Hudson, 1973).

Yang (1972) states that optimizing asphalt pavement design requires a procedure in which all the elements have the same reliability level. A design procedure should provide consistent pavement performance at the desired level of reliability (Kim & Lee, 2002) or a design at a relatively lower cost without compromising reliability (Rajbongshi & Das, 2008). Reliability is a performance measure expressed as the probability that the pavement will perform its intended functions under certain conditions over a specified period (Deshpande, Damnjanovic, & Gardoni, 2010). The performance measure may be the number of load applications before the pavement structural and functional integrity fall below predefined thresholds (Dilip & Sivakumar Babu, 2013). The variability may be described by the mean, the standard deviation, and the probability density distribution (Dalla Valle & Thom, 2016b).

The uncertainties in pavement performance include four categories: (1) spatial variability, including heterogeneity and fluctuations in as-built thickness, (2) variability in quantifying the parameters affecting pavement performance, (3) model bias due to assumptions and idealizations of mathematical models, and (4) statistical errors due to lack-of-fit of regression equations (Kim & Lee, 2002). The sources of uncertainty are the pavement design parameters and their response (Dilip, Ravi, & Sivakumar Babu, 2013).

There is not a single approach to a probabilistic-based design, as illustrated by several design methods:

1. The 1981 Asphalt Institute design method considers three percentiles to define the subgrade design value (resilient modulus) as a traffic function. Heavy traffic requires a smaller subgrade design value (Asphalt Institute, 1981).
2. The 1993 Overseas Road Note considers the 10^{th} percentile of the subgrade bearing capacity as design value (Transport Research Laboratory, 1993).

3. The 1993 AASHTO design method considers the variabilities of (a) the estimated traffic and (b) the pavement condition based on the present serviceability index concept (PSI). All other variables in the AASHTO design equation must be averages (AASHTO, 1993).
4. The 1997 French Guide considers the allowable tensile-stress or tensile-strain variability in bounded materials based on material and construction-quality scattering. Another source of implicit variability is the bearing capacity of the subgrade for the design (LCPC - SETRA, 1994).
5. The ROADENT software (Timm, Newcomb, & Galambos, 2000) accounts for the design reliability with a Monte Carlo simulation technique applied to the variability of the thicknesses and mechanical properties of the layers and the axle weights.
6. The 2008 MEPDG design procedure independently considers the reliability of each damage mode in flexible pavements: fatigue cracking, thermal cracking, rutting, and smoothness (AASHTO, 2008). However, the MEPDG does not consider the change of reliability due to parameter variability (Maji & Das, 2008) because field-observed variabilities are externally incorporated to estimate the predicted distress probability (Rajbongshi & Das, 2008). It appears that MEPDG overestimates pavement reliability, and some authors suggest using load and resistance factors (LRFD) to select the design parameters (Luo et al., 2018) or implementing local calibration (Luo, Hu, & Pan, 2019).

Traditional design methods use a single factor to solve a problem with several random variables with different uncertainties and influences on pavement performance. Consequently, these methods yield inconsistent pavement designs, requiring partial safety or load and resistance factors (Dilip, Ravi, & Sivakumar Babu, 2013).

The last two decades have seen significant research production on reliability-based pavement design. Some research deals with reliability-based optimization analysis. The following paragraphs summarize the research on this subject in two areas: (a) applied reliability and (b) reliability-based design optimization.

3.2.5.1 Applied reliability in asphalt pavement design

Timm et al. (2000) developed a framework to account for the variability of input design parameters incorporating Monte Carlo simulation in an M-E program based on field-calibrated performance observed in Minnesota. They considered fatigue and rutting damage and found that hot-mix asphalt modulus and thickness largely influence fatigue performance variability. The hot-mix asphalt and base thicknesses and the subgrade modulus influence the rutting performance variability. Any variability in axle weight has an *"overwhelming"* effect on the variability of both performance predictions.

Kim & Lee (2002) developed a reliability analysis model for quantifying uncertainties in flexible pavement M-E design. They applied the first-order reliability method (FORM) to a reliability index, β, only based on rutting damage. Comparing with the AASHTO 1993 method shows that the empirical procedure does not produce designs of consistent reliability for the mechanistic failure criterion.

Maji & Das (2008) studied the reliability issues of asphalt pavement design by the ME method. They compared the first-order second-moment (FOSM) and the simulations methods considering four failure definitions based on fatigue and rutting individual or combined thresholds. The variation of fatigue and rutting performances follow a log-normal distribution. They conclude that the thickness of the hot-mix asphalt has the most significant influence on reliability.

Dilip et al. (2013) developed a reliability-based design procedure with the first-order (FORM), second-order (SORM), and Monte Carlo reliability methods. The results were similar among the methods. The thickness of the surface layer is the critical parameter in the reliability of fatigue and rutting failure. The critical strain computations used the response surface methodology (RSM) surrogate technique instead of the layered elastic software KENPAVE. Timm et al. (2000) found that minor traffic variations significantly increase the probability of system failure.

Dilip & Sivakumar Babu (2013) coupled a Bayesian approach to estimate model parameters and a Markov chain Monte Carlo simulation to estimate the distributions of individual parameters. The authors compute the critical strains with the response surface

methodology (RSM) to back-analyze post-failure parameter statistics. The authors found a significant role of the untreated base and the hot-mix asphalt moduli in pavement failure.

Dalla Valle & Thom (2016b) explored how the variability of asphalt modulus, surface thickness, and subgrade modulus affects pavement performance. The authors did not consider the traffic loading variability. A surrogate method of structural analysis allows the rapid and repeated calculation of performance life for Monte Carlo simulation on several sites in UK highways. The research found that the distribution of pavement life has a log-normal distribution.

Dinegdae & Birgisson (2016) developed a load and resistance factor design procedure (LRFD) for Florida's top-down cracking model to provide a reliability-based design. The top-down cracking prediction considers viscoelastic principles and calibration in field pavement sections. The authors used the first-order reliability method (FORM) coupled with a central composite design-based (CCD) response surface approach to surrogate the multilayered elastic model to compute the dissipated creep strain energy due to traffic applications.

Dinegdae et al. (2018) continued the previous work on LRFD by exploring three response surface methods (RSM): central composite design (CCD), Box-Behnken design (BBD), and Dochlert design (DOD). The authors used the Rackwitz-Fiessler algorithm as a first-order reliability method (FORM) for the analysis. The surrogate response surface methods estimate the dissipated creep strain energy limit ($DCSE_{lim}$), which governs the mix resistance to fracture, compared to the accumulated dissipated creep strain energy ($DCSE_{accum}$), which is a function of the structure and traffic. The surrogates, especially CCD, clearly agree with the actual performance values. The reliability analysis produced partial safety factors to implement in LRFD for pavement application. The authors concluded that a reliability analysis framework could capture the influence of the different design input variables, supporting an LRFD procedure for pavement application.

Luo et al. (2018) developed a system reliability-based ME pavement design procedure considering fatigue and rutting for the hot-mix asphalt layer based on the MEPDG models. The authors use the multilayered elastic program MultiSmart3D to generate data for response surface second-order polynomial functions for critical strains. The reliability analysis uses the first-order reliability method. The system is implemented on a

spreadsheet and compared with Monte Carlo simulations. Results show that the uncertainty of the hot-mix asphalt modulus, base modulus, and surface thickness significantly impacts pavement design, which is not surprising considering that the authors focused on the bituminous layer distresses.

Luo et al. (2019) introduced the concept of robust design in pavement applications to minimize the variation in the design outcomes by adjusting the uncertain design parameters. The reliability analysis uses the point estimate method (PEM). The robustness is the signal-to-noise ratio of fatigue cracking and rutting safety factors of the hot-mix asphalt layer. The authors use the non-dominated sorting genetic algorithm II (NSGA-II) to find a Pareto front considering safety (a failure probability lower than an acceptable value), robustness, and construction cost. The conflicting objectives are the minimization of cost and the maximization of reliability. The optimal design is the best compromise between reliability and cost, in contrast with selecting the minimum cost that meets a required failure probability.

3.2.5.2 Reliability-based design optimization

Several references deal with implementing *"reliability-based design optimization (RBDO)"* or any explicit pavement management and design optimization.

Sánchez-Silva et al. (2005) proposed a framework to RBDO. They concluded that pavement design and maintenance require a precise prediction of the distressing process influenced by the uncertainties in traffic loading distribution, material properties, structural behavior, and socioeconomic considerations, especially the discount rate. The reliability-based design optimization is conceptually different from the traditional mechanistic design and produces appropriate designs within a long-term maintenance policy.

Rajbongshi & Das (2008) developed a methodology to obtain cost-effective probabilistic designs for the combined fatigue and rutting risk of failure based on numerical simulation. A comparison with a deterministic ME design shows that it is possible to propose an optimal design with a lower cost for any given reliability level. A subsequent work by Rajbongshi (2014) illustrated an automated design approach to find the most cost-effective solution for independent fatigue and rutting reliability levels.

Deshpande et al. (2010) considered the effect of rehabilitation actions on pavement reliability. The authors define rehabilitation as treatments that improve the functional condition and increase the pavement structural capacity, for example, overlays. They applied a multiobjective genetic algorithm to minimize the rehabilitation costs, maximize the reliability, or satisfy both objectives accounting for the effects of hot-mix asphalt overlay construction. The structural model considered a three-layer system plus the overlay and fatigue and rutting failure modes estimated through regressions based on layered elastic computations. The discount rate, budget limits, and target reliability affect the optimal solutions.

Saride et al. (2019) developed a reliability-based design optimization method for flexible pavements considering probability functions of layer moduli other than normal or log-normal and safety against fatigue and rutting considering the variability of design parameters. The authors proposed a nonlinear surrogate analysis to compute critical strains for hot-mix asphalt fatigue and subgrade rutting in a four-layer pavement. Comparing the proposed and published surrogate elastic solutions shows an imperfect agreement with the multilayered elastic program. The analysis uses the first-order reliability (FORM) and Monte Carlo methods for comparison. The hot-mix asphalt thickness and the untreated bases moduli significantly affect the reliability indexes against fatigue and rutting failure. The mean and COV values of base thickness and subgrade modulus do not affect the reliability index against fatigue failure. The subgrade modulus' mean value and COV significantly affect the rutting performance. The review of a structure designed with the AASHTO 1993 procedure, with nominal reliability of 95%, showed that the actual reliability is 10% to 40% lower due to the variability associated with random design variables.

Following the previous work, Peddinti et al. (2020) proposed a system reliability-based design optimization (SRBDO) for a four-layer flexible pavement considering the dependency between fatigue and rutting. The analysis uses the first-order reliability method (FORM). A four-layer elastic surrogate model estimates critical strains to compute reliability indexes against fatigue and rutting failure modes (Saride, Peddinti, & Basha, 2019). The correlation coefficient evaluates the interrelation of the failure modes. They found that the assumption of statistical independence between failure modes overpredicts the failure probability. The mean thicknesses, resilient moduli, and COV of hot mix asphalt thickness

and subbase modulus significantly influence the system's performance. A particular conclusion in this research suggests the existence of a set of optimum moduli without recognizing the moduli dependency between the subgrade and untreated materials or the climate-frequency dependency of hot-mix asphalt moduli.

Dilip & Sivakumar Babu (2021) proposed a quantile-based reliability-based design optimization (RBDO) to optimize the initial cost to ensure a prescribed reliability level in flexible pavements. The independent failure modes are fatigue and rutting. A Kriging model is used to surrogate the finite-element method based on the ABAQUS and EverStressFE programs. However, as the pavement materials are linear elastic, there is no evident benefit from the FEM solution, for example, using non-linear properties. The reliability analysis uses a Monte Carlo simulation to compute the failure probabilities in an inner loop. An outer loop minimizes the cost using sequential quadratic programming. The authors developed several cases and recognized that future research should focus on the interdependence of layer thickness and moduli, the differential costs due to material quality, and the conjugate failure probability of fatigue and rutting.

3.3 Summary

Dede et al. (2019) point out that there is no *"best"* optimization algorithm for all types of problems in civil engineering. Pavement engineering is a crossroads between geotechnical, transportation, and materials engineering. It is not surprising that there are multiple applications of optimization algorithms in this area, with a clear emphasis on pavement management, for its socioeconomic implications, followed by backcalculation of layer properties. The following sections summarize the major topics of applied optimization in pavement engineering.

3.3.1 Summary of applications in pavement design

Flexible pavement design optimization must minimize the total life-cycle cost (agency and users) constrained to structural or functional conditions.

Although results are similar in the reviewed experiences, the restrictions depend on the pavement analysis method: functional conditions in empirical AASHTO 1993 or damage failure in the mechanistic-empirical procedure. Design optimization may be independent of

the pavement type, as shown by Hadi & Arfiadi (2001), who proposed a method to optimize Australian rigid pavement design with a genetic algorithm and the Portland Cement Association performance models.

Chong et al. (2018) applied the incremental design method based on the MEPDG software to a heavy-traffic road in Hong Kong. Figure 3-9 shows results in terms of total life-cycle costs (thousands of Hong Kong currency), energy consumption (GJ), and greenhouse emissions (ton CO_2) based on IRI (m/km) and roadbase thickness (mm).

Figure 3-9: Search spaces and Pareto front for pavement design optimization.

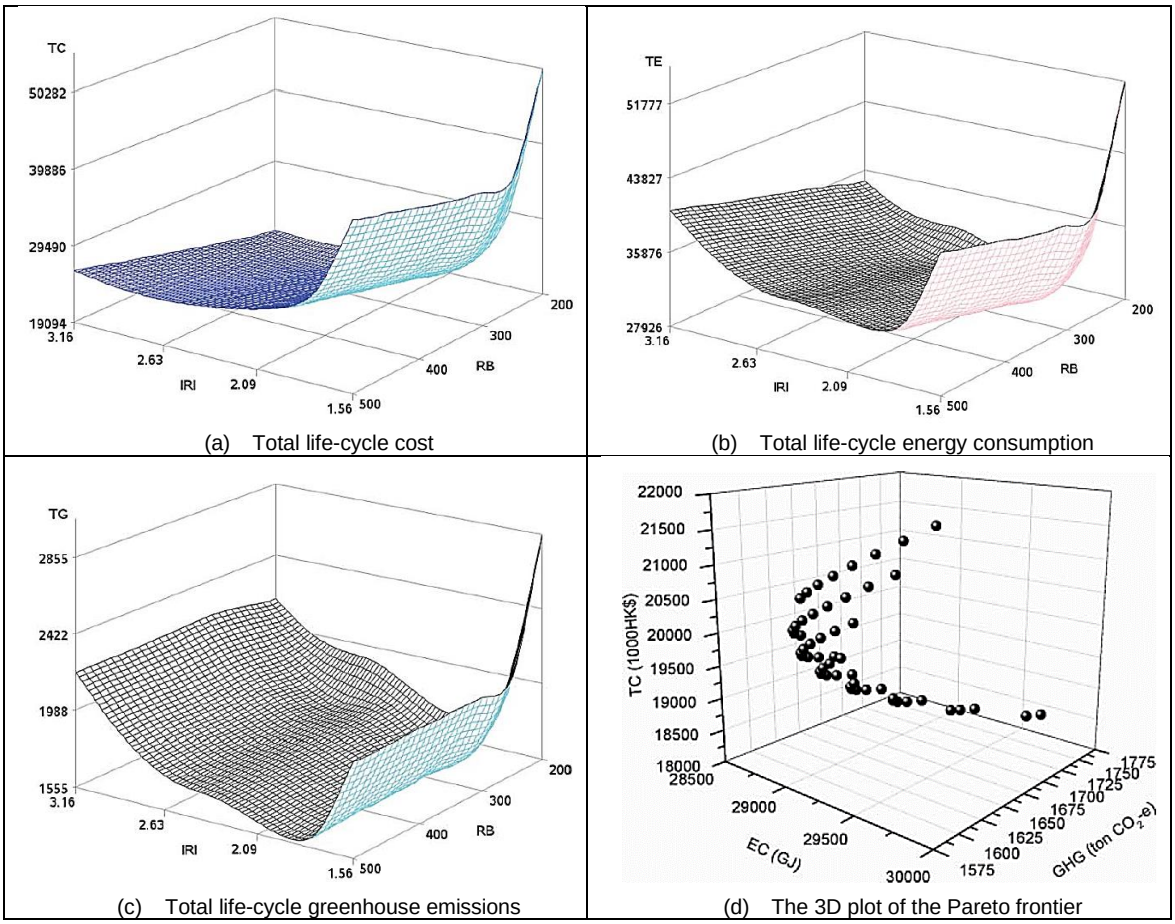

Source: Chong et al. (2018)

The authors explored the whole search space for the proposed problem and identified a tridimensional Pareto front. They did not include variations in the subgrade, climate, or pavement materials other than the roadbase thickness.

The approach is computationally expensive. Suppose each ME computation takes three hours for input setup, run, output interpretation, and data processing for life-cycle cost and energy consumption. The complete analysis may take 206 hours for one traffic level. The time would multiply accordingly for every new variable in pavement design, like subbase thickness, a chemically stabilized base, or a different subgrade (in the same project).

Chong et al. propose a multiobjective pavement design optimization based on mechanistic-empirical incremental damage analysis and sustainability principles. However, it is mandatory to implement efficient search techniques to reduce the computational effort and make the analysis available to practicing Engineers.

3.3.2 Summary of applications in pavement management

Random-search techniques are powerful tools to optimize pavement management activities, especially for multiobjective problems such as minimizing costs and maximizing the pavement state from network to project levels. However, beyond the encouraging published case studies, one must consider testing new GA applications on small-size problems to compare their results to global optimum solutions obtained through complete enumeration (Ferreira, Antunes, & Picado-Santos, 2002). It would be appropriate to implement parallelization techniques to expand the problem sizes beyond the typical examples with some pavement sections and a handful of management activities (Abu-Lebdeh, Chen, & Ghanim, 2014).

According to the reviewed applications, one may classify the used objective functions into three groups based on costs or expenditures, resource consumption, or pavement condition:

1. Based on cost or expenditures:
    a. Minimization of maintenance costs or fluctuations of yearly demand for pavement expenditures.
    b. Maximization of usage of the allocated budget.
    c. Maximization of saving in vehicle operating costs.
    d. Maximization of saving in vehicle operating costs over cost.
2. Based on resource consumption:

   a. Maximization of usage of available workforce or minimization of workforce requirements.
   b. Maximization of usage of available equipment or minimization of equipment requirements.
   c. Maximization of maintenance production.
3. Based on pavement condition or network operation:
   a. Maximization of effectiveness.
   b. Maximization of overall network pavement condition.
   c. Maximization of skid resistance.
   d. Minimization of total travel time of vehicles in a network under maintenance.
   e. Minimization of accidents.

Cost-based functions are the preferred objective functions or constraints (fixed budget). Resource-consumption-based objective functions may interest highway agencies with in-house capabilities beyond administrative management (self-construction). Pavement-condition-based may be the most comprehensive objective function because it can be related to agency and user costs (vehicle operating costs, delay of users, cost of accidents).

Multiobjective optimization is fundamental for a better implementation of pavement management activities because it allows exploring a single optimum solution and a set of near-optimum solutions that may offer trade-offs for the highway agency. Pilson (1999) applied conflicting objectives, while Meneses (2013) considered cost components as M&R strategies, user's costs, and residual value, which may be reduced to a single objective function of the discounted total cost.

To the author´s knowledge, all efforts in multiobjective optimization focused on two, maximum three, complementary, or conflicting objective functions. Mathematically, it is possible to define N objective functions and obtain an incumbent solution with the minimum vector from the origin to the normalized N-dimensional Pareto front. However, the current state of research and technology transfer may demand a simple and graphically understandable approach to mitigate the resistance to embracing these new methods. Future research in multiobjective optimization calls for sustainable aspects, such as environmental and social impacts, to assess maintenance alternatives' costs and benefits (Yepes, Torres-Machi, Chamorro, & Pellicer, 2016).

Most of the reviewed applications used small-size numerical cases with pavement networks comprising less than 100 uniform sections with longitudes near 500 meters. Typical pavement sections may provide a programming scheme, but further work is necessary to execute the management activities on individual pavement sections.

The genetic algorithm performance improves significantly with hybridization with expert systems, reducing the production of invalid individuals or parallelizing with subset migration among populations. One must consider the stochastic process of pavement deterioration with Markov-chain models as proposed in the Arizona pavement management system (Ferreira, Antunes, & Picado-Santos, 2002) or by Morcous & Lounis (2005) and Shahin (2006) for the pavement condition index (PCI) prediction.

Table 3-2 summarizes the main characteristics of some of the described applications of genetic algorithms and other techniques in pavement management systems.

Table 3-2: Summary of pavement management applications with soft computing

Author	Description	Methods	Crossover type & rate	Mutation type & rate	Population range (selected)	Maximum generations
Applications reviewed in this thesis:						
Chan et al. (1994)	Road network maintenance	GA & RA	OP	UF-SG (0.10)	10 – 80 (50)	50
Fwa et al. (1994)	Road network maintenance	GA & RA	OP (0.80)	SG (0.20)	80	100
Taha & Hanna (1995)	Road maintenance based on optimized weights of the ANN	GA & ANN	(0.70)	(0.10)	10	50
Fwa et al. (1996)	Road network maintenance	GA & RA	OP (0.80)	UF-SG (0.20)	30	100
Fwa et al. (1998)	Pavement management activities programming	GA	OP (N.R.)	UF (N.R.)	N.R.	N.R.
Pilson et al. (1999)	Multiobjective optimization in pavement management	GA & RA	OP (0.60)	UF (0.01)	60	70
Fwa et al. (2000)	Multiobjective programming of pavement management activities	GA & RA	OP (0.80)	UF (0.10)	200	500
Shekharan (2000)	Evaluation of pavement deterioration models	GA & RA	OP (N.R.)	UF (N.R.)	N.R.	Up to 9600
Chan et al. (2001)	Constraint handling methods in pavement maintenance programming	GA & RA	TP (N.R.)	UF (N.R.)	100 to 400	250
Ferreira et al. (2002)	Pavement management optimization model	GA	OP-U (0.85)	UF (0.05)	1000	N.R.
Tack & Chou (2002)	Multiyear pavement repair scheduling optimization	GA & ES	N.R.	N.R.	40	Up to 39000
Cheu et al. (2004)	Pavement maintenance scheduling for road closure	GA & S	TP (0.80)	UF (0.05)	4	20
Herabat & Tangphaisankun (2005)	A multiobjective optimization model for Thailand highway network	GA & RA	MP (0.90)	UF (0.045)	50	100

Author	Description	Methods	Crossover type & rate	Mutation type & rate	Population range (selected)	Maximum generations
Morcous & Lounis (2005)	Maintenance optimization of infrastructure networks	GA & MC	DA (0.50)	DA (0.01)	50	10000
Bosurgi & Trifirò (2005)	Pavement maintenance management	GA & ANN	OP (0.90)	UF (0.001)	924	1270
Chootinan et al. (2006)	Multilayer pavement maintenance program	GA, RA & MC	U (0.50)	UF (0.01)	32	50000
Wang et al. (2007)	Network optimization system with multiple objectives	GA, LP & MC	OP (0.90)	UF (0.01)	45	150
Maji &Jha (2007)	Highway infrastructure maintenance schedule	GA	OP (0.70)	UF (0.30)	100	200
Shen et al. (2009)	Chaos particle swarm optimization applied in pavement maintenance decision	CPSO vs. NSGA-II	-- N.R.	-- N.R.	-- N.R.	50 50
Unnikrishnan et al. (2009)	Design and management strategies for mixed public-private transportation networks	GA	OP (0.75)	UF (0.004)	100	100
Quian (2010)	Road pavement performance evaluation	GA & ANN	OP (N.R.)		30	
Tayebi (2010)	Pavement management activities programming	PSO	--	--	15	100
Javed (2011)	Integrated prioritization and optimization approach for pavement management	GA	N.R. (0.85)	N.R. (0.05)	300	N.R.
Shahnazari et al. (2012)	Prediction of Pavement Condition Index	GP & ANN	--	--	--	--
Golroo & Tighe (2012)	Optimum genetic algorithm structure selection	FA & RA	U (0.90)	SG (0.10)	50	500
Farhan & Fwa (2012)	Incorporating priority preferences into pavement maintenance programming	GA	OP (0.85)	UF (0.05)	300	N.R.
Di Mino et al. (2013)	Advanced pavement management system	GA	OP (0.80)	UF (0.90)	100	500
Tayebi et al. (2014)	Analysis of Pavement Management Activities	GA & RA vs. PSO & RA	N.R. (0.90)	N.R. (0.005)	100	1000
Terzi & Serin (2014)	Planning maintenance works on pavements	ACO	--	--	40 ants	33 tours
Yang et al. (2015)	Pavement maintenance scheduling	GA	OP (0.60)	UF (0.01)	500	5000
Elhadidy et al. (2015)	Multiobjective optimum analysis of pavement maintenance	GA & MC	N.R. (0.60)	N.R. (0.01)	100	N.R.
Rifai et al. (2016)	Optimization of pavement maintenance under overload traffic	GA	N.R.	N.R.	N.R.	100
Matin et al. (2017)	Comparative study of metaheuristic algorithms for road maintenance planning	NSGA II MOPSO	N.R. (0.75) N.R.	N.R. (0.30) N.R.	45 N.R.	400 N.R.
Ahmed et al. (2018)	Multiobjective optimization of pavement maintenance	PSO	--	--	100	100
Panda & Swamy (2018)	Improved artificial bee colony algorithm for pavement resurfacing problem	ABC	--	--	100 50 foragers 50 onlookers	5000
Other applications mentioned by Golroo & Tighe (2012):						
Fwa & Sinha (1986)	Relationships between pavement performance and routine maintenance	RA	--	--	--	--
Fwa & Chan (1993)	Model priority assessment of highway pavement maintenance needs	ANN	--	--	--	--

Author	Description	Methods	Crossover type & rate	Mutation type & rate	Population range (selected)	Maximum generations
Carnahan (1988)	Pavement maintenance scheduling	MC	--	--	--	--
Dekker (1996)	Applications of maintenance optimization models (review)	NN	--	--	--	--
Fwa et al. (1996)	Road maintenance and rehabilitation programming	GA	N.R. (0.80)	N.R. (0.20)	60	--
Fwa et al. (1998)	Mathematical programming for routine maintenance	IP	--	--	--	--
Bosurgi & Trifirò (2005)	Road pavement maintenance management	GA & ANN	N.R. (0.90)	N.R. (0.001)	N.R.	N.R.
Hegazi (2006)	Efficient delivery of infrastructure	GA	--	--	--	--

Methods: GA: Genetic algorithm. RA: Regression analysis. ANN: Artificial neural network. S: Simulation. ES: Expert system. MC: Markov chain. IP: Integer programming. LP: Linear programming. PSO: Particle-swarm optimization. ACO: Ant colony optimization. CPSO: Chaos particle swarm optimization. NSGA-II: Non-dominated sorted genetic algorithm. ABC: Artificial Bee Colony.
Crossover type: OP: One-point. TP: Two-point. U: Uniform. MP: Multi-point. DA: Dynamically adjusted by the software.
Mutation type: UF: Uniform flipping. SG: Switching genes. DA: Dynamically adjusted by the software.
Other: N.R..: Non-reported.
Source: Modified after Golroo & Tighe (2012).

Pavement management is a heavily constrained problem. Consequently, the random generation may produce a high rate of invalid individuals. The penalty, decode, and repair methods are preferred to deal with them. It could be more convenient to consider the constraints before the encoding process, avoiding the creation or reparation of invalid individuals. The constraint implementation requires careful consideration and knowledge because it may threaten diversity.

3.3.3 Summary of applications in backcalculation of pavement moduli

Based on the previous discussion, Figure 3-10 shows a proposed classification of backcalculation procedures applied in pavement engineering according to the forward calculation model, background theory, and backcalculation procedure objectives.

The usual objective function in static backcalculation minimizes the *"relative root-mean-square error"* (RMSE) between measured and computed deflections. The RMSE can be the objective and the fitness function in the optimization processes.

Figure 3-10: Extended backcalculation procedures classification

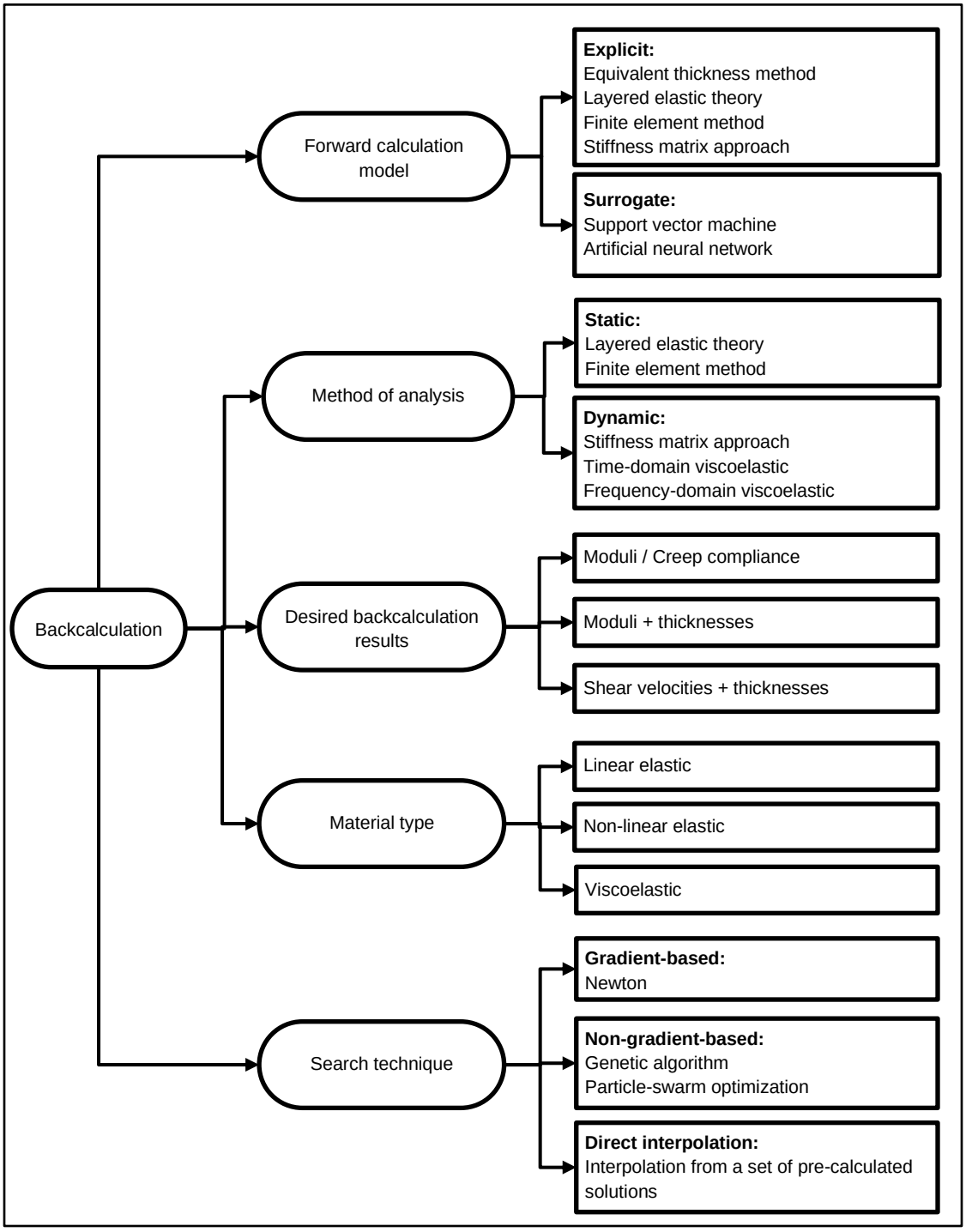

It is possible to propose a different fitness function to improve the optimization process as follows (Alkasawneh, 2007):

$$f = \frac{1}{\alpha \cdot (1 + RMSE)}$$

Eq. 3-13

With the following generalized RMSE function:

$$RMSE = \sqrt[2]{\frac{1}{m} \cdot \sum_{i=1}^{m} w_i \cdot \left(\frac{d_i - D_i}{D_i + \beta}\right)^2} \cdot 100\%$$

Eq. 3-14

Where m is the number of measuring sensors, d_i is the calculated or predicted deflection, D_i is the measured deflection, and w_i is a weighting factor for each deflection point (Kameyama, Himeno, Kasahara, & Maruyama, 1998). The α factor may range between a small number (0.0001) and 1.0 adding significant numbers to the fitness evaluation. In such a case, the analyst seeks to maximize the fitness function to obtain the minimum RMSE and, hopefully, appropriate pavement moduli. The β factor may be 0.001 µm or zero, and it is helpful to avoid *"division by zero"* errors when the computed deflection is low.

In RMSE computation, the user must consider the significant figures and the measurement precision. For example, if the measured deflection is 4 µm, and the calculated deflection is 8 µm, the contributed error in Eq. 3-14 is 100% even though the absolute difference is 4 µm. However, if the FWD precision is 5 µm, and one considers that any difference equal to or less than the precision is zero, the contributions to error are null (Jooste, 2016).

An alternative objective function to RMSE is the *"squared differences summation"* (RSS) used by Reddy et al. (2004), Tsai et al. (2004), Gopalakrishnan (2009, 2010), Park et al. (2010), or Li et al. (2012):

$$RSS = \sum_{i=1}^{m} (d_i - D_i)^2$$

Eq. 3-15

For dynamic backcalculation, one must consider the time histories from FWD load and deflection sensors with the *"relative mean absolute error"* (RMAE) (Zaabar, Chatti, Suk-Lee, & Lajnef, 2014):

$$RMAE = \sum_{k=1}^{m} 100 \cdot \sum_{i,o=1}^{n} \frac{\left|d_i^k - d_o^k\right|}{\{d^k\}_{max}}$$

Eq. 3-16

Where m is the number of sensors, d_i^k is the input deflection information obtained from the field at sensor k, d_o^k is the output deflection information obtained from forward calculation at sensor k, n is the total number of deflection data points recorded by a sensor, and $\{d^k\}_{max}$ is the maximum value of the input deflection information obtained from the field at sensor k.

Based on multiple case studies, Alkasawneh (2007) concluded that the RMSE is an inadequate objective function and postulated that the AREA parameter might be a better objective or fitness function. The AREA parameter is:

$$AREA = \frac{1}{2 \cdot d_0} \cdot \left\{ d_0 \cdot r_1 + \left[\sum_{i=1}^{n-1} d_i \cdot (r_{i+1} - r_{i-1}) \right] + d_n \cdot (r_n - r_{n-1}) \right\}$$

Eq. 3-17

Where $AREA$ is the normalized area of a vertical section of a deflection basin, expressed in units of length; and d_i is any surface deflection at a distance r_i from the test load center. The usual computation of AREA requires four sensors ($d_0, \dots d_3$) equally spaced at 300 millimeters between them ($r_0 = 0\ mm, \dots, r_3 = 900\ mm$).

Nevertheless, researchers keep using RMSE in static backcalculation, with remarkable exceptions, as Kosasih (2011), who used the maximum deflection (d_0) as the objective function and the AREA parameter as the fitness function. Likewise, Horak et al. (1989) proposed several basin-shape-based indexes that might be objective functions in backcalculation procedures.

Further improvements in materials characterization consider non-linear or viscoelastic behavior, which requires load and deflection time histories for the objective function.

Constraints in backcalculation may consider the range of moduli or *"seed values,"* usually from databases or experts' judgment.

A surrogate artificial neural network may avoid the high computation cost of the layered-elastic or viscoelastic theories or the finite element method. However, there is no guarantee that it performs equally or better than the LET or FEM solutions. There are reported difficulties in the backcalculation of the moduli of intermediate granular layers in multilayer systems, both in optimization with LET and ANN and for linear-elastic and non-linear elastic materials (Gopalakrishnan, 2010).

Quijano-Bernal (2016) developed an artificial neural network to backcalculate the moduli of four-layer structures based on a database of 8,640 forward-calculated pavements. The results were discouraging because of the lack of continuity of moduli, as seen in the following figures for asphalt concrete and unbound granular base.

Figure 3-11: Predicted versus exact moduli from ANN based on a database

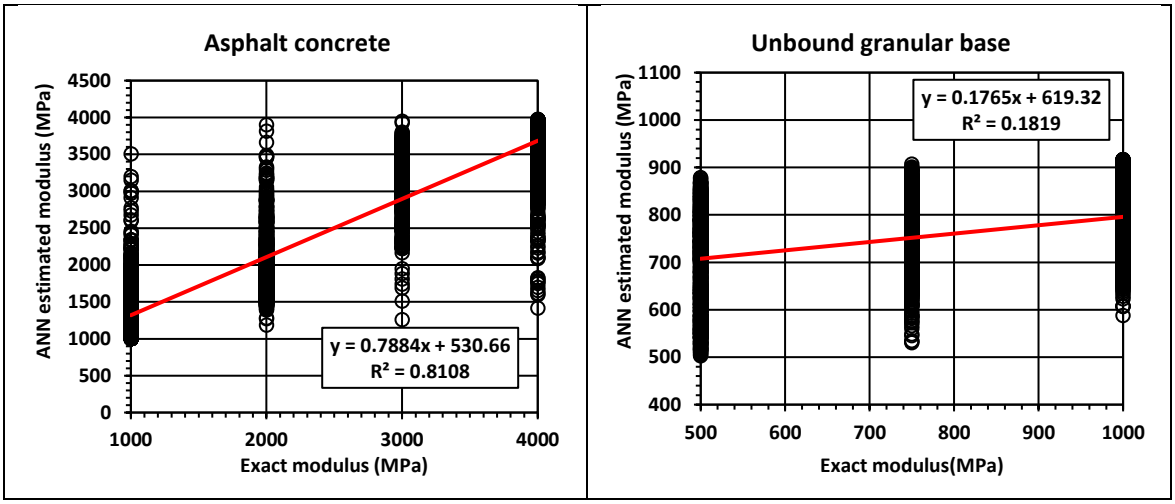

Source: Adapted from Quijano-Bernal (2016).

The following table summarizes the characteristics of the backcalculation applications with metaheuristics. There is a predominance of genetic algorithms with at least two particle swarm optimization implementations described as a promising technique.

Table 3-3: Summary of backcalculation applications with metaheuristics

Author	Program name	Method[1]	Objective function[2]	Forward model[3]	Crossover	Mutation	Pop.[4]	Gen.[5]	Lay[6]
Fwa et al. (1997)	NUS-GABACK	GA	RMSE	LET (BISAR) MET	0.85	0.15	60	150	3-4
Hunaidi (1998)	N.R.	GA	Minimize measured versus computed dispersion curves	Thomson-Haskel & SASW	0.50	Jump: 0.02 Creep: 0.04	50	100	3
Terzi et al. (2003)	N.R.	GA	Minimize layer thickness Maximize elastic moduli	ANN from LET	N.R.	N.R.	10	200	N.R.
Reddy et al. (2004)	BACKGA	GA	RSS	LET (ELAYER)	0.60-0.95 (0.74)	0.001-0.20 (0.10)	20-160 (60)	20-160 (60)	3-4
Tsai et al. (2004)	N.R.	GA	RSS	LET (ELSYM5)	N.R.	N.R.	500-2000	50-200	3
Terzi (2005)	N.R.	GA	N.R.	GEP (Karva)	0.30	0.044	50	10000	N.R.
Rakesh et al. (2006)	BACKGA	GA	RMSE	ANN from LET (ELAYER)	0.90	0.02	200-700	60	2-5
Hu et al. (2007)	DBFWD-GA	GA	RMSE	Dynamic stress wave propagation	0.50	0.10 0.15 0.20	60-140	N.R.	3-4
Alkasawneh (2007)	BackGenetic3D	GA DPGA	RMSE AREA	LET (MultiSmart3D)	Varies	Varies	Varies	Varies	4-20
Gopalakrishnan (2009)	N.R.	PSO SCE	RSS	ANN from FEM (ILLIPAVE)	N.R.	N.R.	N.R.	N.R.	3
Park et al. (2010)	GAPAVE	GA	RSS	FEM	0.70-0.86	0.01-0.05	100-140	70-120	3
Gopalakrishnan (2010)	N.R.	PSO[7] W = 1.0 Cc = 2.8 Cs = 1.3	RSS	ANN from FEM (ILLIPAVE)	--	-	25	--	3
Pekcan et al. (2010)	SOFTSYS	GA	RMSE	ANN from FEM (ILLIPAVE)	N.R.	N.R.	N.R.	N.R.	2-3
Kosasih (2011)	BackCalc	GA	Do AREA	Closed-form equations	0.50	0.01	N.R.	N.R.	4
Li et al. (2012)	N.R.	PSO[7] W = 1.0 Cc = 0.5 Cs = 0.5	RSS	LET (BISAR)	--	--	50	60	3
Senseney et al. (2013)	N.R.	GA	Minimize measured versus computed time history deflection LWD curves	FEM	0.50	0.10	60	60	2
Varma et al. (2013)	BACKLAVA	GA	RMAE	LAVA Layered viscoelastic algorithm	N.R.	N.R.	300-400	15	5
Zaabar et al. (2014)	DYNABACK-VE	GA	RMAE	ViscoWave II (Viscoelastic dynamic solution in the time domain) LET for unbound layers	N.R.	N.R.	N.R.	N.R.	4
Scimemi et al. (2016)	N.R.	ACO[8] ξ = 0.85 q = 0, 1 α = 1.8 k = 50	RMSE	LET (LEAF)	--	--	--	50	4
Li & Wang (2017)	N.R.	GA	RMSE	ANN from FEM (ABAQUS)	0.85	0.15	N.R.	50	3

1. Methods: GA: Genetic algorithm; DPGA: Dynamic parameterless genetic algorithm; PSO: Particle Swarm Optimization; SCE: Shuffled Complex Evolution; ACO: Ant Colony Optimization.
2. Objective functions: RMSE: root-mean-square error; RSS: Squared differences summation; RMAE: Relative mean absolute error.

3. Forward model: LET: Layered-elastic theory; MET: method of equivalent thickness; SASW: Spectral analysis of surface waves; ANN: Artificial neural network; GEP: Gene expression programming.
4. Pop.: Population.
5. Gen.: Generations.
6. Lay: Number of layers in case studies.
7. Parameters of Particle Swarm Optimization: W: Inertia factor; Cc: Cognitive acceleration coefficient; Cs: Social acceleration coefficient.
8. Parameters of Ant Colony Optimization: ξ = 0.85 is the convergence speed (rate of pheromone evaporation); q = (0, 1) is the elitism; α = 1.8 is the stability index (diversification); and k = 50 is the archive dimension (number of ants).
9. N.R.: non-reported.

3.3.4 Summary of applications in data-fitting

Data fitting uses soft computing techniques, including metaheuristics, to improve phenomenological models based on extensive experimental data without a specific physical model. Other applications include image processing for pavement distress detection and segmentation or dielectric coefficient estimation from reflected waves from ground-penetrating radar. The hybridization of artificial neural networks with metaheuristics improves the prediction capabilities of the ANN.

3.3.5 Summary of applications in reliability-based design optimization

It has been recognized that pavement design must consider the variability of the design input parameters and their effect on the long-term performance of the structure. The uncertainties in materials, traffic loads, environmental conditions, and as-built conditions may explain the poor performance due to early functional and structural distress in all pavements.

Numerous authors proposed different reliability-based approaches to pavement design, considering target reliability, evaluating the resultant reliability of a given structure, or proposing reliability-based design optimization considering cost restrictions. The benefits of the reliability-based design are evident in more reliable structures, better material selection, or lower initial or life-cycle costs.

For a given pavement structure, a set of mean values, coefficients of variance, and probability density functions for moduli and thickness allow the estimation of the probability of failure with an equation of the form (Dilip & Sivakumar Babu, 2021):

$$P(N_x < N_{lim}) = P\left(\frac{N_x}{N_{lim}} - 1 < 0\right) = P[g_x(\boldsymbol{P}) < 0]$$

Eq. 3-18

Where $P(N_x < N_{lim})$ is the probability of failure for a specific distress x, N_x is the allowable number of load repetitions associated with the distress, N_{lim} is the expected number of load repetitions, $g_x(\boldsymbol{P})$ is a performance function, and $\boldsymbol{P}$ is a vector with the input parameters (thicknesses and moduli) that govern the pavement life.

Even though the benefits of the reliability-based design are evident, there are aspects of interest in the reviewed research that demand attention:

1. The authors highlight that the uncertainty in traffic loadings significantly affects pavement reliability. However, the case studies use a simplified representation of traffic loadings based on an equivalent axle wheel load on the pavement surface. There is no discussion about converting the mixed traffic into equivalent single-wheel repetitions considering the uncertainties of the axle projection per type or the load magnitudes.
2. The case studies consider pavements with three or four linear-elastic layers. The reliability analysis is computationally expensive, and researchers focused on different surrogate models to substitute the layered elastic system to estimate the critical strains for damage analysis. In one case, the authors use two finite element programs with linear elastic moduli, wasting the capabilities of non-linear modeling.
3. Most of the research focuses on the traditional distress of mechanistic-empirical design: fatigue of the hot-mix asphalt and rutting of the whole structure. Some research includes new models of top-down fatigue cracking and partial rutting for asphalt layers. The authors agree that the reliability analysis can include any number of distresses; however, there are no alternative proposals, for example, for roughness progression prediction, which would be significant for users' cost predictions.
4. The reliability against combined distresses appears to define a critical condition with lower values of reliability or thicker structures for target reliability. However, several reports disregard this condition and focus on one distress only.
5. In some cases, the authors assume or replicate previously published mean values and coefficients of variance of thicknesses and moduli. Some significant conclusions, even with cost computations, depend on these values, but the authors do not discuss them further.
6. In the last two decades, the research on reliability-based pavement design highlighted the drawbacks of the previous pavement design methods, including the MEPDG. However, it is unclear how the incremental pavement design proposed in MEPDG could

consider reliability analysis with the dependency of the parameter variability considering its computational cost and the use of complex traffic and climate models.

Reliability-based pavement analysis and design offer an exciting and productive area for future research. However, this dissertation will not apply reliability concepts considering the complexities associated with reliability incorporation in an incremental pavement design scheme as the MEPDG-type proposed in the next section of this document.

4 Analysis method

The road to success is paved with the hot asphalt of failure.

Craig D. Lounsbrough.

An abridged version of this chapter was presented at the ASCE International Airfield and Highway Pavements Conference in Chicago, Illinois (U.S.A.) in July 2019 (Vásquez-Varela & García-Orozco, 2019).

4.1 Layered elastic analysis

4.1.1 Overview of layered elastic theory

Layered elastic theory (LET) has been the preferred method of analyzing asphalt pavements in highways and airports since its introduction by Burmister (1943). The LET models the pavement as a semi-infinite continuum, divided into discrete layers of finite thickness overlaying an elastic half-space (see Figure 4-1). The mechanical properties are the elastic modulus (resilient modulus) and the Poisson ratio.

The main characteristics of the layered elastic theory, with some up-to-date variations, are:

1. The pavement corresponds to a series of N horizontal layers, infinite in the horizontal plane, and with finite thicknesses (h_i) except for the infinite lower layer, as in the Boussinesq model. Figure 4-1 shows a layered elastic medium in cylindrical coordinates and axial symmetry around the center of the uniformly loaded area representing a vehicular wheel applied on the surface.
2. The materials are weightless, so the stresses, strains, and displacements are solely due to the applied traffic loads. Including the density modifies the stress-equilibrium equations, which is necessary to analyze non-linear (stress-sensitive) elastic materials.

It is also possible to prescribe normal, or shear stresses on the upper boundary as traffic loads.

3. The mechanical properties are the modulus (E) and Poisson ratio (ν); hence, the solution considers isotropic linear elastic materials, but it is possible to consider non-linear behavior in discrete points with a proper definition of the stress-moduli relationship.
4. The elastic layered medium is a composed system. There is a continuity of stresses and strains in the interfaces between layers. The continuity is a mathematical concept, but it may represent the effect of prime and tack coats in asphalt layer interfaces or the compatibility of fine fractions in granular and soil materials. Broadly, the friction between particles develops structural continuity in the interfaces. When there is a significant contrast between the rigidities, there may be a loss of continuity, as is reported in pavements with Portland cement stabilized bases under asphalt concrete (LCPC - SETRA, 1994).

Figure 4-1: Example of a layered elastic system with a uniform load on its surface

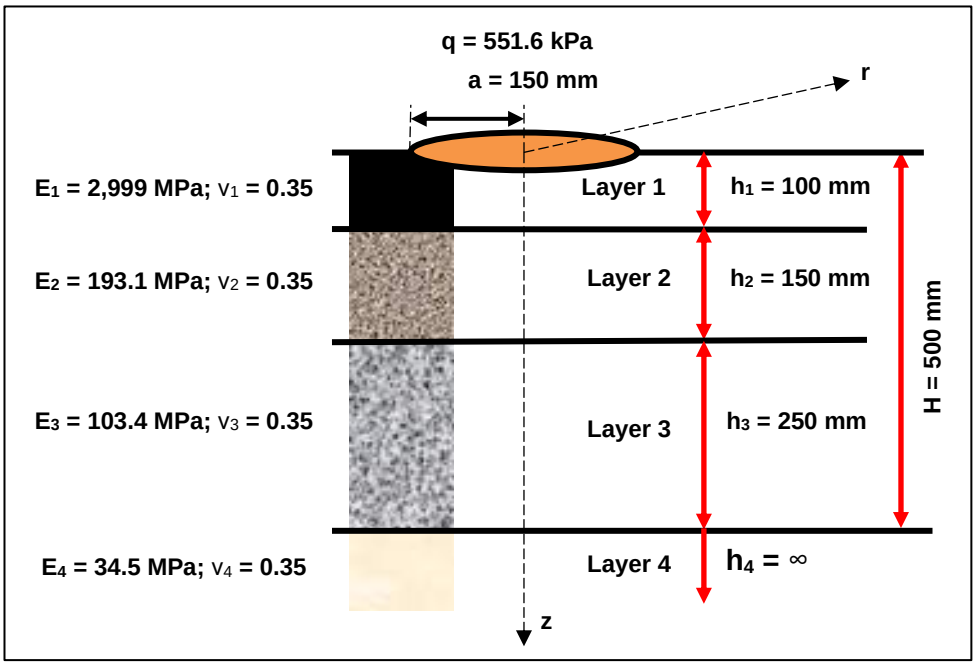

LET usually employs uniform pressure to simulate the effect of wheel loads. However, non-uniform axisymmetric loadings are of interest. Pioneering work by Harr and Lowell (1963) allowed the computing of vertical stresses under parabolic boundary load with superposition to overcome the inaccuracy of uniform contact pressures. Charyulu (1964)

also considered a parabolic pressure distribution on a circular surface. Chen (1971) evaluated an elliptically distributed pressure over a circular area and a uniform pressure applied over a rectangular area in two and three-layer structures. Yoshimura et al. (1972) presented solutions for three-layer systems under normally distributed and tangential loads. Kai (1987) developed expressions for vertical, centripetal-horizontal, unidirectional horizontal, and rotational-horizontal loads in N-layer systems. The BISAR software (De Jong, Peutz, & Korswagen, 1979) applies vertical and horizontal loads (braking, accelerating, cornering), considers a friction tire-pavement factor, and the direction of traffic flow. Maina et al. (2012) analyzed a uniformly distributed rectangular model, with normal and shear components, as a more realistic approach to the tire footprint and found differences in the tensile strains of the HMA and compressive-strains in the subgrade of a three-layer example. They also found that wide-base tires are more damaging than dual tires. More recently, Kimura (2014) found, in two-layer systems, that shear stresses at the surface tend to spread horizontally instead of vertically, disregarding the modulus ratio of the structure, and that the effect of shear stress may be more significant than that of the vertical component in curves and crossings.

There are some concerns about the capacity of LET to represent real stresses and strains. For example, Loulizi et al. (2006) analyzed an instrumented section of the Virginia Smart Road project. They found that LET overestimates pavement responses at low and intermediate temperatures and underestimates the response at high temperatures. Tensile strains in HMA vary linearly with temperature, disregarding that the HMA modulus varies exponentially with temperature.

4.1.1.1 Differential equations

Appendix B by Huang (2004) presents the differential equations for the stresses and displacements components in a layered elastic structure with axial symmetry in a cylindrical coordinate system (r, z, θ), as shown in Figure 4-1. For example, stress in the z-direction (σ_z) can be determined by:

$$\sigma_z = \frac{\partial}{\partial z}\left[(2-\nu)\nabla^2\phi - \frac{\partial^2\phi}{\partial z^2}\right]$$

Eq. 4-1

Where σ_z is the normal stress in the z-direction, ν is the Poisson ratio, and ϕ is a stress function that satisfies the following governing differential equation at any point of the layered system.

$$\nabla^4\phi = \left(\frac{\partial^2\phi}{\partial r^2} + \frac{1}{r}\frac{\partial\phi}{\partial r} + \frac{\partial^2\phi}{\partial z^2}\right)\left(\frac{\partial^2\phi}{\partial r^2} + \frac{1}{r}\frac{\partial\phi}{\partial r} + \frac{\partial^2\phi}{\partial z^2}\right) = 0$$

Eq. 4-2

Where ∇ is the Laplace operator. There are five additional equations for the normal stresses in r (σ_r, Eq. 4-3) and θ directions (σ_θ, Eq. 4-4), the shear stress in the $r-z$ plane (τ_{rz}, Eq. 4-5), and the vertical (w, Eq. 4-6 [a] & [b]) and radial (u, Eq. 4-7) displacements:

$$\sigma_r = \frac{\partial}{\partial z}\left(\nu\cdot\nabla^2\phi - \frac{\partial^2\phi}{\partial r^2}\right)$$

Eq. 4-3

$$\sigma_\theta = \frac{\partial}{\partial z}\left[\nu\cdot\nabla^2\phi - \frac{1}{r}\frac{\partial\phi}{\partial r}\right]$$

Eq. 4-4

$$\tau_{rz} = \frac{\partial}{\partial r}\left[(1-\nu)\nabla^2\phi - \frac{\partial^2\phi}{\partial z^2}\right]$$

Eq. 4-5

$$w = \frac{1+\nu}{E}\left[(1-2\nu)\nabla^2\phi + \frac{\partial^2\phi}{\partial r^2} + \frac{1}{r}\frac{\partial\phi}{\partial r}\right](a)$$

$$w = \frac{1+\nu}{E}\left[2(1-\nu)\nabla^2\phi - \frac{\partial^2\phi}{\partial z^2}\right](b)$$

Eq. 4-6

$$u = -\frac{1+\nu}{E}\left[\frac{\partial^2\phi}{\partial r\partial z}\right]$$

Eq. 4-7

Where E is the Young modulus, ν is the Poisson ratio, and ϕ is the stress function. One can demonstrate that both equations for vertical displacement (Eq. 4-6 [a] & [b]) are equivalent. Several authors employ Eq. 4-6 (b), like Peutz, Van Kempen, & Jones (1968); Yoshimura, Ushio, & Sugawara (1972); Ioannides & Khazanovich (1998); Maina & Matsui (2004); Khazanovich & Wang (2007); and Kimura (2014).

One must propose a stress function that satisfies the differential equations to solve the layered system. The stress function proposed by Burmister (1943) is:

$$\phi_i = J_0(mr)[(A_i + C_i z)e^{mz} - (B_i + D_i z)e^{-mz}]$$

Eq. 4-8

Where ϕ_i is the stress function of the i^{th} layer, r is the radial coordinate, and z is the vertical coordinate of any point of interest inside the i^{th} layer, J_0 is the Bessel function of the first kind and order zero, and m is a parameter used in the Hankel transformation to solve the stresses and displacements due to a circular loaded area. A_i, B_i, C_i, and D_i are integration constants for each layer obtained from the boundary and interface conditions. The stress function includes the exponential function of the "$\pm m \cdot z$" product, which is prone to underflow and overflow errors in computational solutions for large values of depth and the m parameter.

Other authors propose alternative stress functions by normalizing the exponential and Bessel functions by the radius of the loaded area (Kai, 1987) or the total depth. Huang (1969) applies the latter case as follows:

$$\phi_i = \frac{H^3 J_0(m\rho)}{m^2}\left[(A_i + C_i m\lambda)e^{-m(\lambda_i - \lambda)} - (B_i + D_i m\lambda)e^{-m(\lambda - \lambda_{i-1})}\right]$$

Eq. 4-9

Where ϕ_i is the stress function of the i^{th} layer, H is the full depth of the pavement (500 mm in Figure 4-1), $\rho = r/H$ is the normalized radial coordinate and $\lambda = z/H$ is the normalized vertical coordinate of any point of interest inside the i^{th} layer. For the i^{th} layer, λ_i is the normalized depth of its bottom and λ_{i-1} are the normalized depth of its top.

Eq. 4-9 is substituted in the differential equations for each structural response. For example, the stress in the z-direction is:

$$(\sigma_z^*)_i = -mJ_0(m\rho)\left\{[A_i - C_i(1 - 2\nu_i - m\lambda)]e^{-m(\lambda_i - \lambda)} + [B_i + D_i(1 - 2\nu_i + m\lambda)]e^{-m(\lambda - \lambda_{i-1})}\right\}$$

Eq. 4-10

Where $(\sigma_z^*)_i$ is the normal stress in the z-direction of any point in the i^{th} layer due to a vertical load equal to $-mJ_0(m\rho)$. The other terms in Eq. 4-10 are defined above. The Hankel transformation gives the actual normal stress in the z-direction (σ_z) due to a constant load (q) distributed over a circular area of radius (a) as follows:

$$\sigma_{zi} = q\alpha \int_0^\infty \frac{(\sigma_z^*)_i}{m} J_1(m\alpha)dm$$

Eq. 4-11

Where σ_{zi} is the actual normal stress in the z-direction of any point in the i^{th} layer due to load q, J_1 is the Bessel function of the first kind, and order one, $\alpha = a/H$ is the normalized radius of the loaded area, and m is a parameter used in the Hankel transformation. The other terms in Eq. 4-11 are already defined.

Similarly, the normal stresses in r (σ_r) and θ directions (σ_θ), and the shear stress in the $r-z$ plane (τ_{rz}) are as follows:

$$(\sigma_r^*)_i = \left[mJ_0(m\rho) - \frac{J_1(m\rho)}{\rho}\right]\left\{[A_i + C_i(1+m\lambda)]e^{-m(\lambda_i-\lambda)} + [B_i - D_i(1-m\lambda)]e^{-m(\lambda-\lambda_{i-1})}\right\} + 2\nu_i m J_0(m\rho)\left[C_i e^{-m(\lambda_i-\lambda)} - D_i e^{-m(\lambda-\lambda_{i-1})}\right]$$

Eq. 4-12

$$(\sigma_\theta^*)_i = \frac{J_1(m\rho)}{\rho}\left\{[A_i + C_i(1+m\lambda)]e^{-m(\lambda_i-\lambda)} + [B_i - D_i(1-m\lambda)]e^{-m(\lambda-\lambda_{i-1})}\right\} + 2\nu_i m J_0(m\rho)\left[C_i e^{-m(\lambda_i-\lambda)} - D_i e^{-m(\lambda-\lambda_{i-1})}\right]$$

Eq. 4-13

$$(\tau_{rz}^*)_i = mJ_1(m\rho)\left\{[A_i + C_i(2\nu_i + m\lambda)]e^{-m(\lambda_i-\lambda)} - [B_i - D_i(2\nu_i - m\lambda)]e^{-m(\lambda-\lambda_{i-1})}\right\}$$

Eq. 4-14

The author of this dissertation reviewed all the equations in Appendix B of Huang (2004) and found an inconsistency in the vertical and radial displacement equations units. The corrected equations are:

$$(w^*)_i = -\frac{(1+\nu_i)\cdot H}{E_i} J_0(m\rho)\{[A_i - C_i(2-4\nu_i - m\lambda)]e^{-m(\lambda_i-\lambda)} - [B_i + D_i(2-4\nu_i + m\lambda)]e^{-m(\lambda-\lambda_{i-1})}\}$$

Eq. 4-15

$$(u^*)_i = \frac{(1+\nu_i)\cdot H}{E_i} J_1(m\rho)\{[A_i + C_i(1+m\lambda)]e^{-m(\lambda_i-\lambda)} + [B_i - D_i(1-m\lambda)]e^{-m(\lambda-\lambda_{i-1})}\}$$

Eq. 4-16

Where $(w^*)_i$ is the vertical displacement and $(u^*)_i$ is the radial displacement of any point in the i^{th} layer due to a vertical load equal to $-J_0(m\rho)$ or $J_1(m\rho)$, respectively. The Hankel transformation method gives the actual displacements. Other terms in Eq. 4-15 and Eq. 4-16 are already defined. The difference between Eq. 4-15 and Eq. 4-16 with those presented by Huang (2004) is the multiplication by the total thickness (H).

4.1.1.2 Interface conditions

The boundary and continuity conditions are defined by the relationship between the structural responses in the pavement surface, the foundation, and the interfaces. Each layer has four integration constants. Thus, one needs at least four independent equations for the pavement layers and two for the foundation. For a full friction interface, one can propose that the normal stress in the z-direction, the shear stress in the r-z plane, and the vertical and radial displacements are equal across the interface.

Other boundary conditions require different equations. Huang (2004) proposed zero shear stress in the r-z plane to represent the unbounded condition at the interface; this reduces to zero an entire row in the matrix equations, which impedes its inversion in the computation of the coefficients.

The current version of UNLEA considers both full friction interfaces and partially bonded interfaces based on the strategy implemented by Hayhoe (2002) for the LEAF computer program. The partially bonded condition allows the relative horizontal movement between two layers at the interface with a shear spring that represents the connection according to the following equation (Hayhoe, 2002):

$$\tau_i = k_i(u_i - u_{i+1})$$

Eq. 4-17

Where τ_i is the radial shear stress at the interface between layers i and $i+1$, $(u_i - u_{i+1})$ is the relative radial displacement across the interface, and k_i is the interface spring stiffness with force units over a length raised to the cube (F/L³). The model is simplified with the following change of variable:

$$k_i = \frac{l_i}{1 - l_i}$$

Eq. 4-18

Where l_i is a non-dimensional parameter for fully bonded layers, $k_i = \infty$ and $l_i = 1.0$, and for unbounded layers, $k_i = 0$ and $l_i = 0.0$. According to Hayhoe (2002), the JULEA program uses this variable change with a further logarithmic transformation in the input data parameter. LEAF and UNLEA use the input parameter directly in the computational routines. Thus, the matrix equation for bonded interfaces ($l_i = 1.0$) is (Huang, 2004):

$$\begin{bmatrix} 1 & F_i & -(1-2\nu_i - m\lambda_i) & (1-2\nu_i + m\lambda_i)\cdot F_i \\ 1 & -F_i & 2\nu_i + m\lambda_i & (2\nu_i - m\lambda_i)\cdot F_i \\ 1 & F_i & 1 + m\lambda_i & -(1-m\lambda_i)\cdot F_i \\ 1 & -F_i & -(2-4\nu_i - m\lambda_i) & -(2-4\nu_i + m\lambda_i)\cdot F_i \end{bmatrix} \begin{Bmatrix} A_i \\ B_i \\ C_i \\ D_i \end{Bmatrix}$$

$$= \begin{bmatrix} F_{i+1} & 1 & -(1-2\nu_{i+1} - m\lambda_i)\cdot F_{i+1} & 1-2\nu_{i+1} + m\lambda_i \\ F_{i+1} & -1 & (2\nu_i + m\lambda_i)\cdot F_{i+1} & 2\nu_{i+1} - m\lambda_i \\ R_i \cdot F_{i+1} & R_i & (1+m\lambda_i)\cdot R_i \cdot F_{i+1} & -(1-m\lambda_i)\cdot R_i \\ R_i \cdot F_{i+1} & -R_i & -(2-4\nu_{i+1} - m\lambda_i)\cdot R_i \cdot F_{i+1} & -(2-4\nu_{i+1} + m\lambda_i)\cdot R_i \end{bmatrix} \begin{Bmatrix} A_{i+1} \\ B_{i+1} \\ C_{i+1} \\ D_{i+1} \end{Bmatrix}$$

Eq. 4-19

Where all terms are already defined, and:

$$F_i = e^{-m(\lambda_i - \lambda_{i-1})}$$

Eq. 4-20

$$R_i = \frac{E_i}{E_{i+1}} \cdot \frac{1+\nu_{i+1}}{\nu_i}$$

Eq. 4-21

Each row defines the continuity of the vertical stress (σ_z), the shear stress (τ_{rz}), the horizontal displacement (u), and the vertical displacement (w), respectively.

Also, the matrix equation for unbounded interfaces ($l_i = 0.0$) is:

$$\begin{bmatrix} 1 & F_i & -(1-2\nu_i-m\lambda_i) & (1-2\nu_i+m\lambda_i)\cdot F_i \\ 1 & -F_i & 2\nu_i+m\lambda_i & (2\nu_i-m\lambda_i)\cdot F_i \\ 1 & -F_i & -(2-4\nu_i-m\lambda_i) & -(2-4\nu_i+m\lambda_i)\cdot F_i \\ -1 & F_i & (sml-1)\cdot(2\nu_i+m\lambda_i)+sml\cdot(1+m\lambda_i) & [(sml-1)\cdot(2\nu_i-m\lambda_i)-sml\cdot(1-m\lambda_i)]\cdot F_i \end{bmatrix} \begin{Bmatrix} A_i \\ B_i \\ C_i \\ D_i \end{Bmatrix}$$

$$= \begin{bmatrix} F_{i+1} & 1 & -(1-2\nu_{i+1}-m\lambda_i)\cdot F_{i+1} & 1-2\nu_{i+1}+m\lambda_i \\ F_{i+1} & -1 & (2\nu_i+m\lambda_i)\cdot F_{i+1} & 2\nu_{i+1}-m\lambda_i \\ R_i\cdot F_{i+1} & -R_i & -(2-4\nu_{i+1}-m\lambda_i)\cdot R_i\cdot F_{i+1} & -(2-4\nu_{i+1}+m\lambda_i)\cdot R_i \\ sml\cdot R_i\cdot F_{i+1} & sml\cdot R_i & sml\cdot(1+m\lambda_i)\cdot R_i\cdot F_{i+1} & -sml\cdot(1-m\lambda_i)\cdot R_i \end{bmatrix} \begin{Bmatrix} A_{i+1} \\ B_{i+1} \\ C_{i+1} \\ D_{i+1} \end{Bmatrix}$$

Eq. 4-22

All terms are already defined, and sml is a small number (0.0001) to avoid singular matrices. Each row defines the continuity of the vertical stress (σ_z), the shear stress (τ_{rz}), and the vertical displacement (w); and the partial continuity of the horizontal displacement (u) related to the shear stress (τ_{rz}).

At the upper surface ($i = 1,\ \lambda = 0$), the boundary conditions are $(\sigma_z^*)_1 = -m \cdot J_0(m\rho)$, and $(\tau_{rz}^*)_1 = 0$, which defines the following equation:

$$\begin{bmatrix} e^{-m\lambda_1} & 1 \\ e^{-m\lambda_1} & -1 \end{bmatrix} \begin{Bmatrix} A_1 \\ B_1 \end{Bmatrix} + \begin{bmatrix} -(1-2\nu_1)\cdot e^{-m\lambda_1} & 1-2\nu_1 \\ 2\nu_1\cdot e^{-m\lambda_1} & 2\nu_1 \end{bmatrix} \begin{Bmatrix} C_1 \\ D_1 \end{Bmatrix} = \begin{Bmatrix} 1 \\ 0 \end{Bmatrix}$$

Eq. 4-23

Where all terms are already defined.

The stresses and displacements vanish when $\lambda \to \infty$, so it can be concluded that $A_n = C_n = 0.0$. Consequently, there are $4n-2$ constants for an n-layer system. By successive multiplications, the constants for the first layer are related to those of the last layer (Huang, 2004):

$$\begin{Bmatrix} A_1 \\ B_1 \\ C_1 \\ D_1 \end{Bmatrix} = [4x2\ matrix] \begin{Bmatrix} B_n \\ D_n \end{Bmatrix}$$

Eq. 4-24

According to Kruntcheva et al. (2005), pavement performance is severely affected by the bonding condition between layers. The lower bearing capacity and slippage failures reduce the ride quality. The design assumes complete bonding between layers, but the actual interface condition is in an intermediate state. The de-bonding of the asphalt layers may reduce up to 80% of the fatigue life. Ziari & Kharibi (2007) obtained similar conclusions and

estimated a 20% increase in granular bases and subgrade compressive strain with a corresponding reduction in allowable repetitions by the conventional rut limiting model.

Duong et al. (2017) reviewed the French practice over an instrumented asphalt pavement with LET (Alizé) and a viscoelastic FEM (Viscoroute) solution. They found that the interlayer condition is neither bonded nor unbounded but varies with temperature. At higher temperatures, there is evidence that de-bonding occurs between asphalt layers.

Viscoelastic FEM allows better modeling of the bonding-temperature dependency. Alae et al. (2018) modeled, with an enhanced LET, the tensile strain at the surface in pavements with cement-treated (CTB) and granular bases. They found thick asphalt pavements with CTB prone to top-down longitudinal cracking. In contrast, conventional flexible pavements are prone to bottom-up cracking except when interfaces are bonded at high temperatures. The partial de-bonding of asphalt layers results in considerable longitudinal tensile strain at the bottom of the corresponding HMA layer and a slight increase in transverse strain at the top of pavements. The HMA over CTB may develop both cracking patterns at high temperatures simultaneously. De-bonding has a significant impact on pavements with granular bases.

4.1.2 Available software

Table 4-1 summarizes 22 pavement analysis and design computer programs, including recent layered elastic theory and finite element method developments.

Table 4-1: Computer programs for the analysis of asphalt pavements

Program	Author(s)	Method of analysis	Max. layers	Max. loads	Remarks
CHEVRON	Warren & Dieckman (1963) and Michelow (1963) (Chevron Research)	Layered elastic	5	1	CHEV5L. First layered elastic program (1963).
BISAR	De Jong et al. (1979) (Shell Petroleum, UK)	Layered elastic	5	10	BISAR replaces the BISTRO program. Currently, in version 3.0
ELSYM5	G. Ahlborn (1972) (University of California at Berkeley)	Layered elastic	5	10	It was widely used. Non-compatible with a modern OS.
PDMAP (PSAD)	Finn et al. (1977) (NCHRP Project 1-10)	Layered elastic	5	2	It includes provisions for iteration to reflect non-linear response in untreated aggregate layers.
KENPAVE	Yang H. Huang (1993) (University of Kentucky)	Layered elastic	19	6	It allows for simplified viscoelastic and non-linear analysis.

Program	Author(s)	Method of analysis	Max. layers	Max. loads	Remarks
JULEA	Jacob Uzan (1994) (Technion, Israel)	Layered elastic	19	4+	Currently, in the MEPDG. It has limitations in near-surface points.
LEAF	Gordon Hayhoe (2002) (FAA, USA)	Layered elastic	20	Multiple	Base program for the FAA software. Open-source.
WESLEA	Van Cauwelaert & Lequeux (1986)	Layered elastic	5		Extended code with several versions: EVERSTRESS, WFW, and PerROAD.
Alizé 3	Laboratoire Central des Ponts et Chaussés (Francia)	Layered elastic	6	2	16-bit MS-DOS program. Extensively used in Colombia as "DEPAV."
ALIZÉ-LCPC			10		Current Windows version. Focused on the French Design Guide.
CIRCLY	Wardle (1977) (Mincad Systems, Australia)	Layered elastic	5+	100	It includes horizontal loads and variable interface conditions.
VESYS	Kenis, W. J. (1982) (FHWA)	Layered viscoelastic	5	2	It considers the response of the elastic and viscoelastic materials.
VEROAD	Nilsson, Oost & Hopman (1996) (Delft Technical University)	Layered viscoelastic	15		It considers the viscoelastic response in shear and the elastic response to volumetric change.
MnLayer	Khazanovich y Wang (2007) (University of Minnesota)	Layered elastic	20+	100	It includes an optimized recodification of Burmister equations. It improves near-to-surface responses.
GAMES	Maina & Matsui (2004)	Layered elastic			It includes variable interface conditions. It improves near-to-surface responses.
SAPSI-M	Chatti & Yun (1996) (Michigan State University & University of California at Berkeley)	Layered, damped elastic medium	N layers	Multiple	Complex response method of transient analysis-continuum solution in the horizontal direction and finite element solution in the vertical direction
ILLI-PAVE	Thompson & Elliot (1988) (University of Illinois)	Finite element		1	
SENOL	Brown & Pappin (1981) (Universidad de Nottingham)	Finite element			
GT-PAVE	Tutumluer & Barksdale (1995) (Georgia Institute of Technology)	Finite element			It considers non-linear analysis for granular bases and subgrade.
FENLAP	Brunton & d'Almeida (1992) (Universidad de Nottingham)	Finite element		1	It is developed to consider non-linear elastic properties.
TTIPAVE	Kim, Little & Masad (2005) (Texas Transportation Institute)	Finite element	4	2	It is developed to consider non-linear elastic properties.
3D-Move	Al-Qadi & Wang (2009) (Asphalt Research Consortium)	Continuum-based finite layer			It includes three-dimensional dynamic analysis and viscoelastic materials.

Source: Adapted from Brown (1993), Monismith (2004), Haas et al. (2007) and Vásquez Varela (2015).

Chen et al. (1985) compared several computer programs for pavement analysis, including LET and FEM codes. Their main concerns are the satisfaction of boundary conditions, especially in FEM codes, and the divergences in the structural responses in the whole

spectrum of software. The most significant drawback of the FEM codes was their inability to handle more than one surface load, except for an earlier version of ABAQUS.

In Europe, The AMADEUS project did a detailed review of computer programs (2000). The project aimed to establish an analytical, incremental pavement design procedure. Apparently, the objective was not achieved in the following 16 years (Pereira & Pais, 2017); however, it is required to note that the focus was equal to the MEPDG project and the new Californian method CAL-ME (Lu, Ullidtz, Basheer, Ghuzlan, & Signore, 2009).

Some of the oldest programs are incompatible with modern operating systems like Windows, OSX, or Linux 32 or 64 bits. The following section describes some general features of the most used programs:

1. The CHEVRON algorithm (Michelow, 1963) is one of the earliest developments, now available in multiple versions. Its first version was known as CHEV5L (Monismith, 2004). The Kentucky Transportation Center of the University of Kentucky modified the original CHEVRON N-Layer program from five to 15 layers, but it is limited to full frictional interfaces (Southgate, Deen, Cain, & Mayes, 1987).
2. The University of California developed the ELSYM5 program for structures up to five layers (Ahlborn, 1972). Pavement researchers and designers used ELSYM5 extensively. However, it is incompatible with modern operative systems and requires MS-DOS emulators with associated disadvantages.
3. The Shell Petroleum Company developed the BISAR program (De Jong, Peutz, & Korswagen, 1979). The program is used in pavement research and design as the baseline for benchmarking new programs and algorithms. Although the last version still runs on the Windows OS, it has compatibility issues because it dates from 1993 (Strickland, 2000).
4. Huang (2004) developed the KENLAYER program. The software allows simplified non-linear and viscoelastic analysis and includes unique features like seasonal design and multi-axle loading. KENPAVE has some compatibility issues with modern operative systems.
5. Uzan developed the program JULEA (Uzan, 1994). JULEA was the layered elastic procedure adopted in the MEPDG (NCHRP, 2004). However, the program has issues

in the computation of near-surface responses, which are critical in the new deterioration models of that procedure.

6. The Federal Aviation Administration (FAA) developed the program LEAF (Hayhoe, 2002), an open-source solution applied in airport pavement research and design. Despite the availability of its code, there are no independent developments based on it. At present, working codifications of LEAF are the BAKFAA and LEDFAA software.

In the last 15 years, several authors proposed new developments for the numerical solution and software implementation of LET by improving the number of layers, loads, and analysis points. Some authors consider complex-load combinations, simplified non-linear properties, and enhance the Bessel functions' numerical integration procedure. The accuracy of near-to-surface structural responses and computation speeds are critical in using LET in the new MEPDG or any future design methods related to surface responses and damage prediction (Zhao, Zhou, Zeng, & Ni, 2015). Some new LET programs are:

1. GAMES: A component of the South African design software mePADS (Maina & Matsui, 2004).
2. MnLayer: Developed by the University of Minnesota as an alternative to JULEA in the MEPDG (Khazanovich & Wang, 2007).
3. ERAPAVE: An ongoing development with fast computation and non-linear procedures developed at the Swedish National Road and Transport Research Institute (Erlingsson & Ahmed, 2013).
4. OpenPave: An open-source project developed by Jeremy Lea in California (2014). It supports any number of layers, loads, and evaluation points. It is based on the FORTRAN code of ELSYM5.
5. PITRAPAVE: Developed by Universidad de Costa Rica as part of their CR-ME pavement design method (Rojas-Pérez, Aguiar-Moya, & Loría-Salazar, 2015). It supports up to 40 layers and any number of loads and evaluation points.
6. NonPAS: A non-linear LET program developed in Iran (Ghanizadeh & Ziaie, NonPAS: A Program for Nonlinear Analysis of Flexible Pavements, 2015)
7. MultiSmart3D: A program with imperfect interface conditions developed at the University of Akron, Ohio (Liu, Pan, & Cai, 2018).

Most of these programs are written and compiled in high-level languages like C++, Java, or FORTRAN, and they are available, free of charge, from the developers but not as open-source solutions. Also, there are new algorithms for improved accuracy with double exponential integration (Wang, Roesler, & Guo, 2011), improved computation of near-surface responses (Zhao, Zhou, Zeng, & Ni, 2015), and non-circular loaded areas (Maina, Ozawa, & Matsui, 2012).

4.1.3 Surrogates for the layered elastic theory

The layered elastic method is preferred to compute asphalt pavement responses. Each computation may be computationally expensive, including multiple wheel loads, sub-layering, rutting, and fatigue estimations. Therefore, several authors evaluated alternative approaches to LET computations as follows:

4.1.3.1 Method of equivalent thickness

The method of the equivalent thickness (MET) allows the fast computation of responses by transforming a multi-layered media to a single layer with a corresponding thickness increased (or decreased) by the one-third power ratio of moduli. Odemark's procedure is based on the equality of the rigidity against flexural stress with adjustment factors for better agreement with layered elastic solutions. Dalla Valle & Tom (2016a) propose improvements to the MET method by transforming the subbase and subgrade layers into equivalent foundation modulus before computing the asphalt layer bottom-tensile strain. A non-linear prediction equation based on the asphalt layer thickness is presented. The analysis considers three-layer systems and the asphalt and subgrade layers' tensile and compressive strain criteria.

4.1.3.2 Probabilistic stress distribution

Freeman & Harr (2004) proposed an alternative method to predict stress distributions in flexible pavement systems based on the central limit theorem of probability and a coefficient of lateral stress for each material. From the original work by Harr (1977 in Op. Cit., 2004), they conclude that elastic solutions are cases without assumptions about the transference of boundary energy in the interfaces. As far as this dissertation author knows, there has not been any practical application of this proposal to flexible pavement analysis and design.

4.1.3.3 Supervised learning algorithms

Ghanizadeh & Ahadi (2015) and Ghanizadeh (2017) employ artificial neural networks (ANN) and support vector machines (SVM) to estimate the tensile strain in asphalt layers and compressive strain in the subgrade under a standard axle load of 80 kilonewtons. Both techniques give coefficients of determination higher than 0.99 in training and testing against synthetic four-layer LET database solutions. The parametric analysis in both studies indicates that tensile strain in HMA is heavily influenced by HMA thickness and modulus. The thicknesses of all layers and the subgrade modulus control the roadbed compressive strain. The increased speed in computations with both techniques analyzes multiple combinations of thicknesses and materials. However, individual ANN and SVM must be developed for axle type and load magnitude spectra.

4.1.3.4 Response surface methods (RSM)

In reliability-based pavement analysis and design, it is necessary to evaluate the structural performance a significant number of times. Simulation methods such as Monte Carlo imply a high computational cost even with layered elastic solutions (Timm, Newcomb, & Galambos, 2000). Multiple linear regressions yield low correlation coefficients to predict critical strains for performance evaluation. Second-order regressions improve the predictive capabilities of closed-form solutions applying the response surface method (RSM). The central composite design (CCD), the Box-Behnken design (BBD), or the Dochlert design (DOD) methods define a small sample of structural responses encompassing the variability of the performance, for example, the strains in the hot-mix asphalt or the subgrade (Dinegdae, Onifade, Birgisson, Lytton, & Little, 2018).

4.1.3.5 Finite element method (FEM)

The layered theory has limitations, such as the inability to capture the exact load geometry and boundary conditions (Cho, McCullough, & Weismann, 1996). Initial applications of the finite element method used linear elastic properties. However, it was clear that FEM offers "*little or no advantage over layered systems analyses*" unless it includes non-linear material properties (Duncan, Monismith, & L., 1968). Cho et al. (1996) evaluated three approaches to FEM computations (2D, axisymmetric, and three-dimensional) in pavement structural analysis. They concluded that axisymmetric models give a reasonable solution to problems unaffected by boundary or discontinuity conditions. The main advantage of FEM is that it

can consider elastic non-linear, or viscoelastic materials and complex load conditions. The disadvantages are that FEM requires more computational processing time and more information about the behavior of the materials.

Anisotropy is a crucial issue in FEM implementation. Kim (2007) improved the resilient non-linear response of geomaterials with stress-dependent modulus models in ABAQUS™ software. Critical pavement responses present significant errors when the three-dimensional analysis is compared with responses obtained with the superposition principle from axisymmetric solutions. Cai et al. (2015) analyze the effect of anisotropy and thin layers. Anisotropy is a recognized feature of pavement materials beyond the capacities of LET. Also, they report the analysis of thin layers (i.e., geotextiles), which significantly affect the performance of in-service pavements. Every meaningful pavement response is affected by anisotropy; hence, the LET-based calibration is invalid for another analysis method. Liu et al. (2015) developed the SAFEM program for predicting the asphalt pavement structural responses under static loads and compared it with ABAQUS software with favorable results. SAFEM seeks to reduce model complexity by implementing a semi-analytical approach using the Fourier series to represent the vertical displacements and exploit orthogonal directions. The algorithm implements infinite elements at the model boundaries.

4.2 UNLEA - Universidad Nacional Layered Elastic Analysis

4.2.1 Program description

The author developed UNLEA in the Scilab ® software for numerical computation. Scilab has an extensive library of proven mathematical functions to operate with variables and constants represented as matrices. UNLEA is also available in Python and MATLAB®, with the same features described below.

The UNLEA program includes four functions:

1. *“mD*” computes the coefficients of the continuity of stresses and displacement functions for each interface.
2. *“Coeff”* computes the integration coefficients for each computing increment of the Hankel inversion for the N-layers.

3. *"BOUSS"* computes near-to-surface responses of a two-layer structure, and
4. *"PPLSTRESS"* computes the principal stresses in the coordinate system of each problem.

As a custom Scilab or Python function, UNLEA is called from any script as follows:

[RESPONSES] = fUNLEA (E, V, H, L, R, P, MMAX, OnlyW)

Where:

RESPONSES: Matrix of NPoint rows and 26 columns with the following responses for each point of interest: Point number (from 1 to NPoint), point coordinates (x, y & z), normal stresses (σ_x, σ_y & σ_z), shear stresses (τ_{xy}, τ_{yz} & τ_{xz}), displacements (u_x, u_y & u_z), normal strains (ε_x, ε_y & ε_z), shear strains (γ_{xy}, γ_{yz} & γ_{xz}), minor principal strain (ε_t), principal stresses (σ_1, σ_2 & σ_3), and principal strains (ε_1, ε_2 & ε_3).

E: Vector with moduli of the layers.

V: Vector with Poisson ratios of the layers.

H: Vector with thicknesses of layers.

L: Vector with interface conditions. UNLEA considers bonded (1.0) and unbounded interfaces (0.0). The program also can consider intermediate bonding conditions based on the JULEA and LEAF proposals.

R: Matrix with load characteristics: x & y coordinates, applied uniform pressure, and radius of the loaded area.

P: Matrix of evaluation points: x, y & z coordinates, and layer number to guarantee that the strain computations consider the appropriate material.

MMAX: Maximum number of iterations of the *"m"* parameter of the Hankel inverse transformations.

OnlyW: A Boolean variable; if OnlyW = *"true,"* UNLEA only computes vertical displacements, which is helpful in backcalculation procedures to reduce running time.

4.2.2 Numerical integration

In early UNLEA versions, the author applied the spline integration procedure (Rabinovitz, 1990) instead of the conventional integration-then-summation (ISE) approach between the zeros of the Bessel functions to solve the Hankel inverse transformations for each structural response. Due to some instability for points far from the load, the author implemented an ISE approach based on the code developed by Al-Rumahiti (2021). In the integration of functions like Eq. 4-11, one must consider the singularity at $m = 0$ for the ratio:

$$\lim_{m \to 0} \frac{J_1(m\alpha)}{m} = \frac{0}{0}$$

Eq. 4-25

Which, applying the L'Hopital-Bernoulli rule, becomes:

$$\frac{\frac{\partial}{\partial m}[J_1(m\alpha)]}{\frac{\partial}{\partial m}(m)} = \frac{\frac{1}{2} \cdot \alpha \cdot [J_0(m\alpha) - J_2(m\alpha)]}{1.0}$$

Eq. 4-26

Where $J_2(m\alpha)$ is the Bessel function of the first kind and second-order applied to the product $(m \cdot \alpha)$. For $m = 0$, the ratio in Eq. 4-25 becomes $\left({}^{\alpha}/_{2}\right)$.

4.2.3 Near-to-surface responses

Accurate determination of near-surface responses in flexible pavements is required since the new MEPDG (NCHRP, 2004) includes a top-down cracking distress model (Zhao, Zhou, Zeng, & Ni, 2015). Novak et al. (2003) employed the FEM code ADINA to evaluate near-surface responses based on measured radial tire contact in pavements and found non-uniform vertical stress and significant contact stresses in transverse and longitudinal directions. Both responses are critical for the prediction of rutting in the HMA layers.

Khazanovich and Wang (2007) improved the near-to-surface responses in MnLAYER software by subtracting one-layer system responses from the N-layer structure responses. The one-layer structure has the same mechanical properties as the upper layer of the original pavement. Khazanovich and Wang use a one-layer system because they employ Burmister's stress function.

The author of this dissertation uses the stress function proposed by Huang, so it is necessary to have at least two layers because the full depth of the pavement, H, is needed to normalize the arguments of the exponential and Bessel functions. Both layers have the same mechanical properties as in the half-space of Boussinesq. The following equation summarizes the strategy to improve any near-to-surface structural response:

$$R_{N-LEA} = (R_{N-LEA} - R_{2-LEA}) + R_{2-A\&U}$$

Eq. 4-27

Where:

$R_{N\text{-}LEA}$: Any near-to-surface response in the N-layer structure computed with LET.

$R_{2\text{-}LEA}$: Any near-to-surface response in the 2-layer structure computed with LET.

$R_{2\text{-}A\&U}$: Any near-to-surface response in the 2-layer structure computed with the *"BOUSS"* function based on Ahlvin & Ulery coefficients for a one-layer semispace.

The *"BOUSS"* function in UNLEA applies spline interpolation to the coefficients published by Ahlvin & Ulery (1962) or the point-load equations derived by Boussinesq (Timoshenko & Goodier, 1951) to compute the structural responses of a two-layer structure. Several trials showed the validity of the principle of Saint-Venant to apply the point load equations for points outside the bounds of the Ahlvin & Ulery tables. The *"BOUSS"* function is also helpful for other geotechnical computations, for example, stress increments computations under foundations.

Figure 4-2 shows the σ_z integrands for the n-layer solution ($\sigma_{ZN\text{-}LEA}$), the equivalent two-layer solution ($\sigma_{Z2\text{-}LEA}$), and their subtraction ($\sigma_{ZN\text{-}LEA} - \sigma_{Z2\text{-}LEA}$) for a point near the surface (Figure 4-1).

Both integrands show slow convergence with the "m" parameter of the Hankel inversion. In contrast, the subtraction ($\sigma_{ZN\text{-}LEA} - \sigma_{Z2\text{-}LEA}$) shows a fast convergence. For this case, the computation in UNLEA used 41 integration cycles, while KENPAVE took up to 200 computation cycles to achieve the same result with a precision of 0.001.

Figure 4-2: Convergence of near-to-surface integrands for vertical stress, σ_Z

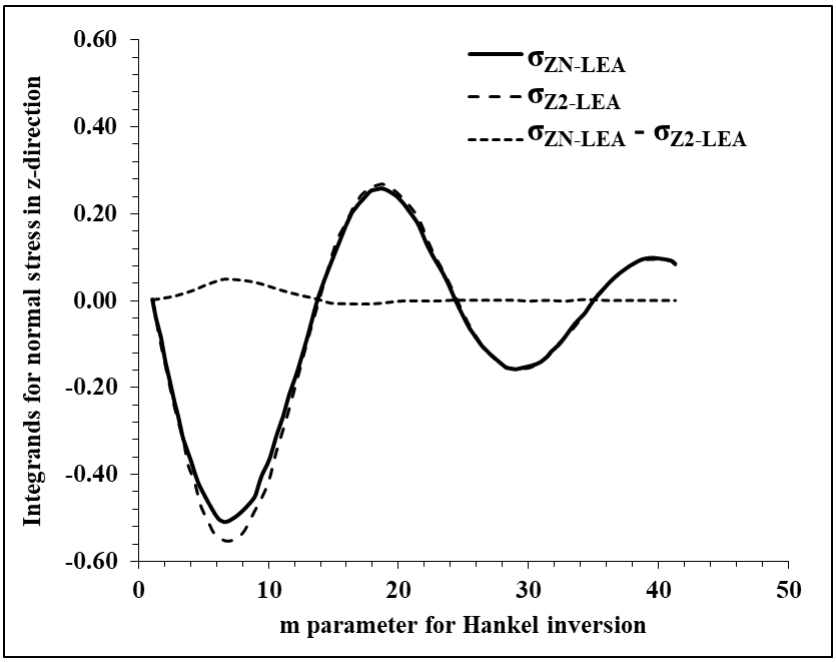

4.2.4 Some results of UNLEA applications

Figure 4-3 compares KENPAVE (Huang, 2004) and JULEA (ERDC, 2002) software with UNLEA results in the pavement axis of symmetry shown in Figure 4-1.

There is a good agreement between the results of the three programs. The near-to-surface computations of UNLEA show good agreement with KENPAVE. However, KENPAVE uses up to 200 computation cycles to achieve its default numerical integration tolerance of 0.001, while UNLEA uses 50. JULEA shows a lack of convergence for the vertical stress for depths under 40 mm; this is a known issue for depths smaller than one-fifth of the loaded area radius (Zhao, Zhou, Zeng, & Ni, 2015).

Concerning tire-pavement interaction, Figure 4-4 shows vertical stress (σ_z) verification against the boundary conditions based on the example presented by Zhao et al. (2015). The pavement has three layers: asphalt concrete (h_1 = 20 cm, E_1 = 5,000 MPa, v_1 = 0.30), base layer (h_2 = 40 cm, E_2 = 300 MPa, v_2 = 0.35), and subgrade (E_3 = 80 MPa, v_3 = 0.40). The load is a uniform pressure of 0.70 MPa over a circular area with a radius of 10 cm. All interfaces are bonded.

Figure 4-3: Comparison between UNLEA, KENPAVE, and JULEA

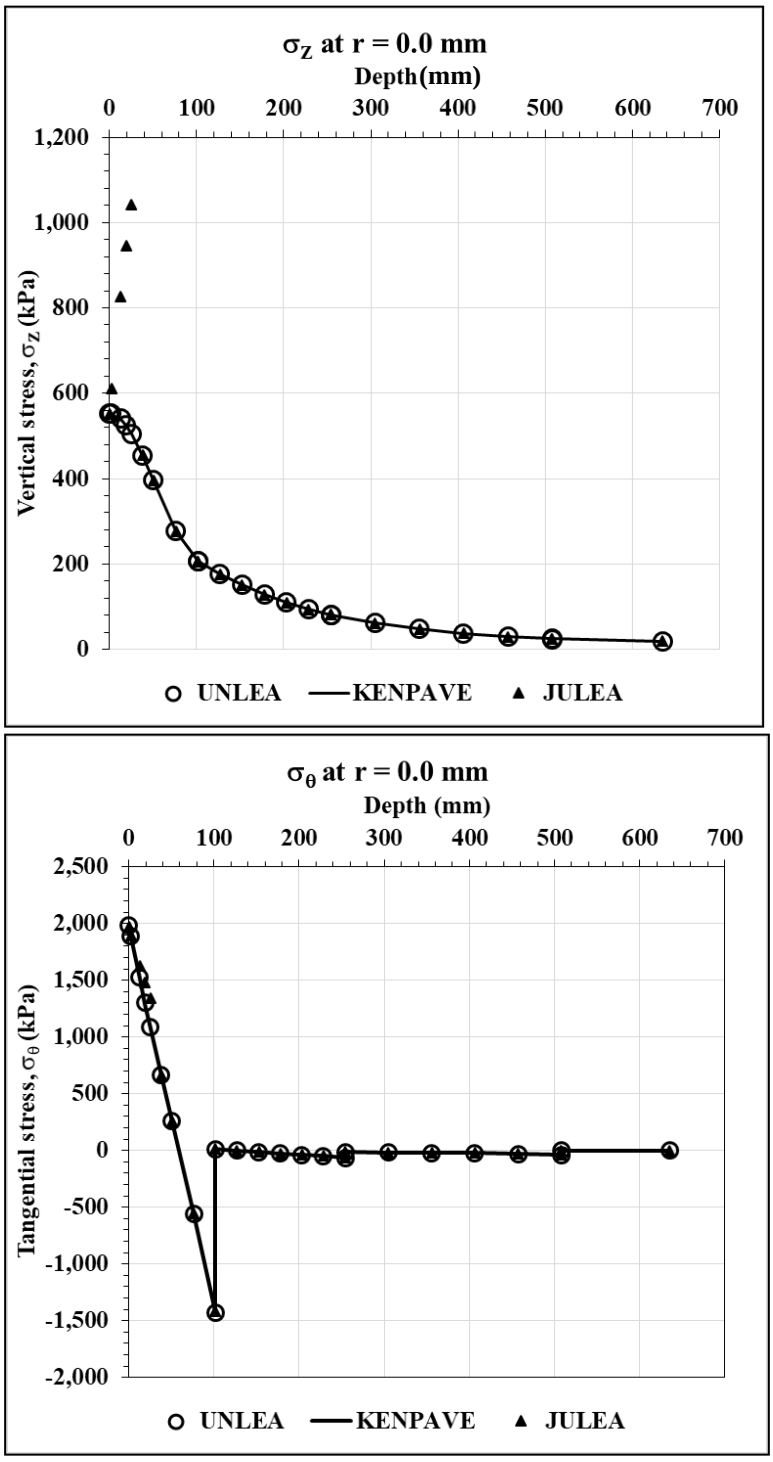

In Figure 4-4, the author of this dissertation did not obtain the same results as Zhao et al. with the KENPAVE program (*"KENLAYER"* in the quoted reference). The Windows-based KENPAVE program (Huang, 2004) reports vertical stresses equal to the applied pressure

for all points inside the loaded area, including the edge. Also, KENPAVE only used three computation cycles, maybe with a specific subroutine with the boundary conditions for $z = 0\ cm$.

Figure 4-4: Verification of vertical stress against the boundary conditions

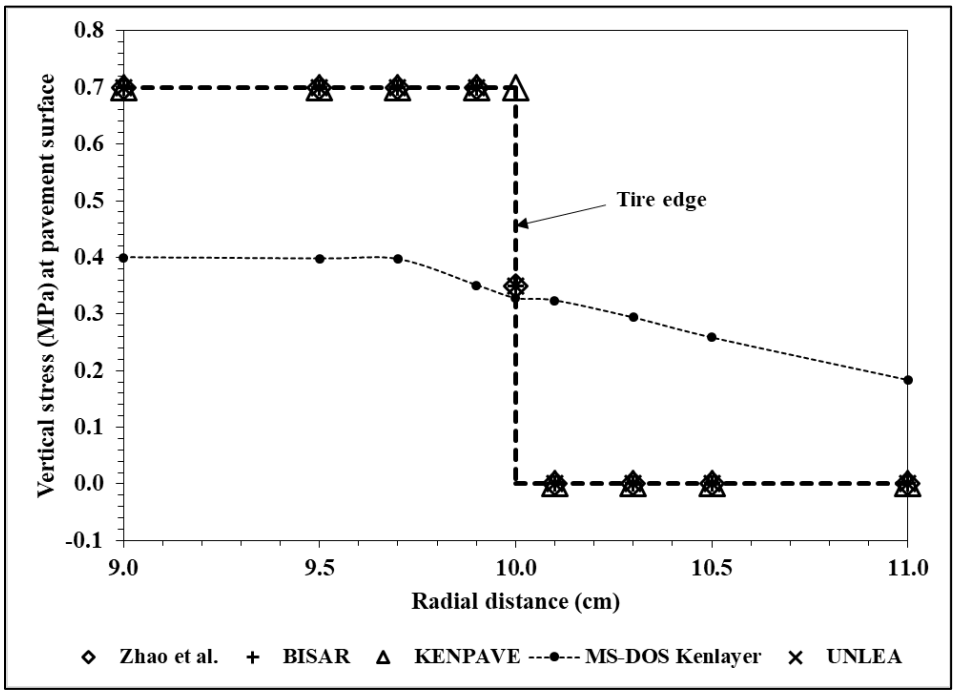

Source: Redrawn from Zhao et al. (2015) with UNLEA and MS-DOS KENLAYER results.

The author of this dissertation also used the MS-DOS version of KENLAYER (Huang, 1993) and obtained a set of unacceptable results. Zhao et al. indicate that the vertical stress in the tire edge is analytically half of the applied pressure. The Ahlvin & Ulery coefficients (1962) used in the *"BOUSS"* subroutine of UNLEA include the same result. Consequently, the UNLEA results match Zhao et al. and BISAR results (De Jong, Peutz, & Korswagen, 1979) for all the points, including the tire edge.

Finally, Figure 4-5 shows another application with a design chart based on the Shell Oil pavement design procedure of 1978 (Shell Oil, 1978). An independent script defines 10,248 three-layer structures with variable structural properties. It calls the UNLEA function and computes the allowable load repetitions in the asphalt and subgrade layers with fatigue and rutting models.

Figure 4-5: Chart for a three-layer pavement with a granular base and HMA

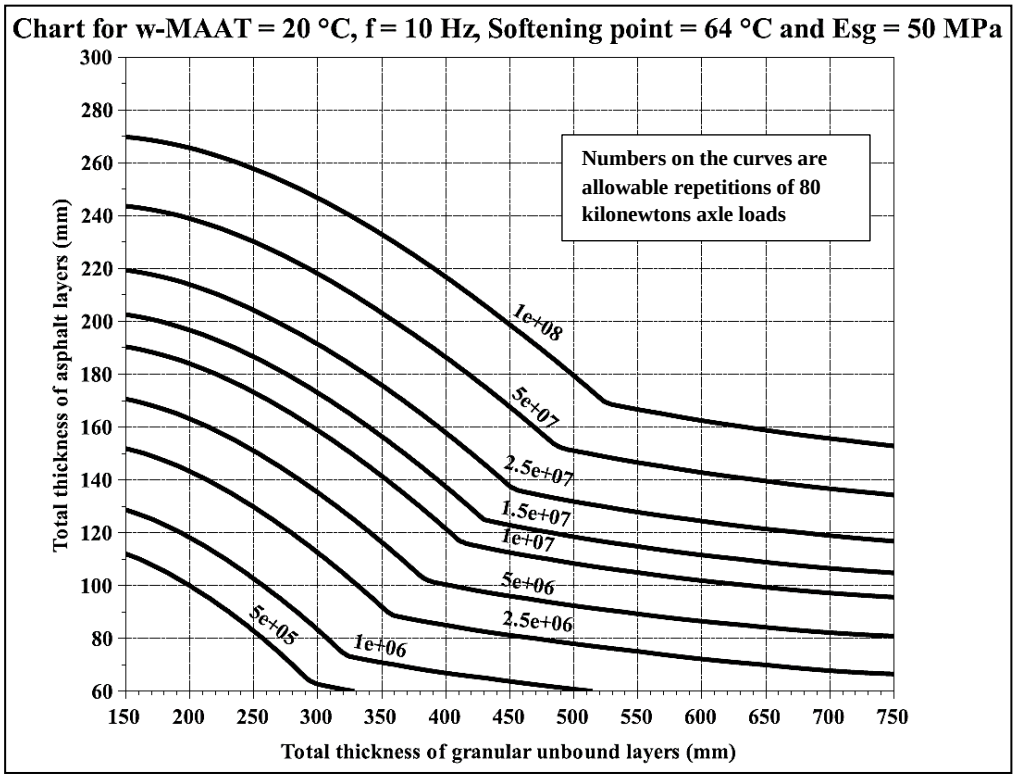

4.3 Summary

The author of this dissertation developed UNLEA, a new software for layered elastic analysis of pavements in highways and airports. UNLEA is an open-source, interpreted, and not-compiled code written in the Scilab software for numerical computation. Python and MATLAB versions are also available.

The program solves a known issue in LET software: the convergence of near-to-surface points, which is dealt with by the strategy proposed by Khazanovich and Wang (2007). Comparison with published results shows good agreement between UNLEA and other programs such as BISAR (De Jong, Peutz, & Korswagen, 1979) and KENPAVE (Huang, 2004) with a lower computing cost.

UNLEA considers both fully bonded and partially bonded interface conditions, the latter following the strategy proposed by Hayhoe (2002) in the LEAF program.

Users can implement the UNLEA script on other highways, airport pavements, or geotechnical engineering programs. UNLEA has no practical limitations for layers, points of analysis, or applied loads, so it has good potential for airport pavement analysis and other complex-load scenarios.

The batch-processing capability of UNLEA may be an advantage over compiled closed-source programs to produce custom design charts or analyze multiple properties and load combinations as required by the MEPDG. Also, UNLEA can run on Windows ®, MacOS ®, or any Linux distribution compatible with the Scilab software without any code rewriting or emulators, so the full power of the computer hardware is available for analysis. Also, UNLEA can compute only vertical deflections and speed up backcalculation applications.

Finally, the author believes that UNLEA has an intrinsic value as an educational tool because it gives an insight into the layered elastic theory instead of the blind application of a *“black box.”*

5 Particle swarm optimization in pavement analysis and design

Under the pavement, the dirt is dreaming of grass.
Wendell Berry.

This chapter presents the application of particle swarm optimization in two pavement analysis and design problems: moduli backcalculation and incremental design. The first part of the chapter presents the fundamentals of PSO. The second and third sections discuss the development of PSO-UNLEA, UNPAVE, and PSO-PAVE, three programs written in MATLAB that implement the PSO in backcalculation and incremental pavement design. Each section includes a practical example and pertinent conclusions.

5.1 Particle swarm optimization (PSO)

The particle swarm optimization (PSO) is a population-based heuristic or metaheuristic algorithm for the global optimization of continuous nonlinear functions proposed by Kennedy & Eberhart (1995). The algorithm is based on a simplified abstraction of the social behavior of animals as fish schools or flocks of birds; however, it stands without metaphorical support (Kennedy & Eberhart, 1995; Shen, Bu, & Yuan, 2009; Marini & Walczak, 2015).

The PSO algorithm is suitable for nonlinear, non-differentiable optimization problems and is characterized by simple principles, easy implementation, and fast convergence speed. In PSO, each weightless individual or agent is called a *"particle"* and is subjected to movement in a D-dimensional space looking for a potential solution. The trajectory of each particle in the search space is adjusted by altering its velocity, which has three components: (a) an inertial component to control the increase of speed, (b) the individual (experience) particle's best position, and (c) the global swarm best position. The resultant velocity vector

compromises its previous best experience and the global best particle by exchanging information between particles and iterations (Shen, Bu, & Yuan, 2009).

The PSO requires a swarm of particles defined by vectors with a dimensionality D according to the search space; x_i is the position of the i^{th} particle as follows:

$$x_i = (x_{i1}, x_{i2}, x_{i3}, \dots, x_{iD})$$

Eq. 5-1

Where $i = 1,2, \dots, m$; and m is the number of particles. For example, for the backcalculation of a four-layer pavement, D is equal to four, and the coordinates of each particle are:

$$x_i = (E_{i1}, E_{i2}, E_{i3}, E_{i4})$$

Eq. 5-2

Where E_{ij} is the modulus of the j[th] layer in the i[th] iteration.

The individual particles move through the search space by a change in the position defined as:

$$x_{i,d}^{k+1} = x_{i,d}^{k} + v_{i,d}^{k+1} \cdot \Delta t$$

Eq. 5-3

Where $x_{i,d}^{k}$ is the d^{th} dimension current position of particle i in cycle k, $x_{i,d}^{k+1}$ is the d^{th} dimension next position of particle i in cycle $k+1$, $v_{i,d}^{k+1}$ is the d^{th} dimension updated velocity of particle i in cycle $k+1$, and Δt is the time increment between cycles k and $k+1$, equal to 1.0. The updated velocity of each particle is equal to the following:

$$v_{i,d}^{k+1} = \omega \cdot v_{i,d}^{k} + \frac{c_1 \cdot r_1^k \cdot \left(p_{i,d}^{k} - x_{i,d}^{k}\right)}{\Delta t} + \frac{c_2 \cdot r_2^k \cdot \left(v_{g,d}^{k} - x_{i,d}^{k}\right)}{\Delta t}$$

Eq. 5-4

Where $v_{i,d}^{k}$ is the d^{th} dimension current velocity of particle i in cycle k, $p_{i,d}^{k}$ is the d^{th} dimension best personal position of particle i in cycle k, and $p_{g,d}^{k}$ is the d^{th} dimension best global position of particle i in cycle k. The PSO parameters are the inertia weight (ω), the cognition weight (c_1), and social weight (c_2). The parameters r_1 and r_2 are two random values uniformly distributed in the range [0, 1].

The inertia weight (Shi & Berhart, 1998) controls the relationship between exploration and exploitation, and it may decrease its value throughout optimization to improve the solution (Xinchao, 2010). Larger ω values are helpful to avoid local minima, and smaller ω values are useful to improve the convergence speed. The IWPSO algorithm applies the following linear decrease strategy for the inertial weight (Shen, Bu, & Yuan, 2009):

$$\omega = \omega_{max} - t \cdot \frac{\omega_{max} - \omega_{min}}{T_{max}}$$

Eq. 5-5

Where T_{max} is the maximum number of evolution iterations, ω_{max} and ω_{min} are the maximum and the minimum inertia weights in the range of [0.1, 0.9] for better convergence performance. According to Li and Chen, if the inertia weight is greater than 1.2, the particle group will not converge (2018).

Clerc (1999) proposed a modified form of Eq. 5-4 with a convergence factor (χ) that is a function of the cognition and social weights:

$$v_{i,d}^{k+1} = \chi \cdot \left[v_{i,d}^{k} + c_1 \cdot r_1^k \cdot \left(p_{i,d}^{k} - x_{i,d}^{k}\right) + c_2 \cdot r_2^k \cdot \left(v_{g,d}^{k} - x_{i,d}^{k}\right)\right]$$

Eq. 5-6

$$\chi = \frac{2}{\left|2 - \varphi - \sqrt{\varphi^2 - 4\varphi}\right|}$$

Eq. 5-7

All variables are as previously defined, and: $\varphi = c_1 + c_2 > 4$. The usual φ value is 4.1 giving a convergence factor of 0.7289.

The cognition and social weights (c_1, c_2), also known as *"learning factors,"* are equal to 2.0 in several applications according to the original swarms studied by Kennedy & Eberhart (1995).

The original PSO has some disadvantages, such as the high convergence speed and a rapid loss of diversity (Xinchao, 2010). Consequently, some authors improved the PSO efficiency by adjusting the code pattern, inertia weight, mutation operators, neighborhood operations, boundary conditions, and maximum particle speed (Li & Chen, 2018).

Van den Bergh & Engelbrecht (2002) proposed the *"Guaranteed Convergence PSO (GCPSO)"* with a separate velocity update formula for the best particle. Xinchao (2010) proposed a *"perturbed Particle Swarm algorithm (pPSA)"* based on the global best disturbance to keep diversity in the swarm.

PSO implementation requires the appropriate knowledge of the specific problem, especially the practical limits of the search space. Several methods can adjust particles that may be stranded out of the boundaries. Li & Chen (2018) proposed the following treatment with a randomized proportion of the valid range of the particle position:

a) For a particle that exceeds the highest boundary value:

$$x_{ik} = x_{k,max} - \left(x_{k,max} - x_{k,min}\right) \cdot rand()$$

Eq. 5-8

b) For a particle that falls below the lowest boundary value:

$$x_{ik} = x_{k,min} + \left(x_{k,max} - x_{k,min}\right) \cdot rand()$$

Eq. 5-9

Where the $rand()$ function generates a random number in the range [0, 1].

5.2 Backcalculation of pavement moduli

Particle swarm optimization is a promising technique for moduli backcalculation in pavement engineering considering the following features:

1. The PSO does not require the codification of solutions to explore and exploit the search space. Consequently, controlling unfeasible solutions requires no computational-expensive decodification, repairing, or other penalty techniques.
2. The PSO requires only three parameters with narrow values, so the parameter-problem dependency is not essential.
3. The PSO does not require seed moduli, which are critical for gradient-based methods. If the user provides a reasonable range for the moduli, the results may converge faster to a satisfactory result.

Besides these advantages and the promising results, the author of this dissertation must emphasize that PSO, like any other optimization technique, is a tool to get a job done and not the job itself. The practitioner must always confirm the reasonableness of the results according to other data sources such as pavement condition and materials sampling and testing.

5.2.1 The PSO-UNLEA program

The author developed PSO-UNLEA in the MATLAB programming language. PSO-UNLEA stands for *"Particle Swarm Optimization – Universidad Nacional Layered Elastic Analysis."*

Figure 5-1 shows the PSO-UNLEA flowchart. For a proposed backcalculation problem, the program reads the layer thicknesses, the measured deflection basin, and the NDT load characteristics as input values. Then, it creates several swarm populations of pavement structures with random moduli and computes their deflection basins with the UNLEA code described in section 4.2.

The program applies two population generation restrictions: (a) fixed moduli ranges for each pavement material and (b) maximum moduli ratios between soil and aggregate layers. Table 5-1 shows the suggested moduli ranges for several materials identified in the program by a three-letter code.

The stopping criterion is a fixed number of iterations; other criteria may include a fitness function threshold to save computing time in fast-converging cases.

The author implemented an error check between actual and backcalculated moduli as a quality measure for PSO-UNLEA testing on hypothetical cases with known properties

The fitness value is the RMSE of the measured versus computed deflections:

$$RMSE = \sqrt[2]{\frac{1}{m} \cdot \sum_{i=1}^{m} w_i \cdot \left(\frac{d_i - D_i}{D_i + \beta}\right)^2} \cdot 100\%$$

Eq. 5-10

Where, m is the number of measuring sensors, d_i is the calculated or predicted deflection, D_i is the measured deflection, and w_i is a weighting factor for each deflection point (Kameyama, Himeno, Kasahara, & Maruyama, 1998). The fitness function should be between 1.0% to 2.5% in a proper backcalculation process (Von Quintus & Simpson, 2002) *despite the goodness of the obtained moduli*.

Figure 5-1: PSO-UNLEA flowchart

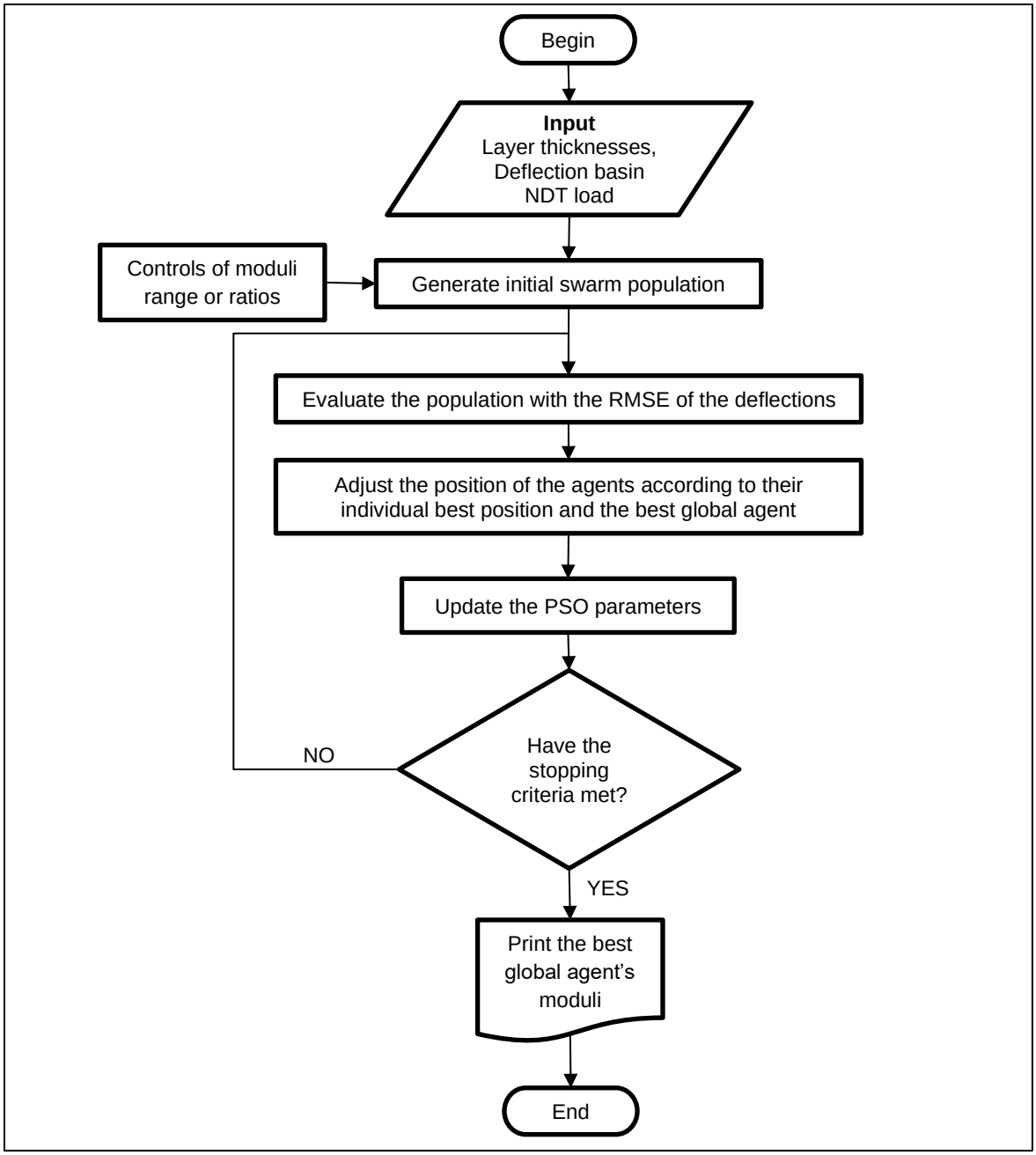

Table 5-1. Suggested moduli range according to layer type in PSO-UNLEA

Layer type	Code	Minimum E (MPa)	Maximum E (MPa)
Hot-Mix Asphalt	HMA	1,000	4,000
Portland Cement Concrete	PCC	18,000	60,000
Asphalt-Treated Base	ATB	300	3,500
Cement-Treated Base	CTB	2,500	8,000
Lean Concrete	LC	6,000	25,000
Granular Base	GB	80	500
Granular Base in Inverted Structure	SDW (1)	400	500
Granular Subbase	GSB	80	300
Granular Subgrade Soil	GSG	30	250
Fine-Grained Subgrade Soil	FSG	10	100
Other	OTR	10	60,000

(1) A Sandwich or inverted construction includes an untreated granular layer between two bounded layers.

Source: Modified from Alkasawneh (2007).

PSO-UNLEA modifies the swarm population, updates the PSO parameters to evolve from exploration to exploitation to achieve the best solution, ends upon reaching the stopping criteria, and reports the best agent's moduli.

5.2.2 PSO-UNLEA example

In this section, the author evaluates the PSO-based backcalculation performance with a four-layer structure with known mechanical properties under the FWD test. Table 5-2 shows the pavement mechanical properties, thicknesses, and interface conditions, and Table 5-3 shows the deflection basin due to a 40 kN load applied over an area with a 0.15 m radius.

Table 5-2: Four-layer pavement structure for PSO parameter evaluation

Layer	Elastic modulus (MPa)	Poisson´s ratio ()	Thickness (m)	Interface condition
Asphalt concrete	3,500	0.35	0.10	Rough
Untreated granular base	400	0.35	0.15	Rough
Untreated granular subbase	200	0.35	0.45	Rough
Subgrade	100	0.45	Semi-infinite	

Table 5-3: Deflection basin of the four-layer pavement structure

Radial distance (m)	0.00	0.20	0.30	0.60	0.90	1.20	1.50	1.80
Deflection (μm)	395.9	303.9	251.7	160.7	116.8	90.70	73.15	60.72

Table 5-4 shows the particle swarm parameters implemented in PSO-UNLEA. The program computes three-independent swarms with 2,250 calls to the UNLEA subroutine.

Table 5-4: Parameters of the particle swarms for backcalculation

Feature	Value
Number of independent swarms	3
Maximum number of iterations	50
Cognitive correction factor	2.0
Social correction factor	2.0
Maximum inertia coefficient	0.90
Minimum inertia coefficient	0.10
Inertia coefficient reduction type	Linear with iterations
Number of agents (particles)	15

In a conventional backcalculation process, the elastic moduli are unknown. This case study evaluates the ability of the PSO to achieve not only an acceptable agreement between measured and computed deflections but between the actual and estimated moduli of each layer with the following ratio:

$$RME = \frac{\left|E_i^{actual} - E_i^{backcalculated}\right|}{E_i^{actual}} \cdot 100\%$$

Eq. 5-11

Where RME is the relative difference between the actual (E_i^{actual}) and the backcalculated moduli ($E_i^{backcalculated}$) of the layer i, and it helps to evaluate the PSO capabilities when the actual moduli are known.

The author develops three approaches to the backcalculation problem with or without controls of moduli range and subgrade seed modulus.

5.2.2.1 Backcalculation without control of the range of moduli

In this analysis, the materials are “OTR” type in Table 5-1 with a moduli range between 10 and 60,000 MPa. Also, there are no limitations to the modular ratio between layers or provisions to set the subgrade modulus. This case examines the PSO's uncontrolled exploratory capabilities in searching for the actual pavement moduli.

Figure 5-2 shows the results of the three random-generated independent swarms in three graphs: (a) a *“Convergence curve”* shows the fitness function change in each iteration, (b) the *“Moduli”* graph shows the RME change of each layer throughout the process, and (c) the *“Last iteration deflection basin”* graph shows the actual and computed deflection basins.

Figure 5-2: Backcalculation without control of the range of elastic moduli

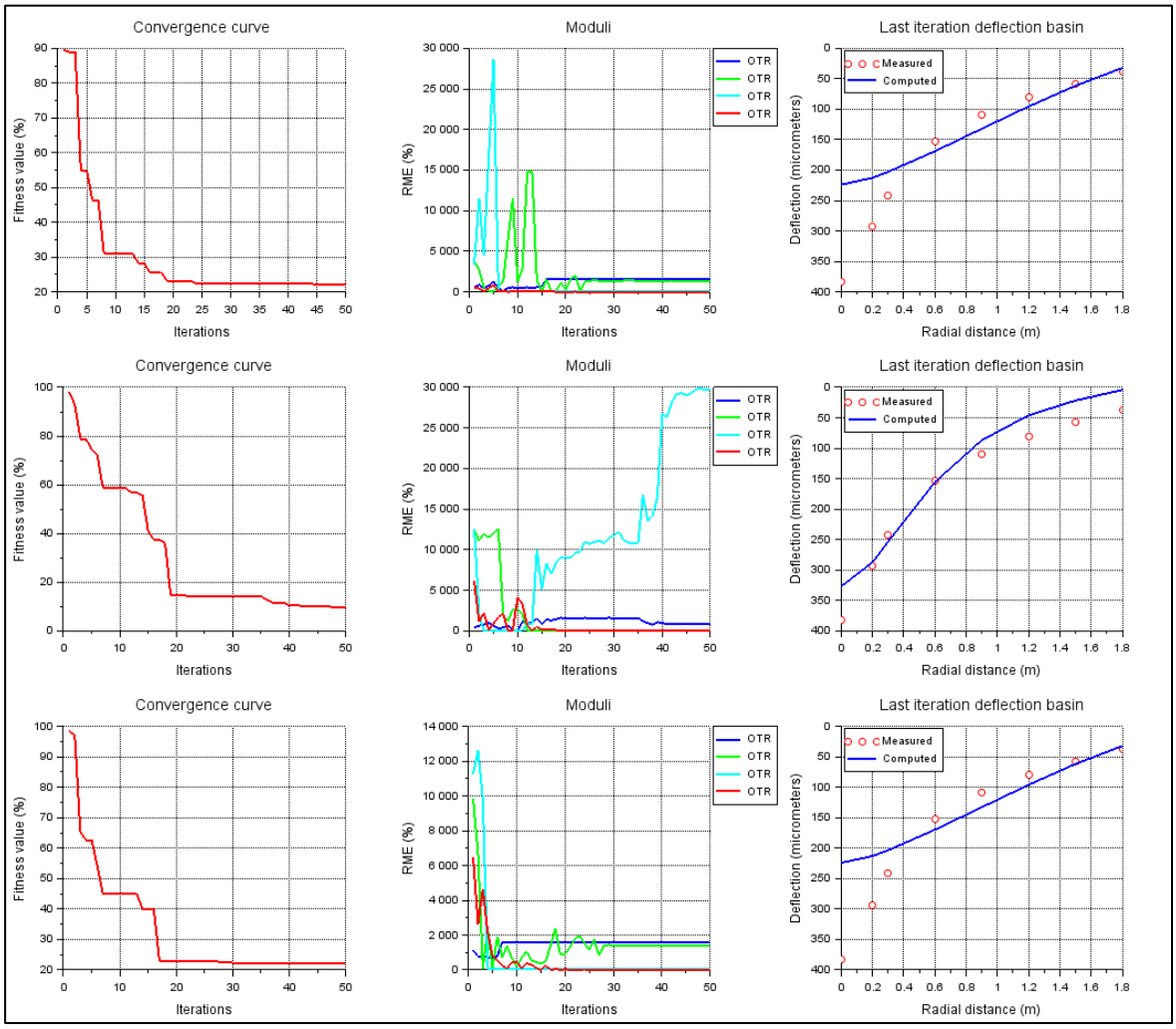

At the end of the iterations, the three swarms produced the results summarized in Table 5-5. The three independent swarms show that uncontrolled PSO cannot return suitable moduli for asphalt concrete and untreated bases. The RMSE values are greater than 2.5%.

Table 5-5: Moduli and RMSE without control of the range of elastic moduli

Swarm	RMSE (%)	E1 (MPa)	Error	E2 (MPa)	Error	E3 (MPa)	Error	E4 (MPa)	Error
1	22.156	58,737	1,578%	5,674	1,318%	12.03	94.0%	106.6	6.61%
2	9.597	32,354	824%	10.54	97.4%	59,563	29,681%	97.34	2.66%
3	22.336	59,666	1,605%	5,883	1,371%	10.13	94.9%	105.9	5.88%

The relative errors of moduli in the asphalt concrete and the untreated granular base and subbase are significant. The PSO compensated for the differences by assigning higher or lower values to the layers. For example, untreated bases with 10 MPa (the lower limit) and asphalt concrete layers with almost 60,000 MPa (the upper limit). The convergence towards the subgrade modulus of 100 MPa, with an average error of 5.05%, is noteworthy in this uncontrolled case. The third panel shows that the swarms do not obtain deflection basins comparable to the reference case.

This *"uncontrolled case"* shows that it is necessary to implement measures to keep the moduli between proper values according to the material type. The following cases develop that approach with and without using a subgrade seed modulus.

5.2.2.2 Backcalculation with control of the range of moduli and without subgrade seed modulus

Each material has a specific type of material and moduli range, as shown in Table 5-6. Any untreated granular base or subbase should not have an elastic modulus larger than three times the underlying layer's modulus. Based on their quality, the user can define different moduli ratios (2.0, 2.5, 3.0) between untreated layers (LCPC - SETRA, 1994).

Table 5-6: Moduli ranges for the conditioned backcalculation process

Layer	Code	Minimum E (MPa)	Maximum E (MPa)
Asphalt concrete	HMA	1,000	4,000
Untreated granular base	GB	80	500
Untreated granular subbase	GSB	80	300
Fine-grained subgrade	FSG	10	100

Figure 5-3 shows the results of the three random-generated independent swarms used in this case.

Figure 5-3. Backcalculation with moduli ranges and without subgrade seed modulus

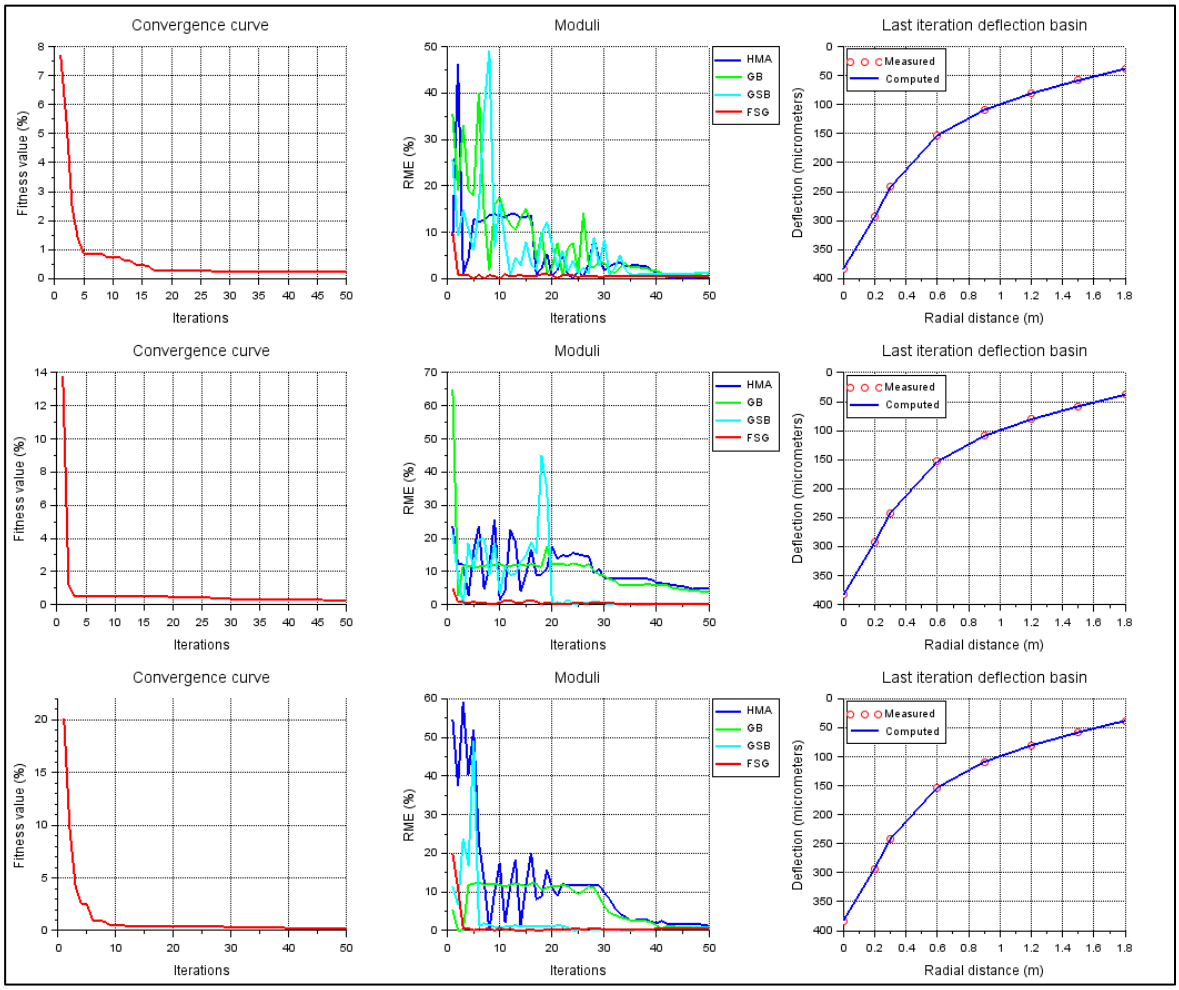

The first graph shows that the three swarms converged to a proper fitness value in 20 iterations. However, the second panel shows that the moduli errors require more than 40 iterations to achieve values below 10%. This difference is significant as the actual backcalculation objective is to obtain a set of suitable moduli, while the RMSE only considers the deflections. Should PSO-UNLEA include a routine to end the inverse calculation based only on RMSE, it would stop exploring better solutions, as seen in this case.

In a practical case, where the actual moduli are not known a priori, it is necessary to verify the quality of the solution according to the material type and laboratory testing.

The third graph shows a significant coincidence between the measured and computed deflection basins, despite the differences between actual and backcalculated moduli in each swarm.

At the end of the 50 iterations, the three swarms yielded the results summarized in Table 5-7. There is a good agreement between the estimated and computed deflections in all cases. The second swarm yields the maximum RMSE (0.273%), but it is not significantly different from the others (0.242%).

Table 5-7: Moduli and RMSE with moduli ranges and without subgrade seed modulus

Swarm	RMSE (%)	E1 (MPa)	Error	E2 (MPa)	Error	E3 (MPa)	Error	E4 (MPa)	Error
1	0.242	3,493	0.194%	397.2	0.691%	202.4	1.197%	99.4	0.594%
2	0.273	3,326	4.961%	415.9	3.972%	200.2	0.112%	99.6	0.372%
3	0.242	3,457	1.241%	402.5	0.636%	201.6	0.815%	99.5	0.520%

The absolute errors in moduli are below 5%. The asphalt concrete layer in the second swarm has the most prominent error (4.961%). The subgrade moduli have errors below 0.6% in the three swarms *without using* a seed value.

5.2.2.3 Backcalculation with control of the range of moduli and subgrade seed modulus

This case considers the moduli range shown in Table 5-6 and the moduli ratio limit between untreated layers. Also, the author proposes an equation to estimate the seed modulus of the subgrade based on two-layer solutions presented by Huang (1969):

$$E_{sr} = \frac{0.08 \times q \times a}{\frac{D_{10a}}{10^6}}$$

Eq. 5-12

Where E_{sr} is the estimated modulus of the subgrade in MPa, q is the applied pressure by the FWD device in MPa, a is the radius of the loaded plate of the FWD device in meters, and D_{10a} is the deflection measured on the pavement surface, in micrometers, at ten times the FWD load-plate radius. The PSO-UNLEA program allows a range for the subgrade modulus between 0.80 to 1.20 of the estimated value.

Figure 5-4 shows the results of three random-generated independent swarms. The first graph shows that the three swarms converged to the minimum fitness value within 40 iterations. The second graph also shows that the errors in moduli fall to 12% or less after 40 iterations. The third graph shows the coincidence between the actual and computed deflection basins.

Figure 5-4. Backcalculation with moduli ranges and subgrade seed modulus

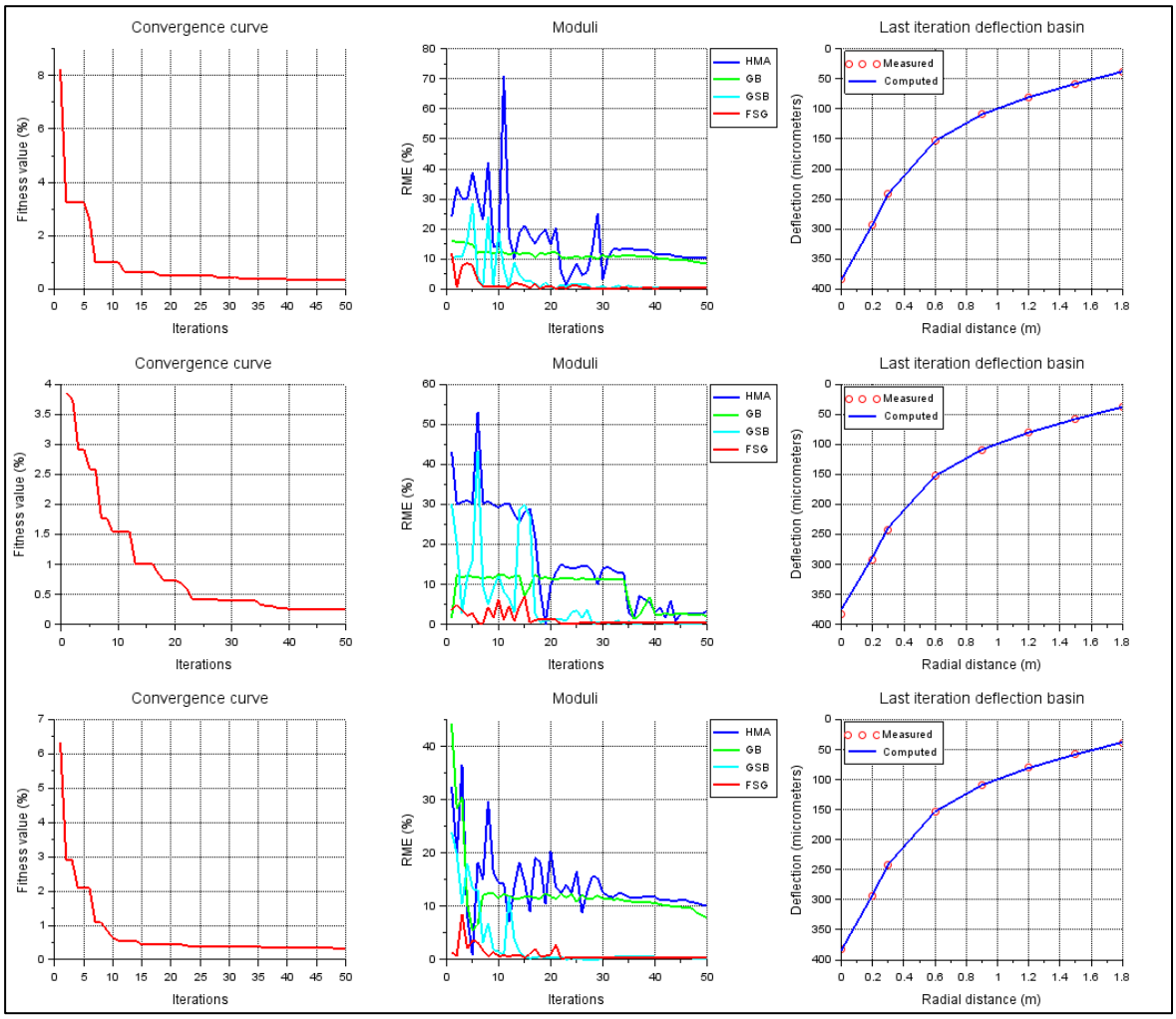

At the end of the 50 iterations, the three swarms yielded the results summarized in Table 5-8. The results show excellent agreement between the estimated and the computed deflections with a maximum RMSE of 0.336% in the first swarm. The predicted absolute errors in moduli are more significant than 5% for the asphalt concrete and the granular base in the first and third swarms.

Table 5-8: Moduli and RMSE with moduli ranges and subgrade seed modulus

Swarm	RMSE (%)	E1 (MPa)	Error	E2 (MPa)	Error	E3 (MPa)	Error	E4 (MPa)	Error
1	0.336%	3,137	10.37%	434.5	8.630%	199.4	0.320%	99.7	0.319%
2	0.249%	3,385	3.278%	407.5	1.881%	201.6	0.777%	99.5	0.511%
3	0.328%	3,148	10.05%	431.6	7.907%	199.6	0.208%	99.6	0.388%

Compared with the two previous cases, the subgrade seed modulus did not improve the backcalculation process.

5.3 Pavement design

As previously stated in section 3.2.1, pavement design optimization is a field of ongoing research on bioinspired techniques with significant contributions based on genetic algorithms. However, one cannot identify a pavement design method that includes a specific module or procedure to obtain *"the best"* properties and thickness combinations for a particular subgrade, traffic, and climate conditions.

The traditional design approach produces the thicknesses of one or more pavement layers. In such methods, construction cost optimization is possible, for example, in charts of equally performing designs such as the Shell Pavement Design Method (Shell Oil, 1978).

Figure 5-5 shows a Shell-type pavement design chart for specific climate, load, and subgrade conditions with thicknesses combinations of hot-mix asphalt and untreated granular base layers for the design traffic in 80 kN axle load repetitions (ESAL). The red lines in the figure indicate the construction cost in US dollars per square meter based on the following unit costs per cubic meter: U$90 for hot-mix asphalt and U$30 for untreated granular material.

Old pavement design methods encouraged using untreated materials and thin asphalt surfacings. However, it is remarkable in Figure 5-5 that the less expensive structures are those at the left side of the chart with significant hot mix asphalt thickness instead of thick untreated granular bases.

Figure 5-5. Shell-type chart with structure costs per square meter

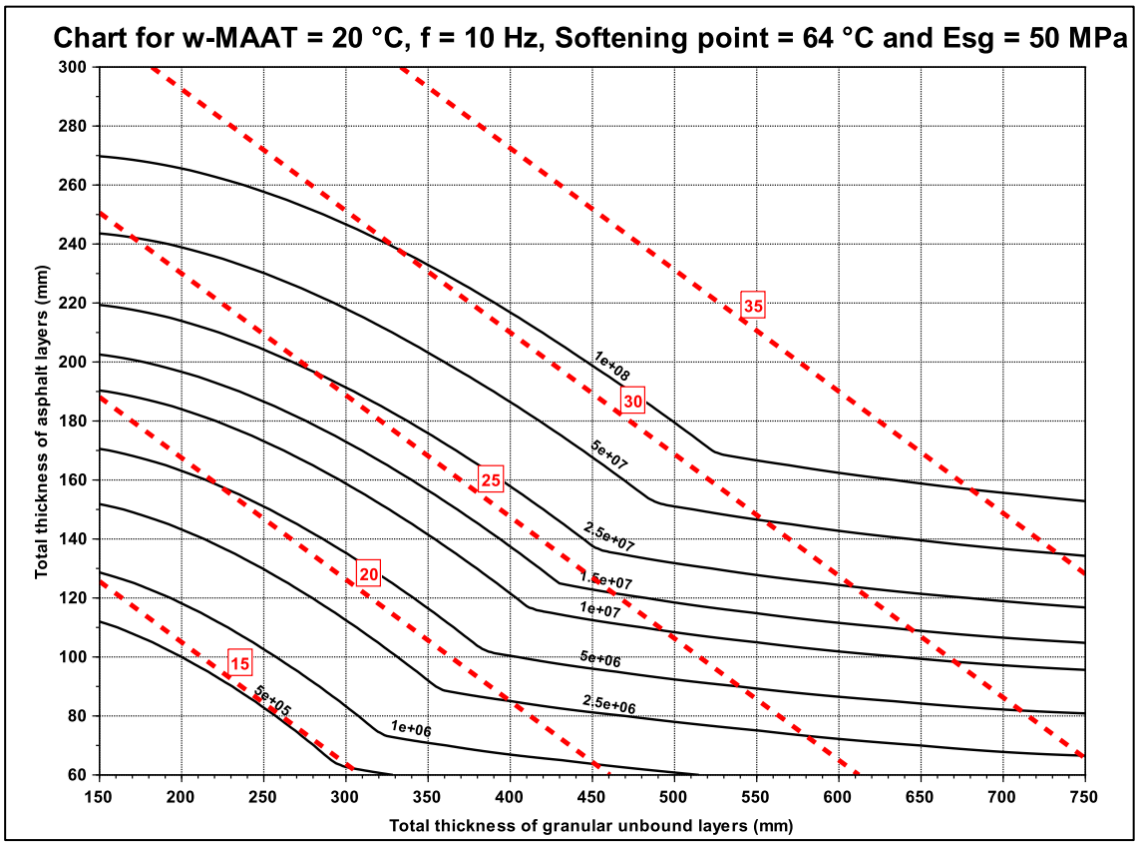

For example, for 5 million ESAL, a pavement composed of 225 mm of untreated granular base and 155 mm of hot-mix asphalt (U$20/m²) is 23% cheaper than an alternative composed of 580 mm of untreated granular base and 87 mm of hot-mix asphalt (U$26/m²). The result depends on local conditions. It does not include maintenance costs; however, each solution in the chart represents a similar state at the end of the performance period according to the fatigue and rutting calibration.

To explore the potential of bioinspired techniques in pavement design optimization, the author developed two computer programs:

1. UNPAVE, for incremental pavement design based on the performance models proposed in the new MEPDG (AASHTO, 2008), includes a module to compute the vehicle operating costs based on the IRI throughout the performance period (National Academies of Sciences, Engineering, and Medicine, 2012).

2. PSO-PAVE implements UNPAVE in a PSO scheme to search the optimum thicknesses for asphalt pavements with untreated granular layers under specific traffic, climate, and subgrade conditions.

The following sections present the main characteristics of each program, including an example of UNPAVE and multiple runs of PSO-PAVE on the same case but with different objective functions.

5.3.1 The UNPAVE program

UNPAVE is an acronym for *"Universidad Nacional de Colombia Pavement Design Program."* The program implements the incremental pavement design approach discussed in section 2.3.2 of this dissertation. As such, UNPAVE requires detailed information about traffic, subgrade, and climate to model the response of the pavement throughout its performance life divided into discrete subperiods.

The current American MEPDG is the model of an incremental pavement design method. The equations included in UNPAVE correspond to the U.S. national calibrated performance equations presented between 2004 to 2008 (NCHRP, 2004) (AASHTO, 2008). In UNPAVE development, the author considered bottom-up fatigue cracking, rutting, and roughness deterioration models. Future developments may include other models or local calibration. The program includes the following modules:

5.3.1.1 Traffic module

This module computes the traffic on the design lane throughout the performance life. It requires the following input:

a) The average daily traffic (ADT) in the first year of operation.
b) The annual traffic growth rate.
c) The directional factor.
d) The lane factor for multilane highways.
e) The traffic composition as percentages of ADT and classified as light vehicles (A), buses (B), two-axle trucks (C2), three to four-axle trucks (C3C4), five-axle trucks (C5), and six-axle trucks (C6). INVIAS uses this classification for the Colombian traffic database (INVÍAS, 2007).

f) The design period is in years.
g) The axle load distribution per axle type (single directional, single, tandem, and tridem) and load magnitude in kilonewtons.
h) The monthly variation of ADT.
i) The initial month of operation.
j) The traffic distribution for the three air temperature periods in the climate module.

The number of subperiods is the design period in years multiplied by 36 (12 months per year times three daily periods). The traffic module output is a table of daily traffic, vehicles per type, axles per weight range, and axles per type for each subperiod.

5.3.1.2 Structure module

This module defines the pavement structure for each subperiod throughout the performance life. It requires the following input:

a) The number of subperiods in the performance life.
b) A vector with the nominal thicknesses in meters.
c) A vector with the nominal Poisson ratios.
d) A vector with the nominal interface conditions.
e) A vector with the type of material for each layer. A three-letter code identifies the following materials: “HMA” for hot mix asphalt, “BG” for the granular base, and “SBG” for the granular subbase.
f) The annual average resilient modulus of the subgrade in kPa.
g) The monthly variations of subgrade strength as a fraction of the annual average value.
h) For the hot mix asphalt concrete:
    i. The volume of air voids in percentage.
    ii. The volume of bitumen in percentage.
    iii. The volume of aggregate in percentage (computed).
    iv. The penetration of the recovered bitumen in 1/10 mm (pen).
    v. The representative velocity of buses and trucks in km/h.
    vi. To compute the hot mix asphalt modulus, the daily subperiods of air temperature, in °C.
    vii. The thickness of the hot-mix asphalt in meters.

The module applies a sublayering procedure to divide the untreated granular layers with thicknesses over 0.15 meters for the base or 0.20 meters for the subbase. The first sublayer of the granular base is 0.05 meters. Each untreated granular layer has the same nominal Poisson ratio, type of material, and interface conditions as the original layer. The following equation estimates the untreated layers moduli (Joint Departments of the Army and Air Force, 1994):

$$E_n = E_{n+1} \cdot [A + B \cdot \log(t) + C \cdot \log(E_{n+1}) \cdot \log(t)]$$

Eq. 5-13

Where E_n is the modulus of the n^{th} the untreated granular layer of the pavement in psi, E_{n+1} is the modulus of the layer beneath in psi, and t is the thickness of the layer in inches. Table 5-9 presents the values of A, B and C for base and subbase materials. Figure 2-17 of this document shows the solution of this equation for both materials. UNPAVE converts the moduli to kPa.

Table 5-9: Parameters to estimate untreated granular materials moduli

Untreated layer	A	B	C
Granular base	1.00	10.52	- 2.10
Granular subbase	1.00	7.18	- 1.56

Source: (Joint Departments of the Army and Air Force, 1994).

The dynamic stiffness of the hot-mix asphalt for each subperiod is computed with the Shell nomographs (Huang, 2004). The equation following equation (Ullidtz, 1987) estimates the bitumen stiffness:

$$S_{bit} = 0.1157 \cdot t_w^{-0.368} \cdot e^{-PI} \cdot (T_{rb} - T_{mix})^{5.0}$$

Eq. 5-14

Where S_{bit} is the bitumen stiffness in Pa, t_w is the traffic loading time in seconds, PI is the penetration index of bitumen (Eq. 2-10), T_{rb} is the softening point of bitumen in °C, and T_{mix} is the hot-mix asphalt temperature in °C.

The traffic loading time is estimated with the following equation (Brown S. F., 1973):

$$t_w = 10^{[0.5 \cdot H - 0.2 - 0.94 \cdot \log(V)]}$$

Eq. 5-15

Where t_w is the traffic loading time in seconds, H is the layer thickness in meters, and V is the vehicle speed in km/h.

The bitumen aging is evaluated with the following equations (Dauzats & Rampal, 1988):

$$pen_t = 11.9925 - 1.2578 \cdot \sqrt{t} + 0.3322 \cdot pen_0 + \frac{0.7656 \cdot pen_0 - 2.9965 \cdot V_v}{\sqrt{t+1}}$$

Eq. 5-16

$$T_{rb} = 64.4448 + 1.5755\sqrt{t} - 0.2531 \cdot pen_0 + 0.5518 \cdot V_v$$

Eq. 5-17

Where pen_t is the retained penetration of the bitumen in 0.1 mm after a time, t, in months, pen_0 is the penetration of the recovered bitumen in 0.1 mm, T_{rb} is the softening point of the bitumen, in °C, after the time, t, and V_v is the volume of voids of the hot-mix asphalt in percent.

With pen_t and T_{rb}, UNPAVE computes the thermal susceptibility, A, and penetration index, PI, of the bitumen using the following equations:

$$A = \frac{\log(pen_t) - \log(800)}{25°C - T_{rb}}$$

Eq. 5-18

$$PI = \frac{20 - 500 \cdot A}{1 + 50 \cdot A}$$

Eq. 5-19

UNPAVE estimates the hot-mix asphalt temperature with the following equation, based on the *"Chart T"* of the Shell Pavement Design Manual (Shell Oil, 1978), and applying interpolation for the specific thickness:

$$T_{mix} = A \cdot T_{air}^2 + B \cdot T_{air} + C$$

Eq. 5-20

Where T_{mix} is the hot-mix asphalt temperature in °C, T_{air} is the air temperature in °C, and A, B, & C are regression coefficients for different thicknesses, as shown in Table 5-10.

Table 5-10: Parameters to estimate hot-mix asphalt temperature from air temperature

Layer thickness (meters)	A	B	C
0.05	-0.00706	1.75728	-1.28783
0.10	-0.00829	1.73114	-1.30369
0.20	-0.00897	1.66774	-1.04389
0.40	-0.01036	1.67077	-1.82581
0.60	-0.00961	1.56068	-1.65616

The hot-mix asphalt modulus is computed with the following equations (Huang, 2004):

$$\beta_1 = 10.82 - 1.342 \cdot \frac{100 - V_g}{V_g + V_b}$$

Eq. 5-21

$$\beta_2 = 8.0 + 0.00568 \cdot V_g + 0.0002135 \cdot V_g^2$$

Eq. 5-22

$$\beta_3 = 0.6 \cdot \log\left(\frac{1.37 \cdot V_b^2 - 1}{1.33 \cdot V_b - 1}\right)$$

Eq. 5-23

$$\beta_4 = 0.7582 \cdot (\beta_1 - \beta_2)$$

Eq. 5-24

Where V_g is the volume of aggregate in percent, V_b is the volume of bitumen in percent, and V_v is the volume of voids in percent of the hot-mix asphalt.

If the bitumen stiffness, S_{bit}, is between 5 and 1,000 MPa, the dynamic stiffness of the hot-mix asphalt is:

$$S_{mix} = 10^{\left\{\frac{\beta_4+\beta_3}{2}\cdot[\log(S_{bit})-8]+\frac{\beta_4-\beta_3}{2}\cdot|\log(S_{bit})-8|+\beta_2\right\}}$$

Eq. 5-25

If the bitumen stiffness, S_{bit}, is between 1,000 MPa and 3,000 MPa, the dynamic stiffness of the hot mix asphalt is:

$$S_{mix} = 10^{\left\{\beta_2+\beta_4+2.0959\cdot\left(\beta_1-\beta_2-\beta_4\right)\cdot[\log(S_{bit})-9]\right\}}$$

Eq. 5-26

Where S_{mix} is the dynamic stiffness of the hot-mix asphalt in Pa, and S_{bit} is the bitumen stiffness in Pa.

The preceding equations are not state-of-the-art on the subject. Other models may be incorporated in UNPAVE to consider more recent research based on the master curve of asphalt concrete. The following paragraphs present the revised dynamic modulus predictive equation for asphalt mixes (NCHRP, 2004):

$$\log_{10}|E^*| = -1.249937 + 0.029232 \cdot P_{200} - 0.001767 \cdot (P_{200})^2 - 0.002841 \cdot P_4 - 0.058097 \cdot Va - 0.802208 \cdot \frac{Vb_{eff}}{Vb_{eff} + Va} + \frac{3.871977 - 0.0021 \cdot P_4 + 0.003958 \cdot P_{38} - 0.000017 \cdot (P_{38})^2 + 0.005470 \cdot P_{34}}{1 + e^{[-0.603313 - 0.313351 \cdot \log_{10}(f) - 0.393532 \cdot \log_{10}(\eta)]}}$$

Eq. 5-27

Where $|E^*|$ is the asphalt mix dynamic modulus (10^5 psi), η is the binder viscosity (10^6 Poise) at any temperature and degree of aging, f is the load frequency (Hz), Va is the air voids in the mix (% by volume), Vb_{eff} is the effective binder content in the mix (% by volume), P_{34} P_{38} P_4 are the cumulative percentages retained on the ¾", ⅜", and No. 4 sieves by total aggregate weight, and P_{200} is the percentage passing the No. 200 sieve by total aggregate weight.

The MEPDG incorporates the Global Aging System with four models: (a) original to mix/lay-down model, (b) surface aging model, (c) air void adjustment, and (d) viscosity-depth model.

- Original viscosity: The original viscosity for unaged conditions is determined from the ASTM viscosity-temperature relationship:

$$\log_{10}\left[\log_{10}\left(\eta_{original}\right)\right] = A + VTS \cdot \log_{10}(T_R)$$

Eq. 5-28

Where $\eta_{original}$ is the unaged viscosity of the asphalt binder (centiPoises: cP), A is the regression intercept, VTS is the regression slope of viscosity-temperature susceptibility, and

T_R is the temperature (°Rankine). Table 5-11 summarizes recommended values of A and VTS for several binder grades.

Table 5-11: Recommended RTFOT A and VTS parameters based on binder grades

Grade method	Grade	A	VTS
Performance grades	PG 58-16	12.248	-4.147
	PG 58-22	11.787	-3.981
	PG 58-28	11.010	-3.701
	PG 64-16	11.375	-3.822
	PG 64-22	10.980	-3.680
	PG 64-28	10.312	-3.440
	PG 70-16	10.641	-3.548
	PG 70-22	10.299	-3.426
	PG 70-28	9.715	-3.217
Viscosity grades	AC-2.5	11.5167	-3.8900
	AC-5	11.2614	-3.7914
	AC-10	11.0134	-3.6954
	AC-20	10.7709	-3.6017
	AC-30	10.6316	-3.5480
	AC-40	10.5338	-3.5104
Penetration grades	40-50	10.5254	-3.5047
	60-70	10.6508	-3.5537
	85-100	10.8232	-3.6210
	120-150	11.0897	-3.7252
	200-300	11.8107	-4.0068

Source: NCHRP (2004).

- Original to mix/lay-down aging: This model considers short-term aging due to construction practices ($\eta_{t=0}$).

$$\log_{10}[\log_{10}(\eta_{t=0})] = (0.054405 + 0.004082 \times code) + (0.972035 + 0.010886 \times code) \cdot \log_{10}[\log_{10}(\eta_{original})]$$

Eq. 5-29

Where $\eta_{t=0}$ is the short-term aged viscosity of the asphalt binder (cP), and $code$ depends on the hardening ratio. Table 5-12 presents the code values for the binder mix/lay-down hardening resistance.

Table 5-12: Recommended code values for short-term aging

Mix/Lay-down hardening resistance	Expected hardening ratio values	Code value
Excellent to good	HR ≤ 1.030	-1
Average	1.030 < HR ≤ 1.075	0
Fair	1.075 < HR ≤ 1.100	1
Poor	HR > 1.100	2

Source: NCHRP (2004).

- Surface aging model: This model considers the effect of the environment on the long-term aging of the binder for surface conditions (η_{aged}).

$$\log_{10}[\log_{10}(\eta_{aged})] = \frac{\log_{10}[\log_{10}(\eta_{t=0})] + A \cdot t}{1 + B \cdot t}$$

Eq. 5-30

Where η_{aged} is the long-term aged viscosity of the asphalt binder (cP) for surface conditions, and t is the aging time (months). The parameters A and B are defined as:

$$A = -0.004166 + 1.41213 \cdot (C) + (C) \cdot \log_{10}(MAAT) + (D) \cdot \log_{10}[\log_{10}(\eta_{t=0})]$$

Eq. 5-31

$$B = 0.197725 + 0.068384 \cdot \log_{10}(C)$$

Eq. 5-32

Where C and D are:

$$C = 10^{[274.4946 - 193.831 \cdot \log_{10}(T_R) + 33.9366 \cdot (\log_{10}(T_R))^2]}$$

Eq. 5-33

$$D = -14.5521 + 10.47662 \cdot \log_{10}(T_R) - 1.88161 \cdot (\log_{10}(T_R))^2$$

Eq. 5-34

Where $MAAT$ is the mean annual air temperature (°F), and T_R is the binder temperature (°R).

- Air void adjustment: This model adjusts the viscosity from the surface aging model for air voids effects (η_{aged_va}).

$$\log_{10}[\log_{10}(\eta_{aged\_va})] = F_v \cdot \log_{10}[\log_{10}(\eta_{aged})]$$

Eq. 5-35

Where η_{aged} is the long-term aged viscosity of the asphalt binder (cP) for surface conditions. The parameter F_v is defined as:

$$F_v = \frac{1 + 1.0367E - 04 \cdot (VA) \cdot (t)}{1 + 6.1798E - 04 \cdot (t)}$$

Eq. 5-36

Where VA is the air void ratio (percent), and t is the aging time (months). VA is defined as:

$$VA = \frac{VA_{original} + 0.0111 \cdot (t) - 2}{1 + 4.24E - 04 \cdot (t) \cdot (MAAT) + 1.169E - 03 \cdot \left(\frac{t}{\eta_{original\ 77°F}}\right)} + 2$$

Eq. 5-37

Where $VA_{original}$ is the initial air void content of the mix, t is the aging time (months), $MAAT$ is the mean annual air temperature (°F), and $\eta_{original\ 77°F}$ is the original binder viscosity at 77°F.

- Viscosity-depth model: This model describes the aged viscosity (cP) as a function of depth $(n_{t,z})$.

$$n_{t,z} = \frac{\left(\eta_{aged\_va}\right) \cdot (4 + E) - (E) \cdot (\eta_{t=0}) \cdot (1 - 4z)}{4 \cdot (1 + E \cdot z)}$$

Eq. 5-38

Where η_{aged_va} is the viscosity from the surface aging model for air voids effects (cP), $\eta_{t=0}$ is the short-term aged viscosity (cP), and z is the depth (inches). The parameter E is defined as:

$$E = 23.83 \cdot e^{(-0.0308 \cdot MAAT)}$$

Eq. 5-39

Where $MAAT$ is the mean annual air temperature (°F).

These four models estimate the long-term aged viscosity used in Eq. 5-27 with the unit conversion from centiPoises to MegaPoises.

The structure module output module is:

a) A vector with the thicknesses after the sublayering procedure.
b) A vector with the Poisson ratios after the sublayering procedure.

c) A vector with the interface conditions after the sublayering procedure.
d) A vector with the layer type after the sublayering procedure.
e) A matrix with the moduli of the layers for each subperiod.
f) A matrix with the hot-mix asphalt temperature and bitumen stiffness per subperiod.

5.3.1.3 Structural analysis points module

This module defines the structural analysis points for each subperiod, considering the pavement profile obtained from the sublayering procedure. The module generates vectors with the x, y & z coordinates of the points of analysis, the type of material, and the type of performance analysis: fatigue or rutting.

The points pattern follows the spacings defined in Figure 2-21 for single, tandem, and tridem axles, which are necessary to perform the wander analysis to summarize the structural responses to compute the critical strains in each layer. The z-coordinates correspond to critical fatigue and rutting strains in pavement and subgrade. The module output is four vectors with the x, y, & z coordinates and the layer number in the original structure before the sublayering procedure.

5.3.1.4 Structural analysis computations module

This module calls the UNLEA algorithm (see section 4.2) to evaluate the pavement structures on each subperiod for all load types and combinations and obtain the strains for the fatigue and rutting performance models.

The module requires the following information:

a) The thickness of each layer.
b) The Poisson ratio of each layer.
c) The interface condition between layers.
d) The type of material of each layer, for example, hot-mix asphalt (HMA), untreated granular base (BG), untreated granular subbase (SBG), or subgrade (SG).
e) The new pavement's initial International Roughness Index (IRI) in m/km.
f) The radius of the wheel contact area. Default value: 0.10 meters.
g) The distance between wheels in dual-wheel axles. Default value: 0.30 meters.

h) The axle separation for multiple axles. Default value: 1.311 meters. The MEPDG proposes a spacing of 1.250 meters for tridem axles. UNPAVE can use both values, but the author unified them to reduce the computation cost.
i) The axle weight or applied load. Default value: 100 kN per axle.
j) The traffic transversal wander. Default value: 0.30 meters.

The UNLEA code computes stresses, strains, and displacements for each type of axle load in each subperiod throughout the pavement performance life. Computations consider 100 kN per axle, but UNLEA linearly transforms the responses for each load in the axle load spectrum. This procedure disregards the non-linear characteristics of the subgrade and the untreated granular materials to reduce the computing cost. The module output is a matrix with the critical strains for each subperiod and analysis point identifying a fatigue or rutting point.

5.3.1.5 Summarize responses module

This module reads the critical strains computed by UNLEA. It calculates the effect of each type of axle load by applying the superposition principle for tandem and tridem axles, as specified in the MEPDG (NCHRP, 2004). Then, it simulates the transversal wander of traffic to define the critical strain position under each type of axle per subperiod, considering a normal distribution of transversal wheel position in five percentiles. The module output is four matrices with the five percentile values of critical strains for each subperiod and analysis points under each type of axle load: steer, single, tandem, and tridem.

5.3.1.6 Rutting prediction module

This module reads the summarized critical strains and computes the accumulated plastic vertical deformation for each rutting-susceptible layer with the MEPDG models for hot-mix asphalt, untreated aggregate layers, and subgrade (NCHRP, 2004). The module output is a matrix with the accumulated rutting in each sublayer for each subperiod. The sum of each layer contribution yields the total rut depth in the pavement surface per subperiod.

5.3.1.7 Fatigue prediction module

This module reads the summarized critical strains and computes the accumulated bottom-up and top-down cracking fatigue for the hot-mix asphalt layer with the MEPDG model

(NCHRP, 2004). The module output is a matrix with the accumulated fatigue damage in each sublayer for each subperiod.

5.3.1.8 Roughness prediction model

This module computes the International Roughness Index (IRI), considering an initial roughness value and the accumulated cracking and rutting damage per subperiod with the updated MEPDG model for flexible pavements (AASHTO, 2008). The module output is a vector with the IRI for each subperiod.

5.3.1.9 Vehicle operating costs module

This module computes the vehicle operating costs (VOC) considering each subperiod's fleet and pavement roughness. The VOC includes fuel and tire consumptions and repair and maintenance costs based on the models presented by Chatti & Zaabar (2012) for the representative traffic speed.

The module output is a matrix of VOC per item in U.S. currency. According to vehicle type, the costs per kilometer are U$ 0.609 / liter of fuel, U$ 60 to U$ 400 / tire, and U$ 0.015 to U$ 0.046 per repair and maintenance. The vehicular fleet for cost computation considers three types of vehicles: *"medium car"* for automobiles; *"light truck"* for buses, C2P, and C2G trucks; and *"articulated truck"* for C3-C4 to >C6 in the INVIAS traffic classes. Future research may incorporate costs considering different fuel types, locally calibrated consumption, and maintenance and repair rates.

5.3.1.10 Graphic output module

This module generates six charts with (a) bottom-up fatigue cracking, (c) accumulated rutting, (c) IRI, (d) cumulative burnt fuel in liters per kilometer, (e) cumulative used tires in units per kilometer, and (f) cumulative vehicle operating cost in U$ per kilometer throughout the pavement performance period.

5.3.1.11 Climate modeling

UNPAVE selects the air temperature for each subperiod throughout the performance life considering three daily periods: "dawn" (07:00), "noon" (13:00), and "night" (19:00), as available in IDEAM (Colombian Institute for Hydrology, Meteorology, and Environmental

Studies) climate databases. Air temperatures are necessary to compute the dynamic modulus of hot-mix asphalt throughout the performance life.

The required information is as follows:

a) Monthly variation of the dawn, noon, and night average air temperatures.
b) The initial month of traffic operation.
c) Average annual precipitation in millimeters

UNPAVE does not include an integrated climate model. Users must estimate the moisture variation on the subgrade during the life period and include it as monthly fractions of the average resilient modulus. The untreated layers' moduli depend on the subgrade modulus and indirectly consider the moisture variation.

5.3.2 Design example with the UNPAVE program

The following example illustrates the capabilities of UNPAVE for a given set of conditions in a specific project.

The design period is ten years divided into monthly periods to consider climate effects on the subgrade and untreated granular layers. Each month is divided into three temperature periods representing different conditions for hot-mix asphalt. The total subperiods are ten years comprising twelve months per year and three air temperature periods per month.

At the end of the 360th subperiod, the program presents the damage (fatigue and rutting), roughness progression in the pavement, accumulated fuel and tire consumptions, and vehicle operating costs per kilometer for the whole performance period.

5.3.2.1 Input information

1. Traffic. Data traffic corresponds to the counting station “444 La Esperanza – Petaqueros,” shown in Figure 5-6. The author considers a multilane highway with two lanes for each travel direction for the case study. The actual road is a two-lane highway. Table 5-13 summarizes the traffic data for incremental pavement analysis based on the counting station and some assumptions by the author.

The UNPAVE program requires the axle load magnitude and relative distribution. Table 5-14 presents the axle load distribution in the Chinchiná – Manizales Road, corresponding to counting station 338 in Figure 5-6 (INVÍAS, 2003).

Figure 5-6. 444. La Esperanza – Petaqueros traffic count station – not to scale

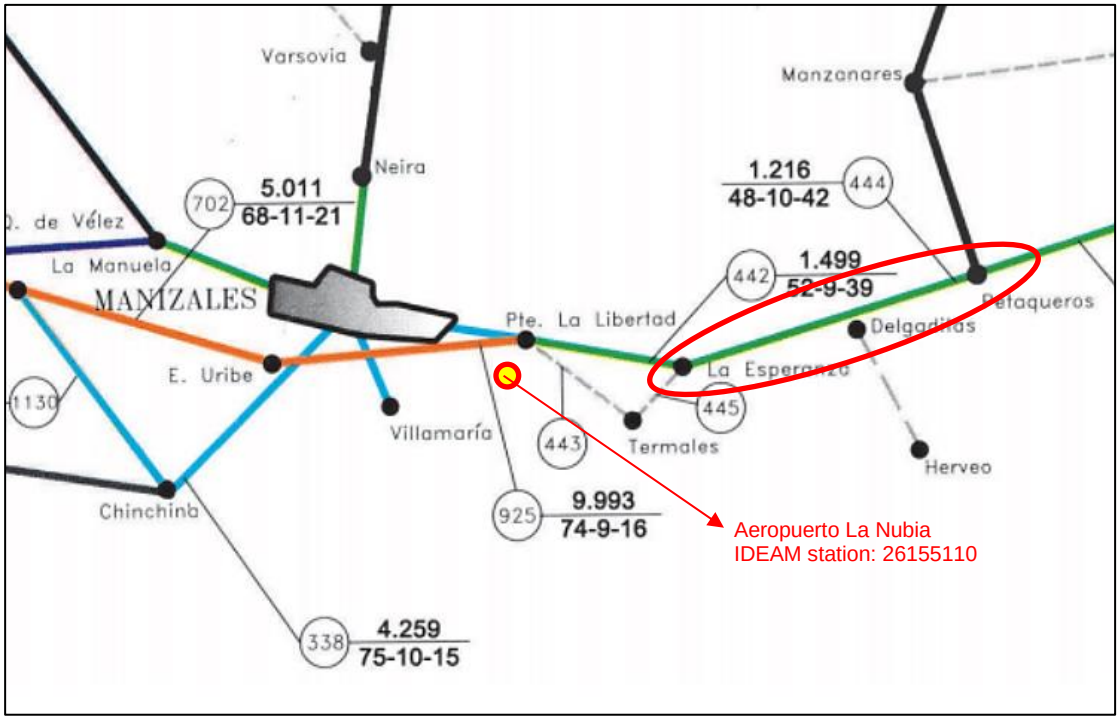

Source: INVÍAS (2011).

Table 5-13: Traffic data for pavement design 444. La Esperanza - Petaqueros

Item	Value
Average daily traffic	1,786
Annual traffic growth rate (%)	4.99%
Directional factor (%)	50%
Lane factor (%)	90%
Traffic composition as a percentage of the ADT (%)	
A	53.54%
B	8.33%
C2	26.74%
C3C4	3.65%
C5	3.42%
C6	4.36%
Design period (years)	10
Representative speed (km/h)	50

Source: Adapted from INVIAS (2011).

The traffic in each subperiod depends on monthly and hourly distribution factors. Table 5-15 presents the monthly factor to adjust the ADT assumed in this case. Databases from toll booths contain actual monthly and hourly distributions in the road network.

Table 5-14: Axle load distribution Chinchiná – Manizales at Cenicafé weighing station

Range of load (kN)	Load value (kN)	Steer axle (%)	Single axle (%)	Tandem axle (%)	Tridem axle (%)
0 – 20	10	1.75	0.03	0.00	0.00
20 – 40	30	58.34	30.65	0.75	1.00
40 – 60	50	38.50	25.55	11.19	21.04
60 – 80	70	1.31	12.68	25.52	17.53
80 – 100	90	0.08	11.85	10.77	5.68
100 – 120	110	0.02	13.64	5.66	4.84
120 – 140	130	0.00	5.26	7.50	7.35
140 – 160	150	0.00	0.25	4.02	4.67
160 – 180	170	0.00	0.09	4.44	4.17
180 – 200	190	0.00	0.00	6.96	2.17
200 – 220	210	0.00	0.00	13.75	6.34
220 – 240	230	0.00	0.00	8.21	9.35
240 – 260	250	0.00	0.00	1.22	11.85
260 – 280	270	0.00	0.00	0.00	3.84
280 – 300	290	0.00	0.00	0.00	0.00
300 – 320	310	0.00	0.00	0.00	0.17

Source: INVÍAS (2003).

Table 5-15: Assumed monthly traffic variation of ADT

Month	Jan.	Feb.	Mar.	Apr.	May	Jun.	Jul.	Aug.	Sep.	Oct.	Nov.	Dec.
Factor	0.95	1.01	1.00	0.89	0.85	1.05	1.09	1.03	0.95	0.90	0.95	1.15

The proposed hourly factor considers three times with different air temperatures directly affecting the hot-mix asphalt moduli. The numbers in Table 5-16 represent the assumed ADT percentages that operate in each air-temperature period.

Table 5-16: Assumed traffic distribution per daily temperature periods

Period of the day	Dawn	Noon	Night
Percentage of ADT	10%	60%	30%

2. Climate: Table 5-17 shows the monthly distribution of the average wet air temperature in the three daily periods defined for the design. The author selected the IDEAM station “26155110 Aeropuerto La Nubia” for the case study. Figure 5-6 also indicates the airport location in Manizales.

Table 5-17: Mean monthly wet air temperature at three periods per day

Month	Dawn (7:00)	Noon (13:00)	Night (18:00)
January	11.70	16.14	13.31
February	12.02	16.08	13.47
March	12.34	16.14	13.31
April	12.79	16.22	13.28
May	12.92	15.92	13.09
June	12.74	15.85	13.09
July	12.32	15.77	13.14
August	12.32	15.86	13.34
September	12.33	15.69	12.59
October	12.37	15.43	12.39
November	12.35	15.56	12.45
December	12.14	16.00	13.05

Source: Adapted from IDEAM (2021).

The project considers the start of traffic operation in May (5th month). The design period ends in May of the tenth year. UNPAVE does not include an integrated climate model; however, it requires the average annual precipitation for site factor computation in the roughness model. For this case study, it is equal to 1,500 millimeters.

3. Materials: Table 5-18 summarizes the characteristics of the hot-mix asphalt to estimate the moduli based on the air temperature and aging on each subperiod.

Table 5-18: Mean hot-mix asphalt properties to assess subperiod moduli

Item	Value
The volume of air voids in the mix (%)	4.0
The volume of aggregate in the mix (%)	11.0
The volume of bitumen in the mix (%)	85.0
Original penetration of the bitumen (0.1 mm)	65

The untreated aggregate base and subbase moduli depend on the subgrade moduli computed for each subperiod and the USACE model described in Table 5-9.

4. Trial structure: Table 5-19 presents the pavement structure considered for this case with an initial IRI of 2.0 m/km.

Table 5-19: Case study pavement structure

Layer No.	Material type	Poisson ratio	Thickness (m)	Interface condition
1	HMA	0.30	0.15	Rough
2	BG	0.35	0.20	Rough
3	SBG	0.35	0.45	Rough
4	SR	0.45		

5.3.2.2 Output information

The UNPAVE program execution takes 33.6 minutes on MATLAB R2021b on a PC with Windows 11®, Intel® Core i7® processor, and 8GB of RAM. UNPAVE calls the UNLEA subroutine 19,800 times. Figure 5-7 to Figure 5-12 show the results of the trial pavement for the design conditions described above.

Figure 5-7. Bottom-up fatigue cracking progression in the case study

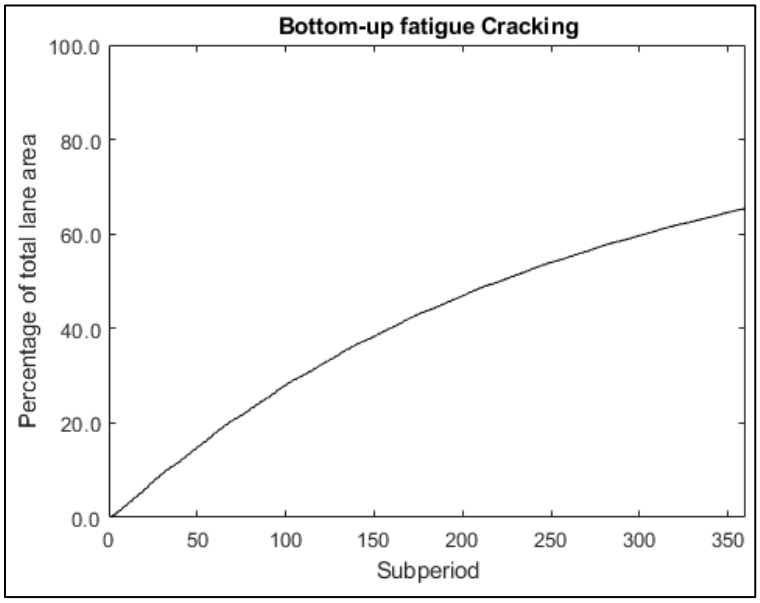

The total lane area with bottom-up fatigue increases throughout the pavement life up to 65% (Figure 5-7). The rut depth increases primarily in the first 24 months of traffic operation and up to 32 mm in ten years (Figure 5-8). This rut depth represents a safety risk for traffic under wet conditions.

Cracking and rutting are well above some commonly accepted thresholds. For example, the 1982 Asphalt Institute method considers 20% cracking of the total lane area and 12.5 mm of total rut depth (Asphalt Institute, 1982). Consequently, the pavement trial section

should be increased in thickness or improved in quality with cement-treated bases. This dissertation deals only with hot-mix asphalt and untreated granular bases and subbases.

Figure 5-8. Rut depth progression in the case study

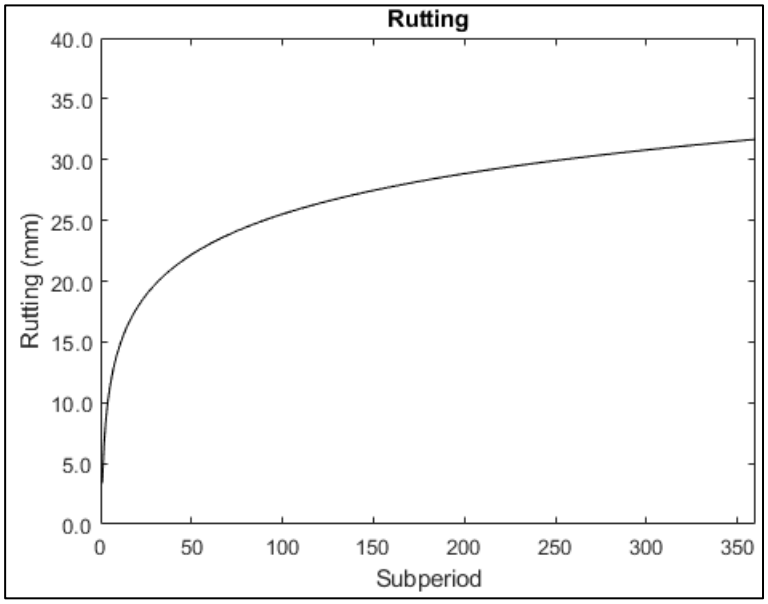

Figure 5-9 shows a final IRI of 3.3 m/km, corresponding to an *"older pavement"* condition, according to Sawyers et al. (1986). The total IRI change is 1.3 m/km throughout the design period.

Figure 5-10 and Figure 5-11 show the cumulative consumption of fuel (1.63 million liters) and tires (958 tires) per kilometer in the 10-year design period. The fuel and tire consumption may help compare the environmental impact of a proposed pavement structure independently of fluctuating fuel and tire costs

Figure 5-12 presents the cumulative vehicle operating costs which add to U$ 1.554 million in the ten years. The construction cost per kilometer for a 7.2-meter-wide road is U$ 0.244 million, so the total cost is U$1.798 million.

Figure 5-9. International roughness index (IRI) progression in the case study

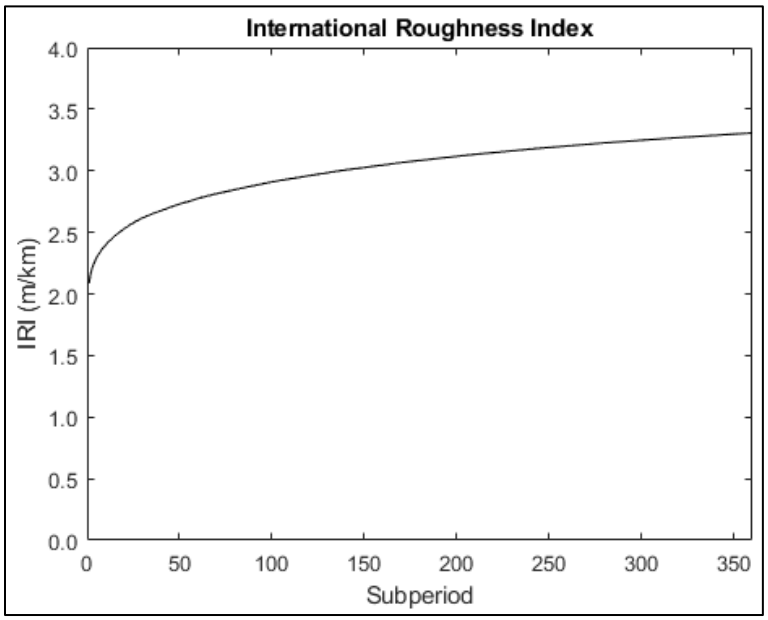

Figure 5-10. Cumulative fuel consumption in the case study

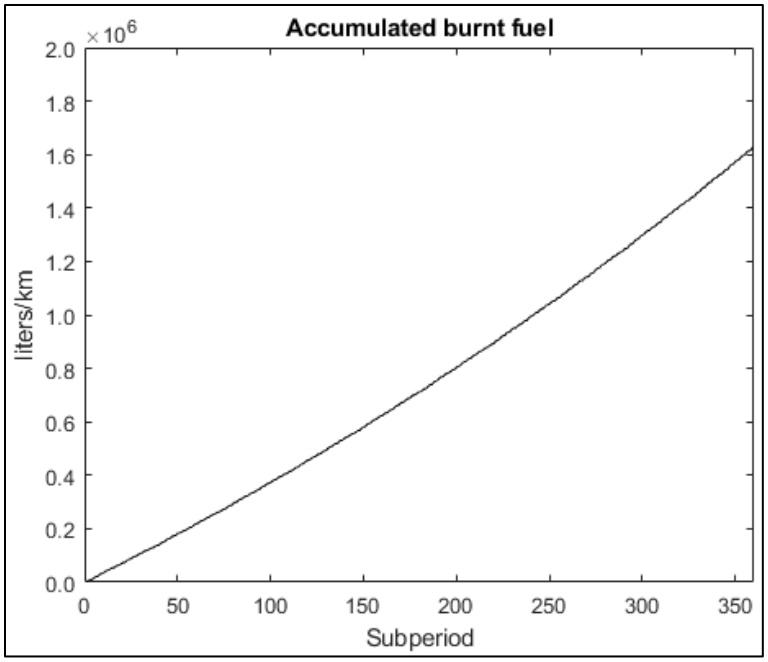

Figure 5-11. Cumulative tire consumption in the case study

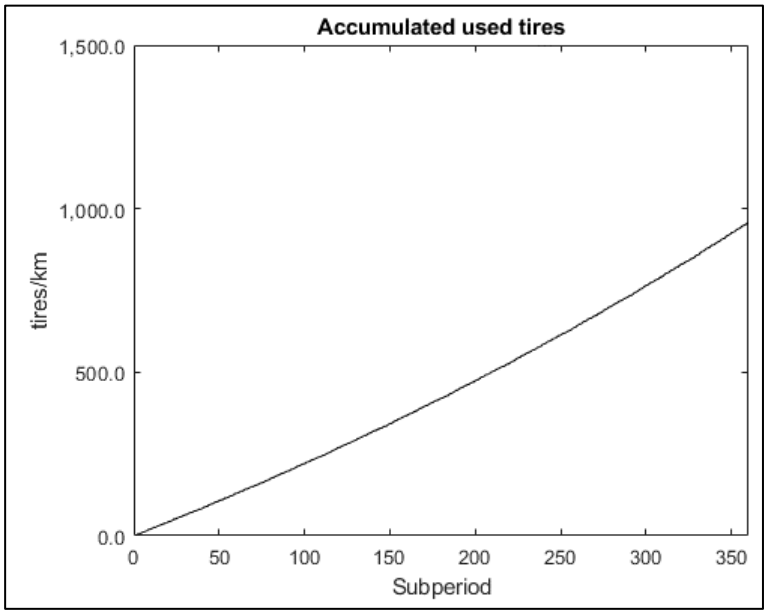

.

Figure 5-12. Cumulative total vehicle operating costs in the case study

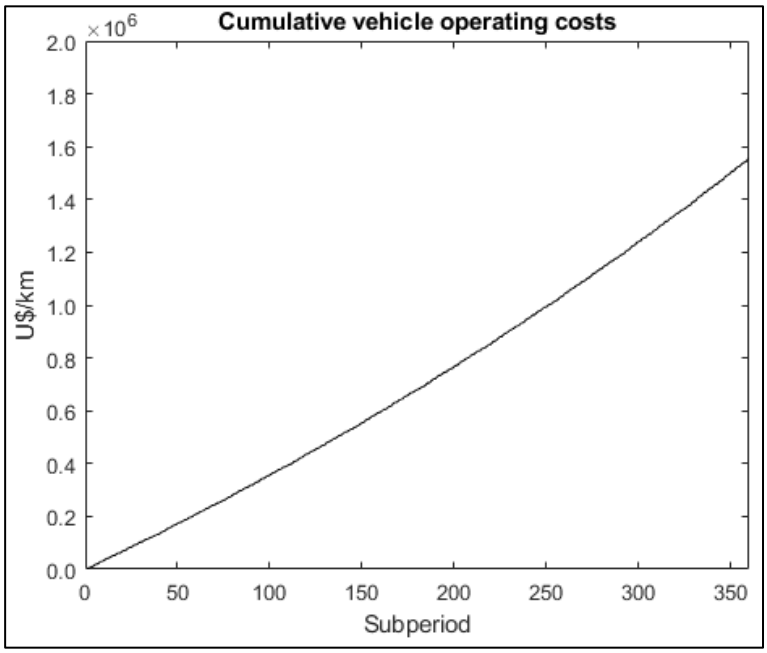

5.3.3 Climate change effects on pavement performance

Climate change poses a significant risk to human life, nature, and the built environment (IPCC, 2014). Road networks are part of the built environment, especially vulnerable to

extreme weather. Increased rainfall intensity may exceed the capacity of hydraulic works, saturate artificial or natural slopes, or weakens treated and untreated pavement materials. Temperature gradients impose cyclic volumetric deformations in pavement surface materials. Asphalt binders are well-known thermosensitive materials, so their ability to store energy from load-imposed deformation reduces with heat, while their susceptibility to fatigue increases at low temperatures.

Gudipudi et al. (2017) summarized previous studies in the U.S. on climate change effects on pavements. Heat waves, phreatic level changes, or rainfall infiltration may impact pavement integrity or subgrade bearing capacity. Previous studies reviewed the effect of temperature changes but not prediction models based on climate change. Other studies integrated temperature and precipitation changes but did not identify the factor with the most significant impact on pavement performance.

Gudipudi et al. used data from the Climate Analytics website and 19 climate prediction models. They concluded that the use of climate change projections impacts the estimation of pavement performance irrespective of climate location and prediction models based on the results of the AASHTOWare algorithms calibrated in five different locations in the U.S. contrasted with historical climate data. The impacts correspond to increased distress (2% to 9% for fatigue cracking and 9% to 40% for rutting) and early pavement failure due to higher temperatures. In contrast, precipitation projections did not affect pavement performance substantially. The uncertainty of these projections is considerable, but the conclusion is consistent: *it is necessary to consider temperatures that deviate from historical norms in pavement analysis and design*.

The Climate Analytics website (https://climateanalytics.org/) offers a Climate Risk Dashboard tool to explore the future impacts of climate change in a geographical location with multiple scenarios and the corresponding impacts (Climate Analytics, 2022). Table 5-20 summarizes two scenarios and temperature indicators of climate change for the southeastern area of the Department of Caldas (Colombia) applicable to the case study.

Table 5-20: Case study scenarios and indicators of climate change (°C)

Scenario	Indicator	Value for the case study		
		2030	2050	2100
Current policies in 2020	Mean temperature	1.3	1.8	3.1
	Hot extreme	1.8	2.2	3.7
	Cold extreme	0.8	1.2	2.4
Delayed action: Decarbonization is delayed in earnest to the 2030s. Renewable energy never displaces all fossil fuel use – carbon dioxide is captured from the air and buried instead, along with reforestation	Mean temperature	1.2	1.6	1.8
	Hot extreme	1.8	2.0	2.2
	Cold extreme	0.8	1.0	1.2
Nationally Determined Contributions are more ambitious than current policies.	Mean temperature	1.3	1.8	3.1
	Hot extreme	1.8	2.2	3.7
	Cold extreme	0.8	1.2	2.4

Source:

- Source: Scenario trajectories modeled with FaIR: Lamboll, R., Rogelj, J., & Schleussner, C. F. (2022) A guide to scenarios for the PROVIDE project. Earth and Space Science Open Archive.
- Temperature data modeled with MESMER: Schwaab et al., in preparation

For the 2030–2050 period, the estimated increments in the mean, extreme hot and extreme cold temperatures reach up to 1.8, 2.2, and 1.2 degrees Celsius, respectively.

The *"Critical Climate Change Concerns for the Road Sector in Colombia"* (CDKN, 2012) estimates an increase of the temperature of 1.6 to 2.2 °C for a high emission scenario in the 2041–2070 term. This range coincides reasonably well with those obtained from the Climate Analytics website. Concerning rainfall, the total annual precipitation shows positive and negative trends. For the case study area, IDEAM studies (Op. Cit., 2012) indicate an increase of 4.1 mm/year in annual precipitation, which equals an increase of 123 mm/year for the 2020 – 2050 term.

Consequently, the effect of climate change in the UNPAVE study case considers two modified inputs: (a) An average annual precipitation equal to 1,623 millimeters (an 8.2% increment), and (b) the three-period air temperatures summarized in Table 5-21.

Table 5-21: Climate-change-adjusted mean monthly wet air temperature

Month	Dawn (7:00)	Noon (13:00)	Night (18:00)
January	12.90	18.34	14.51
February	13.22	18.28	14.67
March	13.54	18.34	14.51
April	13.99	18.42	14.48
May	14.12	18.12	14.29

Month	Dawn (7:00)	Noon (13:00)	Night (18:00)
June	13.94	18.05	14.29
July	13.52	17.97	14.34
August	13.52	18.06	14.54
September	13.53	17.89	13.79
October	13.57	17.63	13.59
November	13.55	17.76	13.65
December	13.34	18.20	14.25

The UNLEA program is re-run with the new climatic information. Figure 5-13 shows the damage, roughness, fuel and tire consumptions, and cumulative vehicle operating cost progression through the analysis period.

Figure 5-13. Performance of the UNPAVE case study considering climate change

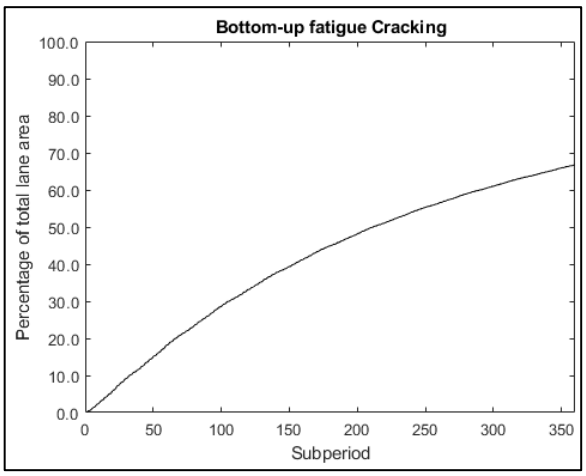

(a) Bottom-up fatigue cracking

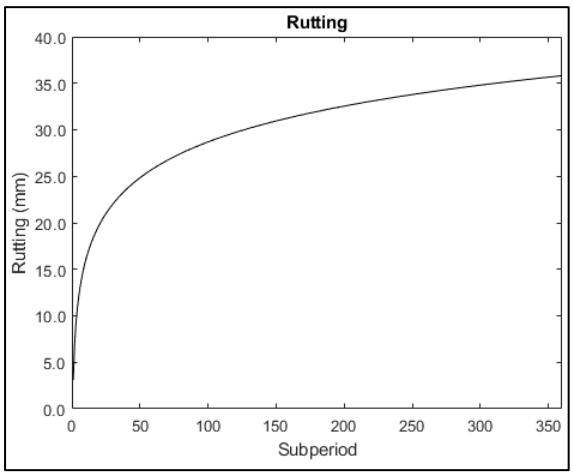

(b) Rut depth

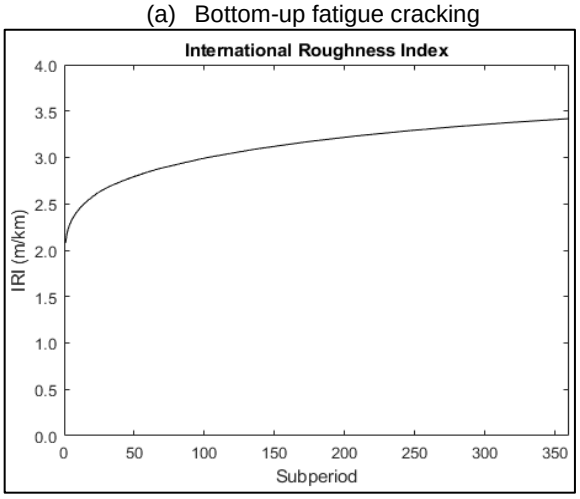

(c) IRI

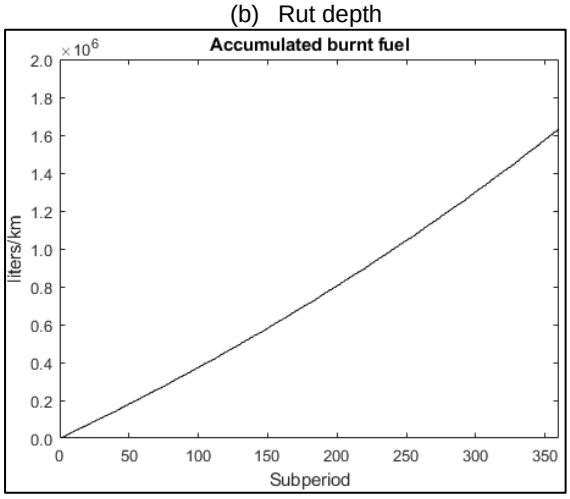

(d) Fuel consumption

Figure 5-13. Performance of the UNPAVE case study considering climate change (cont.)

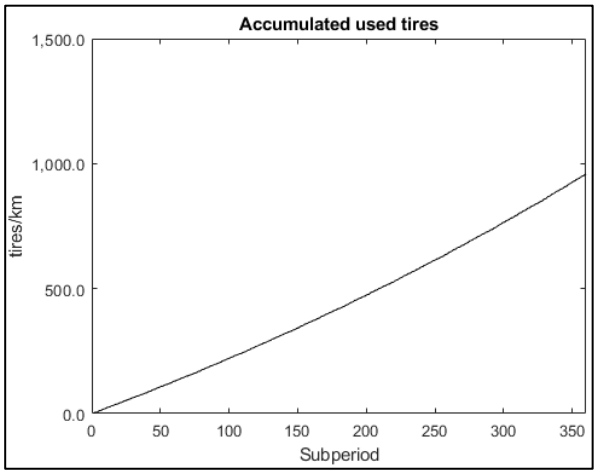

(e) Tire consumption

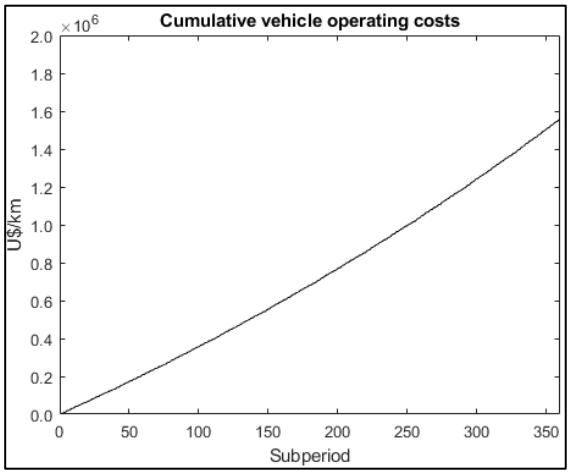

(f) Cumulative vehicle operating cost

The fatigue-cracked area adds up to 67% of the total lane area, i.e., it shows an increment of 2% from the case based on historical climate information or baseline case. In relative terms, there is a 3.1% increase in fatigue damage. The rutting is 36 mm, which is 4.0 mm larger than the 32 mm obtained in the baseline case, so the relative rutting increase is 12.5%. Both fatigue and rutting increments coincide with the findings of Gudipudi et al. (Op. Cit., 2017).

The IRI reaches a value of 3.42 m/km, which is 0.12 m/km larger than the 3.30 m/km of the baseline case, i.e., the relative increase is 3.64 %.

The fuel consumption is 1.632 million liters per kilometer, i.e., 2,000 liters per kilometer more than in the baseline case, with a 0.12% increment. The tire consumption is 958 tires per kilometer, and there is not a significant numerical difference with the baseline case. Finally, the vehicle operating cost is U$ 1.558 million per kilometer, i.e., U$ 4,000 per kilometer more than in the baseline case, with a 0.25% increment.

The fatigue cracking and rutting increase in the *"current policies"* scenario is similar to that reported in previous studies. The fuel and tire consumptions and vehicle operating costs per kilometer are less sensitive than damage because these also depend on the bulk numbers of traffic vehicle mix.

5.3.4 Application of the MEPDG |E*| model

The UNLEA program is re-run with the climatic information proposed in the previous section considering climate change (Table 5-21) and other characteristics of the binder and the asphalt mix to use the MEPDG model.

- Regression intercept of viscosity-temperature susceptibility: A = 10.6508.
- Regression slope of viscosity-temperature susceptibility: VTS = -3.5537.
- Initial air voids in the asphalt mix: Vv_init = 8.0%.
- Particle size distribution for an MDC19 asphalt mix:
  - ¾" sieve: 100.0 % passing by total weight of aggregate.
  - ⅜" sieve: 79.0 % passing by total weight of aggregate.
  - No. 4 sieve: 57.0 % passing by total weight of aggregate.
  - No. 200 sieve: 6.0 % passing by total weight of aggregate.

Figure 5-14 shows the damage, roughness, fuel and tire consumptions, and cumulative vehicle operating cost progression through the analysis period.

The fatigue-cracked area adds up to 54.43% of the total lane area, i.e., it shows a reduction of 10.57% from the case based on historical climate information or baseline case using the Shell Oil model to estimate the asphalt mix dynamic modulus.

The rutting is 26.44 mm, which is 5.56 mm less than the 32.0 mm obtained in the baseline case. The IRI reaches a value of 3.11 m/km, which is 0.19 m/km less than the 3.30 m/km under the same conditions.

The fuel consumption is 1.622 million liters per kilometer, i.e., 10,000 liters per kilometer less than in the baseline case (0.67% reduction). The tire consumption is 954 tires per kilometer, and there is not a significant numerical difference with the baseline case. Finally, the vehicle operating cost is U$ 1.549 million per kilometer, i.e., U$ 43,000 per kilometer less than in the baseline case (2.70% reduction).

Figure 5-14. Performance of the UNPAVE case study with the MEPDG |E*| model

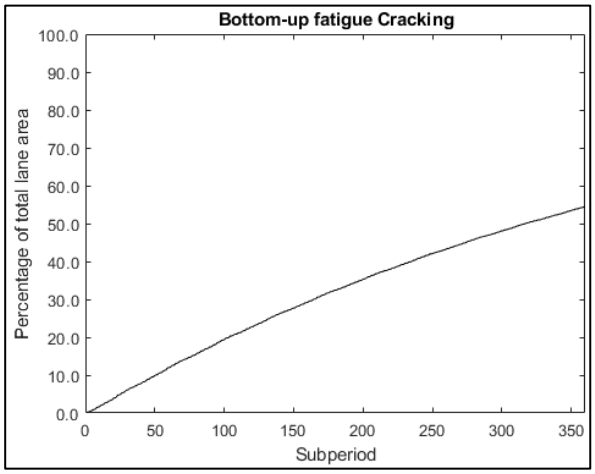

(a) Bottom-up fatigue cracking

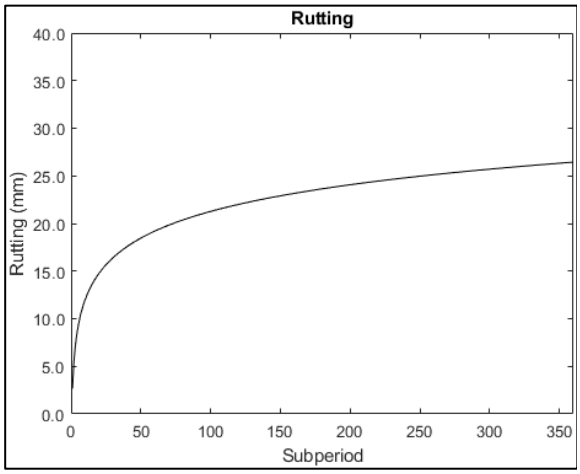

(b) Rut depth

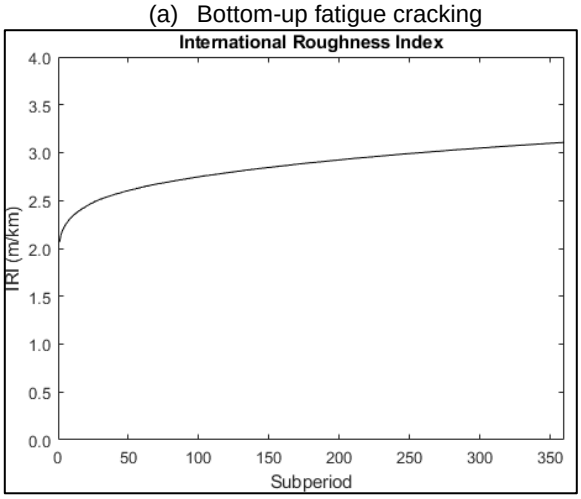

(c) IRI

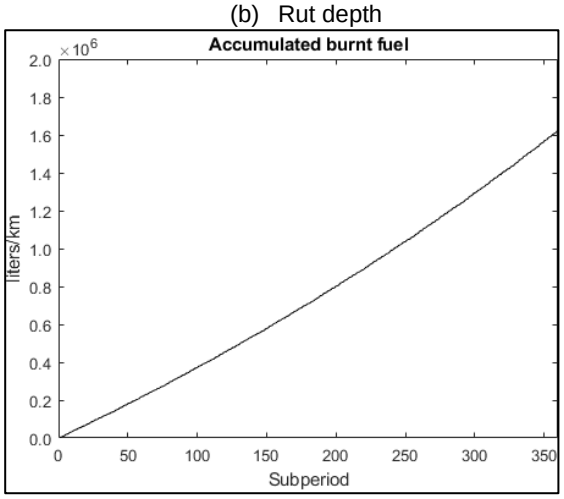

(d) Fuel consumption

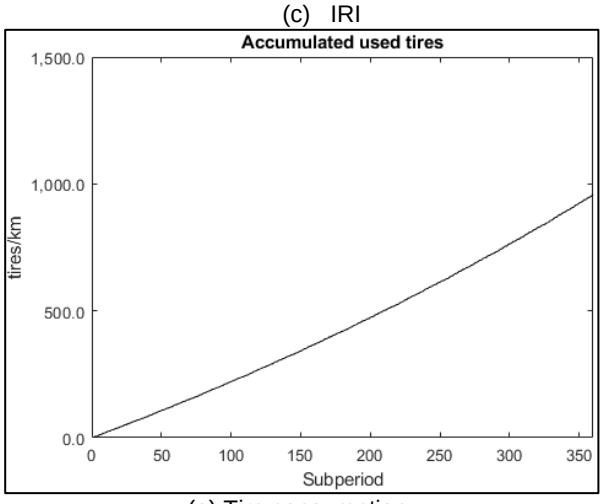

(e) Tire consumption

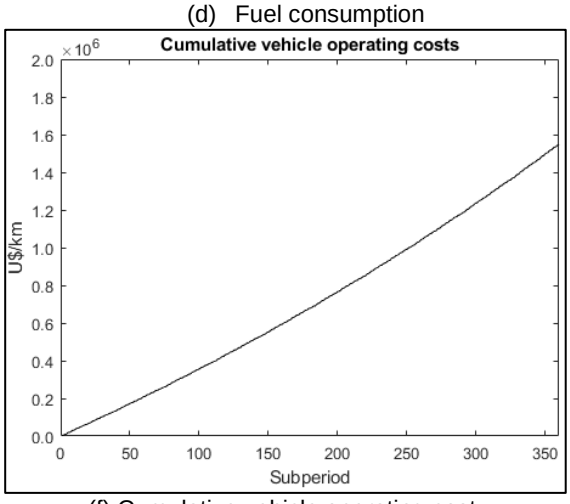

(f) Cumulative vehicle operating cost

The use of the MEPDG model for predicting the dynamic modulus of the asphalt mix, including the aging process, produces less damage than the Shell Oil model. The output

sensitivity to this parameter reinforces the need for proper materials characterization in applied cases.

5.4 The PSO-PAVE program

PSO-PAVE is an acronym for "Particle Swarm Optimization – Pavement design." The program uses the PSO metaheuristic to search for an optimum set of thicknesses according to the results of multiple calls of the UNPAVE program. The objective function seeks the minimum total costs based on construction and vehicle operating costs without any maintenance investment throughout the performance period.

The author developed several cases with PSO-PAVE to evaluate the optimization capabilities of the particle swarm optimization applied to incremental pavement design. All cases consider the same design example developed in the previous section to illustrate the capabilities of the UNPAVE program. In one case, the author considers an increased average daily traffic (ADT) to assess the program's sensibility to such change.

Table 5-22 summarizes the particle swarm optimization parameters. The inertia coefficient varies at each cycle. A PSO-PAVE run takes up to 45 hours for structures like the case study developed in the previous section.

Table 5-22: PSO parameters for pavement design optimization

Parameter	Value
Maximum number of iterations	15
Cognitive correction factor, C1	2.0
Social correction factor, C2	2.0
Maximum inertia coefficient	0.90
Minimum inertia coefficient	0.10
Number of agents	5

The PSO-PAVE program produces three graphics summarizing the optimization process results. The left graph shows the convergence of the fitness function, the central graph shows the thicknesses change throughout the optimization process, and the right graph shows the total or the cumulative vehicle operating costs (VOC) in US dollars per kilometer for a 7.2 meters wide road.

The total cost is the construction cost plus the vehicle operating cost throughout the performance period without maintenance costs. The unit costs per cubic meter are U$ 95.0 for hot-mix asphalt, U$ 31.0 for the untreated granular base, and U$ 30.0 for the untreated granular subbase.

5.4.1 PSO-PAVE Case 1

In this case, the fitness function seeks *the minimum total cost of the pavement*. Figure 5-15 shows that the algorithm converged in five cycles to the predefined minimum thicknesses for each layer in PSO-PAVE: 0.05 m of hot-mix asphalt, 0.10 meters of the granular base, and 0.10 meters of the granular subbase.

Figure 5-15. PSO-PAVE Case 1. Total cost minimization

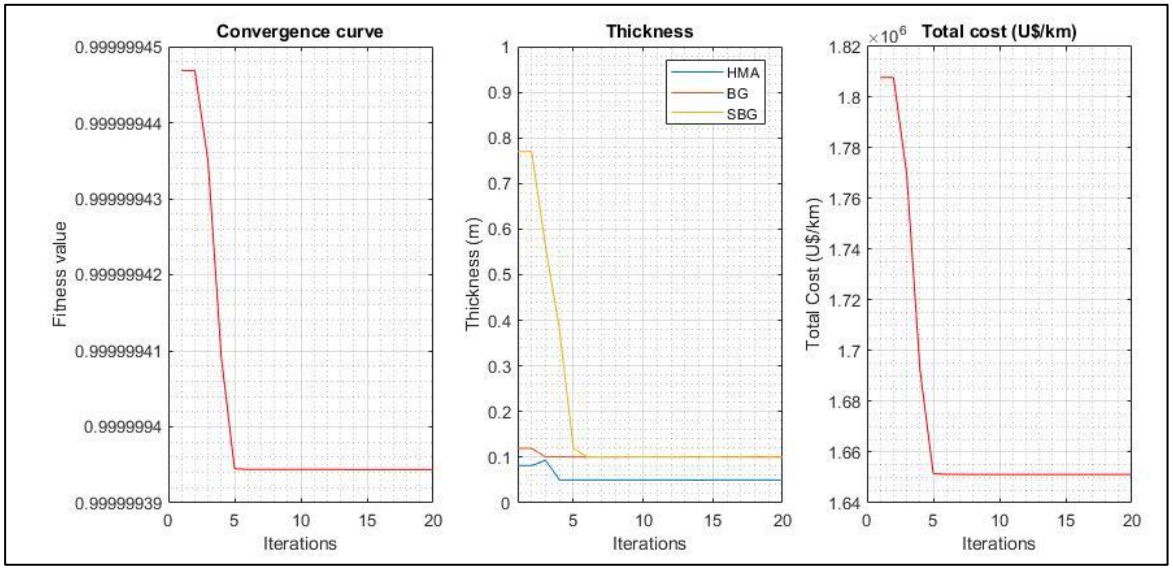

This solution satisfies the minimum total cost disregarding any concern about the pavement state at the end of the performance period. Figure 5-16 shows the damage (cracking and rutting), roughness, fuel and consumptions, and vehicle operating cost progression.

The cracked area adds up to 99.8% of the total lane area, the rut depth is 39.6 mm, and the IRI reaches a value of 3.69 m/km. The fuel and tire consumptions per kilometer are 1.647 million liters and 961 tires per kilometer. The cumulative vehicle operating cost is U$ 1.576 million, the construction cost is U$ 0.078 million per kilometer, and the total cost is

U$ 1.654 million per kilometer. *The structure is unacceptable* even though it satisfies the objective function of minimizing the total cost of the pavement.

Figure 5-16. PSO-PAVE Case 1. Performance of the structure

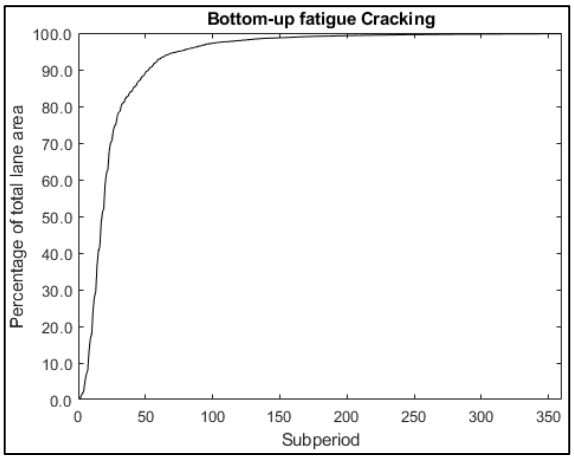

(e) Bottom-up fatigue cracking

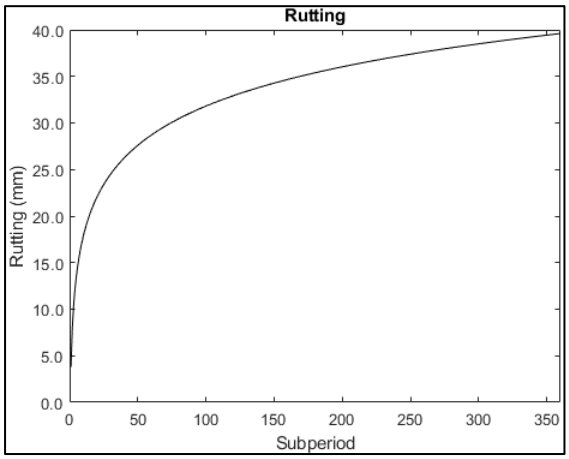

(f) Rut depth

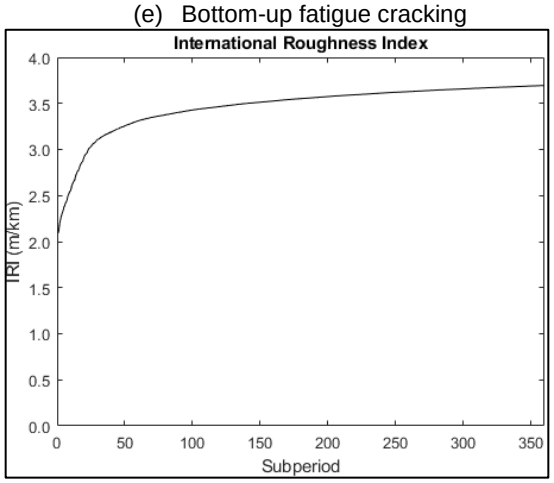

(g) IRI

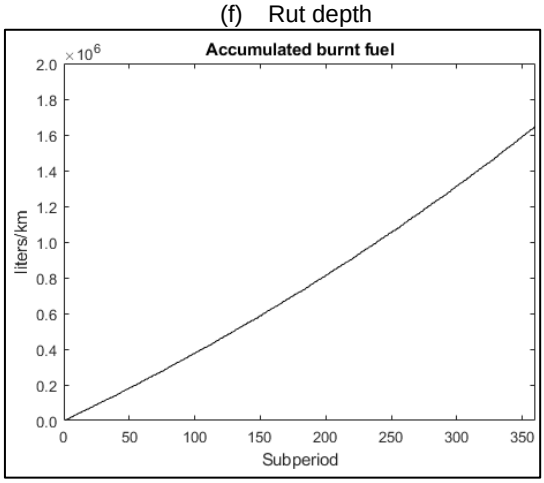

(h) Fuel consumption

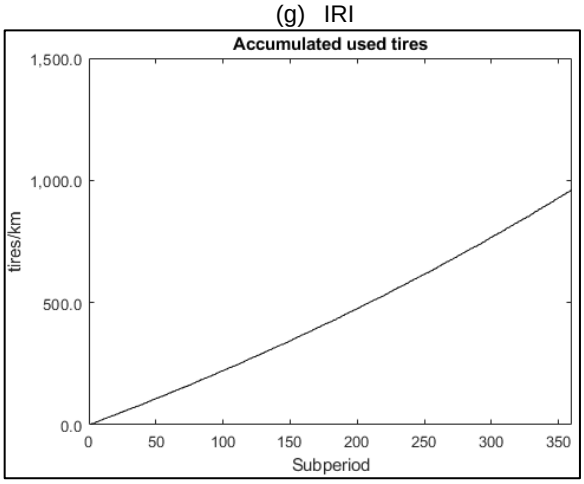

(e) Tire consumption

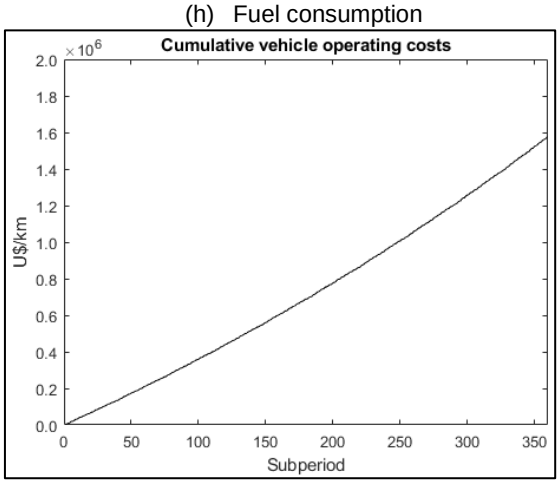

(f) Cumulative vehicle operating cost

5.4.2 PSO-PAVE Case 2

The minimum thickness of the untreated layers increases from 0.10 to 0.15 meters based on construction recommendations (INVÍAS, 2007), reducing the search space. Once again, PSO-PAVE identified the structure with minimum thicknesses as the optimum solution based on a total cost of U$ 1.661 million per kilometer. Figure 5-17 shows the optimization process in seven iterations.

Figure 5-17. PSO-PAVE Case 2. Total cost minimization

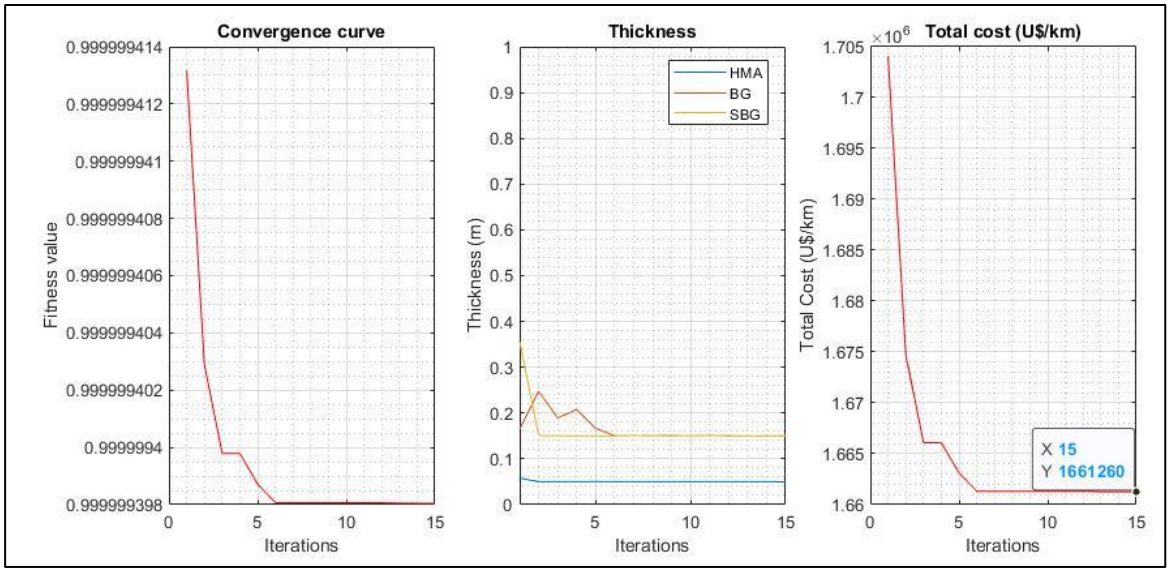

Figure 5-18 shows the damage, roughness, fuel and tire consumptions, and cumulative vehicular operating cost progression. As in Case 1, this solution satisfies the minimum total cost disregarding the pavement state at the end of the performance period.

The cracked area adds up to 98.7% of the total lane area, the rut depth is 33.8 mm, and the IRI reaches 3.50 m/km. The fuel and tire consumptions per kilometer are 1.638 million liters and 960 tires. The cumulative vehicle operating cost is U$ 1.561 million, the construction cost is U$ 0.100 million, and the total cost is U$ 1.661 million per kilometer.

The structure is unacceptable, although it satisfies the objective function of minimizing the total cost of the pavement; however, there were reductions compared to Case 1: -1.1% in total cracked lane area, -5.8 mm in total rutting, -0.19 m/km in IRI, -9,000 liters in fuel consumption per kilometer, and -1 tire used per kilometer.

Figure 5-18. PSO-PAVE Case 2. Performance of the structure

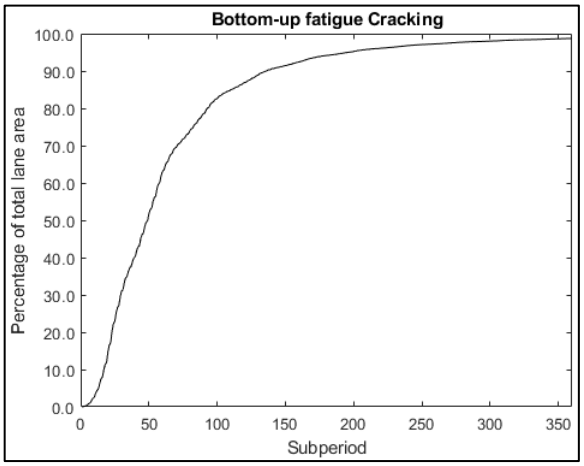

(a) Bottom-up fatigue cracking

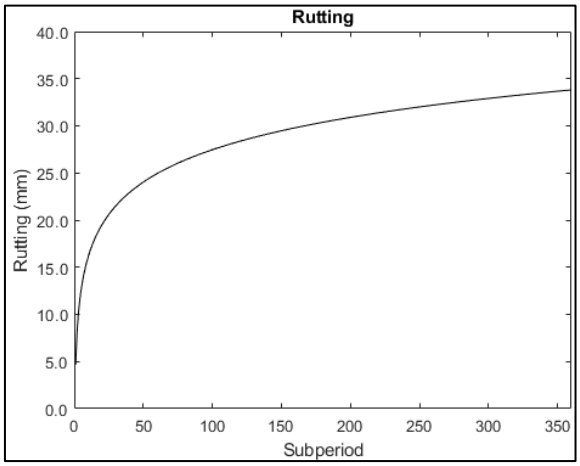

(b) Rut depth

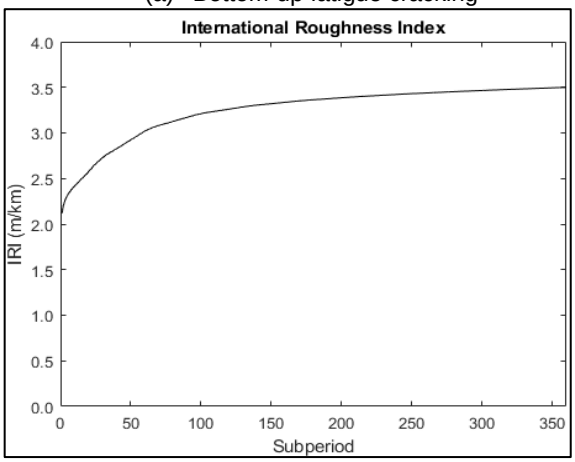

(c) IRI

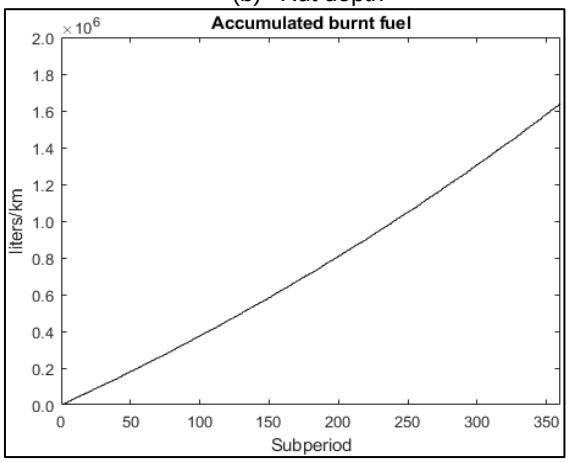

(d) Fuel consumption

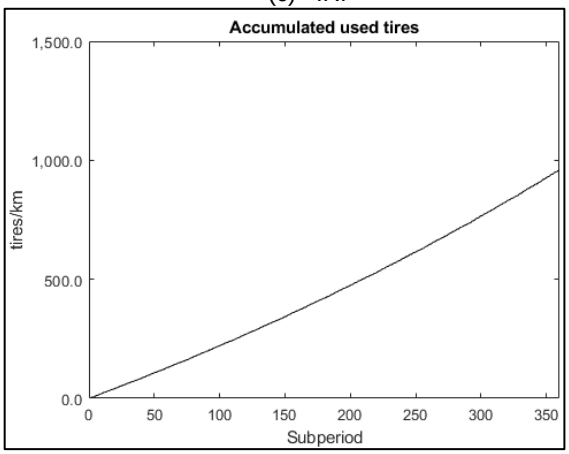

(e) Tire consumption

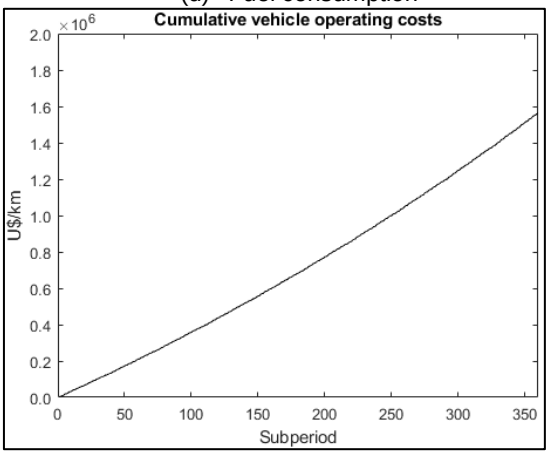

(f) Cumulative vehicle operating cost

5.4.3 PSO-PAVE Case 3

The objective function in Cases 1 and 2 minimized the total cost per kilometer. Both cases converged to pavements with the minimum thicknesses defined for each layer. The proposed structures developed significant damage, roughness, and fuel and tire consumption. Consequently, those structures have the highest vehicle operating costs. In Case 3, *the objective function minimizes the vehicle operating costs* instead of the total cost.

Figure 5-19 shows that the algorithm converged in eight cycles to the predefined maximum thicknesses for each layer: 0.30 meters of hot-mix asphalt, 0.30 meters of the untreated granular base, and 0.80 meters of the untreated granular subbase. The vehicle operating cost is U$ 1.536 million per kilometer plus the construction cost of U$ 0.445 million per kilometer. The total cost per kilometer is U$ 1.981 million.

Figure 5-19. PSO-PAVE Case 3. Vehicle operating costs minimization

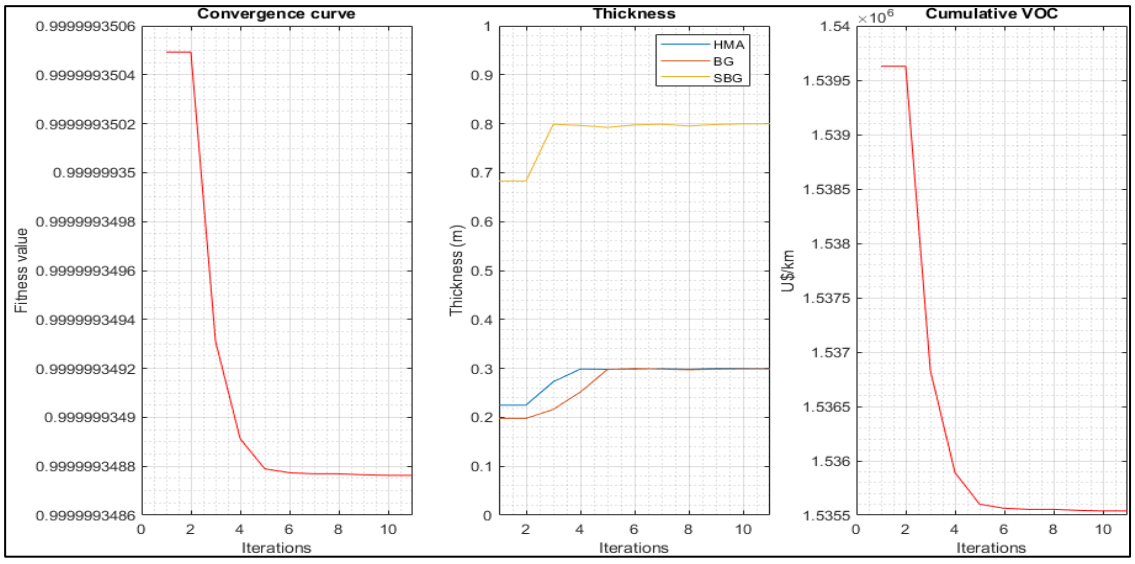

Case 3 satisfies the minimum vehicle operating cost with the maximum thicknesses. Figure 5-20 shows the damage, roughness, fuel and tire consumptions, and vehicle operating cost progression. The cracked area adds up to 4.15% of the total lane area, the rut depth is 17.3 mm, and the IRI reaches a value of 2.50 m/km. The fuel and tire consumptions per kilometer are 1.603 million liters and 955 tires.

Figure 5-20. PSO-PAVE Case 3. Performance of the structure

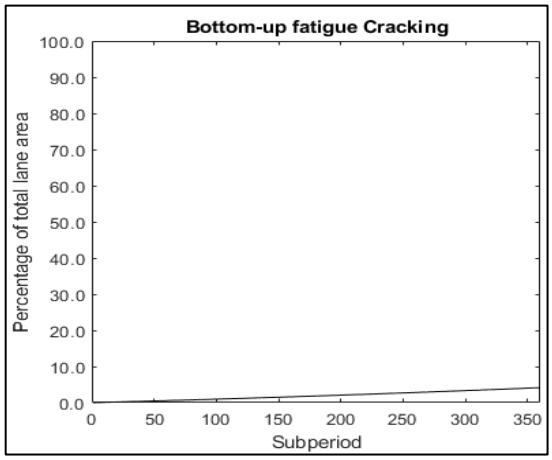

(a) Bottom-up fatigue cracking

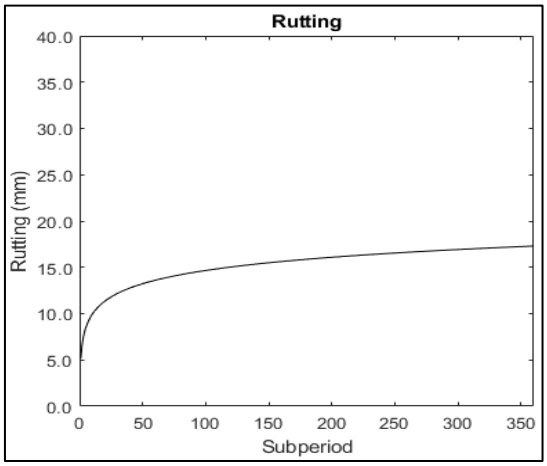

(b) Rut depth

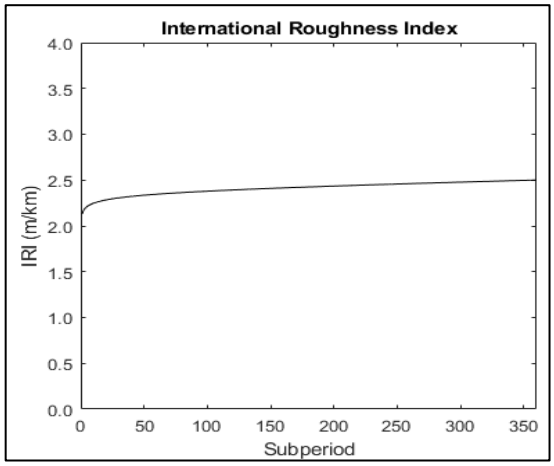

(c) IRI

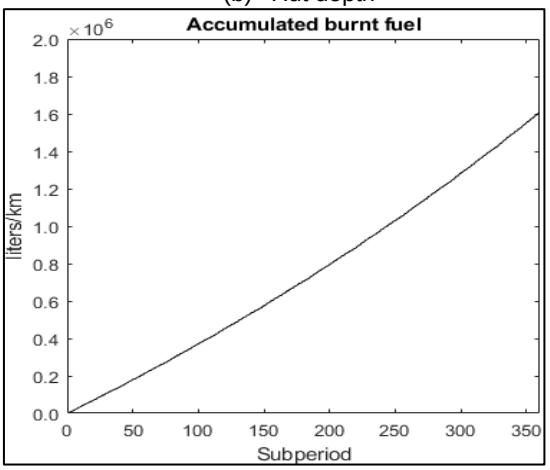

(d) Fuel consumption

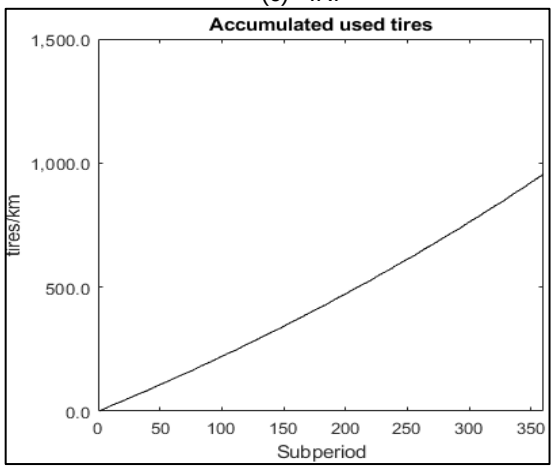

(e) Tire consumption

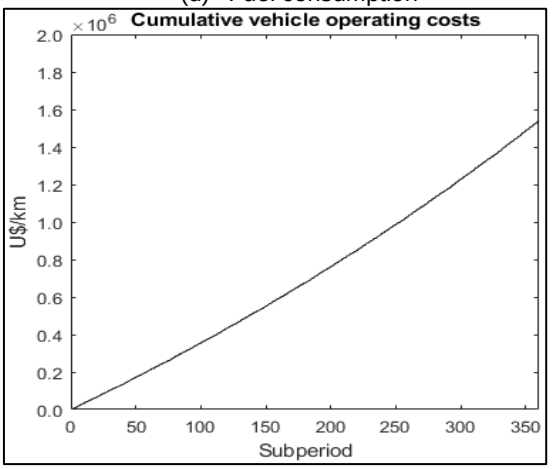

(f) Cumulative vehicle operating cost

The pavement performance is satisfactory for the ten-year design period with little cracked lane area and a minor roughness increment of 0.5 m/km. In contrast, the rut depth is still 4.6 millimeters greater than the 12.7 mm Asphalt Institute's threshold.

The algorithm reached the maximum predefined thicknesses to achieve the optimum solutions. Without such limits, it would increase the thicknesses without control beyond what could be considered a realistic alternative.

5.4.4 PSO-PAVE Case 4

Previous cases consider the same traffic, subgrade, and climate data. In Case 4, the average daily traffic increases from 1,786 to 5,000 vehicles to verify the model sensitivity to traffic conditions and if those conditions effectively change the optimized structure considering the increased vehicle operating costs.

The objective function minimizes the total cost considering that a greater traffic volume increases vehicle operating costs. Hence, the PSO algorithm should reduce those costs instead of converging to the minimum thicknesses like in Cases 1 and 2.

Figure 5-21 shows two independent swarms developed for Case 4. The algorithm converged after ten iterations in the first swarm and five in the second. In both swarms, the optimized structure comprises 0.05 meters of hot-mix asphalt, 0.30 meters of the granular base, and 0.15 meters of the granular subbase.

Figure 5-21. PSO-PAVE Case 4. Increased ADT. Total cost minimization

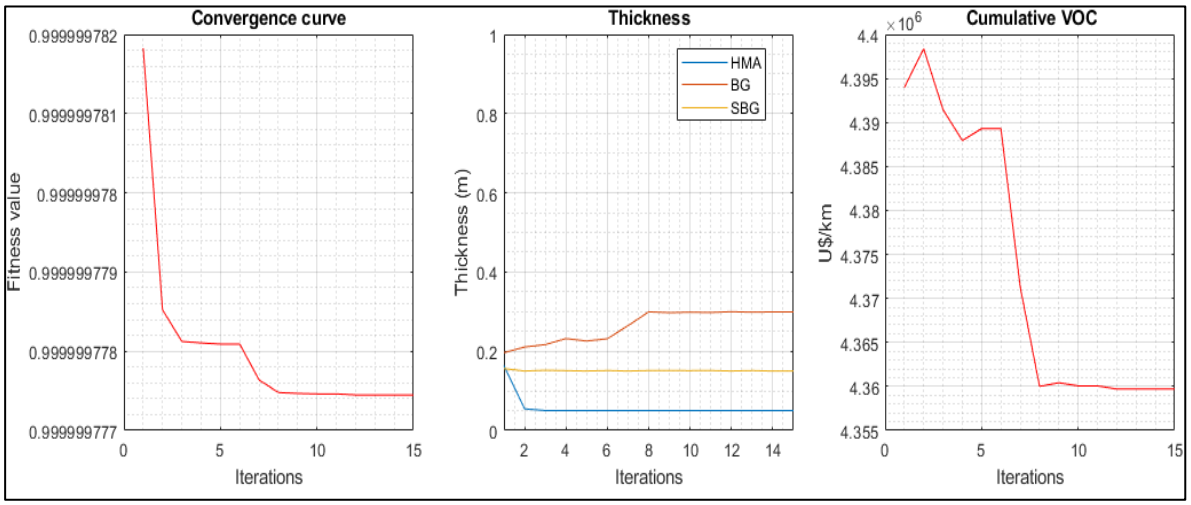

Figure 5-21. PSO-PAVE Case 4. Increased ADT. Total cost minimization (Cont.)

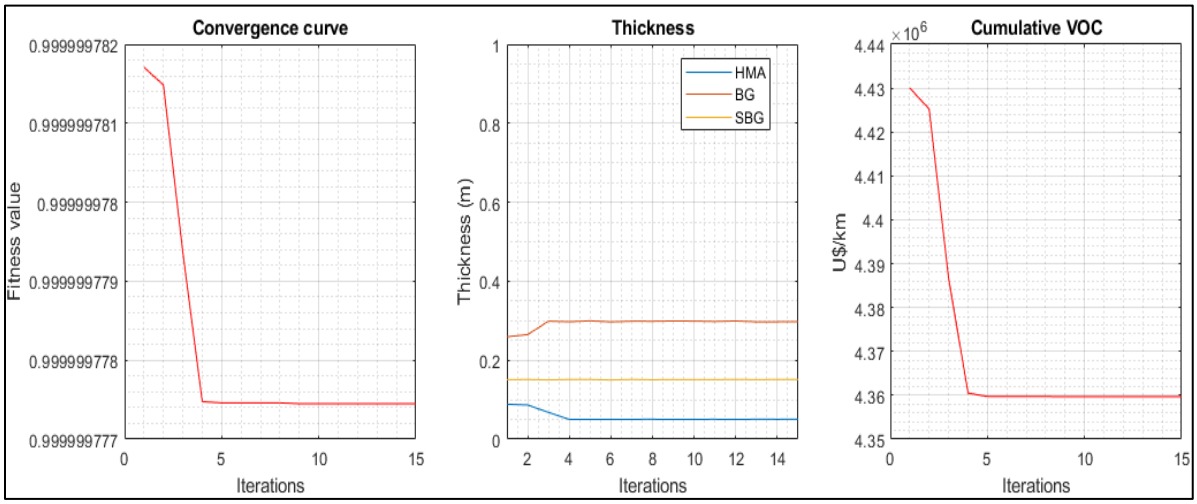

Figure 5-22 shows the performance of this structure. The cracked area adds up to 90.46% of the total lane area, the rut depth is 37.3 mm, and the IRI reaches 3.51 m/km. The cumulative fuel and tire consumptions per kilometer are 4.574 million liters and 2,684 tires. The cumulative vehicle operating cost is U$ 4.356 million, the construction cost is U$ 0.134 million, and the total cost is U$ 4.490 million per kilometer.

As in Cases 1 and 2, Case 4 satisfies the minimum cost, disregarding the pavement state at the end of the performance period. *The structure is unacceptable, although it fulfills the objective function*. Also, Case 4 shows the effect of a change in average daily traffic from 1,786 to 5,000 vehicles with increments in fuel and tire consumptions and cumulative vehicular operating cost. These results will not be considered in further comparisons with the case study.

Figure 5-22. PSO-PAVE Case 4. Performance of the structure

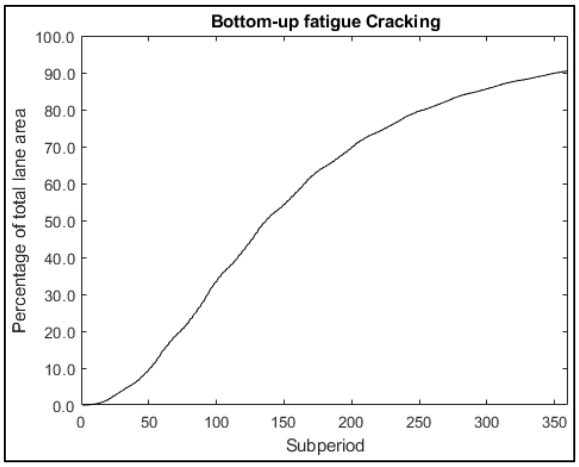

(a) Bottom-up fatigue cracking

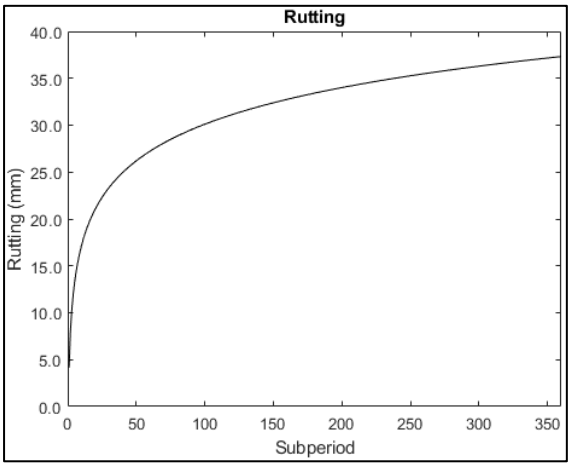

(b) Rut depth

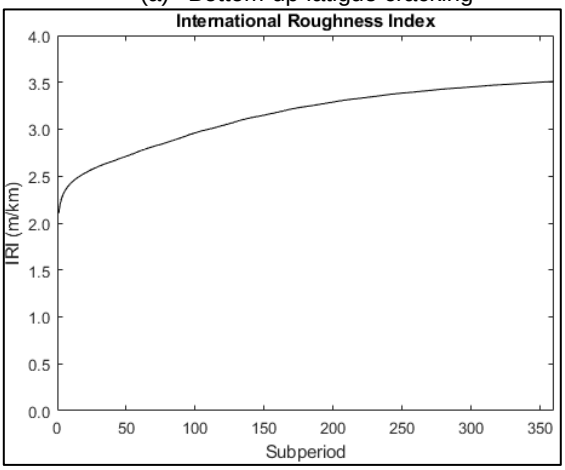

(c) IRI

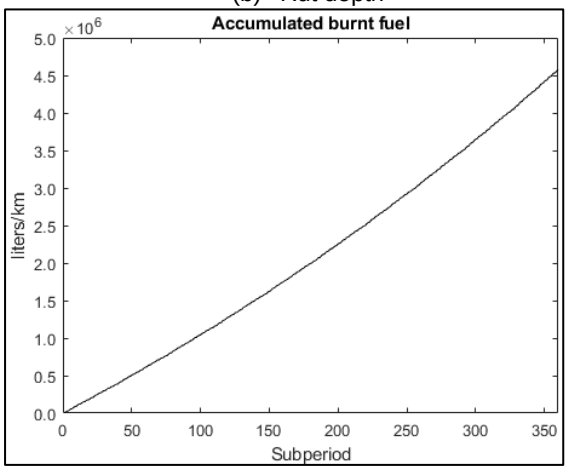

(d) Fuel consumption

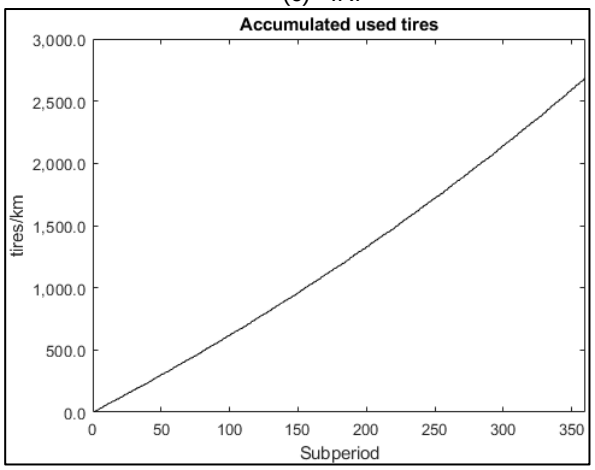

(e) Tire consumption

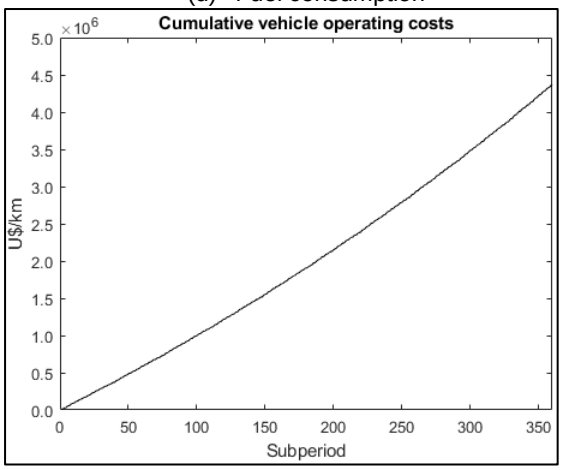

(f) Cumulative vehicle operating cost

5.4.5 PSO-PAVE Case 5

Previous results showed that minimizing construction and vehicle operating costs are opposite objective functions.

If the PSO-PAVE seeks the minimum total cost, it yields a thin structure, limited by minimum thicknesses, with significant damage and roughness, causing considerable vehicle operating costs. On the contrary, if the program seeks the minimum vehicle operating cost, it yields a thick structure, limited by maximum thicknesses, with a more substantial construction cost.

The author analyzed 24 trial structures in UNPAVE to assess the problem's sensitivity to changes in pavement thicknesses. Group G1 varies the hot-mix asphalt thickness, group G2 varies the untreated granular base thickness, and group G3 varies the untreated subbase thickness. Table 5-23 summarizes the results of damage, roughness, and vehicular operating and construction costs.

Table 5-23: Sensitivity analysis with UNPAVE

Trial	HMA (mm)	BG (mm)	SBG (mm)	Cracked area (%)	Rut depth (mm)	IRI (m/km)	VOC (U$/km)	Construction cost ($US/km)
G11	75	200	450	81.280	35.790	3.405	$1,554,000	$193,087
G12	100	200	450	86.240	36.940	3.483	$1,558,000	$210,077
G13	125	200	450	77.300	34.940	3.456	$1,556,000	$227,428
G14	150	200	450	65.400	31.670	3.307	$1,551,087	$244,440
G15	175	200	450	52.620	28.300	3.142	$1,547,000	$261,070
G21	125	150	450	83.510	35.700	3.518	$1,560,000	$215,777
G22	125	180	450	80.430	35.320	3.487	$1,558,000	$221,532
G23	125	230	450	74.190	34.550	3.423	$1,554,000	$233,397
G24	125	250	450	67.930	34.760	3.384	$1,553,000	$238,207
G25	125	280	450	63.900	34.350	3.342	$1,551,000	$244,215
G26	125	300	450	60.114	34.037	3.302	$1,549,810	$249,658
G31	125	250	250	82.320	34.080	3.472	$1,557,000	$195,766
G32	125	250	280	81.104	33.951	3.460	$1,556,820	$200,698
G33	125	250	300	77.542	34.875	3.459	$1,551,970	$210,466
G34	125	250	330	76.080	34.670	3.444	$1,556,000	$211,067
G35	125	250	350	74.701	34.510	3.430	$1,554,890	$216,900
G36	125	250	380	73.410	34.370	3.417	$1,554,000	$222,580
G37	125	250	400	70.442	35.090	3.413	$1,553,900	$227,703
G38	125	250	450	67.930	34.760	3.384	$1,553,000	$238,207
G39	125	250	550	62.645	34.856	3.339	$1,550,990	$260,096
G310	125	250	600	60.260	35.090	3.321	$1,550,000	$271,307

Figure 5-23 shows the vehicle operating cost versus construction cost graph results. Also, it includes the results of Cases 1, 2, and 3 for comparison, identified as *"CX-65,"* indicating

the use of a 65/10 mm recovered bitumen penetration. A MATLAB script (Granada Echeverri, 2009) identifies structure G11 as the non-dominated solution.

Figure 5-23. VOC and construction cost of 24 trial structures and Cases 1 to 3

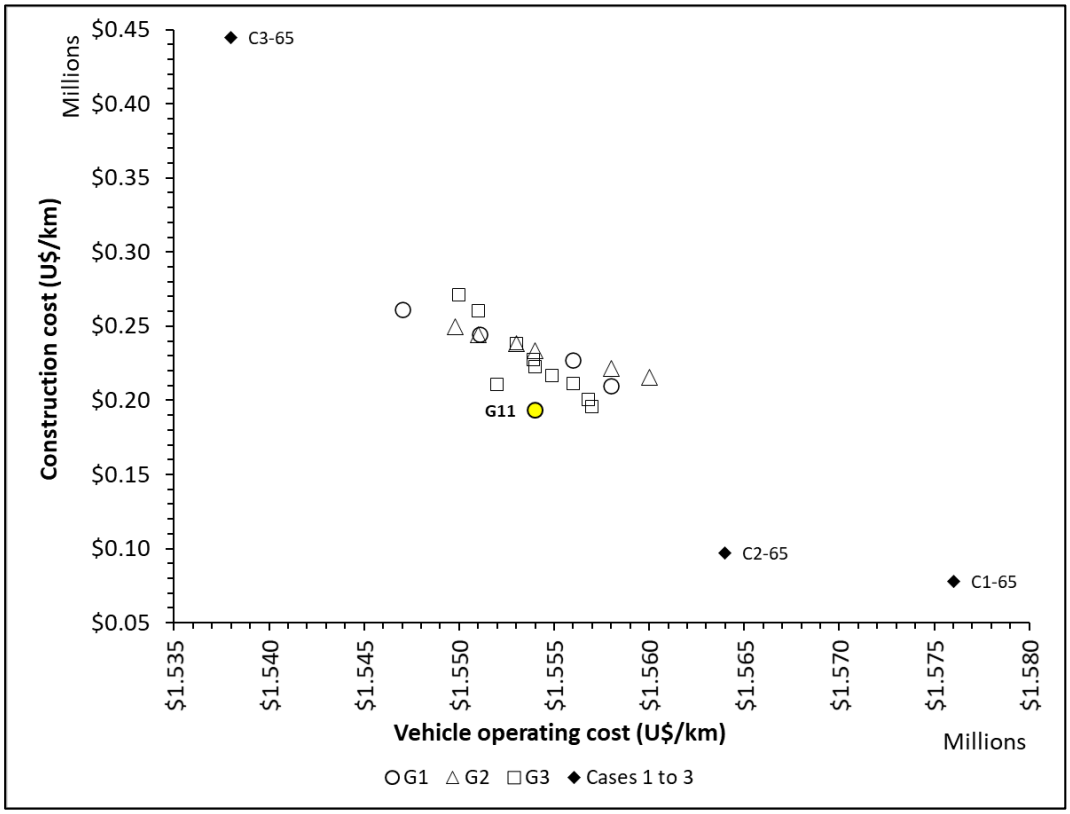

The three groups of structures fall in a narrow band in the mid-section of the graph. That is, pavements with a wide range of thicknesses behave similarly in terms of vehicle operating and construction costs for the conditions of the problem.

Based on Figure 5-23, the author proposes the following alternative objective function:

$$RC = \sqrt{CC^2 + VOC^2}$$

Eq. 5-40

Where RC is the Resultant Cost, CC is the Construction Cost, and VOC is the Vehicle Operating Cost.

A modified version of PSO-PAVE minimizes the resultant cost (RC). Figure 5-24 shows that the algorithm converged to the minimum thicknesses of 0.15 meters for both untreated layers and 0.25 meters for the hot-mix asphalt after 12 iterations.

Figure 5-24. PSO-PAVE Case 5. Resultant cost minimization

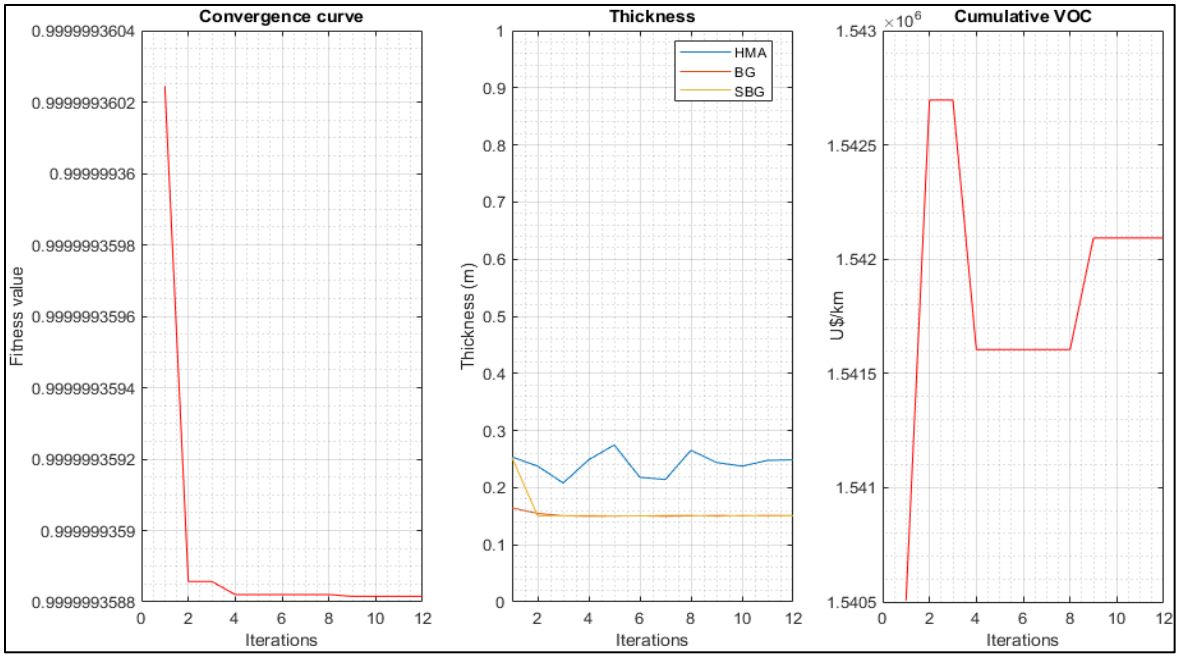

Figure 5-25 shows the damage, roughness, fuel and tire consumptions, and vehicle operating cost progression. The cracked area adds up to 49.17% of the total lane area, the rut depth is 19.89 mm, the IRI reaches 2.91 m/km, and the cumulative fuel and tire consumptions per kilometer are 1.612 million liters and 955 tires.

The cumulative vehicle operating cost is U$ 1.542 million, and the construction and total costs are U$ 0.237 million and U$ 1.779 million, respectively.

Figure 5-25. PSO-PAVE Case 5. Performance of the structure

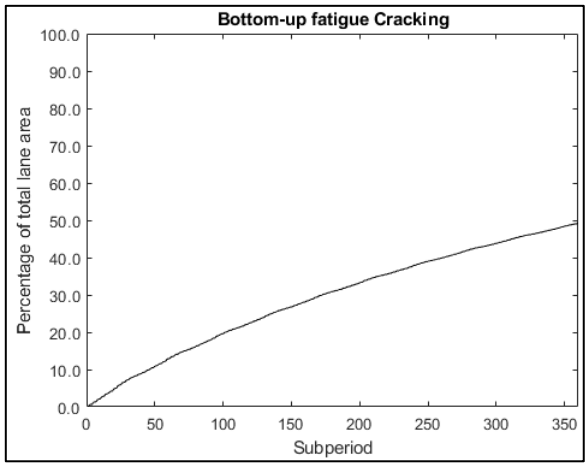

(a) Bottom-up fatigue cracking

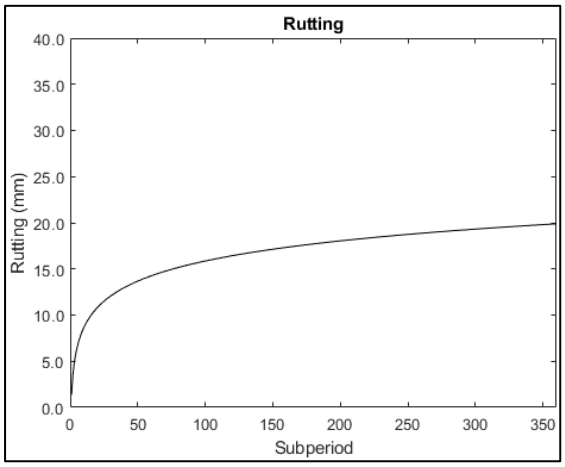

(b) Rut depth

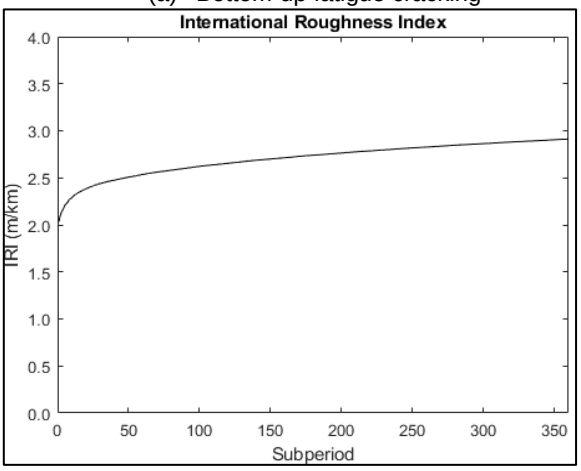

(c) IRI

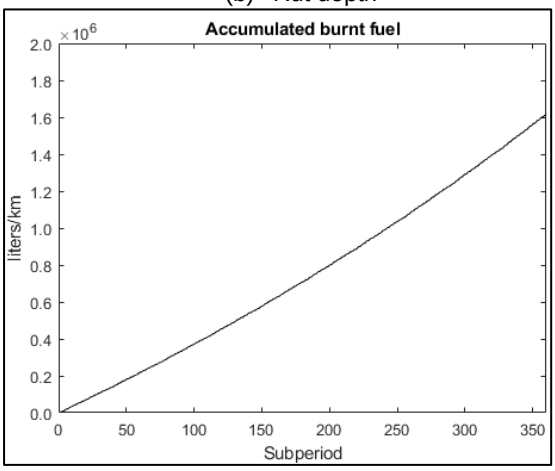

(d) Fuel consumption

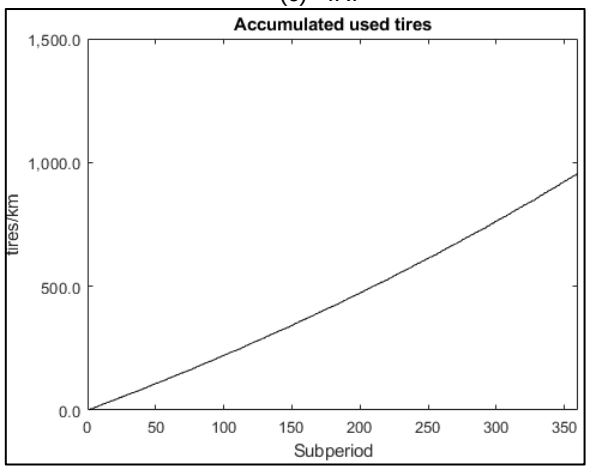

(e) Tire consumption

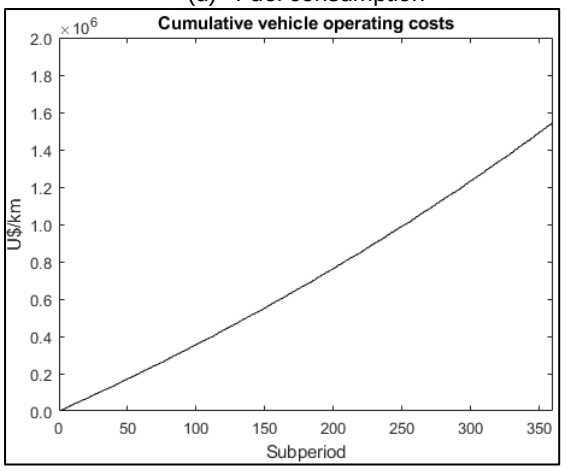

(f) Cumulative vehicle operating cost

5.4.6 PSO-PAVE Case 6

Figure 5-26 shows another solution minimizing the resultant cost (RC) after five iterations. The solution converged to 0.05 meters of hot-mix asphalt, 0.30 meters of the untreated granular base, and 0.15 meters of the untreated granular subbase.

Figure 5-26. PSO-PAVE Case 6. Resultant cost minimization.

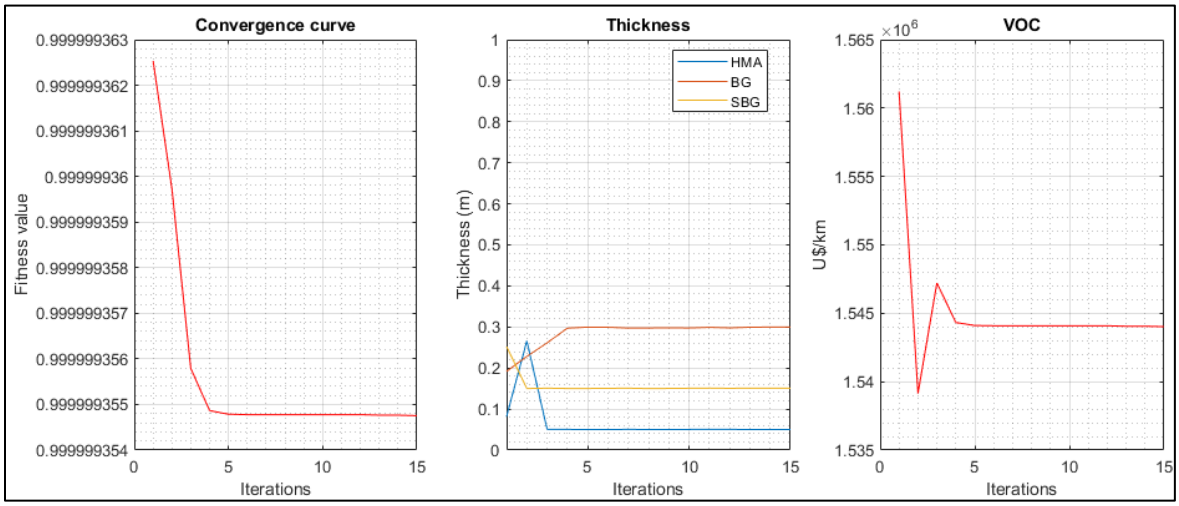

The resultant cost (RC) criterion appears to correct the tendency to select the minimum thicknesses. However, avoiding thin hot-mix asphalt layers requires specific code restrictions. Figure 5-27 shows the damage, roughness, fuel and tire consumption, and vehicle operating cost progression.

The cracked area adds up to 59.34% of the total lane area, the rut depth is 29.67 mm, the IRI reaches 3.12 m/km, and the cumulative consumptions per kilometer of fuel and tires are 1.620 million liters and 954 tires, respectively. The cumulative vehicle operating cost is U$ 1.545 million. The construction and total costs are U$ 0.134 million and U$ 1.681 million, respectively.

The structure is unacceptable, although it achieves the objective function of minimizing the resultant cost of the pavement with reductions in damage compared to Cases 1 and 2.

Figure 5-27. PSO-PAVE Case 6. Performance of the structure

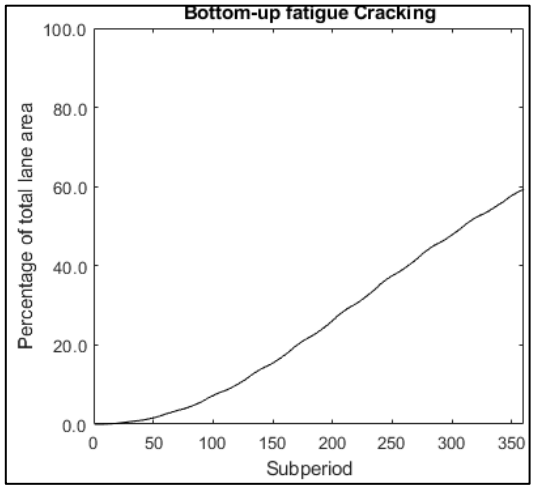

(a) Bottom-up fatigue cracking

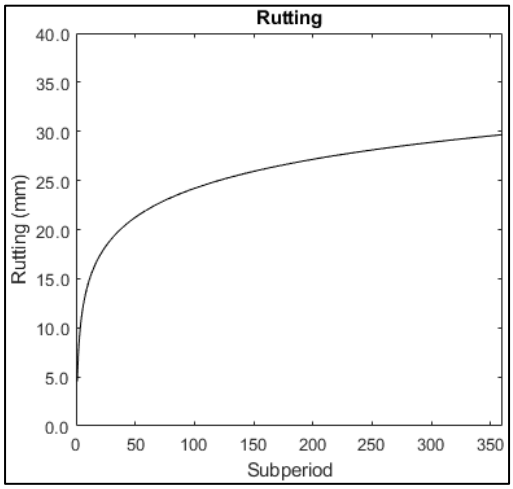

(b) Rut depth

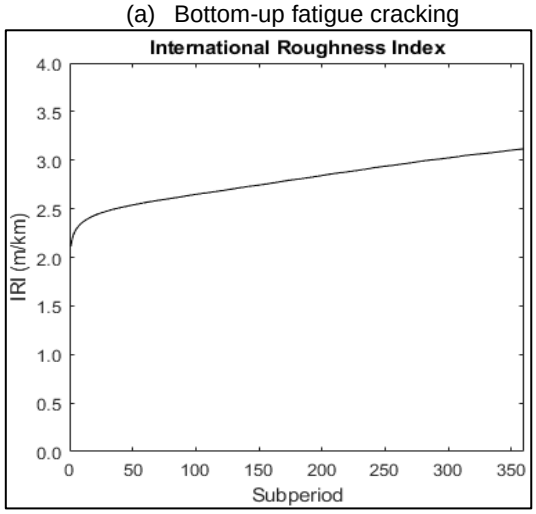

(c) IRI

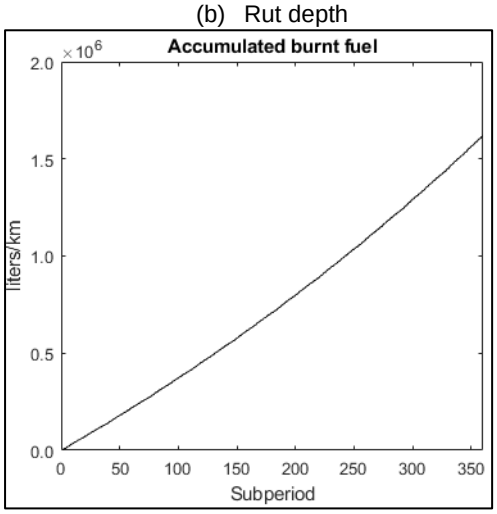

(d) Fuel consumption

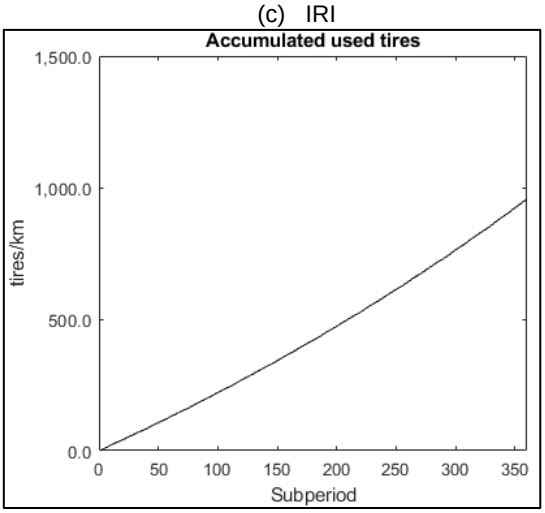

(e) Tire consumption

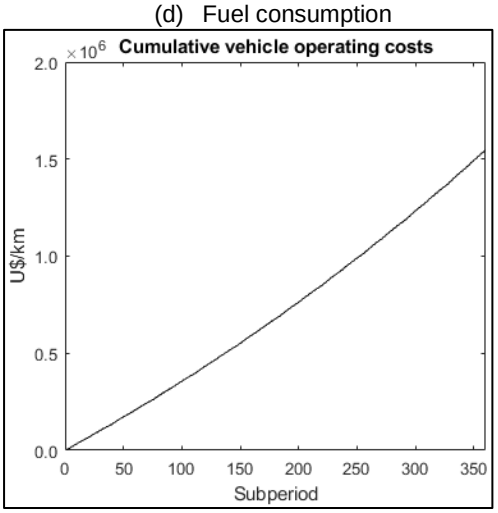

(f) Cumulative vehicle operating cost

5.4.7 PSO-PAVE Case 7

Case 7 focuses on the issue of thin hot-mix asphalt layers. A modified PSO-UNLEA code considers new thickness ranges: hot-mix asphalt from 0.10 to 0.30 meters, granular base from 0.15 to 0.30 meters, and granular subbase from 0.30 to 0.80 meters. Also, the program restricts the granular base from being thicker than the granular subbase.

Figure 5-28 shows that the PSO converged in ten iterations to 0.225 meters of hot-mix asphalt, 0.15 meters of the untreated granular base, and 0.30 meters of the untreated granular subbase.

Figure 5-28. PSO-PAVE Case 7. Resultant cost minimization.

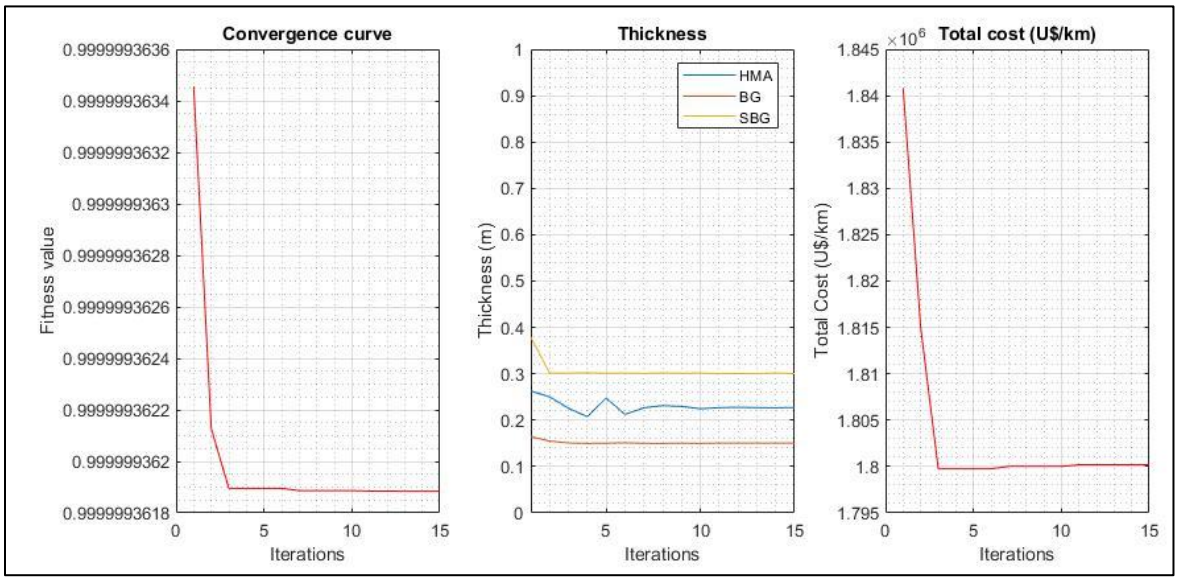

Figure 5-29 shows the damage, roughness, fuel and tire consumption, and vehicle operating cost progression. The cracked area adds up to 47.85% of the total lane area, the rut depth is 24.01 mm, the IRI reaches 3.01 m/km, and the fuel and tire consumptions are 1.619 million liters and 954 tires, respectively.

The cumulative vehicle operating cost is U$ 1.547 million, the construction cost is U$ 0.252 million, and the total cost is U$ 1.799 million per kilometer.

Figure 5-29. PSO-PAVE Case 7. Performance of the structure

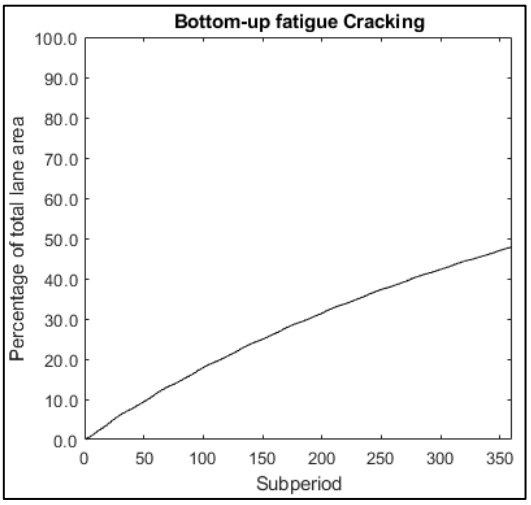

(e) Bottom-up fatigue cracking

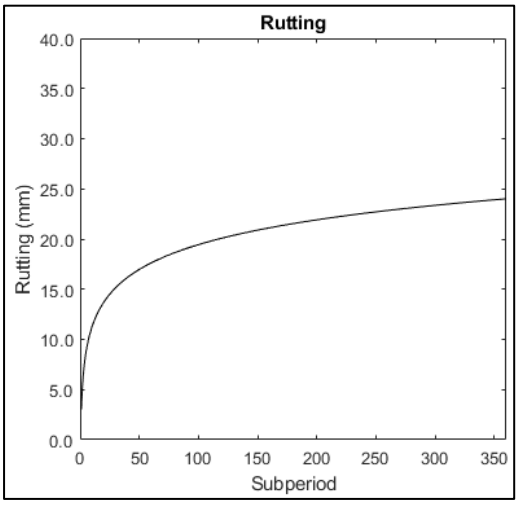

(f) Rut depth

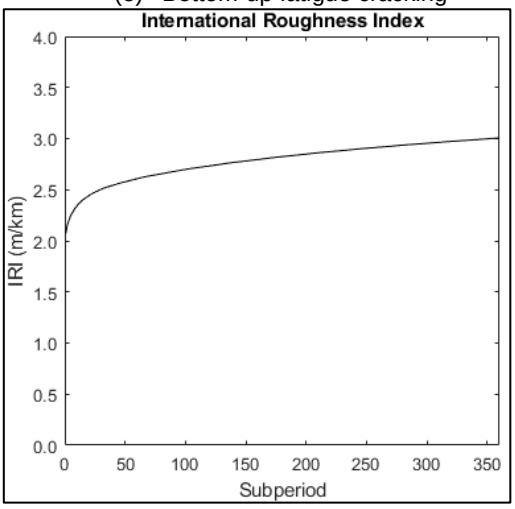

(g) IRI

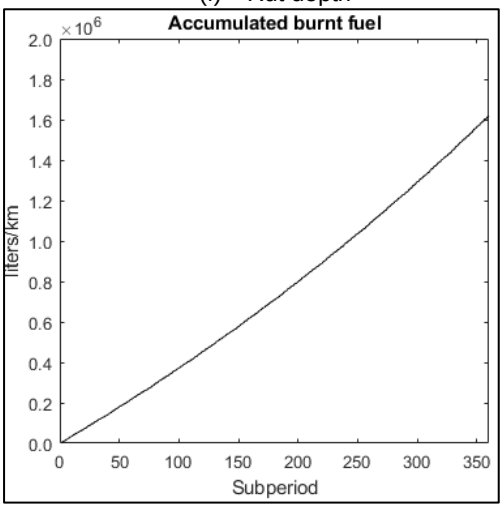

(h) Fuel consumption

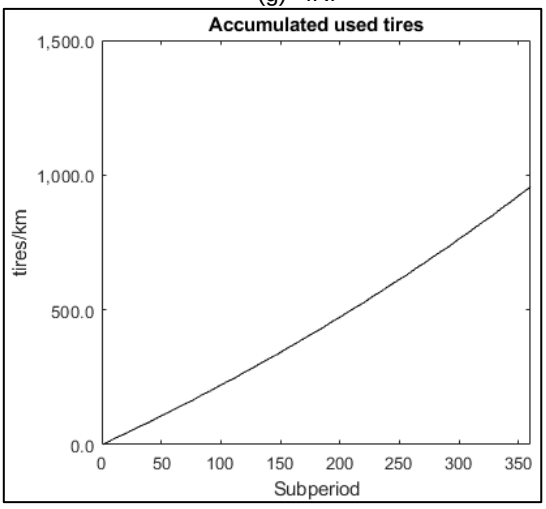

(e) Tire consumption

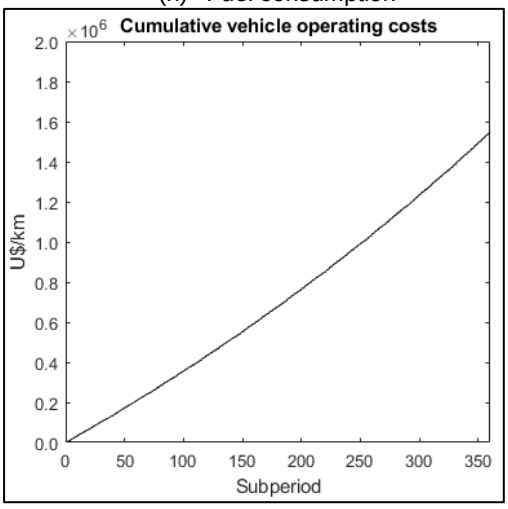

(f) Cumulative vehicle operating cost

5.4.8 Case comparisons

Figure 5-30 shows the cases evaluated in the previous paragraphs. After redefining the objective function to minimize the resultant cost (RC), Case 6 became the best solution despite its significant values of accumulated damage. The author would favor Cases 5 or 7 as solutions after redefining the minimum thickness for hot-mix asphalt to 0.10 meters.

Figure 5-30. PSO-PAVE cases compared with thickness-sensitivity groups

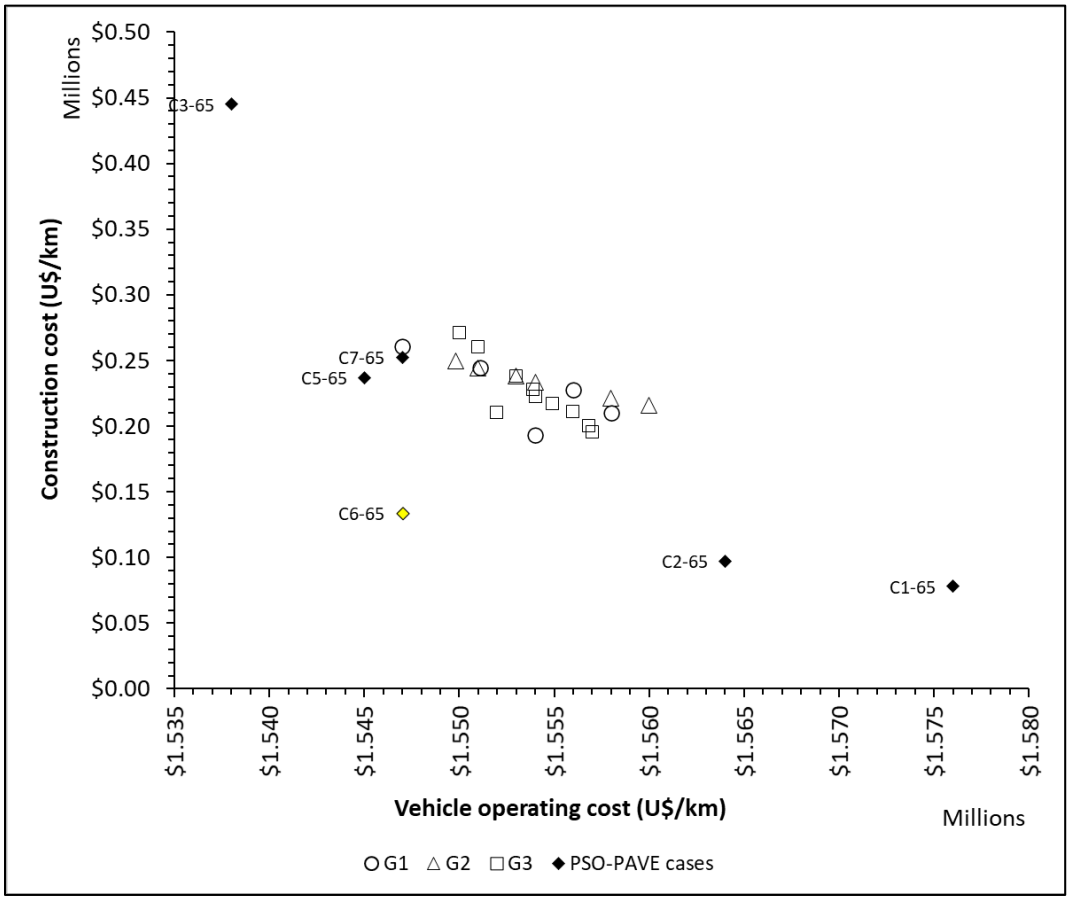

Figure 5-31 shows contour graphics with the sensitivity of cracking and rutting in the proposed structures. The damage reduces toward the left-upper corner of the graphs for higher construction costs and lower vehicle operating costs. From the graphs, it is possible to achieve the Asphalt Institute's 10% cracked area limit; in contrast, the 12.5 mm rutting threshold is outside the search space of the current case study.

Figure 5-31. Damages contours for PSO-PAVE Cases 1 to 7 and Groups 1 to 3

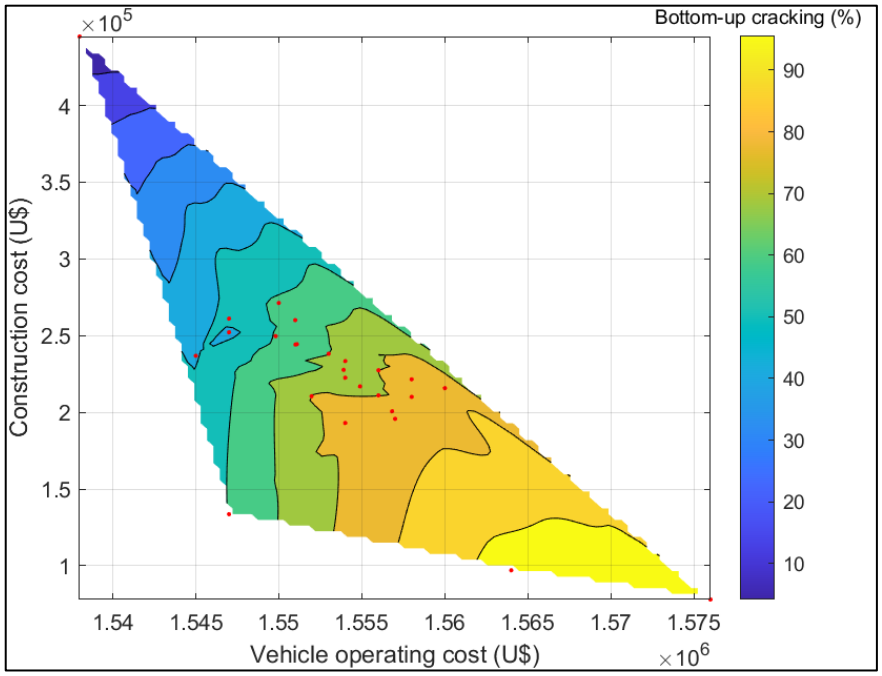

(a) Bottom-up fatigue cracking

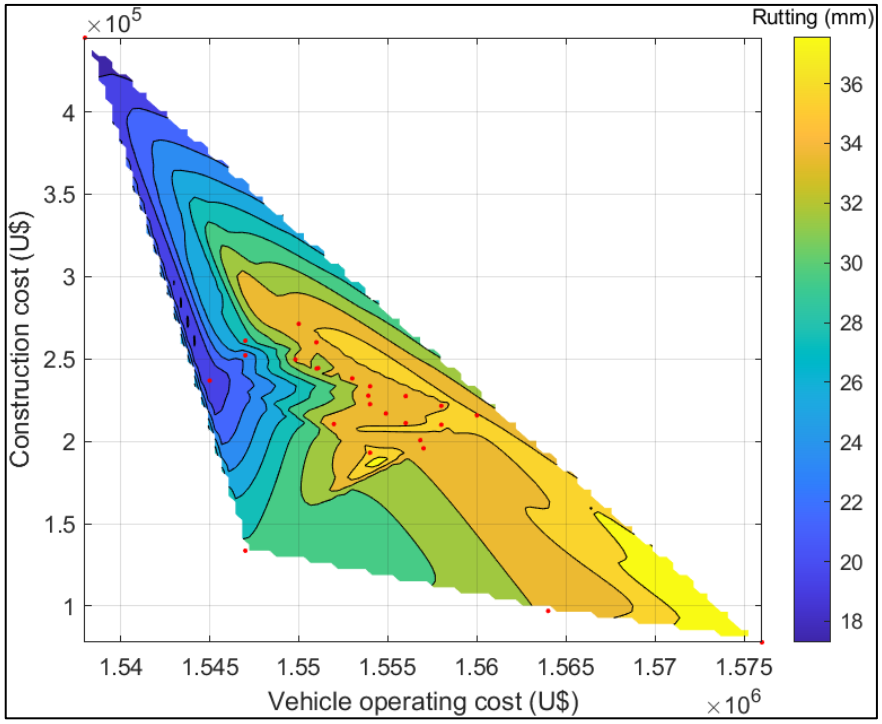

(b) Rut depth

5.4.9 Additional analysis of the optimization process

In this section, the author explores two variations to the previous cases considering a climate-base bitumen modification and the analysis of the case study with traditional pavement design procedures.

5.4.9.1 Modification of the hot-mix asphalt properties

All previous cases show a significant amount of rutting beyond the 12.5 mm threshold defined by the Asphalt Institute. One must remember that the Shell equation for estimating the HMA moduli uses the penetration of recovered bitumen (Huang, 2004); hence a 65/10 mm value may correspond to a 120-150 penetration grade bitumen. According to the climate information for the case study, a better choice would be a 60-70 penetration bitumen with a recovered penetration between 40/10 to 45/10 mm.

The author ran the UNPAVE program to analyze Cases 1 to 7 (except Case 4) with a recovered penetration of 43/10 mm. Figure 5-32 shows a variable reduction in the vehicle operating costs due to the use of the stiffer bitumen. The construction costs are unaffected because the hot-mix asphalt unit price does not change. Case 6 remains the non-dominated solution despite its shortcomings.

5.4.9.2 Comparison with the AASHTO 1993 procedure

1. Traffic projection: The author uses the historical records from 1999 to 2018 at the *"444 La Esperanza – Petaqueros"* station to compute the cumulative equivalent single axle loads.

The traffic projection model for W_{18} is:

$$W_{18i} = 10^{[5.3735+0.0087\cdot(Year-1998)]}$$

Eq. 5-41

Where W_{18i} is the projected ESAL in the design lane for any future year. The standard error of the model (S_w) is 0.0369, which is necessary for the AASHTO design algorithm. A 10-year projection with a 50% reliability yields an accumulated value of 4,183,823 equivalent single axle loads of 18 kips.

Figure 5-32. Comparison between 65-pen and 43-pen bitumen

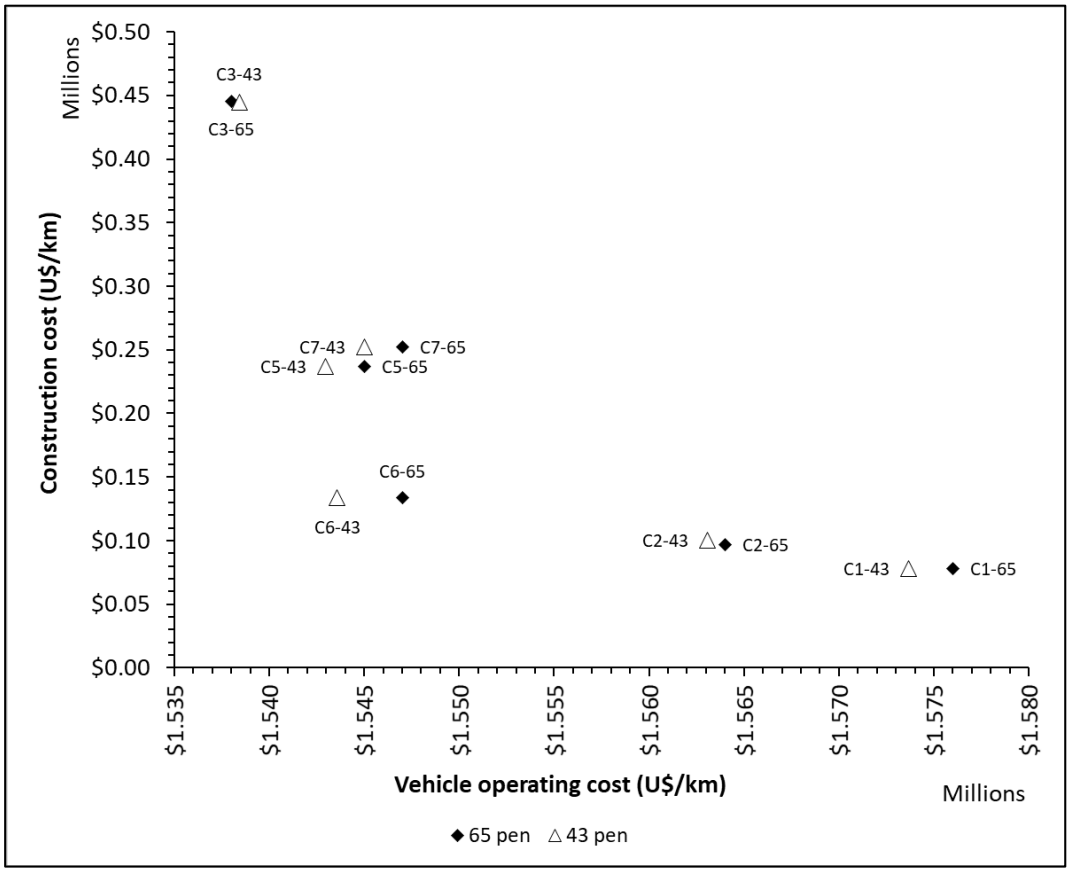

2. Subgrade: The case study considers an average subgrade modulus of 50 MPa (7,252 psi).

3. Reliability: The design considers four reliability levels: 50%, 85%, 95%, and 99%. The standard deviation of performance (S_N) is 0.44, as calibrated in the AASHO Road Test. The overall strander deviation (S_o) is 0.442.

4. Change in the present serviceability index (PSI): The initial PSI is 4.2, and the final PSI is 2.5.

5. Drainage coefficients: The drainage coefficients of the untreated layers (base and subbase) are 1.0.

6. Material properties: The hot-mix asphalt has a modulus of 435,000 psi (a1 = 0.44). The untreated materials moduli consider a simplified non-linear k-θ model for *"wet conditions"* (k1 = 5,000 psi, k2 = 0.6), included in the AASHTO method.

7. Pavement design: Table 5-24 summarizes the designs for the proposed reliability levels.

Table 5-24: Alternative designs for the case study with the AASHTO 1993 procedure

Reliability (%)	Hot-mix asphalt (m)	Granular base (m)	E (psi)	a2	Granular subbase (m)	E (psi)	a3
50	0.152	0.152	18,659	0.086	0.152	11,180	0.080
85	0.203	0.152	13,133	0.060	0.152	11,180	0.080
95	0.229	0.152	13,133	0.060	0.152	11,180	0.080
99	0.254	0.152	13,133	0.060	0.152	11,180	0.080

These structures are analyzed with the UNPAVE program, disregarding the assumed moduli in the AASHTO method. Table 5-25 summarizes the results of each incremental design:

Table 5-25: Damage, roughness, and costs of the AASHTO 1993 alternatives

Structure	Total cracked area (%)	Rut depth (mm)	Final IRI (m/km)	VOC (U$/km)	Construction cost (U$/km)
AA-50	87.715	28.29	3.364	$1,558,240	$170,726
AA-85	64.205	22.50	3.072	$1,548,310	$205,610
AA-95	49.618	20.06	2.919	$1,544,940	$223,394
AA-99	36.635	18.08	2.787	$1,542,620	$240,494

5.4.9.3 Comparison with the Asphalt Institute (AI) 1982 procedure

1. Traffic projection: In this method, it is appropriate to use the same value obtained in the AASHTO procedure: 4,183,823 equivalent single axle loads of 18 kips (80 kN).

2. Subgrade design modulus: The subgrade design modulus is the 87.5 percentile of any set of values for the given traffic. In the case study, monthly factors represent modulus variability throughout the year. The design value is 40.56 MPa.

3. Climate conditions: The method considers a series of charts for three different mean average air temperature values. The case study corresponds to the charts for a MAAT of 15.5°C.

4. Pavement design: For the traffic, subgrade, and climate conditions described above, three designs are proposed for the case study:

Table 5-26: Alternative designs for the case study with the AI 1982 procedure

Structure	Hot-mix asphalt (m)	Untreated aggregate base (m)	Design Chart
AI-150	0.300	0.150	A-7
AA-300	0.265	0.300	A-11
AI-based	0.350	0.300	None

The author analyzes two AI structures, plus an additional one with increased hot-mix asphalt thickness, disregarding the assumed moduli of the AI procedure. Table 5-27 summarizes the results of each incremental analysis in the UNPAVE program.

Table 5-27: Damage, roughness, and costs of the AI 1982 alternatives

Structure	Total cracked area (%)	Rut depth (mm)	Final IRI (m/km)	VOC (U$/km)	Construction cost (U$/km)
AI-150	24.412	17.767	2.700	$1,536,960	$238,104
AI-300	31.859	17.341	2.738	$1,541,850	$247,140
AI-based	9.149	12.769	2.453	$1,537,940	$305,280

Figure 5-33 shows the position of these structures in the VOC versus the CC plane. Cases C1, C2, and C6 are removed from the analysis due to their thin hot-mix asphalt and higher cracking and rutting damage.

In AASHTO designs, the increasing reliability moves the results toward the left side of the graph, reducing vehicle operating costs and construction costs. The pavement with 99% reliability (AA-99) equals Case 5 with 43/10 mm penetration bitumen and Asphalt Institute design with 300 mm untreated aggregate base (AI-300).

The Asphalt Institute design with 150 mm of untreated aggregate base (AI-150) is the non-dominated solution; therefore, it would be the recommended structure. The cracking and rutting of AI-150 are 24.41% and 17.77 mm, respectively. These values are more significant than the method's thresholds of 20% and 12.5 mm because the traffic and materials characteristics in the UNPAVE analysis are not equal to those in the Asphalt Institute's charts.

Figure 5-33. Comparison Cases 3, 5, and 7 with traditional designs

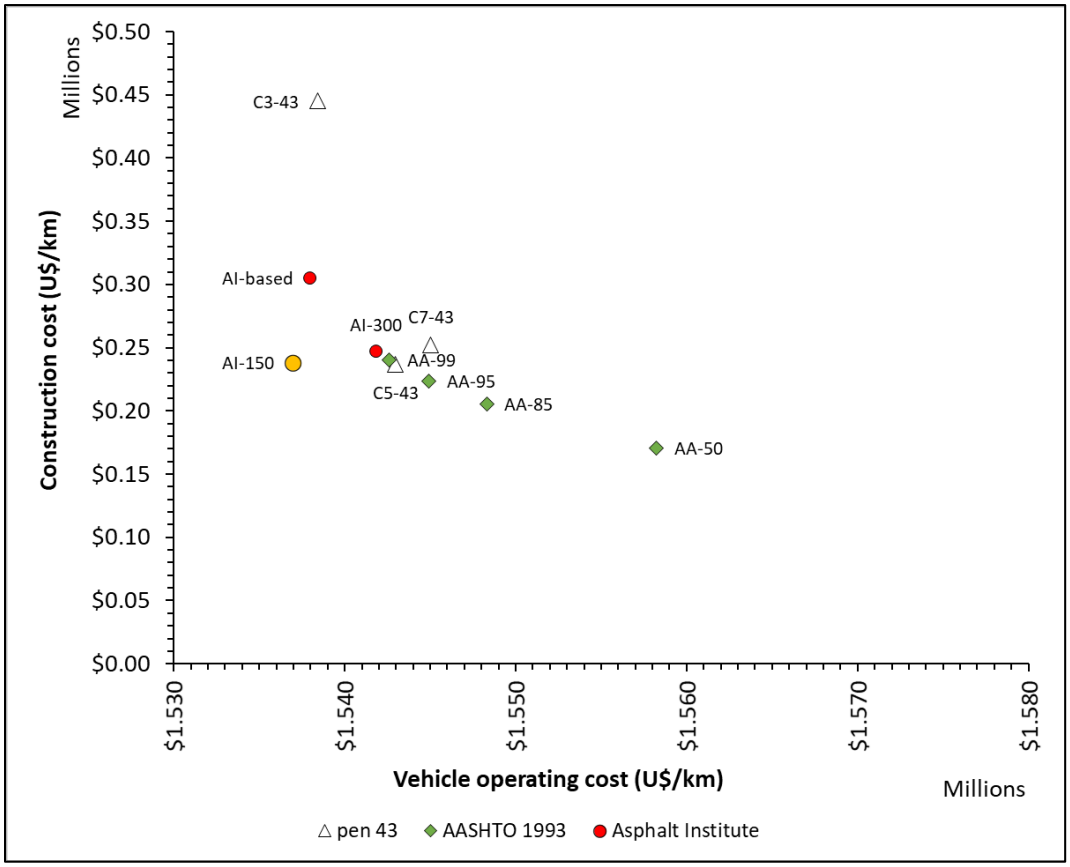

The structure denoted as *"AI-based"* reaches 9.15% of total area cracking and 12.77 mm of rutting, satisfying the AI performance thresholds. However, this structure does not dominate the AI-150 solution regarding the resultant cost.

5.4.9.4 Review of the AI-based structure with the MEPDG |E*| model and climate

All the preceding analyses were based on the Shell Oil model to estimate the dynamic modulus of the asphalt mix considering the variation in temperatures and the effect of bitumen aging. The air temperature comprised historical records of a weather station close to the case study area in the southeastern region of the Department of Caldas (Colombia). In this section, the performance of the *"AI-based"* structure is analyzed using the MEPDG model to estimate the dynamic modulus and with the climate change scenario defined in previous sections. Figure 5-34 summarizes the damage, fuel and tire consumption, and VOC results.

Figure 5-34. *"AI-based"* performance with MEPDG |E*| model and climate change

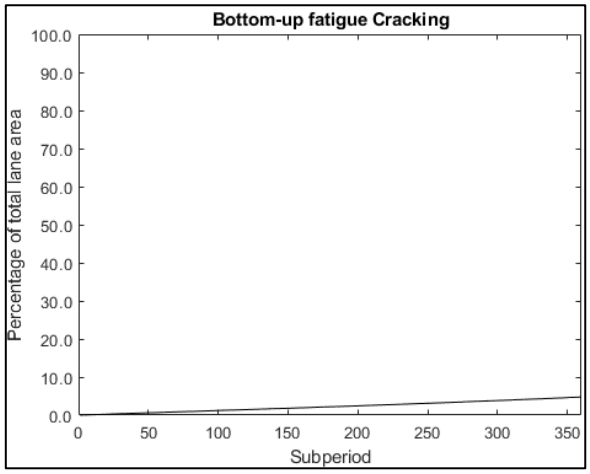

(a) Bottom-up fatigue cracking

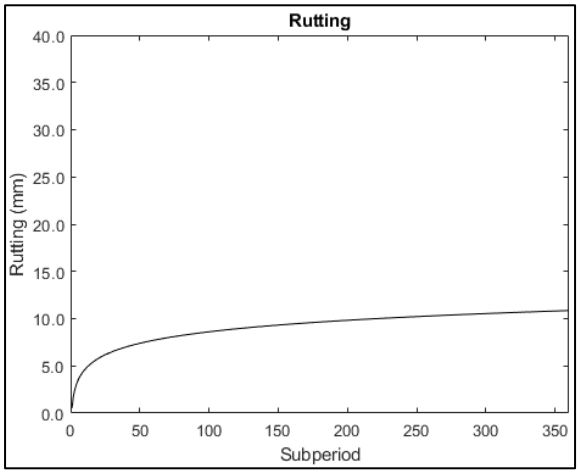

(b) Rut depth

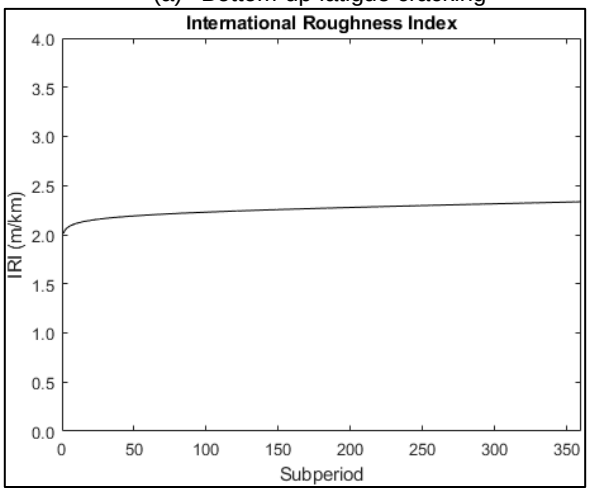

(c) IRI

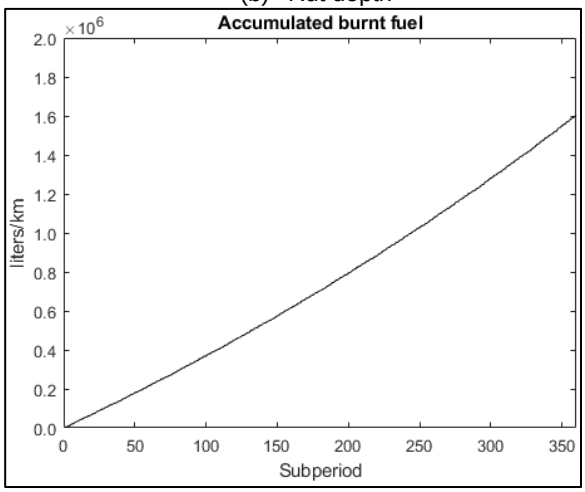

(d) Fuel consumption

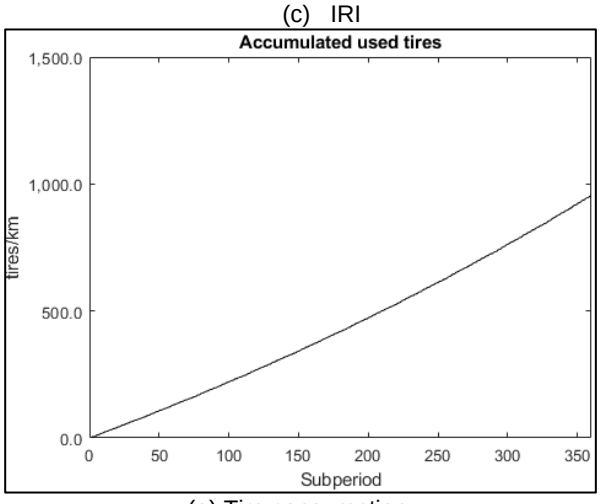

(e) Tire consumption

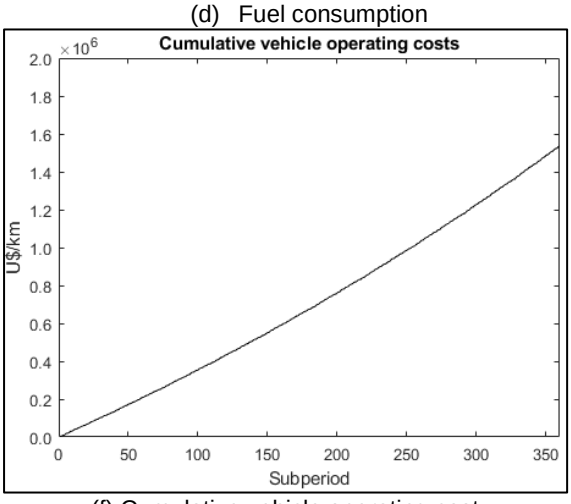

(f) Cumulative vehicle operating cost

All the responses are lower than those obtained in the *"AI-based"* case with the Shell Oil model to predict the dynamic modulus and without the climate change scenario.

The total lane area with fatigue cracking is 4.77% (reduction of 47.9%), the rut depth is 10.86 mm (reduction of 15%), and the final IRI is 2.335 m/km (reduction of 20.8%). The VOC cost is U$ 1.537 million per kilometer, and the construction cost is U$ 0.305 million per kilometer. The VOC is U$ 1,400 less per kilometer, which may be significant in a longer road track.

Despite the notorious reduction in damage and roughness, the vehicle operating cost appears to be less sensitive to the change of dynamic modulus model and climate change scenario.

5.5 Summary

5.5.1 Pavement moduli backcalculation

The author of this dissertation developed PSO-UNLEA, a program based on particle swarm optimization and the layered elastic theory to aid in the backcalculation of pavement mechanical properties. Particle swarm optimization does not need seed moduli values for backcalculation.

A case study shows promising results if the particle swarm optimization includes constraints for the layers moduli, for example, limiting the modular ratio between untreated layers. The results suggest no clear benefit of using narrow-range seed moduli values for the subgrade in the backcalculation procedure. In contrast, this is critical in gradient-based tools.

The computational cost of PSO-UNLEA is significant in Scilab or MATLAB; however, this may be improved by coding the solution in a better-performing language like C or FORTRAN. A surrogate artificial neural network may avoid the high computation cost of the layered-elastic or viscoelastic theories or the finite element method.

Further improvements, considering the non-linear and viscoelastic behavior, are necessary for future developments.

5.5.2 Pavement design

The author developed two programs for pavement design:

a) UNPAVE for incremental pavement design based on some procedures and models of the MEPDG (AASHTO, 2008) with vehicular operating costs (Chatti & Zaabar, 2012), and
b) PSO-PAVE to implement the particle swarm optimization metaheuristic in the flexible pavement design with the UNPAVE program.

The PSO-PAVE program considered two objective functions through a case study with traffic and climate data representative of a mountain road west of Manizales in the central region of Colombia.

The total cost optimization is prone to select the minimum thicknesses for each layer, ignoring damage and roughness levels unacceptable from a serviceability point of view. In contrast, the vehicle operating cost minimization tends to select the maximum thicknesses for each layer. Both objective functions are contradictory, and the optimization process should implement some trade-off between them.

The author proposes an alternative objective function that minimizes the resultant cost (hypotenuse) in the construction cost – vehicle operating costs plane. The optimization process also must include restrictions in minimum thicknesses and material selection to enhance the capabilities of particle swarm optimization.

The author analyzed several case study designs using conventional AASHTO 1993 and Asphalt Institute 1982 methods. According to the resultant cost, the AASHTO 1993 results increase their quality with increased nominal reliability. The AI 1982 charts yield two alternatives with an untreated aggregate base of 150 mm and 300 mm. One of these structures (AI-150) is the non-dominated solution for the problem, but with damage above the same AI thresholds methods because the UNPAVE analysis does not consider the same mechanical properties, only the proposed thicknesses.

Based on the AI alternatives, a 300 mm untreated granular base and a 350 mm hot-mix asphalt design satisfy the cracking and rutting thresholds. However, it is not the non-dominated solution for the resultant cost.

A final analysis of the latter structure, considering the MEPDG dynamic modulus prediction of the hot-mix asphalt and a climate change scenario, shows the importance of adequately characterizing materials. Damage and roughness show significant reductions; however, the vehicle operating cost appears less sensitive to the changes in the dynamic modulus model and climate change scenario.

6 Conclusions and recommendations

In the advance of civilization, it is new knowledge which paves the way, and the pavement is eternal.

Willis R. Whitney.

This chapter presents the conclusions and recommendations for this dissertation. Each section recapitulates the significant ideas from the summaries of Chapters 2 to 5. In those sections, additional information offers further comprehension of each topic.

6.1 Conclusions

6.1.1 About pavement design

Throughout the 20th and 21st centuries, asphalt pavement design for roads and streets evolved from purely empirical to mechanistic-empirical procedures. Empirical methods are simple to use but restricted to a single design condition (subgrade protection), and their applicability is limited by the bounds of the original experimental data. The AASHO Road Test and its subsequent design procedures from 1972 to 1993 improved the design practices and included valuable advances in material characterization and a functional design principle (PSI). However, the increase in vehicular loads and the rise of new materials and construction technologies challenge the current applicability of the empirical components of the AASHTO procedures.

The mechanistic-empirical method (M-E), or analytical method, gained momentum from the 1962 First Conference on Asphalt Pavements to develop the fatigue and rutting criteria coupled with the layered elastic analysis (LEA) developed by Burmister in 1943. Multiple design procedures consider this two-distress approach, like the Shell Pavement Design Manual, the Asphalt Institute Thickness Design, and French Pavement Design Manual. A

subset of the M-E method is the perpetual pavement design approach that considers exceptionally low damage ratios to minimize structural distress as bottom-up fatigue cracking and rutting of the pavement foundation.

Advances in the mechanistic-empiric method include improving the layered-elastic analysis method to the finite element method, considering non-linearity, viscoelasticity, and anisotropy. The main breakthrough in pavement design is the shift from thickness design procedures to incremental damage analysis procedures like the MEPDG.

Adopting an M-E design procedure is not trivial for any Public Highway Agency. Haas et al. (2007) highlighted the need for simplification in catalogs of representative designs to check designs from M-E analysis; they also suggested avoiding using M-E *"black box"* packages to implement checks on the results.

6.1.2 About applied optimization in pavement engineering

Pavement engineering is a crossroads between geotechnical, transportation, and materials engineering. It is not surprising that there are multiple applications of optimization algorithms in this area, with a clear emphasis on pavement management, for its socioeconomic implications, followed by backcalculation for its known complexity.

6.1.2.1 Applications in pavement design

In the design optimization of flexible pavements, the objective function often minimizes the life-cycle total cost (agency and users) by controlling the thicknesses constrained to structural or functional conditions. Although results are similar in the reviewed experiences, there are two defined trends in the analysis method between the AASHTO 1993 and the M-E model to define the restrictions.

There is a trend for multiobjective pavement design optimization based on mechanistic-empirical incremental damage analysis and sustainability principles. It is required to implement efficient search techniques to reduce the computational effort and make the analysis available to practicing Engineers.

6.1.2.2 Applications in pavement management

Random-search techniques are powerful tools to optimize pavement management activities, especially for multiobjective problems such as minimizing costs and maximizing the pavement state from network to project levels. One may classify the objective functions into three groups based on costs or expenditures, resource consumption, or pavement condition:

1. Based on cost or expenditures:
    a. Minimization of maintenance costs or fluctuations of yearly demand for pavement expenditures.
    b. Maximization of usage of the allocated budget.
    c. Maximization of saving in vehicle operating costs.
    d. Maximization of saving in vehicle operating costs over the total cost.
2. Based on resource consumption:
    a. Maximization of usage of available workforce or minimization of workforce requirements.
    b. Maximization of usage of available equipment or minimization of equipment requirements.
    c. Maximization of maintenance production.
3. Based on pavement condition or network operation:
    a. Maximization of effectiveness.
    b. Maximization of overall network pavement condition.
    c. Maximization of skid resistance.
    d. Minimization of total travel time of vehicles in a network under maintenance.
    e. Minimization of accidents.

Cost-based functions are the preferred objective functions or constraints (fixed budget). Resource-consumption-based objective functions may interest highway agencies with in-house capabilities beyond administrative management (self-construction). Pavement-condition-based may be the most comprehensive objective function because it can be related to agency and user’s costs (vehicle operating costs, delay of users, cost of accidents).

Multiobjective optimization is fundamental for better pavement management activities because it explores a single optimum solution and a set of near-optimum solutions that may offer trade-offs for the highway agency. Future research in multiobjective optimization calls for sustainable aspects, such as environmental and social impacts, to assess maintenance costs and benefits (Yepes, Torres-Machi, Chamorro, & Pellicer, 2016).

6.1.2.3 Applications in backcalculation of pavement moduli

The usual objective function minimizes the RMSE between measured and calculated deflections. Alkasawneh (2007) concluded that the RMSE is an inadequate objective function and postulated that the AREA parameter might be a better objective or fitness function. However, as AREA is computed from the same deflections as RMSE, it is unclear how it improves the backcalculation process. Constraints in backcalculation may consider the range of elastic moduli or *"seed values,"* usually from databases or experts' judgment.

A surrogate artificial neural network may avoid the high computation cost of the layered-elastic or viscoelastic theories or the finite element method. However, there is no guarantee that it performs equally or better than the LET or FEM solutions. There are reported difficulties in the backcalculation of the moduli of intermediate granular layers in multilayer systems, both in optimization with LET and ANN and for linear-elastic and non-linear elastic materials (Gopalakrishnan, 2010).

6.1.2.4 Applications in data-fitting

Data fitting uses soft computing techniques, including metaheuristics, to improve phenomenological models based on extensive experimental data without a specific physical model. Other applications include image processing for pavement distress detection and segmentation or dielectric coefficient estimation from reflected waves from ground-penetrating radar.

6.1.2.5 Applications in reliability-based design optimization

Pavement design must consider the variability of the design input parameters and their effect on the long-term performance of the structure. The uncertainties in materials, traffic loads, environmental conditions, and as-built conditions may explain the poor performance due to early functional and structural distress in all pavements.

The benefits of the reliability-based design are evident. However, there are aspects of interest in current research that demand attention, like the traffic loading representation, the limited number of layers and damage criteria, the dependency on surrogate solutions for structural analysis, the combined effect of several modes of damage in the reliability, and the use of assumed or published data on parameters variability.

Recent research on reliability-based pavement design highlighted the drawbacks of the previous pavement design methods, including the MEPDG. However, it is unclear how the incremental pavement design proposed in MEPDG could consider reliability analysis with the dependency of the parameter variability considering its computational cost and the use of complex traffic and climate models.

6.1.3 About layered elastic analysis

The author of this dissertation developed UNLEA, a new software for layered elastic analysis of pavements in highways and airports. UNLEA is an open-source code written in Scilab. Python and MATLAB versions are also available.

The program solves one known issue in LET software: the convergence of near-to-surface points with the strategy proposed by Khazanovich and Wang (2007). Comparison with published results shows good agreement between UNLEA and other programs such as BISAR (De Jong, Peutz, & Korswagen, 1979) and KENPAVE (Huang, 2004) with a lower computing cost.

UNLEA considers both fully bonded and partially bonded interface conditions following the strategy proposed by Hayhoe (2002) in the LEAF program. UNLEA has no practical limitations for layers, points of analysis, or applied loads, so it has good potential for airport pavement analysis and other complex-load scenarios.

6.1.4 About particle swarm optimization in pavement engineering

6.1.4.1 Moduli backcalculation

The author of this dissertation developed PSO-UNLEA, a program based on particle swarm optimization and the layered elastic theory to aid in the backcalculation of pavement mechanical properties.

A case study shows promising results in backcalculation if the particle swarm optimization includes constraints for the moduli, limiting the modular ratio between untreated layers. Constraints in backcalculation should consider the range of elastic moduli from databases or experts' judgment. The results suggest no clear benefit of using narrow-range seed moduli values for the subgrade in the backcalculation procedure.

6.1.4.2 Flexible pavement design

The author of this dissertation developed two programs: UNPAVE for incremental pavement design with vehicular operating costs computation and PSO-PAVE to implement the particle swarm optimization metaheuristic to the flexible pavement design with the UNPAVE program.

The PSO-PAVE program considered two objective functions through a case study with traffic and climate data representative of a mountain road west of Manizales in the central region of Colombia. The total cost optimization is prone to select the minimum thicknesses for each layer, ignoring damage and roughness levels unacceptable from a serviceability point of view. In contrast, the vehicle operating cost minimization tends to select the maximum thicknesses for each layer. Both objective functions are contradictory, and the optimization process should implement some trade-off between them.

The author proposes an alternative objective function that minimizes the resultant cost (hypotenuse) in the construction cost versus vehicle operating costs plane. The optimization process includes restrictions in minimum thicknesses and material selection to enhance the capabilities of particle swarm optimization.

An analysis of alternative designs with the AASHTO 1993 and the Asphalt Institute 1982 methods shows that the latter has a better potential to propose optimal flexible pavement

structures for an objective function based on the hypotenuse of construction and vehicle operating costs. These results are sensitive to the materials characterization, i.e., the dynamic modulus of the hot-mix asphalt or the consideration of climate change scenario. The analysis produces substantially different damage and roughness, but it does not necessarily change the vehicle operating costs significantly.

6.2 Recommendations

From the previous work, it is possible to identify some future research to improve the tools and procedures proposed in this dissertation as follows:

1. Improve the UNLEA program by modifying the matrix solution of interface coefficients for faster executions, as Erlingsson & Ahmed (2013) proposed with regression-based equations.
2. Improve the UNLEA program by including complex load conditions based on the equations proposed by Kai (1987).
3. Develop a finite element method program to implement non-linear viscoelastic materials to optimize pavement backcalculation and design with PSO-UNLEA and PSO-PAVE.
4. Calibrate the MEPDG models for local conditions.
5. Modify UNPAVE by implementing thresholds of rehabilitation activities in the simulation period, such as overlay construction based on a limited roughness value.
6. Develop a reliability-based design optimization based on UNLEA with a full rutting prediction model instead of the subgrade-based model.
7. Update the vehicle operating cost models to incorporate the shift in fuel dependency in transportation systems to alternative energy sources or the change in fuel, tires, and maintenance costs through the design period.
8. Improve the UNPAVE program by including other materials as cement-treated bases.

7 Bibliography

AASHTO. (1993). *AASHTO Guide for Design of Pavement Structures.* Washington, D.C.: American Association of State Highway and Transportation Officials.

AASHTO. (2008). *Mechanistic-Empirical Pavement Design Guide. A Manual of Practice - Interim Edition.* Washington D.C.: American Association of State Highway and Transportation Officials.

Abu-Lebdeh, G., Chen, H., & Ghanim, M. (2014). Improving Performance of Genetic Algorithms for Transportation Systems: Case of Parallel Genetic Algorithms. *Journal of Infrastructure Systems*, 1-8.

Ahlborn, G. (1972). *ELSYM5, Computer Program for Determining Stresses and Deformations in Five Layer Elastic Systems.* Berkeley: University of California.

Ahlvin, R. G., & Ulery, H. H. (1962). Tabulated Values for Determining the Complete Pattern of Stresses, Strains, and Deflections Beneath a Uniform Circular Load on a Homogeneous Half-Space. *Highway Research Board Bulletin, 342*, 1-13. Retrieved from http://onlinepubs.trb.org/onlinepubs/hrbbulletin/342/342-001.pdf

Ahmed, K., Al-Khateeb, B., & Mahmood, M. (2018). A Chaos with Discrete Multiobjective Particle Swarm Optimization for Pavement Maintenance. *Journal of Theoretical and Applied Information Technology, 96*(8), 2317-2326.

Alae, M., Yanqing, Z., Zarei, S., Fu, G., & Cao, D. (2018). Effects of layer interface conditions on top-down fatigue cracking of asphalt pavements. *International Journal of Pavement Engineering*, 1-9.

Alarcón-Guzmán, A. (2004). The geotechnical problem (In Spanish). *Class notes of the "Soil Behavior" course in the Master of Geotechnical Engineering*. Bogotá, Cundinamarca, Colombia.

Ali, H. A., & Shiraz, D. T. (1998). *Mechanistic Evaluation of Test Data from LTPP Flexible Pavement Test Sections Publication No. FHWA-RD-98-012.* McLean, VA: Federal Highway Administration.

Alkasawneh, W. (2007). *Backcalculation of Pavement Moduli Using Genetic Algorithms.* Akron, Ohio, USA: The University of Akron.

Al-Omari, B., & Darter, M. (1994). Relationships Between International Roughness Index and Present Serviceability Rating. *Transportation Research Record 1435*, 130-136.

Al-Qadi, I. L., & Wang, H. (2009). *Evaluation of Pavement Damage due to New Tire Designs Research Report ICT-09-048.* Illinois Center for Transportation.

Al-Rumahiti, A. (2021, November 21). *Multi-layer Elastic Analysis.* Retrieved from Mathworks: https://la.mathworks.com/matlabcentral/fileexchange/69465-multi-layer-elastic-analysis

AMADEUS. (2000). *AMADEUS - Advanced Models for Analytical Design of European Pavement Structures.*

Anderson, M. (1990). *Backcalculation of Composite Pavement Layer Moduli - Technical Report GL-90-15.* Vicksburg, Mississippi: US Army Corps of Engineers.

Asphalt Institute. (1981). *Thickness Design—Asphalt Pavements for Highways and Streets. Manual Series No. 1* (Ninth ed.). Lexington, Kentucky, USA: Asphalt Institute.

Asphalt Institute. (1982). *Research and Development of the Asphalt Institute´s Thickness Design Manual (MS-1) Ninth Edition.* Lexington, Kentucky, USA: Asphalt Institute.

Asphalt Institute. (2000). *Asphalt Overlays for Highway and Street Rehabilitation Manual MS-17.* Lexington, Kentucky: Asphalt Institute.

Asphalt Institute. (2005). *SW-1 Asphalt Pavement Thickness Design Software for Highways, Airports, Heavy Wheel Loads and Other Applications User´s Guide.* Lexington, Kentucky, USA: Asphalt Institute.

Austroads. (1992). *Pavement Design - A Guide to the Structural Design of Road Pavements* (Vols. AP-17/92). Sydney, Australia: Australian Road Research Board.

Austroads. (1994). *Pavement Design - A Guide to the Structural Design of Road Pavements. Interim Version of Revised Overlay Design Procedures.* Sydney, Australia: Austroads Pavement Research Group.

Babkov, V., & Zamakhayev, M. (1967). *Highway Engineering.* Moscow, USSR: Mir publishers.

Baus, R. L., & Stires, N. R. (2010). *Mechanistic-Empirical Pavement Design Guide Implementation.* Columbia, South Carolina: Department of Civil and Environmental Engineering - The University of South Carolina.

Bosurgi, G., & Trifirò, F. (2005). A Model Based on Artificial Neural Networks and Genetic Algorithms for Pavement Maintenance Management. *The International Journal of Pavement Engineering, 6*(3), 201-209.

Brown, S. F. (1967). *Stresses and deformations in flexible layered pavement systems subjected to dynamic loads, Ph.D. Thesis.* Nottingham, UK: The University of Nottingham. Retrieved from http://eprints.nottingham.ac.uk/11667/1/520241.pdf

Brown, S. F. (1973). Determination of Young's modulus for Bituminous Materials in Pavement Design. *Highway Research Record 431. 52nd Annual Meeting of the Highway Research Board* (pp. 38-49). Washington D.C.: Highway Research Board.

Brown, S. F. (1993). Soil Mechanics in Pavement Engineering. *Géotechnique, 46*(3), 383-426.

Brown, S. F., & Pappin, J. W. (1981). Analysis of Pavements with Granular Bases. *Transportation Research Record 810*, 17-22.

Brown, S. F., Bunton, J. M., & Pell, P. S. (1982). The Development and Implementation of Analytical Pavement Design for British Conditions. *Proceedings Fifth International Conference on the Structural Design of Asphalt Pavements* (pp. 17-44). University of Michigan and Delft University of Technology.

Brunton, J. M., & D'Almeida, J. R. (1992). Modeling Material Non-Linearity in a Pavement Back-Calculation Procedure. *Transportation Research Record 1377*, 99-106.

Burmister, D. M. (1943). The Theory of Stresses and Displacements in Layered Systems and Application to Design of Airport Runways. *Proc. HRB* (pp. 120-125). Washington D.C.: Highway Research Board.

Cai, Y., Sangghaleh, A., & Pan, E. (2015). Effect of anisotropic base/interlayer on the mechanistic responses of layered pavements. *Computer and Geotechnics, 65*, 250-257.

Cao, W., Norouzi, A., & Kim, Y. R. (2016). Application of Viscoelastic Continuum Damage Approach to Predict Fatigue Performance of Binzhou Perpetual Pavements. *Journal of Traffic and Transportation Engineering (English Edition), 3*(2), 104-115. doi:http://dx.doi.org/10.1016/j.jtte.2016.03.002

CDKN. (2012). *Critical Climate Change Concerns for the Road Sector in Colombia.* Bogotá: Climate Development and Knowledge Network.

Central Intelligence Agency. (2013). *The World Factbook 2013-2014*. Retrieved March 24, 2016, from https://www.cia.gov/library/publications/the-world-factbook/index.html

Cercevik, A. E., Bozkurt, H., & Toklu, Y. C. (2014). Applications of meta-heuristic algorithms to civil engineering problems, a survey. In Y. C. Toklu, & G. Bekdas (Ed.), *Metaheuristics and Engineering - 14th Workshop of the EURO Working Group* (pp. 63-65). Istambul: The Association of European Operational Research Societies.

Ceylan, H., Kim, S., Gopalakrishnan, K., & Ma, D. (2013). *Iowa Calibration of MEPDG Performance Prediction Models - Final Report.* Iowa State University. Ames, Iowa: Institute for Transportation.

Chan, W. T., Fwa, T. F., & Hoque, K. Z. (2001). Constraint Handling Methods in Pavement Maintenance Programming. *Transportation Research Part C, 9*, 175-190.

Chan, W. T., Fwa, T. F., & Tan, C. Y. (1994). Road-Maintenance Planning Using Genetic Algorithms. I: Formulation. *Journal of Transportation Engineering, 120*(5), 693-709.

Chang, J.-R. (2013). Particle Swarm Optimization Method for Optimal Prioritization of Pavement Sections for Maintenance and Rehabilitation Activities. *Applied Mechanics and Materials, 343*, 43-49.

Chang, J.-R., & Chao, S.-J. (2010). Pavement Maintenance and Rehabilitation Decisions Derived by Genetic Programming. *2010 Sixth International Conference on Natural Computation ICNC* (pp. 2439-2443). IEEE.

Charyulu, M. K. (1964). *Theoretical stress distribution in an elastic multi-layered medium.* Iowa State University. Ames, Iowa: Retrospective Theses and Dissertations 2730.

Chatti, K., & Yun, K. K. (1996). SAPSI-M: A Computer Program for Analyzing Asphalt Concrete Pavements under Moving Arbitrary Loads. (T. R. Board, Ed.) *Transportation Research Record 1539*.

Chatti, K., & Zaabar, I. (2012). *NCHRP Report 720 Estimating the Effects of Pavement Condition on Vehicle Operating Costs.* Washington D.C.: Transportation Research Board.

Chen, D.-H., Zaman, M., Laguros, J., & Soltani, A. (1985). Assessment of Computer Programs for Analysis of Flexible Pavement Structure. *Transportation Research Record 1482*, 123-133.

Chen, W. T. (1971). Computation of Stresses and Displacements in a Layered Elastic Medium. *International Journal of Engineering Science*, 775-800.

Cheu, R. L., Wang, Y., & Fwa, T. F. (2004). Genetic Algorithm-Simulation Methodology for Pavement Maintenance Scheduling. *Computer-Aided Civil and Infrastructure Engineering, 19*, 446-455.

Cho, Y. H., McCullough, B. F., & Weismann, J. (1996). Considerations on Finite-Element Method Application in Pavement Structural Analysis. *Transportation Research Record: Journal of the Transportation Research Board, 1539*(1), 96-101.

Choi, J. W., Wu, R., Pestana, J. M., & Harvey, J. (2010). New Layer-Moduli Back-Calculation Method Based on the Constrained Extended Kalman Filter. *Journal of Transportation Engineering, 136*(1), 20-30.

Chong, D., Wang, Y., Dai, Z., Chen, X., Wang, D., & Oeser, M. (2018). Multiobjective Optimization of Asphalt Pavement Design and Maintenance Decisions Based on Sustainability Principles and Mechanistic-Empirical Pavement Analysis. *International Journal of Sustainable Transportation, 12*(6), 461-472.

Chootinan, P., Chen, A., Horrocks, M. R., & Bolling, D. (2006). A Multi-Year Pavement Maintenance Program Using a Stochastic Simulation-Based Genetic Algorithm Approach. *Transportation Research Part A, 40*, 725-743.

Christensen, P. W., & Klarbring, A. (2009). *An Introduction to Structural Optimization.* Linköping, Sweden: Springer Science + Bussiness Media B. V.

Clerc, M. (1999). The Swarm and the Queen: Towards a Deterministic and Adaptative Particle Swarm Optimization. *Proceedings of the Congress on Evolutionary Computing*, *III*, pp. 1951-1957.

Climate Analytics. (2022). *PROVIDE climate risk dashboard*. Retrieved from https://climate-risk-dashboard.climateanalytics.org/

Coleri, E., Guler, M., Gungor, A. G., & Harvey, J. T. (2010). Prediction of Subgrade Resilient Modulus Using Genetic Algorithm and Curve-Shifting Methodology. *Transportation Research Record: Journal of the Transportation Research Board, 2170*, 67-73.

Corté, J.-F., & Goux, M.-T. (1996, January). Design of Pavements Structures: The French Technical Guide. *Transportation Research Record: Journal of the Transportation Research Board*(1539), 116-124. doi:10.3141/1539-16

Croney, D., & Croney, P. (1998). *The design and performance of road pavements* (Third ed.). London, UK: McGraw-Hill.

Cunha Coelho, N. F. (2016). *Calibration of MEPDG Performance Models for Flexible Pavement Distresses to Local Conditions of Ontario - M.Sc. Thesis.* The University of Texas at Arlington. Arlington, Texas: The University of Texas at Arlington.

Dalla Valle, P., & Thom, N. (2016a). Improvement of method of equivalent thicknesses (MET) for calculation of critical strains for flexible pavements. *International Journal of Pavement Engineering*, 1-8.

Dalla Valle, P., & Thom, N. (2016b). Reliability in pavement design. *E & E Congress 6th Eurasphalt & Eurobitume Congress.* Prague, Czech Republic.

Darter, M. I., & Hudson, W. R. (1973). *Probabilistic Design Concepts Applied to Flexible Pavement System Design - Research Report 123-18.* Texas Highway Department. Austin, Texas: Center for Highway Research - The University of Texas at Austin.

Dauzats, M., & Rampal, A. (1988). Mécanismes de fissuration de surface des couches de roulement. *Bulletin de Liaison des Laboratoires des Ponts et Chaussés, 154*, 57-72.

De Jong, D., Peutz, M. G., & Korswagen, A. R. (1979). *Computer program BISAR, layered systems under normal and tangential surface loads.* Amsterdam: Koninklijke/Shell Laboratorium, Shell Research B.V.

Dede, T., Kripka, M., Togan, V., Yepes, V., & Rao, R. V. (2019). Usage of Optimization Techniques in Civil Engineering During the Last Two Decades. *Current Trends in Civil & Structural Engineering, 2*(1), 1-17.

Deshpande, V. P., Damnjanovic, I. D., & Gardoni, P. (2010). Reliability-Based Optimization Models for Scheduling Pavement Rehabilitation. *Computer-Aided Civil and Infrastructure Engineering, 25*, 227-237.

Di Mino, G., De Blasiis, M. R., Di Noto, F., & Noto, S. (2013). An Advanced Pavement Management System based on a Genetic Algorithm for a Motorway Network. In Y. Tsompanakis (Ed.), *Proceedings of the Third International Conference on Soft Computing Technology in Civil, Structural and Environmental Engineering* (pp. 1-17). Stirlingshire, Scotland: Civil-Comp Press.

Dilip, D. M., & Sivakumar Babu, G. L. (2013). Methodology for Pavement Design Reliability and Back Analysis Using Markov Chain Monte Carlo Simulation. *ASCE Journal of Transportation Engineering, 139*(1), 65-74.

Dilip, D. M., & Sivakumar Babu, G. L. (2021). Reliability-Based Design Optimization of Flexible Pavements Using Kriging Models. *Journal of Transportation Engineering. Part B: Pavements*, 04021046 1-14.

Dilip, D. M., Ravi, P., & Sivakumar Babu, G. L. (2013). System Reliability Analysis of Flexible Pavements. *ASCE Journal of Transportation Engineering, 139*(10), 1001-1009.

Dinegdae, Y. H., & Birgisson, B. (2016). Reliability-Based Design Procedure for Fatigue Cracking in Asphalt Pavements. *Transportation Research Record: Journal of the Transportation Research Board, 2583*(1), 127-133.

Dinegdae, Y., Onifade, I., Birgisson, B., Lytton, R., & Little, D. (2018). Towards a Reliability-Based Pavement Design using Response Surface Methods. *Transportation Research Record, 2672*(40), 97-107.

Diwekar, U. (2008). *Introduction to Applied Optimization.* Clarendon Hils, IL: Springer Science + Business Media, LLC.

Duncan, J. M., Monismith, C. L., & L., W. E. (1968). Finite Element Analyses of Pavements. *Highway Research Record, 228*, 18-33.

Duong, N. S., Blanc, J., & Hornych, P. (2017). Analysis of the behavior of pavement layers interfaces from in situ measurements. In A. Loizos, I. L. Al-Qadi, & T. Scarpas (Ed.), *10th International Conference on the Bearing Capacity of Roads, Railways, and Airfields (BCRRA 2017).* Athens, Greece: CRC Press.

Elhadidy, A. A., Elbeltagi, E. E., & Ammar, M. A. (2015). Optimum Analysis of Pavement Maintenance Using Multi-Objective Genetic Algorithms. *Housing and Building National Research Center HBRC Journal*, 107-113.

ERDC. (2002). *WinLEA ERDC Developed Software WinJULEA Windows Layered Elastic Analysis.* GSL - Airfields & Pavements Branch. Vicksburg, Mississippi: Engineering Research & Development Center.

Erlingsson, S., & Ahmed, A. (2013). Fast layered elastic response program for the analysis of flexible pavement structures. *Road Materials and Pavement Design, 14*(1), 196-210. doi:10.1080/14680629.2012.757558

Farhan, J., & Fwa, T. F. (2012). Incorporating Priority Preferences into Pavement Maintenance Programming. *Journal of Transportation Engineering, 138*(6), 714-722.

Federal Aviation Administration. (1995). *Airport Pavement and Evaluation - Advisory Circular AC 150/5320-6D (Cancelled).* Washington, D.C.: U.S. Department of Transportation - Federal Aviation Administration.

Ferreira, A., Antunes, A., & Picado-Santos, L. (2002). Probabilistic Segment-linked Pavement Management Optimization Model. *Journal of Transportation Engineering, 128*(6), 568-577.

Figueroa, A., Reyes, F., Hernández, D., Jiménez, C., & Bohórquez, N. (2007). Análisis de un asfalto modificado con icopor y su incidencia en una mezcla asfáltica densa en caliente. *Ingeniería e Investigación, 27*(3), 5-15.

Finn, F. N., Saraf, C., Kulkarni, R., Nair, K., Smith, W., & Abdullah, A. (1977). The Use of Distress Prediction Subsystems in the Design of Pavement Structures. *Proceedings Fourth International Conference on the Structural Design of Asphalt Pavements. 1*, pp. 3-38. Michigan: The University of Michigan.

Flintsch, G. W., & Chen, C. (2004). Soft Computing Applications in Infrastructure Management. *Journal of Infrastructure Systems, 10*(4), 157-165.

Freeman, R. B., & Harr, M. E. (2004). Stress Predictions for Flexible Pavement Systems. *Journal of Transportation Engineering, 130*(495-502).

Fwa, T. F., Chan, T. Y., & Hoque, K. Z. (1998). Analysis of Pavement Management Activities Programming by Genetic Algorithms. *Transportation Research Record: Journal of the Transportation Research Board, 1643*, 1-6.

Fwa, T. F., Chan, W. T., & Hoque, K. Z. (2000). Multiobjective Optimization for Pavement Maintenance Programming. *Journal of Transportation Engineering, 126*(5), 367-374.

Fwa, T. F., Chan, W. T., & Tan, C. Y. (1994). Optimal Programming by Genetic Algorithm for Pavement Management. *Transportation Research Record: Journal of the Transportation Research Board, 1455*, 31-41.

Fwa, T. F., Chan, W. T., & Tan, C. Y. (1996). Genetic-Algorithm Programming of Road Maintenance and Rehabilitation. *Journal of Transportation Engineering, 122*(3), 246-253.

Fwa, T. F., Tan, C. Y., & Chan, W. T. (1997). Backcalculation Analysis of Pavement-Layer Moduli Using Genetic Algorithms. *Transportation Research Record: Journal of the Transportation Research Board, 1570*, 134-142.

Gallego, R., Toro, E., & Escobar, A. (2015). *Técnicas Heurísticas y Metaheurísticas.* Pereira, Colombia: Universidad Tecnológica de Pereira.

Gandomi, A. H., Yang, X.-S., Talatahari, S., & Alavi, A. H. (2013). Metaheuristic Algorithms in Modeling and Optimization. In A. H. Gandomi, X.-S. Yang, S. Talatahari, & A. H. Alavi, *Metaheuristics Applications in Structures and Infrastructures* (pp. 1-24). Elsevier Science & Technology.

Gao, L., Xie, C., Zhang, Z., & Waller, S. T. (2012). Network-Level Road Pavement Maintenance and Rehabilitation Scheduling for Optimal Performance Improvement and Budget Utilization. *Computer-Aided Civil and Infrastructure Engineering, 27*, 276-287.

Garnica Anguas, P., & Hernández Domínguez, R. (2013). *Manual de Usuario IMT-PAVE 1.1 Documento Técnico No. 53.* Sanfandila, Qro: Instituto Mexicano del Transporte.

Ghanizadeh, A. R. (2016). An Optimization Model for Design of Asphalt Pavements Based on IHAP Code Number 234. *Advances in Civil Engineering*, 1-8.

Ghanizadeh, A. R. (2017). Application of support vector machine regression for predicting critical responses of flexible pavements. *International Journal of Transportation Engineering, 4*(4), 305-315.

Ghanizadeh, A. R., & Ziaie, A. (2015). NonPAS: A Program for Nonlinear Analysis of Flexible Pavements. *International Journal of Integrated Engineering, 7*(1), 21-28.

Ghanizedeh, A. R., & Ahadi, M. R. (2015). Application of Artificial Neural Networks for Analysis of Flexible Pavements under Static Loading of Standard Axle. *International Journal of Transportation Engineering, 3*(1), 31-43.

Golroo, A., & Tighe, S. L. (2012). Optimum Genetic Algorithm Structure Selection in Pavement Management. *Asian Journal of Applied Sciences, 5*(6), 327-341.

Gonzales, C. R., Barker, W. R., & Bianchini, A. (2012). *Reformulation of the CBR procedure. Report I: Basic report.* U.S. Army Corps of Engineers, Geotechnical and Structures Laboratory. Vicksburg: U.S. Army Engineer Research and Development Center.

Gonzalez, C. R. (2015). *Development and Validation of a Stress-Based Procedure for the Design of Military Flexible Pavements (Ph.D. Thesis).* The University of Illinois at Urbana-Champaign. Urbana, Ilinois: The University of Illinois at Urbana-Champaign.

Gopalakrishnan, K. (2009). Backcalculation of Pavement Moduli Using Bio-Inspired Hybrid Metaheuristics and Cooperative Strategies. *Proceedings of the 2009 Mid-Continent Transportation Research Symposium* (pp. 1-5). Ames, Iowa: Iowa State University.

Gopalakrishnan, K. (2010). Neural Network-Swarm Intelligence Hybrid Nonlinear Optimization Algorithm for Pavement Moduli Back-Calculation. *Journal of Transportation Engineering, 136*(6), 528-536.

Granada Echeverri, M. (2009). *Algoritmos Evolutivos y Técnicas Bioinspiradas. De la Teoría a la Práctica.* Pereira, Colombia: Universidad Tecnológica de Pereira.

Gudipudi, P. P., Underwood, B. S., & Zalghout, A. (2017). Impact of climate change on pavement structural performance in the United States. *Transportation Research*

Part D: Transport and Environment, 57, 172-184. doi:https://doi.org/10.1016/j.trd.2017.09.022

Haas, R., Tighe, S., Dore, G., & Hein, D. (2007). Mechanistic-Empirical Pavement Design: Evolution and Future Challenges. *2007 Annual Conference Transportation Association of Canada*, (pp. 1-23). Saskatoon, Saskatchewan.

Hadi, M. N., & Arfiadi, Y. (2001). Optimum rigid pavement design by genetic algorithms. *Computers and Structures, 79*, 1317-1624.

Harr, M. E., & Lovell, Jr., C. W. (1963). Vertical Stresses Under Certain Axisymmetrical Loadings. *Highway Research Record, 39*, 68-81.

Hasan, M. M., Rahman, A. A., & Tarefder, R. A. (2018). Investigation of Accuracy of Pavement Mechanistic Empirical Prediction Performance by Incorporating Level 1 Inputs. *Journal of Traffic and Transportation Engineering (English Edition)*, 1-10. doi: https://doi.org/10.1016/j.jtte.2018.06.006

Hayhoe, G. F. (2002). LEAF - A New Layered Elastic Computational Program for FAA Pavement Design and Evaluation Procedures. In F. A. Administration (Ed.), *The 2002 Federal Aviation Administration Airport Technology Transfer Conference*, (pp. 1-15).

He, Z., Cai, Y., & Haas, R. (1996). *OPAC 2000 Engineering document.* Ontario: Ministry of Transportation of Ontario.

Herabat, P., & Tangphaisankun, A. (2005). Multi-Objective Optimization Model using Constraint-Based Genetic Algorithms for Thailand Pavement Management. *Journal of the Eastern Asia Society for Transportation Studies, 6*, 1137-1152.

Horak, E., Maree, J. H., & van Wijk, A. J. (1989). Procedures for Using Impulse Deflectometer (IDM) Measurements in the Structural Evaluation of Pavements. *Proceedings of the Annual Transportation Convention*, *5A.* Pretoria, South Africa.

Hu, K.-F., Jiang, K.-P., & Chang, D.-W. (2007). Study of Dynamic Backcalculation Program with Genetic Algorithms for FWD on Pavements. *Tamkang Journal of Science and Engineering, 10*(4), 297-305.

Huang, Y. H. (1969). Computation of Equivalent Single-Wheel Loads Using Layered Theory. *Highway Research Record*(291), 144-155.

Huang, Y. H. (1993). *Pavement Analysis and Design* (First ed.). Englewood Cliffs, NJ, USA: Prentice Hall.

Huang, Y. H. (2004). *Pavement Analysis and Design* (Second ed.). Upper Saddle River, NJ, USA: Pearson Prentice Hall.

Hunaidi, O. (1998). Evolution-Based Genetic Algorithms for Analysis of Non-Destructive Surface Wave Tests on Pavements. *NDT&E International, 31*(4), 273-280.

IDEAM. (23 de 01 de 2021). *Consulta y Descarga de Datos Hidrometeorológicos*. Obtenido de Consulta y Descarga de Datos Hidrometeorológicos: http://dhime.ideam.gov.co/atencionciudadano/

INVÍAS. (2003). *Operativo Móvil de Pesaje Carretera Manizales - Chinchiná en el sitio Cenicafé.* Bogotá D.C.: Instituto Nacional de Vías. Subdirección de Conservación.

INVÍAS. (2007). *Manual de diseño de pavimentos asfálticos para vías con bajos volumenes de tránsito.* Bogotá: Instituto Nacional de Vías.

INVÍAS. (2011). *Volumenes de Tránsito .* Bogotá DC: Instituto Nacional de Vías de Colombia.

Ioannides, A. M., & Khazanovich, L. (1998). General Formulation for Multilayered Pavement Systems. *Journal of Transportation Engineering, 124*(1), 82-90.

IPCC. (2014). *Climate Change 2014-Impacts, Adaptation and Vulnerability: Regional Aspects.* Intergovernmental Panel on Climate Change. Cambridge University Press. doi:https://doi.org/10.1017/CBO9781107415379

Jameson, G. W. (1996). *Origins of AUSTROADS Design Procedures for Granular Pavements. Research Report ARR 292.* Vermont South, Australia: ARRB Transport Research Ltd.

Javed, F. (2011). *Integrated Prioritization and Optimization Approach for Pavement Management.* Ph.D. Thesis, Singapore.

Joint Departments of the Army and Air Force. (1994). *TM 5-822-13/AFJMAN 32-1018 Pavement Design for Roads, Streets and Open Storage Areas, Elastic Layered Method.* Washington D.C.

Jooste, F. (2016, 07 12). *Automated Backcalculation: How the backcalculation error is calculated.* Retrieved 06 04, 2019, from Rubicon Toolbox: Rubicon forum: http://forum.rubicontoolbox.com/pages/topic7-how-the-backcalculation-error-is-calculated.aspx

Kai, W. (1987). Analysis and Calculation of Stresses and Displacements in Layered Elastic Systems. *Acta Mechanica Sinica, 3*(3), 252-260.

Kameyama, S., Himeno, K., Kasahara, K., & Maruyama, T. (1998). Backcalculation of Pavement Layer Moduli using Genetic Algorithms. *8th International Conference on Asphalt Pavements* (pp. 1375-1385). Seattle, Washington: University of Washington.

Kasperick, T., & Ksabaiti, K. (2015). *Calibration of the Mechanistic-Empirical Pavement Design Guide for Local Paved Roads in Wyoming.* Department of Civil and Architectural Engineering - The University of Wyoming. Laramie, Wyoming: The Mountain Plains Consortium.

Kenis, W. J., Sherwood, J. A., & McMahon, R. F. (1982). Verification and Application of the VESYS Structural Subsystem. *Proceedings Fifth International Conference on the Structural Design of Asphalt Pavements. 1*, pp. 333-348. University of Michigan and Delft University of Technology.

Kennedy, J., & Eberhart, R. (1995). Particle Swarm Optimization. *Proceedings of ICNN'95 - International Conference on Neural Networks* (pp. 1942-1948). Perth, WA, Australia, Australia: IEEE. doi:10.1109/ICNN.1995.488968

Khazanovich, L., & Wang, Q. (2007). MnLayer – A high performance layered elastic analysis program. *Transportation Research Record: Journal of the Transportation Research Board*(2037), 63-75.

Kim, H. B., & Lee, S. H. (2002). Reliability-Based Design Model Applied to Mechanistic Empirical Pavement Design. *KSCE Journal of Civil Engineering, 6*(3), 263-272.

Kim, M. (2007). *Three-Dimensional Finite Element Analysis of Flexible Pavements Considering Nonlinear Pavement Foundation Behavior.* The University of Illinois at Urbana - Champaign. Urbana, Illinois: The University of Illinois at Urbana - Champaign.

Kim, S. H., Little, D. N., & Masad, E. (2005). Simple methods to estimate inherent and stress-induced anisotropy of aggregate base. *Transportation Research Record 1913*, 24-31.

Kim, S., Ceylan, H., Ma, D., & Gopalakrishnan, K. (2014). Calibration of Pavement ME Design and Mechanistic-Empirical Pavement Design Guide Performance Prediction Models for Iowa Pavement Systems. (A. S. Engineers, Ed.) *Journal of Transportation Engineering, 140*(10).

Kim, Y. R., Jadoun, F. M., Hou, T., & Muthadi, N. (2011). *Local Calibration of the MEPDG for Flexible Pavement Design - Report FHWA\NC\2007-07.* Raleigh, NC: North Carolina Department of Transportation.

Kimura, T. (2014). Studies on Stress Distribution in Pavements Subjected to Surface Shear Loads. *Proceedings of the Japanese Academy, 90*(2), 47-55.

Kosasih, D. (2011). Back-Calculation of Pavement Modulus Values Using Genetic Algorithms. *Proceedings of the Eastern Asia Society for Transportation Studies, 8*.

Kruntcheva, M. R., Collop, A. C., & Thom, N. H. (2005). Effect of Bond Condition on Flexible Pavement Performance. *Journal of Transportation Engineering, 131*(11), 880-888.

Kuyu, Y. C., & Vatansever, F. (2021). Advanced Metaheuristic Algorithms on Solving Multimodal Functions: Experimental Analyses and Performance Evaluations. *Archives of Computational Methods in Engineering*.

Lamboll, R., Rogelj, J., & Schleussner, C. F. (2022). *A guide to scenarios for the PROVIDE project.* Earth and Space Science Open Archive.

Laurent-Matamoros, P., Loría-Salazar, L.-G., Leiva-Padilla, P., & Trejos-Castillo, C. (2018). PITRA-BACK Herramienta de Cálculo para el Diseño de Sobrecapas Asfálticas de Pavimentos Flexibles en Costa Rica. *Software version Beta 1.0.1*. Costa Rica: Universidad de Costa Rica - Laboratorio Nacional de Materiales y Modelos Estructurales.

LCPC - SETRA. (1994). *Conception et dimensionnement des structures de chaussée - Guide technique.* Paris, France: Laboratoire Central des Ponts et Chaussées - Service d'études sur les Transports, les Routes et leurs Aménagements.

Lea, J. (2014). *About OpenPave.org*. Retrieved 05 29, 2018, from OpenPave.org Open Source Pavement Engineering: http://www.openpave.org/

Li, J., Uhlmeyer, J. S., Mahoney, J. P., & Muench, S. T. (2011). *Use of the 1993 AASHTO Guide, MEPDG and Historical Performance to Update the WSDOT Pavement Design Catalog.* Seattle, Washington: The University of Washington.

Li, M., & Wang, H. (2017). Development of ANN-GA Program for Backcalculation of Pavement Moduli under FWD Testing with Viscoelastic and Nonlinear Parameters. *International Journal of Pavement Engineering*, 1-9.

Li, Q., Xiao, D. X., Wang, K. C., Hall, K. D., & Qiu, Y. (2011). Mechanistic-Empirical Pavement Design Guide (MEPDG): A Bird's Eye Review. *Journal of Modern Transportation, 19*, 114-133.

Li, T., & Chen, Y. (2018). Multiple Improvements to the Particle Swarm Optimization Algorithm. *IOP Conference Series: Materials Science and Engineering*, *435*, pp. 1-10.

Li, X., Li, X., Zhong, Y., & Wang, F. (2012). Modulus Back Analysis of Pavement Structure Based on PSO. *Applied Mechanics and Materials, 178-181*, 1222-1225.

Liu, H., Pan, E., & Cai, Y. (2018). General surface loading over layered transversely isotropic pavements with imperfect interfaces. *Advances in Engineering Software, 115*, 268-282. doi:10.1016/j.advengsoft.2017.09.009

Liu, P., Wang, D., & Oeser, M. (2015). Application of Semi-Analytical Finite Element Method Coupled with Infinite Element for Analysis of Asphalt Pavement Structural Response. *Journal of Traffic and Transportation Engineering (English Version), 2*(1), 45-48. doi:http://dx.doi.org/10.1016/j.jtte.2015.01.005

Liu, W., & Scullion, T. (2011). *Flexible Pavement Design Manual System FPS 21: User´s Manual.* Texas Department of Transportation. College Station, TX: Texas Transportation Institute - The Texas A&M University System.

Loulizi, A., Al-Qadi, I. L., & Elseifi, M. (2006). Difference between In Situ Flexible Pavement Measured and Calculated Stresses and Strains. *Journal of Transportation Engineering, 132*(7), 574-579.

Lu, Q., Ullidtz, P., Basheer, I., Ghuzlan, K., & Signore, J. M. (2009). CalBack: Enhancing Caltrans Mechanistic-Empirical Pavement Design Process with New Back-Calculation Software. *Journal of Transportation Engineering, 135*(7), 479-488.

Lui, M.-y., & Wang, S.-y. (2003). Genetic Optimization Method of Asphalt Pavement Based on Rutting and Cracking Control. *Journal of Wuhan University of Technology, 18*(1), 72-75.

Luo, Z., Hu, B., & Pan, E. (2019). Robust design approach for flexible pavements to minimize the influence of material property uncertainty. *Construction and Building Materials*, 332-339.

Luo, Z., Karki, A., Pan, E., Abbas, A. R., Arefin, M. S., & Hu, B. (2018). Effect of uncertain material property on system reliability in mechanistic-empirical pavement design. *Construction and Building Materials, 172*, 488-498.

Lytton, R. L. (1989). Backcalculation of Pavement Layer Properties. In A. J. Bush, & G. Y. Baladi (Ed.), *Nondestructive Testing of Pavements and Backcalculation of Moduli ASTM STP1026* (pp. 7-38). Philadelphia: American Society for Testing and Materials.

Maina, J. W., & Matsui, K. (2004). Developing software for elastic analysis of pavement structure responses. *Transportation Research Records, 1896*, 107-118.

Maina, J. W., Ozawa, Y., & Matsui, K. (2012). Linear Elastic Analysis of Pavement Structure Under Non-circular Loading. *Road Materials and Pavement Design, 13*(3), 403-421. doi:10.1080/14680629.2012.705419

Maji, A., & Das, A. (2008). Reliability considerations of bituminous pavement design by mechanistic-empirical approach. *International Journal of Pavement Engineering, 9*(1), 1-31.

Maji, A., & Jha, M. K. (2007). Modeling Highway Infrastructure Maintenance Schedules with Budget Constraints. *Transportation Research Record: Journal of the Transportation Research Board, 1991*, 19-26.

Mallela, J., Glover, L. T., Liang, R. Y., & Chou, E. Y. (2009). *Guidelines for Implementing NCHRP 1-37A M-E Design Procedures in Ohio. Volume 2 - Literature Review.* Columbus, Ohio: Applied Research Associates, Inc. - Ohio Department of Transportation.

Mallick, R. B., & El-Korchi, T. (2009). *Pavement engineering. Principles and practices* (First ed.). Boca Raton, Florida, USA: CRC Press Taylor & Francis Group.

Mamlouk, M. S., Zaniewski, J. P., & He, W. (2000). Analysis and Design Optimization of Flexible Pavement. (A. S. Engineers, Ed.) *ASCE Journal of Transportation Engineering, 126*(2), 161.

Marini, F., & Walczak, B. (2015). Particle Swarm Optimization (PSO). A tutorial. *Chemometrics and Intelligent Laboratory Systems, 149*, 153-165.

Matin, A. G., Nezafat, R. V., & Golroo, A. (2017). A Comparative Study on Using Metaheuristic Algorithms for Road Maintenance Planning: Insights from Field Study in a Developing Country. *Journal of Traffic and Transportation Engineering (English Edition), 4*(5), 477-486.

Mendoza, C., & Caicedo, B. (2018). Elastoplastic Framework of Relationships between CBR and Young's Modulus for Granular Material. *Road Materials and Pavement Design, 19*(8), 1796-1815. doi:10.1080/14680629.2017.1347517

Meneses, S. (2013). *Multi-Objective Decision-Aid Tool for Pavement Management.* Ph.D. Thesis, University of Coimbra.

Meneses, S., & Ferreira, A. (2012). Pavement Maintenance Programming Considering Two Objectives: Maintenance Costs And User Costs. *International Journal of Pavement Engineering, 14*(2), 206-221.

Michelow, J. (1963). *Analysis of stresses and displacements in N-layered elastic systems under a load uniformly distributed in a circular area.* Richmond, CA, USA: California Research Corporation.

Ministerio de Transporte - Oficina Asesora de Planeación. (2014). *Transporte en Cifras - Estadísticas 2014.* Bogotá: MinTransporte. Recuperado el 27 de Marzo de 2016, de https://www.mintransporte.gov.co/descargar.php?idFile=12621

Monismith, C. L. (2004). Evolution of Long-Lasting Asphalt Pavement Design. Distinguished Lecture International Society for Asphalt Pavements. *International*

Symposium on Design and Construction of Long-Lasting Asphalt Pavements (pp. 1-77). USA: Auburn University.

Montoya-Rodriguez, C. (2015). *Predicting Pavement Performance Under Traffic Loading Using Genetic Algorithms and Artificial Neural Networks to Obtain Resilient Modulus Values.* Ph.D. Thesis, Ohio State University. Retrieved from https://etd.ohiolink.edu/

Morcous, G., & Lounis, Z. (2005). Maintenance Optimization of Infrastructure Networks using Genetic Algorithms. *Automation in Construction, 14*, 129-142.

Nabhan, P. (2015). *Calibration of the AASHTO MEPDG for Flexible Pavements to Fit Nevada's Conditions - M.Sc. Thesis.* The University of Nevada. Reno, Nevada: The University of Nevada.

Naseri, H., Shokoohi, M., Jahanbakhsh, H., Golroo, A., & Gandomi, A. H. (2021). Evolutionary and swarm intelligence algorithms on pavement maintenance and rehabilitation planning. *International Journal of Pavement Engineering*. doi:10.1080/10298436.2021.1969019

National Academies of Sciences, Engineering, and Medicine. (2012). *Estimating the Effects of Pavement Condition on Vehicle Operating Costos.* Washington, DC: The National Academies Press. doi:10.17226/22808

Nazzal, M. D., & Tatari, O. (2013). Evaluating the Use of Neural Networks and Genetic Algorithms for Prediction of Subgrade Resilient Modulus. *International Journal of Pavement Engineering, 14*(4), 364-373.

NCHRP. (2004). *Mechanistic-Empirical Design of New and Rehabilitated Pavement Structures.* National Cooperative Highway Research Program NCHRP Project 1-37A. Washington D.C.: National Research Council.

Newcomb, D. E., Buncher, M., & Huddleston, B. W. (2001). Concepts of Perpetual Pavements. *Transportation Research Board Circular No. 503*, 4-11.

Nguyen, L. H. (2017, September). Research on the Correlation Between International Roughness Index (IRI) and Present Serviceability Index (PSI), Recommendations on Evaluation Rates in Vietnam's Conditions. *International Journal of Engineering Research & Technology (IJERT), 6*(09), 266-271. Retrieved from http://www.ijert.org

Nik, A. A., Nejad, F. M., & Zakeri, H. (2016). Hybrid PSO and GA Approach for Optimizing Surveyed Asphalt Pavement Inspection Units in Massive Network. *Automation in Construction, 71*, 325-345.

Nilsson, R. N., Oost, I., & Hopman, P. C. (1996). Viscoelastic Analysis of Full-Scale Pavements: Validation of VEROAD. (T. R. Board, Ed.) *Transportation Research Record 1539*, 81-87.

Novak, M., Birgisson, B., & Roque, R. (2003). Near-surface stress states in flexible pavements using measured radial tire contact stresses and ADINA. *Computers and Structures, 81*, 859-870.

Oppenlander, J. J., Heal, S. S., & Burns, L. D. (1971). *Optimization of the Structural Design of Asphalt Pavements JHRP C-36-52I.* Lafayette, Indiana: Purdue University.

Panda, T. R., & Swamy, A. K. (2018). An Improved Artificial Bee Colony Algorithm for Pavement Resurfacing Problem. *International Journal of Pavement Research and Technology, 11*, 509-16.

Papagiannakis, A. T., & Masad, E. A. (2008). *Pavement design and materials* (First ed.). Hoboken, NJ, USA: John Wiley & Sons.

Park, S.-W., Park, H. M., & Hwang, J.-J. (2010). Application of Genetic Algorithm and Finite Element Method for Backcalculating Layer Moduli of Flexible Pavements. *KSCE Journal of Civil Engineering, 14*(2), 183-190.

Peddinti, P. T., Basha, B. M., & Saride, S. (2020). System Reliability Framework for Design of Flexible Pavements. *Journal of Transportation Engineering. Part B: Pavements, 146*(3).

Pekcan, O., Tutumluer, E., & Ghaboussi, J. (2010). Soft Computing Methodology to Determine Pavement Thickness from Falling Weight Deflectometer Testing. *GeoFlorida 2010: Advances in Analysis, Modeling & Design (GSP 199)* (pp. 2621-2630). West Palm Beach, Florida: American Society of Civil Engineers.

Pereira, P., & Pais, J. (2017). Main flexible pavement and mix design methods in Europe and challenges for the development of a European method. *Journal of Traffic and Transportation Engineering, 4*, 316-346.

Peutz, M., Van Kempen, H., & Jones, A. (1968). Layered Systems Under Normal Surface Loads. *Highway Research Record, 228*, 33-45.

Pierce, L. M., & McGovern, G. (2014). *Implementation of the AASHTO Mechanistic-Empirical Pavement Design Guide and Software - NCHRP Synthesis 457.* Washington, D.C.: Transportation Research Board.

Pijarski, P., & Kacejko, P. (2019). A New Metaheuristic Optimization Method: The Algorithm of the Innovative Gunner (AIG). *Engineering Optimization*, 1-20. doi:10.1080/0305215X.2019.1565282

Pilson, C., Hudson, W. R., & Anderson, V. (1999). Multiobjective Optimization in Pavement Management by Using Genetic Algorithms and Efficient Surfaces. *Transportation Research Record: Journal of the Transportation Research Board, 1655*, 42-48.

Porter, O. J. (1942). Foundations for Flexible Pavements. *Proceedings of the Highway Research Board* (pp. 10-36). Washington, D.C.: HRB.

Poulos, H. G., & Davis, E. H. (1974). *Elastic Solutions for Soil and Rock Mechanics.* New York, USA: John Wiley & Sons, Inc. Retrieved 03 24, 2016, from http://research.engr.oregonstate.edu/usucger/PandD/PandD.htm

Powell, M. J. (2004). The NEWUOA Software for Unconstrained Optimization Without Derivatives. *The 40th Workshop on Large Scale Nonlinear Optimization.* Erice, Italy.

Pryke, A., Evdorides, H., & Ermaileh, R. A. (2006). Optimization of Pavement Design Using a Genetic Algorithm. *2006 IEEE Congress on Evolutionary Computation* (pp. 1095-1098). Vancouver: IEEE.

Qian, W.-d. (2010). Road Pavement Performance Evaluation Model Based on Hybrid Genetic Algorithm Neural Network. *2010 Second International Conference on Computational Intelligence and Natural Computing CINC* (pp. 209-212). IEEE.

Quijano-Bernal, C. A. (2016). *Aplicación de Redes Neuronales en el Cálculo Inverso de Pavimentos Flexibles - Trabajo de grado en modalidad de monografía.* Ingeniería Civil. Manizales: Universidad Nacional de Colombia.

Rabinovitz, P. (1990). Numerical integration based on approximating splines. (E. S. B.V., Ed.) *Journal of Computational and Applied Mathematics, 33*, 73-83.

Rajbongshi, P. (2014). Reliability Based Cost Effective Design of Asphalt Pavements Considering Fatigue and Rutting. *International Journal of Pavement Research and Technology, 7*(2), 153-158.

Rajbongshi, P., & Das, A. (2008). Optimal Asphalt Pavement Design Considering Cost and Reliability. *ASCE Journal of Transportation Engineering, 134*(6), 255-261.

Rakesh, N., Jain, A. K., Reddy, M. A., & Reddy, K. S. (2006). Artificial Neural Networks - Genetic Algorithm Based Model for Backcalculation of Pavement Layer Moduli. *International Journal of Pavement Engineering, 7*(3), 221-230.

Reddy, M. A., Reddy, K. S., & Pandey, B. B. (2004). Selection of Genetic Algorithm Parameters for Backcalculation of Pavement Moduli. *The International Journal of Pavement Engineering, 5*(2), 81-90.

Reyes Lizcano, F., Caicedo, B., & Yamin, L. (1997). *Manual de diseño de pavimentos para Bogotá D.C.* Bogotá D.C.: Instituto de Desarrollo Urbano - IDU - Universidad de Los Andes.

Rifai, A. I., Hadiwardoyo, S. P., Comes Correia, A., & Pereira, P. (2016). Genetic Algorithm Applied for Optimization of Pavement Maintenance under Overload Traffic: Case Study Indonesia National Highway. *Applied Mechanics and Materials*, 369-378.

Rojas-Pérez, F., Aguiar-Moya, J.-P., & Loría-Salazar, L.-G. (2015). PITRAPAVE - Software de multicapa elástica. (U. d.-L. (LANAMME), Ed.) San José de Costa Rica, Costa Rica: Laboratorio Nacional de Materiales y Modelos Estructurales.

Romanoschi, S., Lewis, P., Gedafa, D., & Hossain, M. (2014). *Verification of Mechanistic-Empirical Design Models for Flexible Pavements through Accelerated Pavement Testing - Report FHWA-KS-14-02.* Topeka, Kansas: Kansas State University Transportation Center.

Rouphail, N. M. (1985). Minimum-Cost Design of Flexible Pavements. *Journal of Transportation Engineering, 111*(3), 196-207.

Salari, E., & Yu, X. (2011). Pavement Distress Detection and Classification Using a Genetic Algorithm. *IEEE Applied Imagery Pattern Recognition Workshop 41PR* (pp. 1-5). IEEE.

Sánchez-Silva, M., Arroyo, O., Junca, M., Caro, S., & Caicedo, B. (2005). Reliability-Based Design Optimization of Asphalt Pavements. *The International Journal of Pavement Engineering, 6*(4), 281-294.

Santos, J., & Ferreira, A. (2012a). Pavement Design Optimization Considering Costs and Preventive Interventions. *Journal of Transportation Engineering, 138*(7), 911 - 923.

Santos, J., & Ferreira, A. (2012b). Pavement design optimization considering costs and M&R interventions. *Procedia - Social and Behavioral Sciences, 53*, 1184 - 1193.

Santos, J., & Ferreira, A. (2013). Life-Cycle Cost Analysis System for Pavement Management at Project Level. *International Journal of Pavement Engineering, 14*(1), 71-84.

Santos, J., Fereira, A., & Flintsch, G. (2017). An Adaptive Hybrid Genetic Algorithm for Pavement Management. *International Journal of Pavement Engineering, 20*(3), 266-286.

Saride, S., Peddinti, P. R., & Basha, M. B. (2019). Reliability Perspective on Optimum Design of Flexible Pavements for Fatigue and Rutting Performance. *Journal of Transportation Engineering, Part B: Pavements, 145*(2).

Sawyers, M. W., Gillespie, T. D., & Paterson, W. D. (1986). *Guidelines for conducting and calibrating road roughness measurements (No. Technical Paper 46).* Washington, DC: The World Bank.

Schwartz, C. W., & Carvalho, R. L. (2007). *Implementation of the NCHRP 1-37A Design Guide. Final Report. Volume 2: Evaluation of Mechanistic-Empirical Design Procedure* (Vol. 2). College Park, Maryland, USA: University of Maryland.

Schwartz, C. W., Kim, S. H., Ceylan, H., & Gopalakrishnan, K. (2011). *Sensitivity Evaluation of MEPDG Performance Prediction.* College Park, Maryland: University of Maryland - Iowa State University.

Scimemi, G. F., Turetta, T., & Celauro, C. (2016). Backcalculation of airport pavement moduli and thickness using the Lévy Ant Colony Optimization Algorithm. *Construction and Building Materials*, 288-295.

Senseney, C. T., Krahenbuhl, R. A., & Mooney, M. A. (2013). Genetic Algorithm to Optimize Layer Parameters in Light Weight Deflectometer Backcalculation. *International Journal of Geomechanics, 13*(4), 473-476.

Shahin, M. Y. (2006). *Pavement Management for Airports, Roads, and Parking Lots* (Second ed.). Springer.

Shahnazari, H., Tutunchian, M. A., Mashayekhi, M., & Amini, A. A. (2012). Application of Soft Computing for Prediction of Pavement Condition Index. *Journal of Transportation Engineering, 138*(12), 1495-1506.

Sharma, L. K., Singh, R., Umrao, R. K., Sahrma, K., & Singh, T. N. (2017). Evaluating the modulus of elasticity of soil using soft computing system. *Engineering with Computers, 33*, 497-507. doi:10.1007/s00366-016-0486-6

Shekharan, A. R. (2000). Solution of Pavement Deterioration Equations by Genetic Algorithms. *Transportation Research Record: Journal of the Transportation Research Board, 1699*, 101-106.

Shell Oil. (1978). *Shell Pavement Design Manual: Asphalt Pavements and Overlays for Road Traffic.* London, UK: Shell International Petroleum Company, Ltd.

Shen, Y., Bu, Y., & Yuan, M. (2009). A Novel Chaos Particle Swarm Optimization (PSO) and Its Application in Pavement Maintenance Decision. *ICIEA 2019* (pp. 3521-3526). IEEE.

Shi, Y. E., & Berhart, R. C. (1998). A Modified Particle Swarm Optimizer. *Proceedings of the IEEE Congress on Evolutionary Computation. 6*, pp. 69-73. IEEE.

Sidess, A., & Uzan, J. (2009). A design method of perpetual flexible pavement in Israel. *International Journal of Pavement Engineering*, 241-249.

Southgate, H. F., Deen, R. C., Cain, D., & Mayes, J. G. (1987). *Modifications to CHEVRON N-Layer program Research Report UKTRP-87-28.* Lexington, KY: Kentucky Transportation Center Research.

Strickland, D. (2000). *Shell Pavement Design Software for Windows.* London: Shell International Petroleum Company.

Sufian, A. A. (2016). *Local Calibration of the Mechanistic Empirical Pavement Design Guide for Kansas - M.Sc. Thesis.* Kansas State University. Manhattan, Kansas: Kansas State University.

Suh, Y., Mun, S., & Yeo, I. (2010). Fatigue Life Prediction of Asphalt Concrete Pavement Using a Harmony Search Algorithm. *KSCE Journal of Civil Engineering, 14*(5), 725-730.

Sundin, S., & Braban-Ledoux, C. (2001). Artificial Intelligence-Based Decision Support Technologies in Pavement Management. *Computer-Aided Civil And Infrastructure Engineering, 16*, 143-157.

Tack, J. N., & Chou, E. Y. (2002). Multiyear Pavement Repair Scheduling Optimization by Preconstrained Genetic Algorithm. *Transportation Research Record: Journal of the Transportation Research Board, 1816*, 3-9.

Taha, M. A., & Hanna, A. S. (1995). Evolutionary Neural Network Model for the Selection of Pavement Maintenance Strategy. *Transportation Research Record: Journal of the Transportation Research Board, 1497*, 70-76.

Tao, X., Huang, J., & Cai, Y. (2013). Inverse Analysis for Inhomogeneous Dielectric Coefficient of Pavement Material Based on Genetic Algorithm. *Applied Mechanics and Materials, 438-439*, 430-435.

Tarefder, R. A., & Bateman, D. (2012). Design of Optimal Perpetual Pavement Structure. *Journal of Transportation Engineering, 138*(2), 157-175.

Tarefder, R., & Rodriguez-Ruiz, J. I. (2013). Local Calibration of MEPDG for Flexible Pavements in New Mexico. *Journal of Transportation Engineering, 139*(10), 981-991.

Tayebi, N. R. (2010). Analysis of Pavement Management Activities Programming by Particle Swarm Optimization. *Proceedings of the International Conference on Advances in Electrical & Electronics* (pp. 149-154). ACEEE.

Tayebi, N. R., Nejad, F. M., & Mola, M. (2014). Comparison between GA and PSO in Analyzing Pavement Management Activities. *Journal of Transportation Engineering, 140*(1), 99-104.

Teodorovic, D. (2008). Swarm Intelligence Systems for Transportation Engineering: Principles and Applications. *Transportation Research Part C, 16*, 651-667.

Terzi, S. (2005). Modeling the Deflection Basin of Flexible Highway Pavements by Gene Expression Programming. *Journal of Applied Sciences, 5*(2), 309-314.

Terzi, S., & Serin, S. (2014). Planning Maintenance Works on Pavements Through Ant Colony Optimization. *Neural Computing & Applications, 25*(143), 143-153.

Terzi, S., Saltan, M., & Yildirim, T. (2003). Optimization of the Deflection Basin by Genetic Algorithm and Neural Network Approach. In O. Kaynak (Ed.), *ICANN/ICONIP 2003* (pp. 662-669). Springer-Verlag Berlin Heidelberg.

The South African National Roads Agency. (2014). *South African Pavement Engineering Manual - Introduction.* Johannesburg: The South African National Roads Agency.

Thom, N. (2008). *Principles of pavement engineering.* London, UK: Thomas Telford Publishing Ltd.

Thompson, M. R., & Barenberg, E. J. (1989). *Calibrated Mechanistic Structural Analysis Procedures for Pavements: Phase I—Final Report, NCHRP Project 1-26.* Washington, D.C.: Transportation Research Board, National Research Council.

Thompson, M. R., & Elliot, R. P. (1988). “ILLI-PAVE Based Response Algorithms for Design of Conventional Flexible Pavements. *Transportation Research Record 1207*, 145-168.

Timm, D. H., Newcomb, D. E., & Galambos, T. V. (2000). Incorporation of Reliability into Mechanistic-Empirical Pavement Design. *Transportation Research Record: Journal of the Transportation Research Board, 1730*, 73-80.

Timm, D. H., Robbins, M. M., Tran, N., & Rodezno, C. (2014). *Flexible Pavement Design - State of the Practice NCAT Report 14-04.* Auburn, AL: National Center for Asphalt Technology - NCAT.

Timoshenko, S., & Goodier, J. N. (1951). *Theory of Elasticity.* New York, USA: McGraw-Hill Book Company Inc.

Toklu, Y. C. (2014). An Overview of Metaheuristic Algorithms. In Y. C. Toklu, & G. Bekdas (Ed.), *Metaheuristics and Engineering Proceedings of the 15th EU/ME Workshop* (pp. 13-16). Istambul, Turkey: Bilecik Seyh Edebali University.

Tran, N., Robbins, M. M., Rodezno, C., & Timm, D. H. (2017). *Pavement ME Design - Impact of Local Calibration, Foundation Support, and Design and Reliability Thresholds - NCAT Report 17-08.* Auburn University. Auburn, Alabama: National Center for Asphalt Technology.

Transport Research Laboratory. (1993). *Overseas Road Note 31 A Guide to the Structural Design of Bitumen-Surfaced Roads in Tropical and Sub-Tropical Countries.* Crowthorne, Berkshire: Transport Research Laboratory.

Transport Research Laboratory. (2002). *Overseas Road Note 19 A guide to the design of hot mix asphalt in tropical and sub-tropical countries.* London, UK: TRL Limited.

Trejos Castillo, C., Leiva Padilla, P., & Loría Salazar, G. (2014). *Interfaz Gráfica para Diseño Mecanístico-Empírico de Pavimentos en Costa Rica CR-ME Versión 1 Guía del Usuario.* San José: Laboratorio Nacional de Materiales y Modelos Estructurales - Universidad de Costa Rica.

Tsai, B.-W., Harvey, J. T., & Monismith, C. L. (2009). Case Studies of Asphalt Pavement Analysis/Design with Application of the Genetic Algorithm. (K. Gopalakrishnan, & N. O. Attoh-Okine, Eds.) *Studies in Computational Intelligence 259. Intelligent and Soft Computing in Infrastructure Systems Engineering. Recent Advances*, 205-238. doi:10.1007/978-3-642-04586-8

Tsai, B.-W., Kannekanti, V. N., & Harvey, J. T. (2004). *Transportation Research Record: Journal of the Transportation Research Board, 1891*, 112-120.

Tsunokawa, K., Van Hiep, D., & Ul-Islam, R. (2006). True Optimization of Pavement Maintenance Options with What-If Models. *Computer-Aided Civil and Infrastructure Engineering, 21*, 193-204.

Tutumluer, E., & Barksdale, R. D. (1995). Behaviour of pavements with granular bases - prediction and performance. *Unbound aggregates in roads*, 173-183.

Tutumluer, E., & Sarker, P. (2015). *Development of Improved Pavement Rehabilitation Procedures Based on FWD Backcalculation - NEXTRANS Project No. 094/Y04.* Urbana-Champaign, Illinois: NEXTRANS USDOT V Regional University Transportation Center.

Ullidtz, P. (1987). *Pavement analysis.* Amsterdam: Elsevier.

Ullidtz, P., Harvey, J., Basheer, I., Jones, D., Wu, R., Jeremy, L., & Lu, Q. (2010). CalME, a Mechanistic-Empirical Program to Analyze and Design Flexible Pavement Rehabilitation. *Transportation Research Record: Journal of the Transportation Research Board, 2153*, 143-152.

Universidad Nacional de Colombia. (2013). *Cartilla guía de diseño de pavimentos con bajos volúmenes de tránsito y vías locales para la ciudad de Bogotá D.C.* Bogotá: Universidad Nacional de Colombia - Instituto de Desarrollo Urbano - Banco de Desarrollo para América Latina.

Unnikrishnan, A., Valsaraj, V., Damnjanovic, I., & Waller, S. T. (2009). Design and Management Strategies for Mixed Public Private Transportation Networks: A Meta-Heuristic Approach. *Computer-Aided Civil and Infrastructure Engineering, 24*, 266-279.

Uzan, J. (1994). Advanced back-calculation techniques. *Second International Symposium on NDT of Pavements and Backcalculation* (pp. 3-37). Philadelphia, Pa, USA: ASTM Special Technical Publications.

Van Cauwelaert, F. J., & Lequeux, D. (1986). *Computer Programs for the Determination of Stresses and Displacements in Four Layered Structures.* Waterways Experiment Station. Vicksburg, Miss.: U.S. Army Corps of Engineers.

Van den Bergh, F., & Engelbrecht, A. (2002). A New Locally Convergent Particle Swarm Optimizer. *International Conference on Systems, Man and Cybernetics. 3.* IEEE.

Van Hiep, D. (2009). *Optimization of Pavement Designs and / or Maintenance Strategies Using Gradient Search with Option Evaluation Systems.* Ph.D. Thesis, Saitama University.

Varma, S., Kutay, M. E., & Levenberg, E. (2013). Viscoelastic Genetic Algorithm for Inverse Analysis of Asphalt Layer Properties from Falling Weight Deflections. *Transportation Research Record: Journal of the Transportation Research Board, 2369*, 38-46.

Vásquez Varela, L. R. (14 de Mayo de 2015). *Aplicación de la Mecánica de Sólidos en Ingeniería de Pavimentos.* Recuperado el 24 de Marzo de 2016, de Ingepav - Ingeniería de pavimentos por Luis Ricardo Vásquez Varela: https://sites.google.com/site/ingepav/diseno-y-analisis/mecanicadesolidoisaplicadaapavimentos

Vásquez-Varela, L. R., & García-Orozco, F. J. (2019). UNLEA A Multilayer Elastic Program Script in Scilab. *International Airfield and Highway Pavements Conference 2019.* Chicago, IL: American Society of Civil Engineers. doi:https://doi.org/10.1061/9780784482452.010

Vásquez-Varela, L. R., & García-Orozco, F. J. (2020). An overview of asphalt pavement design for streets and roads. *Revista Facultad De Ingeniería Universidad De Antioquia*(98), 10-26. doi:https://doi.org/10.17533/udea.redin.20200367

Vásquez-Varela, L. R., & García-Orozco, F. J. (2021). Applied Metaheuristic Optimization in Asphalt Pavement Management. *Ciencia e Ingeniería Neogranadina*, 75-92. doi:https://doi.org/10.18359/rcin.4371

Velasquez, R., Hoegh, K., Yut, I., Funk, N., Cochran, G., Marasteanu, M., & Khazanovich, L. (2009). *Implementation of the MEPDG for New and Rehabilitated Pavement*

Structures for Design of Concrete and Asphalt Pavements in Minnesota. Saint Paul, Minnesota: Minnesota Department of Transportation.

Verstraeten, J., Veverka, V., & Francken, L. (1982). Rational and Practical Designs of Asphalt Pavements to Avoid Cracking and Rutting. *Proceedings Fifth International Conference on the Structural Design of Asphalt Pavements* (pp. 42-58). University of Michigan and Delft University of Technology.

Von Quintus, H. L., & Simpson, A. L. (2002). *Back-Calculation of Layer Parameters for LTPP Test Sections, Volume II: Layered Elastic Analysis for Flexible and Rigid Pavements - FHWA-RD-01-113.* McLean, Virginia: Federal Highway Administration.

Von Quintus, H. L., Mallela, J., Bonaquist, R., Schwartz, C. W., & Carvalho, R. L. (2012). *Calibration of Rutting Models for Structural and Mix Design - NCHRP Report 719.* Washington, D.C.: Transportation Research Board.

Walker, R. N., Patterson, W. D., Freeme, C. R., & Marias, C. P. (1977). The South African Mechanistic Pavement Design Procedure. *Proceedings, Fourth International Conference on the Structural Design of Asphalt Pavements. 2.* The University of Michigan.

Walls, I. J., & Smith, M. R. (1998). *Life-Cycle Cost Analysis in Pavement Design - Interim Technical Bulletin Report No. FHWA-SA-98-079.* Washington D.C., USA: Federal Highway Administration.

Wang, D., Roesler, J. R., & Guo, D.-Z. (2011). Innovative Algorithm to Solve Axisymmetric Displacement and Stress Fields in Multilayered Pavement Systems. *ASCE Journal of Transportation Engineering, 137*(4), 287-295. doi:10.1061/(ASCE)TE.1943-5436.0000208

Wang, K. C., Nguyen, V., & Zaniewski, J. P. (2007). Genetic Algorithms-Based Network Optimization System with Multiple Objectives. *Transportation Research Record: Journal of the Transportation Research Board, 2016*, 85-95.

Wardle, L. J. (1977). *Program CIRCLY. A Computer Program for the Analysis of Multiple Complex Loads on Layered Anisotropic Media.* Victoria, Australia: Division of Applied Geomechanics and Commonwealth Scientific and Industrial Research Organisation.

Warren, H., & Dieckmann, W. L. (1963). *Numerical Computation of Stresses and Strains in a Multiple-Layered Asphalt Pavement System.* Richmond, California: California Research Corporation.

Watanatada, T., Harral, C. G., Paterson, W. D., Dhareshwar, A. M., Bhandari, A., & Tsunokawa, K. (1987). *The Highway Design And Maintenance Standards Model Volume 1: Description of the HDM-III Model.The Highway Design and Maintenance Standards Series.* The World Bank. Baltimore, USA: Johns Hopkins Press. Retrieved from http://www.worldbank.org/transport/roads/rd_tools/hdm-iii%20_vol-1.pdf

Whiteoak, D. (1991). *The Shell Bitumen Handbook.* Surrey, UK: Shell Bitumen UK.

Williams, R. C., & Shaidur, R. (2013). *Mechanistic-Empirical Pavement Design Guide Calibration for Pavement Rehabilitation - Final report SPR 718.* Salem, Oregon: Oregon Department of Transportation - Federal Highway Administration.

Wu, Z., Flintsch, G., Ferreira, A., & de Picado-Santos, L. (2012). Framework for Multiobjective Optimization of Physical Highway Assets Investments. *Journal of Transportation Engineering, 138*(12), 1411-1421.

Xinchao, Z. (2010). A Perturbed Particle Swarm Algorithm for Numerical Optimization. *Applied Soft Computing, 10*, 119-124.

Yang, C., Remenyte-Prescott, R., & Andrews, J. D. (2015). Pavement Maintenance Scheduling Using Genetic Algorithms. *International Journal of Performability Engineering, 11*(2), 135-152.

Yang, N. C. (1972). *Design of functional pavements.* (W. G. Salo Jr., J. Ely, & D. A. Douglas, Eds.) New York, NY, USA: McGraw-Hill.

Yang, X. -S. (2011). *Metaheuristic Optimization: Algorithm Analysis and Open Problems.* National Physics Laboratory.

Yang, X. S. (2013). Optimization and Metaheuristic Algorithms in Engineering. *Metaheuristics in Water, Geotechnical and Transport Engineering*, 1-23.

Yang, X.-S., Koziel, S., & Leifsson, L. (2014). Computational Optimization, Modelling and Simulation: Past, Present and Future. *Procedia Computer Science ICCS 2014 14th International Conference on Computational Science. Volume 29*, pp. 754-758. Cairns, Australia: Elsevier. doi:10.1016/j.procs.2014.05.067

Yepes, V., Torres-Machi, C., Chamorro, A., & Pellicer, E. (2016). Optimal Pavement Maintenance Programs based on a Hybrid Greedy Randomized Adaptative Search Procedure Algorithm. *Journal of Civil Engineering and Management, 22*(4), 540-550.

Yoder, E. J., & Witczak, M. W. (1975). *Principles of Pavement Design* (Second ed.). New York, USA: John Wiley & Sons, Inc.

Yoshimura, J., Ushio, S., & Sugawara, T. (1972). Stresses in Multi Layered Systems. *Memoirs of the Faculty of Engineering, Hokkaido University, 03*, 75-89.

Zaabar, I., Chatti, K., Suk-Lee, H., & Lajnef, N. (2014). Backcalculation of Asphalt Concrete Modulus Master Curve from Field-Measured Falling Weight Deflectometer Data - Using a New Time Domain VIscoelastic Dynamic Solution and Genetic Algorithm. *Transportation Research Record: Journal of the Transportation Research Board, 2457*, 80-92.

Zhao, Y., Liu, W., & Tan, Y. (2012). Analysis of Critical Structure Responses for Flexible Pavements in NCHRP 1-37A Mechanistic-Empirical Pavement Design Guide. *Journal of Transportation Engineering, 138*(8), 983-990.

Zhao, Y., Zhou, C., Zeng, W., & Ni, Y. (2015). Accurate determination of near-surface responses of asphalt pavements. *Road Materials and Pavement Design, 16*(1), 186-199. doi:10.1080/14680629.2014.979221

Ziari, H., & Khabiri, M. M. (2007). Interface condition influence on prediction of flexible pavement life. *Journal of Civil Engineering and Management*, 71-76.